UNIVERSITY OF TRENTO

Doctoral School in Civil, Environmental and Mechanical Engineering

Curriculum 1. Civil and Environmental Engineering

Maria Vittoria Tenci

Ecological evolution of recent proglacial lakes in the deglaciating Alps (Cevedale Glacier, Italy)

2025 - Doctoral thesis

UNIVERSITÀ DI TRENTO

Doctoral Programme in Civil, Environmental and Mechanical Engineering

XXXVII cycle 2021-2024

Doctoral thesis

Ecological evolution of recent proglacial lakes in the deglaciating Alps (Cevedale Glacier, Italy)

Maria Vittoria Tenci

Supervisors

Walter Bertoldi – University of Trento

Maria Cristina Bruno – Fondazione Edmund Mach

Marco Toffolon – University of Trento

Monica Tolotti – Fondazione Edmund Mach

Abstract

The Alpine cryosphere is strongly affected by the current climate-driven deglaciation. In this context, one of the most evident effects of glacier retreat is the increase in number and volume of new proglacial lakes, that in the past decades progressively became a frequent feature of the high mountain landscape. Common traits of proglacial lakes are related to the inflow of glacial meltwater and include low water temperature and high amounts of inorganic particles suspended in the water column, which results in high turbidity. These factors shape a harsh and rapidly evolving habitat, with only partially known selective effects on lake biota. While planktonic communities in proglacial lakes have attracted more attention from the scientific community, knowledge on benthic communities remains scattered. Nonetheless, given the low input of allochthonous organic matter from bare proglacial forefields, local periphyton may represent a crucial carbon source fuelling the food webs of glacier-fed lakes.

This thesis contributes to the general knowledge of Alpine proglacial lake ecosystems, by integrating observations and modelling of lake hydrodynamic, temperature and turbidity patterns with investigations on benthic biological communities. The synergy between different disciplines allows to provide a broad picture of the dynamics involved in the ecological evolution of proglacial lake ecosystems influenced by the current Alpine deglaciation. For this purpose, a lake cluster formed by the regression of the Cevedale Glacier was investigated over a two-year period, during the ice-free season. Four proglacial lakes were selected, representing the different evolutionary stages of proglacial lake ecosystems, going from one turbid ice-contact lake to intermediate and distal lakes.

Physical, chemical and biological components were extensively monitored in the lakes through the installation of temperature, light and electrical conductivity sensors, and by collecting samples for chemical and biological analyses (eDNA and benthic diatoms). The environmental gradients recorded in the study site are mainly linked to the different lake age and the related glacial influence. Physical dynamics were further analysed in one turbid lake, by installing chains of thermistors in the water column, to observe vertical stratification phenomena. These data were used to calibrate a 2-D hydrodynamic model, which allowed to link the lake thermal dynamics to the turbidity patterns. Input data for the model set-up were obtained from in situ measurements of outlet discharges, water level and the concentration of inorganic suspended solids in the lake. The model simulation showed that during periods characterised by warm air temperatures and rare precipitation events, the lake promptly responds developing a daily thermal stratification, which in turn determines the depth of intrusion of the turbid inflow, often entering the lake as an interflow. Therefore, thermal stratification can influence the light penetration in the water column of shallow layers through the control on turbidity patterns. From an ecological perspective, these results indicate that light availability in the littoral area can occur also in periods of sustained glacier turbid inflow, thus determining the presence of stratification-driven windows of opportunity for periphyton growth. This result was consistent with the seasonal evolution of the biomass of littoral photosynthetic communities in the lake, measured as chlorophyll-*a* and organic content in the biofilm and as benthic diatom density. A peak in photosynthetic biomass was indeed observed in August 2022, suggesting

that periphyton growth can be sustained even during periods of maximum turbid inflow from the glacier.

Detailed analyses on biological communities indicate a progressive increase in littoral α-diversity from the ice-contact lake to the distal lake, for both eukaryotic (including diatoms) and prokaryotic assemblages. However, taxonomic compositions significantly differed from lake to lake. These results indicate that the progressive loss of glacial influence during the evolution of the studied lakes is related to an increase in α-diversity in littoral communities and to a simultaneous homogenisation of communities, which leads to a decreasing β-diversity.

First stages of colonisation (i.e., communities in the most recent lakes), are dominated by psychrophilic, aerophilic, soil-adapted and pioneer species. The selective physical setting of habitat in the Cevedale proglacial lakes, characterised by cold and turbid water inflow and the continuous deposition of high amounts of fine-grained sediment on shores, allows the establishment of specialised diatom communities. One diatom species (i.e., *Pinnularia bullacostae*) not previously recorded in the European Alps was observed in the Cevedale proglacial lakes.

The results of this thesis point out the relevance of proglacial lakes for the Alpine environment: despites strongly dependent on hydrodynamic patterns and characterised by harsh habitats, they can host specialised biodiversity. In a climatic change perspective, proglacial lake habitats are expected to undergo relevant modifications in the upcoming decades, since the projected increase in air temperature and concomitant decrease in summer precipitation could accelerate natural colonisation processes. This will further extend the expected effects of global warming over biodiversity and ecological evolution of Alpine aquatic ecosystems.

Table of Contents

List of figures

Figure 5. 13. Taxonomic composition (relative abundance of reads in the sample) at the division level of the analysed samples, grouped by type (E = epilithic, P = plankton, S = sediment) and lake.

Figure 5. 14. Eukaryotic ASV richness in the analysed epilithic and plankton samples, grouped by lake.

Figure 5. 15.ASV richness of the most abundant (n ASV > 2%) classes detected in the analysed samples, divided into epilithic and plankton samples.

Figure 5. 16. Ordination plot of epilithic diatom samples grouped by lake, based on the method used for the determination of the taxonomic composition at the genus level: 18S = metabarcoding od the 18S rRNA gene; LM = light microscopy. NMDS stress = 0.13.

List of tables

Chapter 1

Introduction

The ongoing climatic changes are affecting biodiversity and functioning of ecosystems worldwide (IPBES, 2019; Nimma et al., 2025), as well as their provision of services to human societies. This determines dramatic effects that encompass the access to food and water, human health, and other human rights (Birkmann et al., 2022). One of the most evident effects of global warming on natural systems is the massive reduction in the extension of glaciated areas worldwide (IPCC, 2022; WGMS, 2023; Al-Yaari et al., 2023). Cycles of glaciation and deglaciation are important agents of transformation of the Earth surface at geological scales, including the formation of lakes, as most lakes on Earth have a glacial origin (Wetzel, 2001). The present deglaciation of mountain areas offers the unique opportunity to directly observe the cascade effects that are involved in this process, many of which related to snow and ice depletion (Pepin et al., 2022). Cryosphere loss in mountain areas has been extensively documented (Hock et al., 2019), together with the connected impacts on hydrological regimes and the seasonality of water availability (Beniston et al., 2018), habitat shifts and biodiversity loss (Cauvy-Fraunié & Dangles, 2019). The consequent effects on ecosystem services provided by the mountain cryosphere have been addressed in relation to quantity and quality of freshwater supply for human activities, climate regulation, culture and tourism (Huss et al., 2017; Milner et al., 2017; Ramel et al., 2020). Mountain areas are considered as "water towers" in relation to their significant contribution in water supply to lowland populated areas (Viviroli et al., 2007). In this context, the European Alps are very sensitive to climatic changes, due to their location in a densely populated geographic area that strongly relies on their ecosystem services (Vanham, 2012). The decline of the Alpine cryosphere has been largely documented (Beniston et al., 2018; Hock et al., 2019), as well as its consequences on downstream ecosystems and human activities (Milner et al., 2017).

As glaciers retreat, they leave a complex of new terrestrial and aquatic proglacial ecosystems, which are characterised by high geodiversity (Bollati et al., 2023) and extraordinarily rapid evolution (Bosson et al., 2023). Among the new ecosystems, proglacial lakes, i.e., lentic water bodies located in the proglacial area and directly linked to the glacier activity (Otto, 2019), are becoming increasingly represented elements of mountain landscapes worldwide (Stokes et al., 2007; Wang et al., 2015; Song et al. 2017; Tweed & Carrivick, 2015; Salerno et al., 2016; Nie et al., 2017; Drenkhan et al., 2018; Shugar et al., 2020; Ma et al., 2021). Furthermore, proglacial lakes pose risks related to sudden floods caused by rapid drainage of glacial basins (Glacier Lake Outburst Floods, GLOFs), that constitute a natural hazard for human populations living in deglaciating areas and can induce catastrophic landscape changes (Haeberli et al., 2011; Carrivick & Tweed, 2016; Viani et al., 2021; Taylor et al., 2023).

Many studies conducted in the European Alps agree that glacier retreat is paralleled by both the increase in the formation of new proglacial lakes and the growth of existing ones (e.g., Emmer et al., 2016; Viani et al., 2016). Ma et al. (2021) reported the existence in the European Alps, in 2019, of 498 glacial lakes with area >0.01 km^2, largely exceeding the number of non-glacier-fed ones.

According to this study, Alpine glacial lakes markedly increased in number and area between 2000 and 2019. Buckel et al. (2018) estimated the formation of 264 new glacial lakes between the Little Ice Age and 2015. The high rate of formation of Alpine proglacial lakes is expected to persist under the present climate change conditions. For example, Steffen et al. (2022) estimated that in the Swiss Alps more than 100 new lakes might form by 2050, and up to 683 potential lakes (with a total volume of up to 1.16 km^3) could form if glaciers will completely disappear. Because of glacier retreat, the elevation at which proglacial lakes form tends to increase (Salerno et al., 2014; Nie et al., 2016).

Proglacial lakes are directly linked to the glacier activity (Otto, 2019) as they are in direct contact with glacier ice (Tweed & Carrivick, 2015) and are fed by glacial meltwater ("glacier-fed lakes", Ashley, 2002), which transports sediments and solutes (Ashley, 2002; Otto, 2019). From a geomorphological point of view, these lakes are classified based on the type of dam that allows the impoundment of meltwater (Tweed & Carrivick, 2015; Otto, 2019), such as ice, bedrock, moraines, and landslides. Another classification considers the position of the lake relative to the glacier, distinguishing between ice-contact and ice-distal lakes. The latter are physically detached from the glacier but still receive glacial meltwater from glacier-fed streams (Ashley, 2002). The altitudinal distribution of the different types of Alpine glacial lakes is uneven (Ma et al., 2021). In particular, supraglacial and ice-contact lakes are generally located at higher elevations (average 2600 m a.s.l.), while ice-distal lakes are found down to 2400 m a.s.l. Ice-dammed lakes have a narrower altitudinal distribution than moraine-dammed and bedrock-dammed lakes, as they are strictly associated with glacier termini.

Alpine proglacial lakes are often ephemeral (Salerno et al., 2014), and their persistence depends on different interconnected factors. First, the rapid formation of these lakes is often accompanied by infilling processes due to the input and deposition of glacial sediment, which reduce lake depth and area (Bogen et al., 2015; Tweed & Carrivick, 2015; Otto, 2019). Second, unstable ice, landslide and moraine dams close to glacier margins can suddenly collapse, leading to the complete drainage of the lake (Rabot, 1905; Masetti et al., 2010; Carrivick & Tweed, 2013). Finally, the increased ratio between evaporation and precipitation induced by global warming can lead to a net lake volume loss after disconnection with the glacier, as observed in low elevation ponds of glacial origin in the Ortles-Cevedale area (Salerno et al., 2014).

Proglacial lake habitats

Altogether, proglacial lake ecosystems are oligotrophic systems, where physical factors such as temperature and turbidity represent the main constraints on biodiversity and productivity. The habitat features in proglacial lakes are largely determined by glacial meltwater, which is cold, turbid, and has distinctive chemical characteristics (Slemmons et al., 2013).

Proglacial lakes are generally colder than their non-glacier-fed counterparts (e.g., Koenings et al., 1990; Tiberti et al., 2020). However, the distance between lake and glacier is a determinant factor for water temperature, with distal lakes exhibiting higher water temperature compared to ice-contact lakes (Peter & Sommaruga, 2017; Harmeier et al., 2024). This results in different lake thermal dynamics. In ice-contact lakes, surface temperatures below 4°C induce inverse stratification or continuous mixing, while in ice-distal lakes temperatures above 4°C can promote the

establishment of thermal stratification (Hardmeier et al., 2024). These thermal differences originate from the inlet temperature, which is often close to 0°C in ice-contact lakes (Carrivick & Tweed, 2013), whereas in distal lakes the inlet is heated in its path from the glacier to the lake (Irwin & Pickrill, 1982; Ashley, 2002). Also, the direct contact with the glacier front, when it forms part of the lake banks, can induce lake water cooling.

Turbidity in glacier-fed lakes is usually higher than in snow-fed lakes at comparable elevations (Barta et al., 2018; Buerpee et al., 2018; Echeverría-Vega et al., 2018; Tiberti et al., 2020; Vanderwall et al., 2023) and is caused by large amounts of fine sediment suspended in the water column (Modenutti et al., 2000). These fine sediments constitute the so-called "glacial flour", which is composed mainly of mineral particles produced by the glacier erosion of underlying bedrock (Herman et al., 2015). The grain size of glacial flour particles ranges from fine silt to clay (Smith, 1978; Gallegos et al., 2008; Chanudet & Filella, 2009; Sommaruga & Kandolf, 2014) and their mineralogical composition depends on bedrock lithology (Ashley, 2002). Glacial flour influences the optical properties of the water column, attenuating the penetration of light radiation, both in the photosynthetic active (PAR) and in the ultraviolet (UV) range of wavelength (Rae et al., 2001; Gallegos et al., 2008; Rose et al., 2014).

Turbidity patterns depend on the distribution of glacial flour in the lake, which is controlled by, and controls, density stratification within the lake, together with temperature (Sugiyama et al., 2016). For example, as explained by Ashley (2002), in stratified distal lakes, the atmospheric heat input on surface layers determines the formation of a warmer epilimnion overlying a colder hypolimnion. The difference in density between the cold and turbid inflow and the warmer lake water layers drives the formation of complex overflows, interflows or underflows. These transport patterns can result in sub-surface turbidity maxima (e.g., Robb et al., 2021).

In comparison to snow-fed mountain lakes, proglacial lakes can be enriched in nutrients of different origin (Ren et al., 2019; Vanderwall et al., 2023). Glacial meltwater is an important source of organic carbon for downstream ecosystems (Singer et al., 2012; Hood et al., 2015). Indeed, glaciers store allochthonous organic carbon originating from atmospheric deposition and organic carbon originating from microbial primary production (Anesio et al., 2009; Singer et al., 2012). Enrichment in total phosphorus mainly derives from particulate phosphorus (P) released by the erosion activity of the glacier mass on underlying bedrocks (Hodson et al., 2004). However, relevant P input can originate also from episodic deposition of desert dust transported by the atmospheric circulation (Brahney et al., 2014). Glacier meltwater is often enriched also in particulate nitrogen (N), resulting in increased total N concentrations in glacier-fed lakes in comparison to other mountain lakes fed by snow (Saros et al., 2010; Slemmons and Saros, 2012; Williams et al., 2016; Warner et al., 2017; Colombo et al., 2019). Nitrogen can derive from atmospheric deposition on glacier surface (Colombo et al., 2019) and microbial processes (Slemmons et al., 2013). Given the spatial variability of sources, nutrient enrichment of meltwater is quite variable at regional scale (Rogora et al., 2008; Williams et al., 2016).

Life in proglacial lakes

Proglacial lakes are unique ecosystems, where the extreme habitat conditions created by glacier meltwater support the presence of special combinations of organisms. Field-based studies showed that proglacial lake communities are markedly different from those found in clear mountain lakes (Slemmons & Saros, 2012; Kammerlander et al., 2016; Peter & Sommaruga, 2016; Barta et al., 2018; Tiberti et al., 2020; Kleinteich et al., 2022) and from those found in glacier-fed rivers (e.g., Hu et al., 2020). The uniqueness of proglacial lake plankton is the result of the environmental characteristics of these ecosystems, as summarised by Sommaruga (2015).

According to Elser et al. (2020), the main factors driving biological dynamics in alpine headwaters are temperature, light, stoichiometry, and efficiency in the use of limiting resources.

Water temperature is an important factor in determining community composition and physiology in proglacial lakes. Cold temperatures pose selective constraints to living organisms, affecting enzyme activity, molecular flexibility, and fluidity of membranes (D'Amico et al., 2006; Elser et al., 2020). Therefore, cryosphere-related organisms have evolved adaptations that involve, for example, the production of cold-adapted enzymes (Collins & Gerday, 2017), antifreeze proteins and cryoprotectants (Kawahara, 2017), modulations in the composition of membrane lipids (Russell, 1997), and the increase of ATP production to maintain appropriate metabolism levels at low physiological temperature (Napolitano, 2004). These costly adaptations become ineffective, or even harmful, at higher temperatures (Elser et al., 2020), so that many cold-adapted organisms are stenotherms. In proglacial lakes, the presence of planktonic cold-adapted species is well documented, and include, for example, bacteria such as *Polaromonas* (Peter & Sommaruga, 2016) and algae such as *Koliella* sp. (Kammerlander et al., 2016). A warmer Alpine hydrosphere leads to a reduction of habitats of cold-adapted species (e.g., Brown et al., 2007; Muhlfeld et al., 2011), with increasing extinction risk (Gobbi et al., 2021).

The presence of glacial flour is another key factor in determining the composition of planktonic communities in proglacial lakes, as it influences the feeding efficiency of grazers (Koenings et al., 1990) and reduces the thickness of the photic zone (Rose et al., 2014), while attenuating UV-induced damage (Tartarotti et al., 2014). In such environments, turbidity induces light limitation and only the most tolerant taxa of phytoplankton can survive. In the Italian Alps, Tiberti et al. (2020) found a negative relationship between glacial influence and the presence of eukaryotic phytoplankton, with the main planktonic primary producers being picocyanobacteria. In some cases, proglacial planktonic communities can lack photosynthetic bacteria (Gaskill et al., 2020; Hu et al., 2020). Harsh conditions favour specialised taxa and life strategies. Algal taxa observed in proglacial lake phytoplankton possess adaptations to low or variable light conditions. Cryptophytes, that are characteristic members of proglacial lake phytoplankton (Kammerlander et al., 2016; Barta et al., 2018), possess, together with chlorophyll *a* and *c*, the phycobilisome light-harvesting complex (Gantt et al 1971; Gervais, 1997). Similarly, autotrophic picocyanobacteria are equipped with accessory light-harvesting phycobiliproteins (Callieri, 2017), an advantageous adaptation to low-light niches (Tiberti et al., 2020; Miserendino et al., 2023). Among chlorophytes, species of the genus *Koliella* such as *K. antarctica* can readily respond to light fluctuations by controlling the xanthophyll content of their photosynthetic apparatus (La Rocca et al., 2015).

Phytoplankton is also highly sensitive to nutrient loads (Wetzel, 2001). N input delivered with glacial meltwater can cause phytoplankton communities to shift from N limitation, rather common for mountain lakes, towards P and N co-limitation (Slemmons & Saros, 2012; Ren et al., 2019) or P limitation (Tiberti et al., 2020), which implies changes in algal community composition (Slemmons et al., 2017) and photosynthetic rates (Slemmons & Saros, 2012). However, despite the nutrient input from meltwater, proglacial lakes are generally oligotrophic or ultraoligotrophic. Indeed, nutrients delivered with meltwater are mainly not readily available to algal consumption (Hodson et al., 2004; Föllmi et al., 2009). Furthermore, the physical constraints posed by glacial meltwater inhibit algal growth even in presence of large nutrient availability (e.g., Rinke et al., 2001), so that in very turbid proglacial lakes light attenuation induced by glacial particles dominates over nutrient enrichment in limiting primary production (Tiberti et al., 2020).

The presence of glacial flour, together with phytoplankton composition of glacial lakes, influences higher planktonic trophic levels. Waibel et al. (2019) identified high mountain oligotrophic lakes as hotspots for mixotrophy, i.e., the capacity of certain algal groups to improve their nutrition by ingesting organic particles or cells. In glacier-fed lakes, mixotrophy represents an advantageous trait for unicellular eukaryotes (Hinder et al., 1999; Sommaruga, 2015; Kammerlander et al 2016). In their experiment, Sommaruga and Kandolf (2014) demonstrated that the mixotrophic flagellate *Dinobryon divergens* was insensitive to the presence of glacial flour, while the abundance of the strictly heterotrophic *Spumella* sp. was significantly affected. This effect was concentration-dependent and linked to the low bacteria to particle ratio. Indeed, the particles of glacial flour have a grain size distribution overlapping the size of the potential prokaryotic preys (Pernthaler, 2005; Sommaruga & Kandolf, 2014). Bacterivory of mixotrophic flagellates is strongly reduced by increased clay concentrations, in relation to the increased time invested in the handling of the prey and ejection of non-edible particles (Schenone et al., 2020). Furthermore, glacial particles typically have low organic coating, which does not support bacterial colonisation (Sommaruga & Kandolf, 2014). Similarly, the high amounts of small-sized mineral particles arriving together with ice meltwater affect the foraging efficiency of filter-feeding zooplankton (Koenings et al., 1990). The main taxonomical groups of zooplankton living in proglacial lakes are copepods and rotifers (Barta et al., 2018; Kammerlander et al., 2016; Tiberti et al., 2020), both known as selective feeders (DeMott et al., 1986; Kirk et al., 1991). With respect to clear lakes, copepods have wider habitats in glacial lakes, thanks to UV-attenuation exerted by turbidity (Tartarotti et al 2017). Cladocerans, such as *Daphnia* sp., are present at very low densities in proglacial lakes (Barta et al., 2018). Tiberti et al. (2020) found significantly lower abundances of cladocerans and copepods in glacier-fed Alpine lakes compared to non-glacier-fed ones, with *Daphnia* sp., *Alona* sp. and the copepode *Eucyclops serrulatus* totally absent in the former ones. Khamis et al. (2014) found a negative relationship between the presence and abundance of the *Daphnia longispina* group, and the percentage of glacier cover in the catchment, thus confirming the link between the glacier activity and plankton structure. Nutrient limitations in phytoplankton interact with light restrictions caused by turbidity, affecting the light:P ratio (Sterner et al., 1997). In turbid glacial lakes, this can lead to a low algal C:P ratio (Ren et al., 2019). Since zooplankton species have different nutrient needs (e.g., Hall et al., 2004), changes in the C:P ratio along turbidity gradients impact food quality and affect grazer species composition (Laspoumaderes et al., 2013).

While the knowledge of composition and ecology of phytoplankton of Alpine proglacial lakes is relatively advanced, information about benthic communities is still scarce and restricted to few taxonomic groups. A rather large information is available for benthic macroinvertebrates, which generally exhibit a lower diversity in glacier-fed lakes than in clear lakes (Barta et al., 2018; Miserendino et al., 2023), and whose communities are dominated by chironomids (Gobbi & Lencioni, 2020). However, macrozoobenthic assemblages in glacier-fed lakes exhibit distinct taxonomic composition, characterised by the presence of cold stenotherms such as the tribe Diamesinae (Jennings, 2021).

Benthic microbial communities have been rarely considered in previous studies conducted in the Alps (e.g., Kleinteich et al., 2022). Even though cyanobacteria, diatoms, chrysophytes, and green algae represent the key component of phytobenthos of both glacial and clear non glacial high altitude water bodies (e.g., Rott et al., 2006; Sudlow et al., 2023), the investigations so far identified benthic microbial assemblages as taxonomically differing in proglacial lakes and clear lakes (Kleinteich et al., 2022). In the French Alps, Feret et al. (2017) individuated distinctive benthic diatom assemblages in proglacial lakes compared to other mountain lakes. However, the spatial and seasonal variability of benthic communities along the Alpine deglaciation chronosequences is still unknown.

Nonetheless, given the reduced planktonic primary production and the low input of allochthonous organic matter from bare proglacial terrestrial ecosystems, benthic primary producers (i.e., periphyton) represent a key autochthonous carbon source for proglacial lake food webs (Vadeboncoeur et al., 2002). For example, Mez et al. (1998) and Kleinteich et al. (2022) observed the formation of conspicuous cyanobacterial mats growing on stones and sediment in proglacial lakes in the Swiss Alps. Despite the high dynamism of the water column, periphytic biofilm likely experiences different environmental conditions in comparison to plankton. However, information on this aspect only comes from studies on glacial streams. The study conducted by Ezzat et al. (2022) demonstrated that both alpha and beta diversity of benthic microbial communities significantly differ from those observed in the water column of glacier-fed streams. The phenology of phytobenthos in glacier-fed streams is determined by the physical properties induced by glacial runoff, i.e., cold temperatures and high turbidity. This suppresses benthic primary production during periods of glacial ablation (summer), when glacial flour induces light limitation, and bedload induces physical disturbance on biofilms. Instead, periphyton growth is concentrated during the so-called “Windows of Opportunity” (WOs, Uehlinger et al., 2010), periods during which environmental conditions are favourable for photosynthesis. WOs typically occur in autumn, when temperatures are still relatively high, but glacier runoff is reduced, and in spring, depending on snowpack conditions. The response of periphyton to WOs has been documented in stream communities and involved biomass, taxonomic composition, diversity, and metabolism (Uehlinger et al., 2010; Busi et al., 2022; Tolotti et al., 2024). Although similar mechanisms may drive WOs in proglacial lakes, the response of lentic water bodies to inflow of glacial meltwater is expected to be mediated also by density stratification (Ashley, 2002; Sugiyama et al., 2016). The consequent timing and characteristics of WOs in glacier-fed lakes remains up to date unexplored in this field.

Aims of the thesis

This thesis aimed at improving the knowledge about Alpine proglacial lake ecosystems and their response to the present deglaciation process. This general aim was addressed by analysing a cluster of 4 proglacial lakes located in the Central European Alps, in the Ortles-Cevedale Massif (details in Chapter 2). The cluster includes four lakes (referred to in this thesis as the Cevedale proglacial lakes) that formed in recent decades due to the progressive retreat of an Alpine glacier, the Zufallferner/Vedretta del Cevedale. Therefore, the lakes have different age and distance from the glacier terminus and potentially represent a deglaciation chronosequence. The study of deglaciation chronosequences, as proposed by Sommaruga (2015), is a valuable approach to observe the changes in lake ecosystem structure over space and time, and to predict future ecological trajectories following their response to deglaciation. The field survey was complemented by the application of a hydrodynamic model, to generalise the observations about the evolution of the physical habitat in proglacial lakes and to explore the role of different processes.

The specific aims of the study were to:

1. Conduct a comprehensive analysis of the physical, chemical, and biological properties of the Cevedale proglacial lakes.
2. Investigate the key parameters that control the physical habitat of the Cevedale proglacial lakes and examine the seasonal evolution of the physical environment in a proglacial lake (Chapter 3).
   Research questions:
   - How is the physical environment structured in a proglacial lake?
   - How do water temperature and turbidity vary during the ice-free season?
   - How can stratification influence ecological windows of opportunity for benthic primary producers?
3. Characterise the community composition and diversity of benthic diatoms in the Cevedale proglacial lakes and assess their response to deglaciation (Chapter 4).
   Research questions:
   - What is the taxonomic composition of littoral benthic diatom communities in proglacial lakes?
   - How do these communities respond to varying levels of glacial influence?
4. Provide the first survey of the community composition and diversity of prokaryotic and eukaryotic organisms in the Cevedale proglacial lakes and investigate their response to deglaciation (Chapter 5).
   - What is the community composition and diversity of prokaryotic and eukaryotic organisms in the Cevedale proglacial lakes?
   - How do these communities respond to deglaciation?
   - Are benthic primary producers more diverse than planktonic ones in proglacial lakes, and how do they adapt to harsh physical conditions and limited resources?

Chapter 2
Study site and methodological approach

Study site

The study area (626746.125 5146297.011; WGS 84/UTM Z 32 N EPSG:32632) is located in the Ortles-Cevedale Group, in the upper Martell Valley, Autonomous Province of Bolzano/Bozen, Italy, and is included in the territory of the Stelvio National Park, in the Central Alps. The upper Martell Valley is characterised by the presence of several Alpine glaciers in its more elevated portions, and proglacial lakes are frequent features of the landscape (Hofmeister et al., 2022). The climate in the study area is classified as "alpine tundra" in the Köppen-Geiger classification map (Kottek et al., 2006). The rock substrate in the area is characterised by mica schists and paragneiss, which are mainly composed of chlorite and sericite, with frequent intercalation with quartz (ISPRA 2012; Montrasio et al., 2012). The underlying rock is extensively covered by glacial deposits and moraines, formed during the last period of glacial expansion, i.e. the Little Ice Age (Montrasio et al., 2012). The land cover classes in the area are glaciers, rocks, and unvegetated debris areas (Autonomous Province of Bolzano/Bozen, 2005), where primary vegetational succession is occurring (Ramskogler et al., 2023). The highest peaks of the area are Ortles (3905 m a.s.l.), Gran Zebrù (3857 m a.s.l.), and Cevedale (3769 m a.s.l.). According to the New Italian Glacier Inventory (Smiraglia & Diolaiuti, 2015), the 129 glaciers of the Ortles-Cevedale Group cover an area of 72.18 km^2, of which 24 are in Trentino (9.22 m^3), 51 in Lombardia (28.85 m^2), and 54 in Alto Adige (34.38 m^2). Among these glaciers, Zufallferner has an area of 3.39 km^2 (Smiraglia & Diolaiuti, 2015). During the Little Ice Age, Zufallferner was connected with Langenferner (Figure 2. 1a) at their lower extremities, and they separated in the second half of the 19th century (Rabot, 1905). At the end of the 19th century, Zufallferner slightly increased in size and became an ice-dam for the glacial lakes fed by the Langenferner. The rupture of this ice dam caused four sudden floods (also known in literature as Glacier Lake Outburst Flood, GLOF, e.g., Taylor et al., 2023) in 1887, 1888, 1889 and 1891, that profoundly changed the morphology of the valley (Rabot, 1905). To protect the towns of the Martell Valley from the devastating effects of the glacial floods, an artificial dam was built between 1892 and 1893.

According to the most recent annual glaciological surveys of Italian glaciers (Baroni et al., 2022; Baroni et al., 2023; Chiarle et al., 2024), the Cevedale glaciers, including Zufallferner and the adjacent Fürkeleferner (Figure 2. 1 a), are facing an important retreat phase. Zufallferner retreated by 251 m between 2013 and 2023 (Servizio Glaciologico Alto Adige, 2023). In 2023, Zufallferner and Fürkeleferner were still connected under the extensive moraine coverage (Servizio Glaciologico Alto Adige, 2023; Chiarle et al., 2024). The front of Zufallferner was located at an elevation of 2782 m a.s.l. in 2021 (Baroni et al., 2022), 2786 m in 2022 (Baroni et al., 2023), and at 2793 m in 2023 (Chiarle et al., 2024).

Within this area, four proglacial lakes (Figure 2. 1) were analysed in the present study. The Cevedale proglacial lakes are located in a remote area, where human frequentation and direct disturbance are rare. There are no official paths to reach the lakes, and tourism is mostly concentrated in other parts of the upper Martell Valley, such as the nearby Fürkeleferner and the alpinist routes that reach

the glaciers of the Cevedale Massif. The closest structure is a mountain hut, Martellerhütte, located at 2610 m a.s.l. about 1.5 km from the downstream lake.

The lakes formed from the progressive retreat of one of the glacier tongues of the Cevedale glaciers, the Zufallferner/Vedretta del Cevedale (Figure 2. 1a). The portion of the Zufallferner that feeds the proglacial lakes is covered with abundant detritus (Figure 2. 1 b).

The proglacial lakes are located above the timberline on almost barren soil, between 2700 and 2900 m a.s.l., within the upper catchment of the Plima Creek, which is the inlet of the Gioveretto/Zufrittsee reservoir (approximately 6 km downstream from the proglacial lakes). Ice melt and snowmelt dominate the hydrological regime of the Plima catchment, and increases in summer flows are caused by glacier melt (Puspitarini et al., 2020). During winter, the lakes are covered with ice and snow, and are accessible only during the ice-free season, i.e., between July (or end of June) and September/October. The lakes formed progressively during the last decades in the depressions of the proglacial area left by the retreat of Zufallferner. Due to their progressive formation, the lakes are located at increasing distance from the glacier terminus (Figure 2. 1 a, b): only the most recent lake, L1, is still in contact with the glacier ice, while the oldest lake, L3, is also the most distant from the glacier ice. Small surface streams connect the water bodies (Figure 2. 1 b). During the ice-free season, the lakes are mainly fed by glacial meltwater. During the study period, lake L1 was in contact with white glacier ice, was ice-dammed and part of the lake bottom was composed of ice. Lake L2 was in contact with debris-covered ice, at least along its upstream shore. The upstream shore was also covered by a conspicuous sediment delta, composed of fine glacial sediment (supplementary material S2.1). Lake LC was dammed by both moraines and bedrock. Lake L3 was dammed by moraines and was divided into two sub-sections by small moraine ridges that caused a narrowing of the lake area in its central part.

The four lakes developed at different times, following the retreat of Zufallferner (Figure 2. 2). The oldest lake, L3, first formed in contact with the terminus of Zufallferner at least in 1992, when its first part was visible in an orthophoto (Figure 2. 2). In the orthophoto of 2015, lakes L1, L2 and LC were not visible, as their positions were still covered by ice or snow. L2 and LC formed between the summer of 2016 and 2017, with L2 initially in contact with ice. L1 appeared for the first time in summer of 2018. By 2020, all four lakes were fully formed and clearly visible in the orthophoto.

In the early ice-free season 2023 (likely during the last week of June), all water in L1 drained following the collapse of the glacier ice dam (Figure 2. 3), allowing meltwater to flow in the direction of the adjacent glacial stream, fed by the Fürkeleferner. After this event, the depression in front of the right part of Zufallferner was no longer filled with water. Consequently, while in 2022 the proglacial lakes selected for the study were L1, L2 and L3, in 2023 LC was added to the study. In the 2023 orthophoto, only the lakes L2, LC, and L3 are visible (Figure 2. 2).

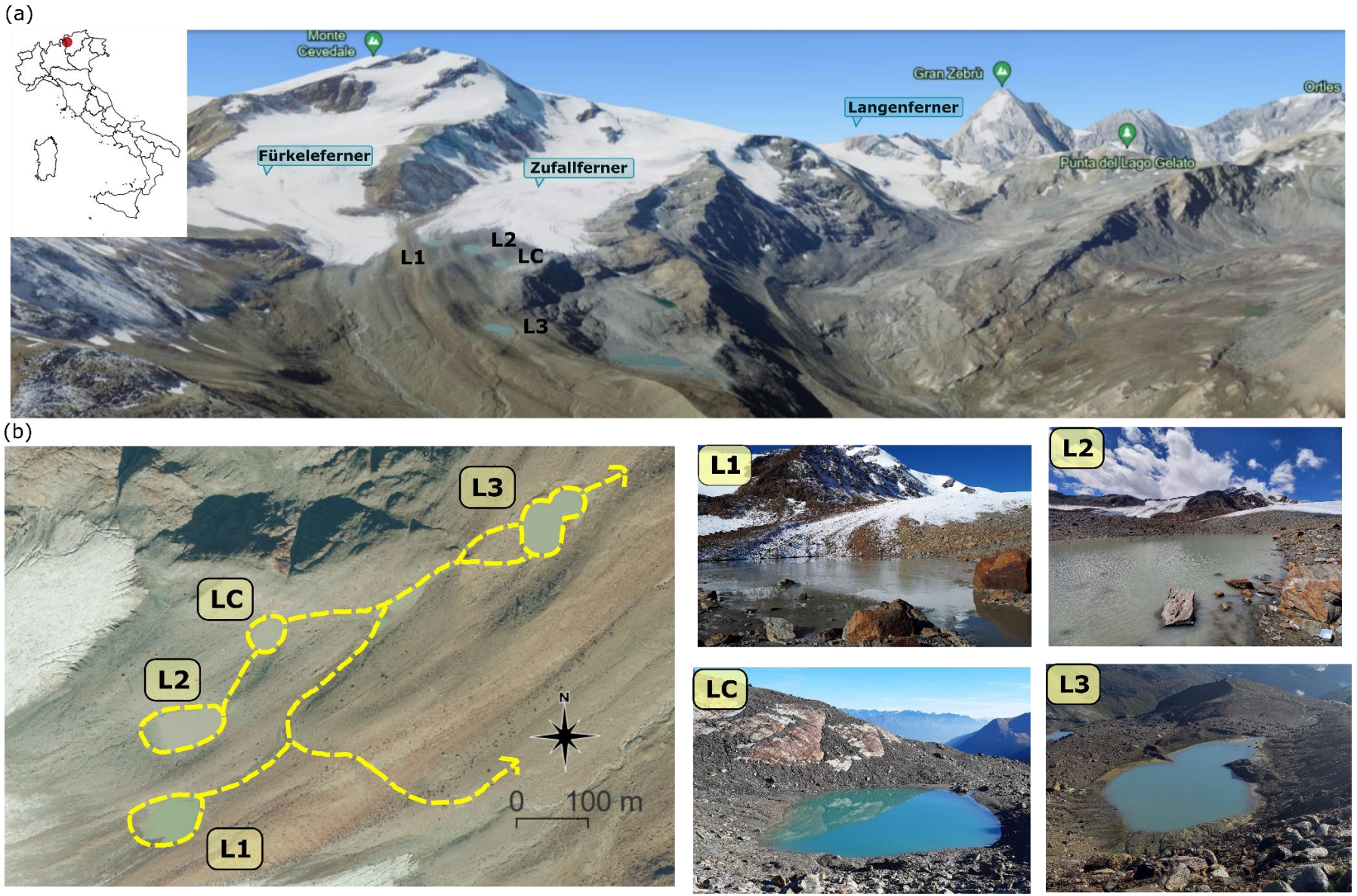

Figure 2. 1. (a) Position of the study site on the Cevedale Massif, in the Upper Martell Valley (from Google Earth). (b) Map of the study area showing the four lakes and the system of superficial streams that connect the lakes (background map: orthophoto 2020, Autonomous Province of Bolzano/Bozen).

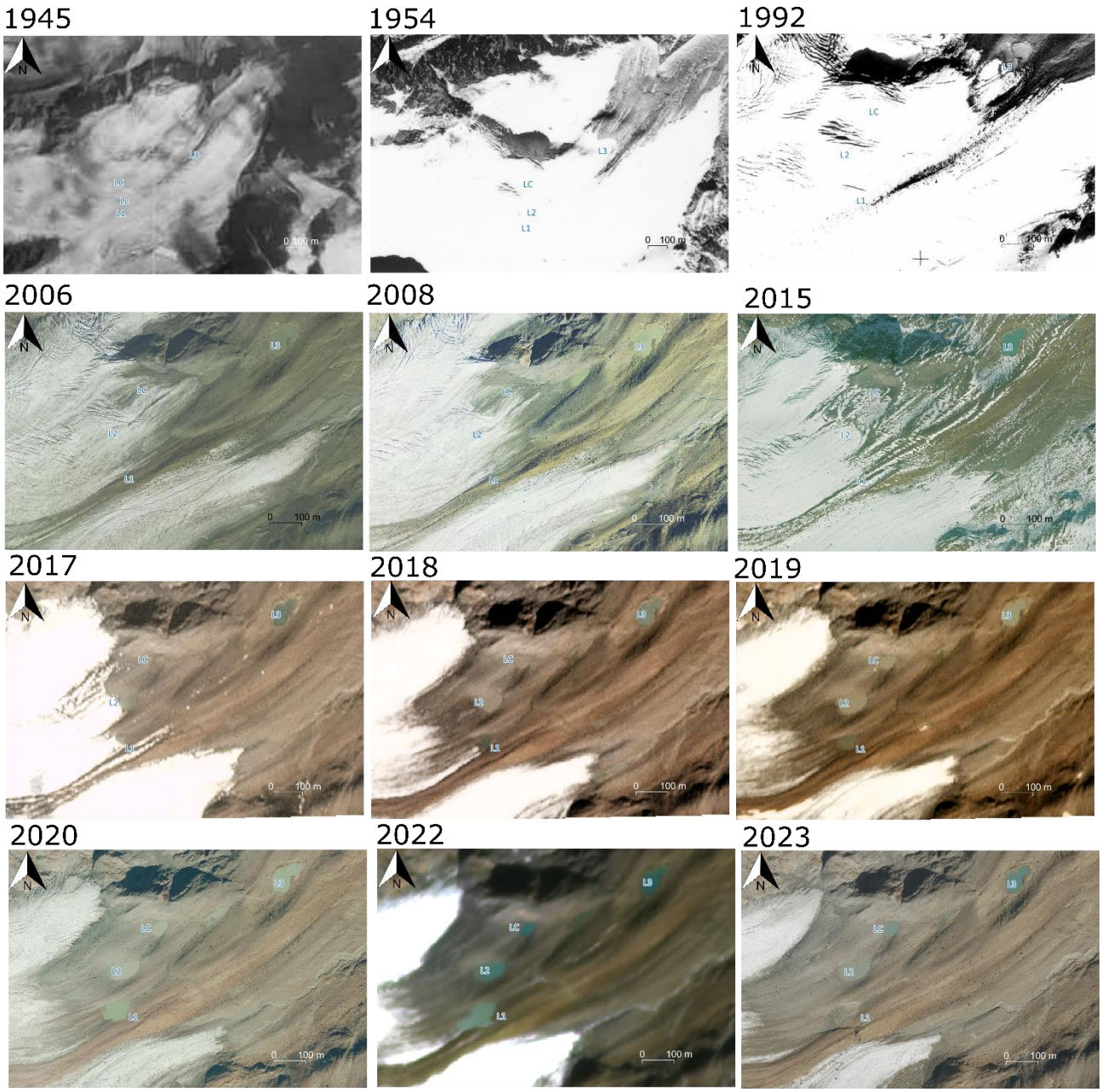

Figure 2. 2. Evolution of the proglacial area around Zufallferner and Fürkeleferner from 1945 to 2023. Note the different scale in images from 1945 and 1954. Sources: 1945, Istituto Geografico Militare Italiano, 1945; 1954, Gruppo Aereo Italiano, 1954; 1992, 2006, 2008, 2015, 2020, 2023, orthophoto Autonomous Province of Bolzano; others, Image ©, 2017, 2018, 2019, 2022, Planet Labs PBC.

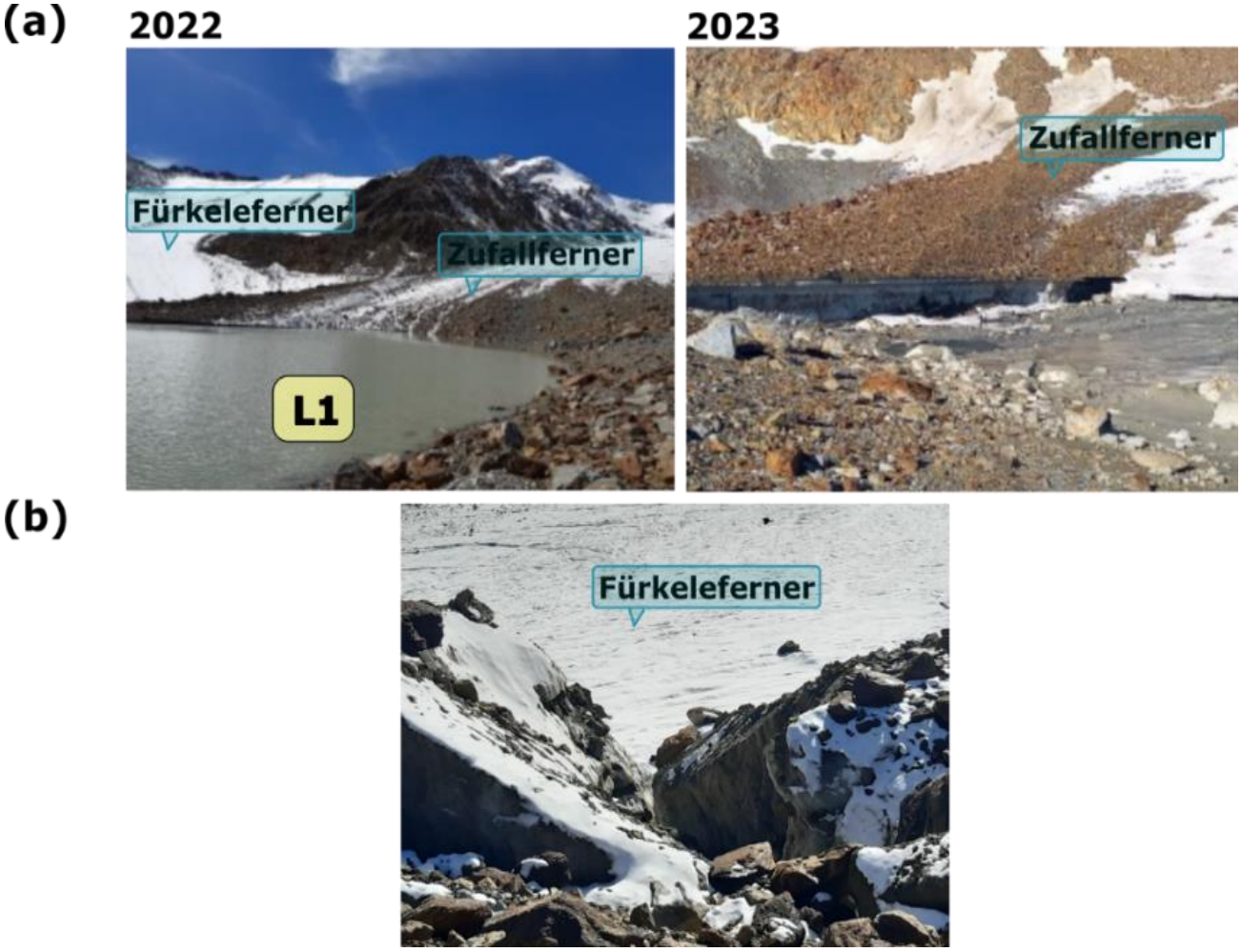

Figure 2. 3. (a) Lake L1 before (13 September 2022) and after (4 July 2023) the dam break and subsequent drainage. (b) Collapsed glacier ice, previously constituting the dam of L1.

The datasets of hydrochemistry and environmental DNA (see next sections) from the four proglacial lakes studied in 2022 and 2023 were integrated with samples collected from the Marmotte Lake, a clear mountain lake (628627.540 5144113.338; WGS 84/UTM Z 32 N EPSG:32632). The Marmotte Lake (Figure 2. 4) is located in the Ortles-Cevedale Group in the upper La Mare Valley (Val de La Mare), in the Autonomous Province of Trento, Italy, at an elevation of 2705 m a.s.l., approximately 2.8 km southeast from the Cevedale proglacial lakes. The lake is currently about 203 m long, 136 m large and 6.5 m deep (Carturan et al., 2021). The geological substrate where this lake is located closely resembles that of the Cevedale proglacial lakes, consisting of Pleistocene glacial deposits overlying a bedrock of mica schists with prevailing chlorite and sericite (ISPRA, 2012). Although the Marmotte Lake has a glacial origin, it no longer receives glacial meltwater. The small Marmotte Glacier (Vedretta Marmotta) occupied the upper portion of the lake catchment until the first half of the 20th century, as reconstructed by Carturan et al. (2021). Vedretta Marmotta completely disappeared around 2003-2007, when the last fragmented glacier remnants melted (Carturan et al., 2021). Today, rock glaciers and permafrost are common in the area (Carturan et al., 2016). Due to the absence of contribution from glacier melt, the water column of Marmotte Lake is highly transparent. The lake shores are composed of coarse sediment (Carturan et al., 2021). The Marmotte Lake was selected because, being once fed by Vedretta Marmotta (Carturan et al., 2021), can represent the possible condition of the proglacial lakes after the complete loss of glacial

influence, in a space-by-time approach. The Marmotte Lake is the closest available clear lake in the Cevedale Massif that can be safely reached.

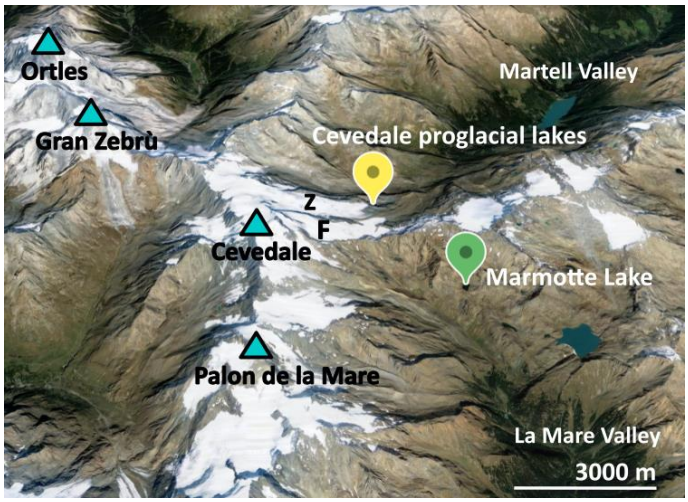

Figure 2. 4. Map of the study area with the location of the Cevedale proglacial lakes (yellow point) and the Marmotte Lake (green point). Light blue triangles indicate the main peaks of the area: Ortles (3905 m asl), Gran Zebrù (3857 m asl), Cevedale (3769 m asl) and Palon de La Mare (3703 m asl). Z and F indicate the sections of the Cevedale glaciers, Zufallferner and Fürkeleferner, respectively. Map: modified from Google Earth, retrieved 21 March 2025, from https://www.google.com/earth.

Methodological approach

The study of the Cevedale proglacial lakes was structured by adopting a multidisciplinary approach, coupling physical, chemical and biological analyses. Physical data, i.e., water temperature, electrical conductivity, light intensity and lake surface level, were monitored by installing dataloggers in the littoral area and the water column of the proglacial lakes. Furthermore, specific measures were acquired targeting the discharge of lake outlets, lake bathymetry, and the granulometric characterisation of littoral sediments. Chemical and biological samples were collected during three dedicated field campaigns each year, to characterise the conditions found in different stages of the Alpine summer, i.e., snow melt in early summer, glacier ablation in mid-summer, and flow recession in early autumn. The samples and data collected in the two seasons, 2022 and 2023, are listed in Table 2. 1. Hydrochemistry data from the Marmotte Lake were available for September of both 2022 and 2023, while eDNA samples (plankton, sediment, and littoral periphyton) were collected in September 2023.

Table 2. 1. Data and samples collected for the present study, in 2022 and 2023.

Measure	2022			2023				Method
	L1	L2	L3	L2	LC	L3	MA	
Water temperature - littoral	x	x	x	x	x	x	x	dataloggers + field probes
Water temperature - vertical profiles				x		x		dataloggers (buoys)
Electrical conductivity	x	x	x	x	x	x	x	dataloggers + field probes
Lake level		x	x	x		x		dataloggers
Discharge measurements		x	x	x		x		salt dilution method
Hydrochemistry	x	x	x	x	x	x	x	water samples and lab analyses (FEM laboratory)
Trace elements	x	x	x	x	x	x	x	water samples and lab analyses (eco-research laboratory)
Suspended solids water column	x	x	x	x	x	x	x	water samples and lab analyses
Biofilm organic content	x	x	x	x	x	x	x	biofilm samples and lab analyses
Biofilm Chlorophyll - a	x	x	x	x	x	x	x	biofilm samples and lab analyses
Benthic diatoms	x	x	x	x	x	x	x	biofilm samples and lab analyses
eDNA	x	x	x	x	x	x	x	plankton, biofilm, sediment samples and lab analyses

The physical habitat of the lakes was characterised by integrating field data and a modelling approach, detailed in Chapter 3.

In the littoral area of the lakes, diatom samples were collected to determine density and taxonomical composition of benthic diatom communities. Further methodological details are provided in Chapter 4.

Other components of biological communities inhabiting the lakes were analysed through the metabarcoding approach on environmental DNA samples. Water, biofilm and sediment samples were analysed, targeting the 16S (prokaryotes) and 18S (eukaryotes) rRNA genes (Chapter 5).

In the next sections of this chapter, the general description of lake morphology, sediment characterisation, and hydrochemistry are provided. These data were used also in the following chapters.

Lake morphology

Bathymetric data were collected on 13 and 14 September 2022 for three of the lakes, L1, L2 and L3. Measurements were taken with a Fish Deeper Chirp+ sonar (Deeper, UAB) acquiring depth and water temperature data 15 times per second, and the GPS position at 1-second intervals. The sonar was mounted on a floating platform, which was moved from one of the lake shores towards the opposite one with ropes. A zig-zag trajectory was followed to cover the lake surface, resulting in 14 transects for L2 and 20 for L3. Due to difficult accessibility along the shores and unfavourable meteorological conditions, only 6 transects could be measured at L1, covering about one half of its bathymetry. The final lake bathymetries were derived by interpolating the point measurements into a raster map using the Triangular Irregular Network method (Figure 2. 5). Bathymetric data were used to compute the lake surface area and the lake volume.

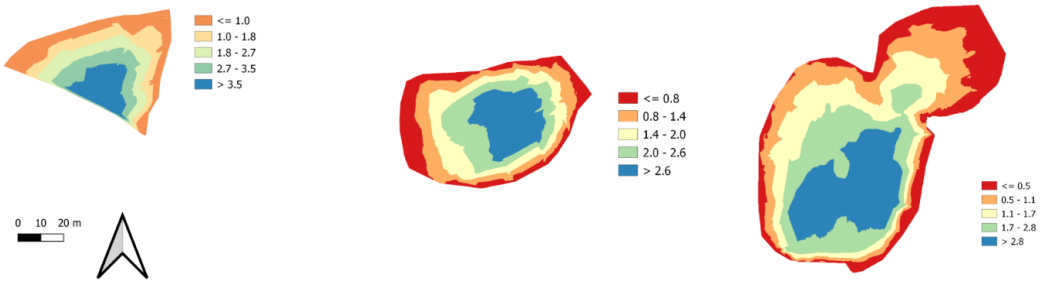

Figure 2. 5. Lake bottom profiles of L1, L2 and L3 (September 2022).

To complement the bathymetric estimates, available remote sensing data were used for comparison (orthophoto 2020, Autonomous Province of Bolzano/Bozen). The contours of the four lakes in the orthophoto 2020 (Autonomous Province of Bolzano/Bozen, 2020) were drawn as polygons with the geometrical tools of QGIS 3.22.14, and the area of each polygon was computed. This approach also allowed the estimation of the area of LC, which was not covered by the field measurements, and to obtain a more complete estimate of the area of L1. For L2, remote sensing estimate was 725.8 m^2 larger than the bathymetric estimate (total area = 4996.3 m^2). In this case, the significant discrepancy is due to the inclusion of the sediment delta in the remote sensing analysis, which was not captured in the field measurements.

The main morphological characteristics of the Cevedale proglacial lakes are summarised in Table 2. 2. Areas of L1 and LC are those estimated from orthophoto 2020, while areas of L2 and L3 are those estimated from bathymetric data.

Table 2. 2. Identification codes and main morphological characteristics (where available) of the analysed lakes. Area estimates for L1 and LC are those measured from orthophoto 2020, for L2 and L3 are those obtained from bathymetric data.

ID	Distance from glacier terminus (m)	Maximum depth (m)	Area (m^2)	Volume (m^3)
L1	0	4.45	4337.3	5526.9
L2	100	2.95	4270.5	7149.4
LC	350	-	1792.3	-
L3	750	4.66	4481.0	7098.9

Lake hydrochemistry and habitat characteristics

During each field campaign in 2022 and 2023, water samples were collected for chemical analyses. Samples were collected in 500 mL polyethylene bottles and preserved at 4°C and in the dark until the analyses, performed at the Hydrochemistry laboratory of the Edmund Mach Foundation according to standardised methods (APHA-AWWA-WPCF, 2017). Analyses addressed turbidity (NTU), pH, electrical conductivity (µS/cm) at 20°C, alkalinity (mg $CaCO_3$/L), concentration of major ions (CO_3^-, Ca^{2+}, Mg^{2+}, Cl^-, Na^+, K^+, SO_4^{2-}, mg/L), nutrients, i.e., total nitrogen TN, NH_4^+- N, NO_3-N (µg/L), total phosphorus TP, soluble PO_4-P (µg/L) and SiO_2 (mg/L). Lake water was also analysed

addressing the concentration of trace elements: 100 mL water samples were filtered through cellulose acetate membranes (0.45 µm) and acidified with 1-1.5 mL of 65% HNO_3. The determination of the content of 24 trace elements was performed by the Ecoresearch S.r.l. laboratory (Bolzano) using a ICP-MS ICAP-Q Thermo Fischer analyser, and addressed concentrations of Be, B, Na, Mg, Al, K, Ca, Ti, V, Cr, Mn, Fe, Co, Ni, Cu, Zn, As, Se, Rb, Sr, Mo, Ag, Cd, Sn, Sb, Ba, Tl, Pb, U, Bi, P (µg/L).
The concentration of suspended solids in the water column of the lakes, divided into organic and inorganic components, was measured by filtering water samples *in situ* (Figure 2. 6) in six sampling occasions (for each month of the ice-free seasons): 24-25 June 2022, 1-2 August 2022, 12 September 2022, 4-5 July 2023, 31 July-1 August 2023, and 26-27 September 2023.

Figure 2. 6. Filtration of water samples in situ for the determination of the concentration of suspended solids in the water column.

Water samples (volume 250-1000 mL) were collected from the surface layers of the water column (20-30 cm depth), from the littoral area. Water was passed through previously calibrated GF/C Whatman glass microfiber filters with 1.2 µm porosity. Filtration was protracted until the filter clogged. Filters were stored in aluminium foils and frozen at temperature below -20°C until laboratory analyses. Filters were oven-dried for 1 hour at 110 °C, followed by 1 hour at 550 °C in a furnace (loss on ignition method, Steinmann et al., 1996). The total dry mass of suspended matter was obtained as the net mass retained in the filter after the treatment at 110°C divided by the filtered volume (TSS in Figure 2. 7, mg/L). After burning the organic matter at 550 °C, the inorganic (ISS in Figure 2. 7, mg/L) and organic (OSS in Figure 2. 7, mg/L) fractions in the sample were obtained as the difference between total dry mass and ashes mass.
The organic content of littoral biofilms (periphyton) was determined in the same six sampling occasions. A known area of biofilm was collected with a clean toothbrush from littoral substrata such as pebbles and cohesive sediment. The reference area was delimited with a nitrile frame (1.5 x 1.5 cm^2), and up to 5 replicates were collected. The total brushed area was dependent on biofilm thickness and the accumulation of mineral sediment on the substrata. The collected material was integrated, dispersed in a small amount of water and passed through previously calibrated GF/C Whatman glass microfiber filters with a fine nominal particle retention of 1.2 µm. Filters were preserved in aluminium foils, frozen as soon as possible and preserved at -20 °C under dark conditions until laboratory analyses, which included the same steps as for the determination of

water suspended solids (Steinmann et al., 1996). The dry mass per unit area (biofilm in Figure 2. 7, g/m^2) was estimated as the net mass retained in the filter after the treatment at 110° divided by the brushed area. The organic content (org_biofilm in Figure 2. 7, g/m^2) was finally computed as the difference between the total dry mass and the ashes mass (ash_biofilm in Figure 2. 7, g/m^2), measured as the net mass retained in the filter after the ignition at 550°C.
During the same sampling campaigns, the content of chlorophyll *a* (Chla-*a*) of littoral biofilms, i.e., periphyton, was determined. Biofilm samples were collected from lake littoral areas by brushing a known area of biofilm, delimited with a nitrile frame. The sampled material was passed through GF/C filters. The filters were preserved in aluminium foils, frozen as soon as possible, and preserved at -20 °C under dark conditions until laboratory analysis. Laboratory analysis was performed in two consecutive days following standardised protocols (Lorenzen, 1967; Hauer & Lamberti, 1996). Algal pigments were extracted from the filters overnight in 90% acetone. After filtering the extract through GF/F Watman filters (pore size 0.7 µm), the absorbance of the extract at 664, 665 and 750 nm was measured with a spectrophotometer before and after acidification with HCl 1N. The chlorophyll *a* per unit area was computed as:

$$Chl - a = \frac{26.7\ (Abs664_b - Abs665_a)\ V_{ext}}{A_s\ L}, \tag{2.1}$$

where $Abs664_b$ is the extract absorbance at 664 nm before acidification, $Abs665_a$ is sample absorbance at 665 nm after acidification, V_{ext} is the volume of acetone used for the extraction (20 mL), A_s is the biofilm sampled area (cm^2) and L is path length of the cuvette (5 cm).

The main chemical and physical properties measured in the Cevedale proglacial lakes are shown in Figure 2. 7. The variables that showed statistically significant differences among the Cevedale proglacial lakes (Kruskal-Wallis test, $p < 0.05$) were water temperature (Tw), suspended solids in the water column (both TSS and ISS), total phosphorus (TP) and silica (SiO_2).

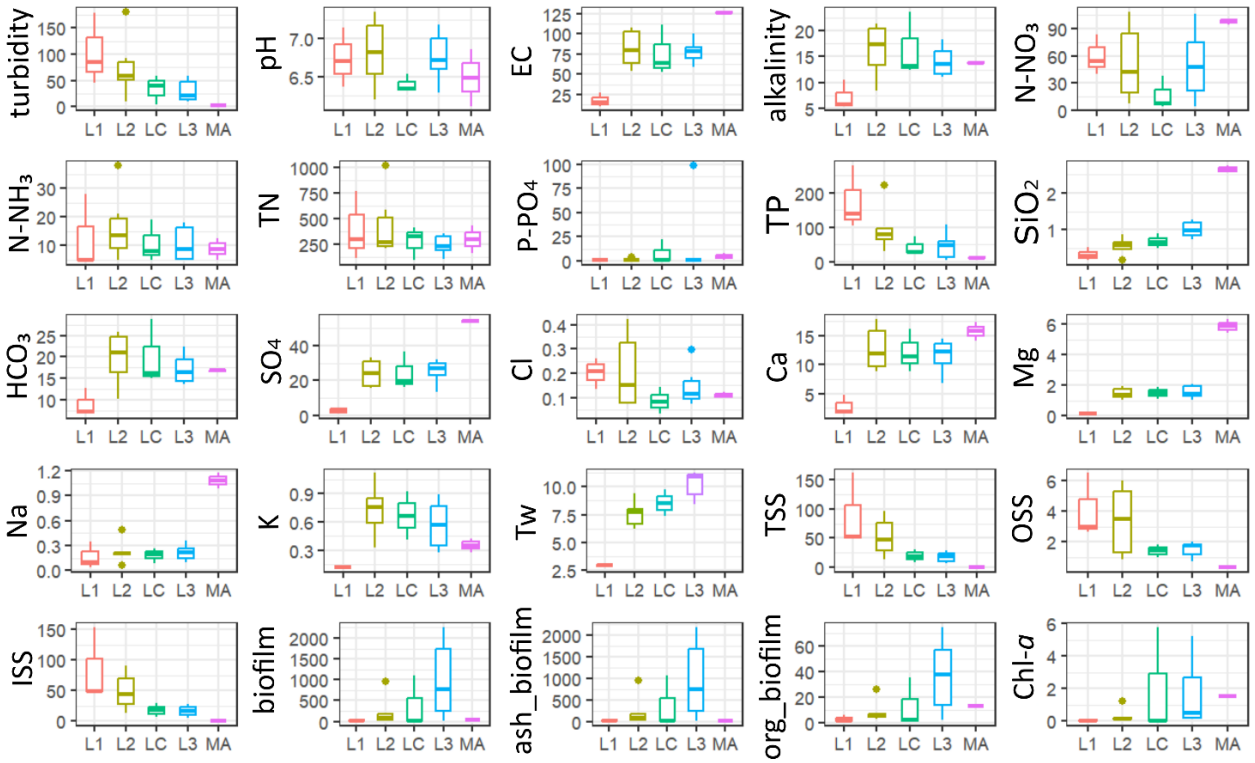

Figure 2. 7. Environmental parameters measured in the Cevedale proglacial lakes and the Marmotte Lake. Units are specified in the text. Tw = water temperature (°C). L1, L2, LC, L3 = Cevedale proglacial lakes; MA = Marmotte Lake.

Turbidity and the concentration of suspended solids in the water column (TSS) decreased progressively from ice-contact to ice-distal and clear conditions, leading to a corresponding decrease in turbidity. Conversely, water temperature (Tw) exhibited an increasing trend from ice-contact to ice-distal lakes, with L1 being the coldest and L3 the warmest.

The pH of the studied lakes was generally circumneutral to slightly acidic. The lowest pH value was recorded in the Marmotte Lake, MA (pH = 6.11 in September 2022), while the highest was observed in L2 (pH = 7.32 in September 2022). Electrical conductivity (EC) was higher in Marmotte Lake (mean = 126.1 µS/cm) compared to the Cevedale proglacial lakes (average = 68.8 µS/cm). Among the Cevedale lakes, L1 exhibited the lowest conductivity (mean = 14.79 µS/cm), while L2, LC, and L3 had similar conductivity values (mean = 81.7, 75.7, and 77.9 µS/cm, respectively).

Regarding nutrient concentrations, total phosphorus (TP) was highest in L1 (mean = 174.13 µg/L) and lowest in MA (mean = 11.43 µg/L). Total nitrogen (TN) was more concentrated in L2 (mean L2 = 428 µg/L). Soluble reactive nitrogen ($N\text{-}NH_3$, $N\text{-}NO_3$) and phosphorus ($P\text{-}PO_4^{3-}$) concentrations were consistently low across the entire proglacial lake system, as well as in the Marmotte Lake. The highest concentrations of TP were found in L1 (104-280 µg/L), gradually decreasing in distal lakes (5-60 µg/L in L3). Within total phosphorus, the particulate fraction predominated, contributing 99% of TP in L1, 93-99% in L2, 21-99% in LC, and 9-98% in L3. These findings are consistent with previous studies reporting extremely low concentrations of soluble phosphorus in glacier-fed freshwaters (Rinke et al., 2001; Uehlinger et al., 2010; Robinson et al., 2016). On the other hand, the particulate fraction of phosphorus is produced by the erosion of sediment and bedrock by the movement of the glacier and is likely less available for photosynthetic organisms (Ren et al., 2019). In absence of the erosive activity of the glacier, in the samples from MA particulate phosphorus had substantially

lower concentrations than in the proglacial lakes (on average 11 µg/L in MA, 83 µg/L in the proglacial lakes).

Silica (SiO_2) concentrations showed an increasing trend from L1 to L3, and MA had the highest mean concentration (mean proglacial = 0.33 mg/L, mean Marmotte = 2.65 mg/L). In L2, SiO_2 concentrations dropped to 0.5 mg/L in the samples collected both in August 2022 and 2023, likely due to dilution from increased meltwater inflow discharge during the period of glacier ablation. A similar seasonal trend, with a decrease in silica concentration in August, was observed also in LC in August 2023 and in L3 in both 2022 and 2023.

Finally, biofilm organic content (org_biofilm) increased from L1 to L3, as well as chlorophyll-*a* concentrations, reaching their peak in L3.

Trace elements

The concentrations of the most relevant trace elements measured in the analysed lakes are shown in Figure 2. 8. Trace elements with concentrations below the sensitivity of the instruments were not considered in the dataset. Nickel (Ni), Strontium (Sr) and Barium (Ba) differed significantly between lakes (Kruskal-Wallis test, $p < 0.05$). Specifically, Nickel decreased from L1 (4.2-7.3 µg/L) to MA (0 µg/L). In L3, the concentration of Ni was higher in 2022 (2.9-5.3 µg/L) than in 2023 (1.1-2.8 µg/L). The contribution of L1 to L3 during the season of 2022 likely increased the concentration of Ni in L3 in 2022, suggesting a local origin of this element. Strontium showed an increasing trend from L1 to MA, and, similarly, Barium was higher in the distal lakes than in L1, while the concentration in MA was more similar to L1. Manganese showed a decreasing, although not statistically significant, trend from L1 to L3. The highest value of Mn, 52.2 µg/L was measured in L1 at the end of June 2022 and exceeded the limits of concentration for human consumption according to Italian laws (50 µg/L). Sr, Li, Ba and Al, together with the sum of the concentrations of all trace elements, showed significant correlations with electrical conductivity (Spearman rho > 0.5, $p < 0.05$).

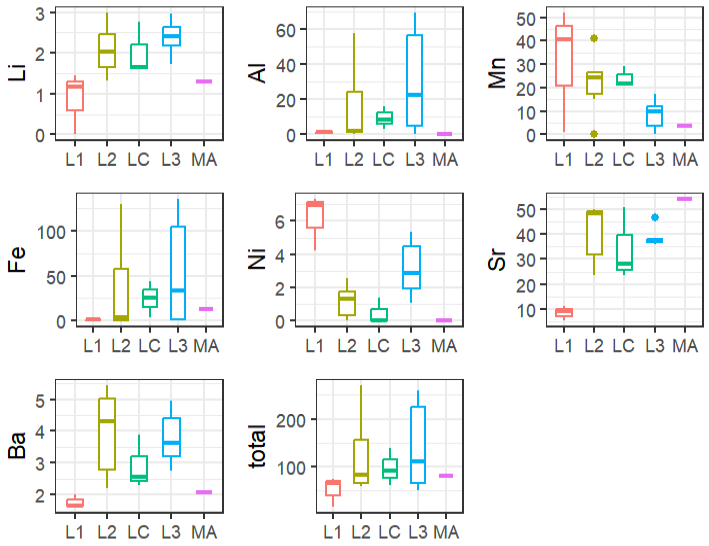

Figure 2. 8. Concentrations of trace elements (µg/L) in the Cevedale proglacial lakes and in the Marmotte Lake. Total = sum of the concentrations of all trace elements in the sample. Only trace elements with concentrations higher than the sensitivity of the instruments are shown.

Sediment characterisation

The sediment deposited on the shore of lake L2 was characterised in terms of grain-size distribution. We collected one integrated sediment sample from the lake shore in the upstream part of L2 in June 2022. The grain size composition of the sample was determined by sieving and sedimentation according to standardised protocols (UNI EN ISO 17892-4:2017), at the Geotechnical Laboratory of DICAM. Gravel and sand fractions were separated from the finer components by sieving the sample. Sieving was performed also by rinsing the sample with distilled water, to separate small particles attached to the surface of gravel and sand grains. Gravel and sand particles represented respectively 0.45% and 10% of the sample mass. The remaining material (grain size < 75 µm) was used for the sedimentation analysis. The material was divided into two subsamples that were analysed separately: subsample "A" was treated with a dispersant agent (sodium hexametaphosphate) that prevents flocculation of sediment particles; subsample "B" was not treated.

The two grain size distributions obtained in the experiment are shown in Figure 2. 9. Subsample A represents the actual grain size composition of the sample, where clays make a relevant portion of the suspended material (26%), and silts represent the 64%. This observation is consistent with literature referring to analogous glacial lake environments, where clay and fine silt are the predominant grain sizes of the suspended sediment (Smith, 1978; Chikita, 1999; Sommaruga & Kandolf, 2014). On the other hand, the experiment without the dispersant is more representative of the real behaviour of the grains in a water column. Specifically, subsample B is composed of 90% silt, indicating that clays in the water column flocculate, thereby exhibiting an increased sedimentation velocity. The aggregation of clay in flocs can occur also in absence of organic material as observed in the glacier-fed Lillooet Lake (Hodder, 2009).

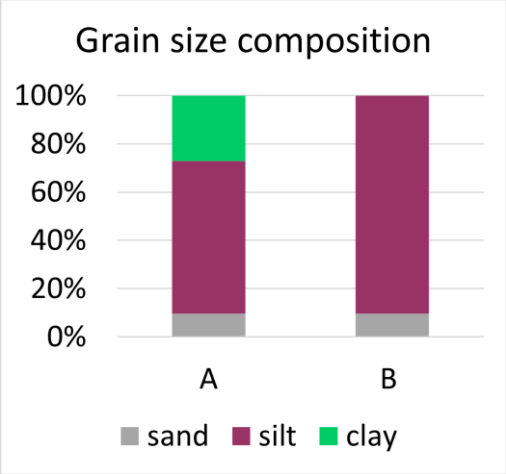

Figure 2. 9. Grain size composition of the sediment sample collected from L2 in June 2022, obtained with (A) and without (B) adding the dispersant.

Chapter 3
Stratification dynamics and implications for proglacial lake habitats

Introduction

Alpine proglacial lakes represent unique aquatic ecosystems that significantly influence the characteristics of high-altitude catchments. Their influence is particularly strong on downstream water temperatures (Uehlinger et al., 2003), turbidity, and sedimentation dynamics (Otto, 2019). Their thermal characteristics are distinct from those of clear, non-glacier-fed high mountain lakes, as proglacial lakes are typically polymictic (Peter & Sommaruga, 2017). Also, they are more turbid (Irwin, 1974; Tiberti et al., 2020), a characteristic that profoundly influences the ecosystem structure by imposing strong selective effects on planktonic biota (Sommaruga, 2015). The dispersal patterns of fine suspended sediment, also called "glacial flour", is strongly influenced by density stratification within the lake (Ashley, 2002). These physical dynamics, particularly the density differences between inflowing meltwater and lake water, play a crucial role in shaping habitat conditions in the surface layers of proglacial lakes and in littoral areas. As recently pointed out by Hardmeyer et al. (2024), small-scale studies on Alpine proglacial lakes are quite rare and rarely consider seasonal patterns (e.g., Masetti et al., 2010; Peter & Sommaruga, 2017).

Studies on glacier-fed streams show that benthic algal growth during the Alpine summer is concentrated in specific periods, called "Windows of Opportunity" (WOs, Uehlinger et al., 2010), mainly occurring in periods of reduced glacial runoff, i.e., autumn. In the euphotic zone of the littoral area of proglacial lakes, local conditions can allow periphyton growth (e.g., cyanobacteria, Mez et al., 1998). However, the timing of occurrence of WOs in glacier-fed lakes, and the influence of stratification patterns on their occurrence, have not previously been addressed (to the best of our knowledge). Understanding how the physical habitat evolves throughout the ice-free season, and the subsequent effects on ecological processes such as periphyton growth, is critical for a complete characterisation of proglacial lake ecology.

This chapter aims to describe the physical habitat of the Cevedale proglacial lakes, focusing on seasonal variations and their ecological implications. The first section analyses data and field observations collected during field campaigns in the ice-free seasons of 2022 and 2023; the second section integrates these data into a modelling approach to provide a more detailed interpretation of the physical dynamics in one of the lakes (L2). Specifically, the following questions are addressed: (i) How is the physical environment structured in the Cevedale proglacial lakes, and how does it evolve seasonally? (ii) How do stratification patterns control ecological Windows of Opportunity for periphyton growth?

Methods

Field data

Field measurements were performed in the Cevedale proglacial lakes over the two ice-free seasons of 2022 and 2023, by installing sensors for continuous data acquisition and with field measurements. Sensors for water temperature (Tw) (HOBO UA-002-08/UA-002-64 Pendant Temperature/Light Data Logger) and electrical conductivity (EC) (HOBO U24-001 Freshwater Conductivity Loggers) were deployed on lake shores. Figure 3. 1 shows the position of the gauging stations; information on the installed data loggers is detailed in Table 3. 1. In lakes L2 and L3, water level was monitored by installing a pressure transducer (Keller AG Messtechnik, Switzerland) in the littoral area, as far from the shore as it was possible to safely reach. The pressure transducer recorded the difference between a submerged pressure sensor and a subaerial sensor at a 10-minute interval.

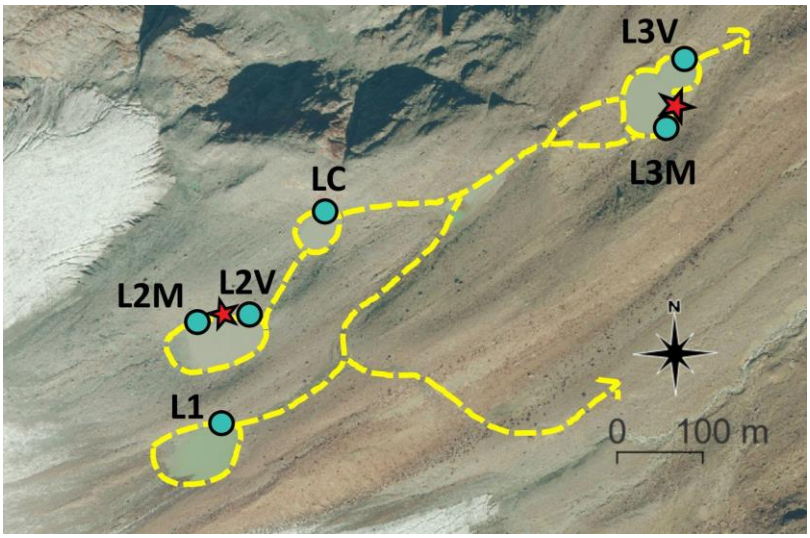

Figure 3. 1. Position of the gauging stations installed at the Cevedale proglacial lakes in 2022 and 2023. Stars represent pressure sensors; circles represent temperature/conductivity stations (for details, see Table 1). Background map: orthophoto 2020, Autonomous Province of Bolzano/Bozen (https://geonetwork1.civis.bz.it).

Table 3. 1. Dataloggers installed in the Cevedale proglacial lakes in 2022 and 2023. The position of the gauging stations is shown in Figure 3. 1. Tw = water temperature, measured in the littoral area and in water column, EC = electrical conductivity, Light = light intensity.

Lake	L1		L2				LC		L3			
Station	**L1**		**L2M**		**L2V**		**LC**		**L3M**		**L3V**	
Season	2022	2023	2022	2023	2022	2023	2022	2023	2022	2023	2022	2023
Tw – littoral	x		x	x	x	x		x	x	x	x	x
EC						x		x		x		
Tw - column				x		x				x		
Light - column				x						x		
Water level			x						X			

In addition, vertical temperature profiles were collected in L2 and L3 between 1 August and 25 September 2023. For this purpose, three chains of temperature data-loggers (MX2202 Pendant - Water Temperature/Light Bluetooth Data Logger and Water Temperature Pro v2 Data Logger, HOBO©, Germany) were installed: two chains in L2, in the upstream (L2M) and downstream (L2V) part of the lake, and one in L3, in the central part. Sensors were secured at 5 fixed depths (i.e., 0,

0.2, 0.4, 0.8, 1.6 m; distances measured starting from the bottom of the immersed part of the buoy, which was approximately 0.05-0.1 m below the water surface) to a rope attached to a buoy and to a weight, as shown in Figure 3. 2. All sensors acquired data every 10 minutes.
Thermal differences between the upstream and downstream parts of L2 were calculated as the difference between the water temperature registered in the downstream buoy and the water temperature registered in the upstream buoy, in each layer.
Starting from water temperature data, the stability of the thermal stratification was quantified by computing the Schmidt stability (Schmidt, 1928; Idso, 1973) for each location where the temperature profiles were measured. The Schmidt stability quantifies the resistance to mechanical mixing of the water column as the amount of work required to make the water column uniformly dense. Calculations were performed by using the Lake Analyzer program (Read et al., 2011) in Matlab version 9.13.0 (The MathWorks Inc., 2022). The obtained time series of Schmidt stability were compared among locations with pairwise comparisons, computing the non-parametric Mann-Whitney test in R version 4.3.2 (R Core Team, 2023).
Sensors installed in the upstream part of L2 and in L3 also included light intensity measurements in units of lumens/ft^2 (lux). Sensors (MX2202 Pendant - Water Temperature/Light Bluetooth Data Logger, HOBO©, Germany) detected light intensity in a wavelength range between 400 and 700 nm, thus covering the spectrum of the Photosynthetically Active Radiation (PAR). Light and temperature data were also integrated in the modelling approach, for model calibration and validation.

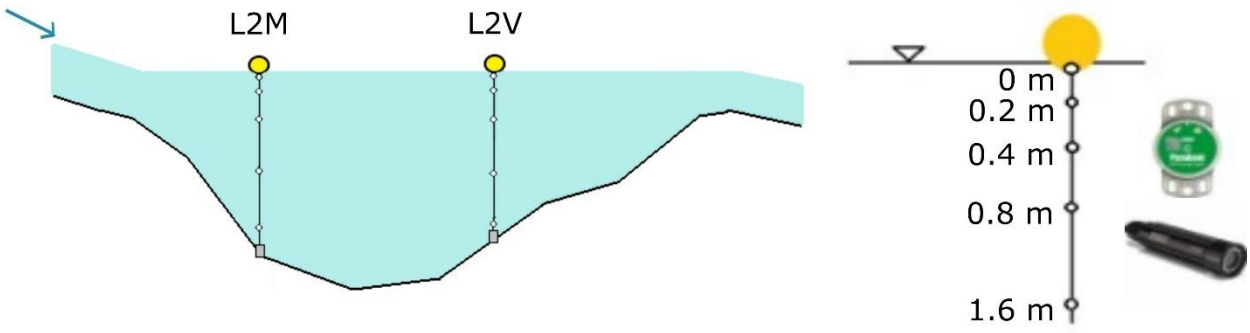

Figure 3. 2. Schematic representation of the chains of thermistors in L2. L2M = upstream; L2V = downstream.

Water light extinction coefficients were calculated based on light intensity measurements according to the Beer-Lambert law:

$$I(z) = I_0 \ e^{-kz}, \tag{3. 1}$$

where $I(z)$ is light intensity at the depth z, I_0 is light intensity at the surface, k is light extinction coefficient, and z is depth. A linear model was fitted to the logarithm of light intensity data versus depth, where the slope of the fitted line is the negative value of the extinction coefficient.
The Secchi disk depth was then estimated by applying, as a first approximation, the relationship originally proposed by Poole & Atkins (1929) and adopted in several models:

$$k \cdot SD = 1.7, \tag{3. 2}$$

where SD is the Secchi disk depth [m] and k is the light extinction coefficient of water [m^{-1}].

The concentration of suspended solids in the lake surface layers was determined by adopting the loss on ignition method, as described in Chapter 2, in six sampling occasions (for each month of the ice-free seasons), representing the main hydrological stages of the Alpine glacial summer, characterised by prevailing snowmelt, ice melt, and base flow.

Modelling

Physical dynamics were further investigated in the L2 lake, by integrating field data analysis and a modelling approach. The model used is the CE-QUAL-W2 model (version 4.5, Wells, 2023a; b), a laterally averaged two dimensional, hydrodynamic and water quality model. Based on the water temperature data observed in the lake, the vertical stratification patterns and their spatial and seasonal evolution were studied. The choice of a laterally averaged 2D model is driven by the need to represent both the longitudinal and the vertical thermal structure observed in the lake, while the lateral variability plays a minor role. Water temperature and the concentration of inorganic suspended solids were simulated in the ice-free seasons of 2022 and 2023, as the main drivers of the evolution of the lake habitat. To run the model, geometric data (bathymetry) and boundary conditions such as meteorological data and inflow and outflow discharges were provided. The model parameters were calibrated using water temperature data collected *in situ*, as described in the following sections.

Bathymetry and computational grid

Bathymetric measurements were performed with a Fish Deeper Chirp+ sonar (© 2023 Deeper, UAB) on 14 September 2022, and the lake bottom profile was obtained from the bathymetric measurements, as described in Chapter 2. Bathymetric data were processed in QGIS 3.22.14 to obtain the final computational grid (2D, laterally averaged, with one main horizontal axis x and vertical axis z), as described in Cole & Wells (2023). Polygon and line vector files were drawn to apply the qgis-cequalw2-bath plugin (https://github.com/WQDSS/qgis-cequalw2-bath/wiki). The final computational grid (Figure 3. 3) is composed of 51 segments along the longitudinal direction and 34 layers along the vertical. Each layer is 0.10 m deep.

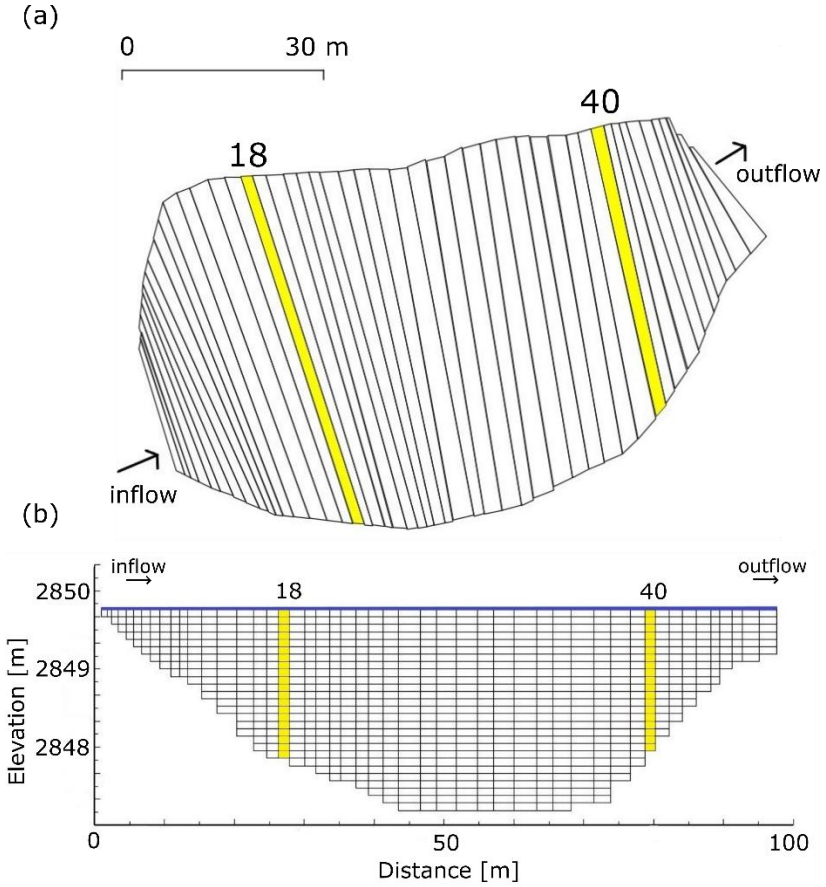

Figure 3. 3. Computational grid used to apply the CE-QUAL-W2 model to the L2 lake. (a): subdivision of the lake surface area into segments (plan view); (b): transect x-z showing segments (along the horizontal axis) and layers (along the vertical axis). The highlighted segments, 18 and 40, correspond to the position of the buoys.

Meteorological conditions

Meteorological forcing was obtained from meteorological data provided by the Autonomous Province of Bolzano/Bozen and eurac research (http://meteobrowser.eurac.edu/). Air temperature, wind velocity, wind direction and relative humidity are those observed at the closest meteorological station available (Figure 3. 4), i.e., Sulden-Madritsch station (2825 m a.s.l., 4.8 km NW from L2). The closest station measuring solar radiation is the Hintermartell station (1720 m a.s.l., 8.7 km NE from L2). Precipitation was also included in the interpretation of data and simulations. Precipitation data came from the Sulden station (1907 m a.s.l., 7.9 km NW from L2).

Figure 3. 4. Map showing the position of the meteorological stations with respect to the Cevedale proglacial lakes. Background map: Google Earth.

Dew point T_d was calculated as:

$$T_d = T_a - \left(\frac{100 - RH}{5}\right), \tag{3. 3}$$

where T_a is air temperature [°C] and RH is relative humidity [%]. Cloud cover was obtained at daily frequency as the ratio between the solar radiation and the maximum measured solar radiation in the reference month, on a daily basis. Given the position of the Madritsch meteorological station (Figure 3. 4), wind direction is affected by a large uncertainty. Indeed, the complex orography of the high mountain landscape makes wind conditions very variable and wind directions can be quite different even in two adjacent valleys. Moreover, the wind at lake L2 is affected by the presence of the glacier, a condition that does not exist at Madritsch station. Therefore, different wind scenarios were analysed, according also to the available scientific knowledge on glacier winds, and a sensitivity analysis was conducted to select the most representative forcing for lake L2's hydro-thermal dynamics.

Outflow and inflow discharge

Water discharge measurements were performed at the outlet of L2 under different flow conditions using the salt dilution method (Gordon et al., 1992). The flow rating curve was reconstructed by fitting the outflow discharge, Q_{out} [m^3/s], as a function of the water level measured in the lake, h [m] (Figure 3. 5 a), using a power law (Figure 3. 5 b). The regression curve allowed us to extrapolate the outflow discharge time series as a function of lake level. To avoid unrealistic values, the maximum outflow discharge was fixed at 0.15 m^3/s.

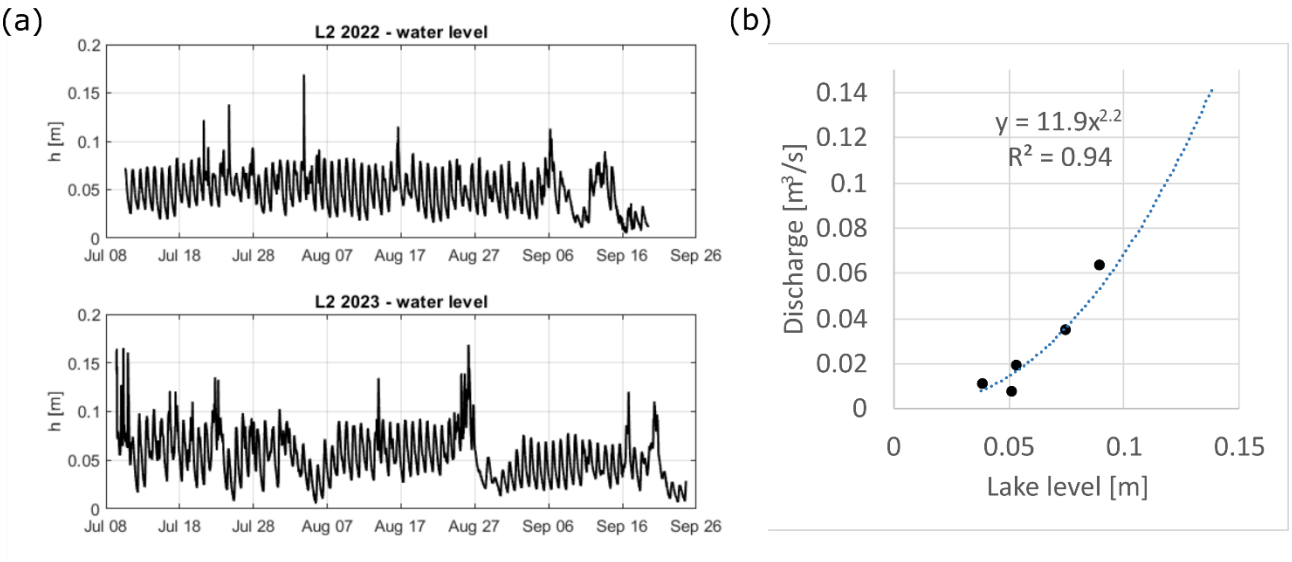

Figure 3. 5. (a)Water level measured in lake L2 in summer 2022 and 2023; (b) flow-rating curve relating outflow discharge to water level (lake L2).

The inflow at lake L2 is composed of diffused glacier runoff flowing on debris-covered ice and moraines (see Figure 3. 6 and S2.1), where direct discharge measurements were not feasible. In order to estimate the total inflow as a single value, Q_{in}, representing the sum of all the streams, we inverted the mass balance

$$\frac{d}{dt}\,(A\,h) = Q_{in} - \,Q_{out},$$

(3. 4)

where t is time [s], and A is the lake surface area [m^2]. Assuming a constant area A_0 (4270.5 m^2) and adopting the flow rating curve shown in Figure 3. 5 b, which allows the computation of the outflow discharge Q_{out} as a function of the water level h, we discretized the continuity equation (3. 4) to obtain:

$$Q_{in}\,(t^k) = A_0\,\frac{h^{k+1}-h^{k-1}}{2\Delta t} + Q_{out}(h^k),$$

(3. 5)

where *k* is the time index and Δt the time step (10 minutes) of the available measurements of the water level.

Inflow qualitative characteristics

The key factors that characterise the glacial meltwater input are water temperature and the concentration of suspended solids. These parameters were estimated with different approaches.

Inflow water temperature

The water temperature time series of the diffused inflow was estimated from a simplified heat balance equation, following a procedure similar to those proposed by Toffolon and Piccolroaz (2015). The heat budget for the region between the melting glacier and the lake can be described as:

$$\rho\, c_p\, V\, \frac{dT_w}{dt} = A\,[R + k_{wa}(T_a - T_w) - L_0],$$

(3. 6)

where T_w is the water temperature [°C], ρ is the water density (≅ 1000 kg m^{-3}), c_p the specific heat capacity of a mixture of water and soil (≅ 4180 J kg^{-1} K^{-1} for water), V the volume of water and soil that is involved in the quantification of the heat capacity (thermal inertia), t the time [s], A the area where the heat flux is exchanged [m^2], R the shortwave solar radiation [W m^{-2}], k_{wa} the heat transfer coefficient [W m^2 K^{-1}] between inflow water and air, and L_0 quantifies the total heat loss [W m^{-2}], a bulk parameter that accounts for the net effect of all the unresolved processes.
Introducing an equivalent thickness of the thermally reactive layer of water and soil, $H = \frac{V}{A}$, equation (3. 6) can be rewritten as:

$$\frac{dT_w}{dt} = \alpha\,[R + k_{wa}(T_a - T_w) - L_0],$$

(3. 7)

where $\alpha = \left(\rho\, c_p\, H\right)^{-1}$ is a lumped coefficient [W^{-1} s^{-1} m^2 K] proportional to the inverse of the characteristic time of the process. Therefore, the variation of temperature over time is a function of the incident solar radiation, the total heat loss, the heat exchange between water and air and the thickness of the thermally reactive layer in the inflow (Figure 3. 6). A simplified linear relation was assumed to describe the increase of the thermally reactive layer, given by the mixture of water and sediment, as a function of the discharge, $H = H_0 + \Delta H \cdot Q/max\,(Q)$, where $H_0$is the base value (also accounting for the effect of the soil), Q is the inflow discharge, and ΔH is the maximum increase corresponding to the maximum discharge estimated from the data.

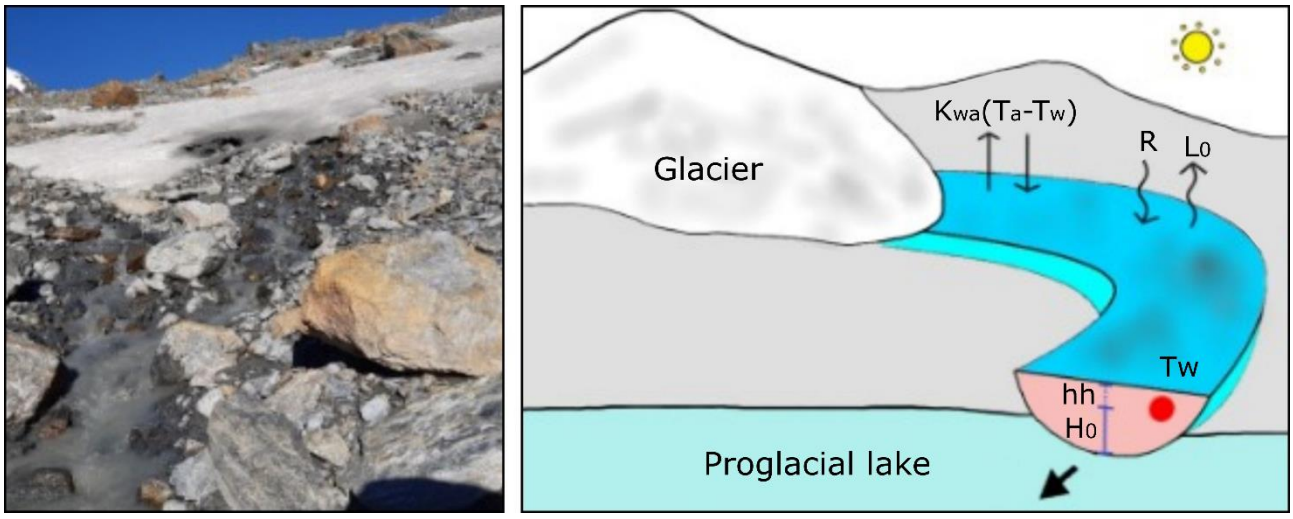

Figure 3. 6. The main glacial meltwater inflow (left) and a schematic description of the heat exchanges (right), modified from Toffolon and Piccolroaz (2015).

For the calibration of the parameters in equation (3. 7), we considered the availability of a few point measurements of the temperature in the lake inlets (performed with a portable probe WTW-Cond-3310 during the 2022 field campaign) and the results obtained with the lake model, compared with the measured temperature profiles, in a trial-and-error procedure. As a first approximation, the total heat loss L_0 was assumed to be equal to the average heat input. The values of the calibrated parameters, H_0, ΔH, and k_{wa}, are reported in Table 3. 2.

Table 3. 2. Parameters used in equation (5) to estimate the inlet water temperature.

Component	Description	Unit	Value
R	Shortwave solar radiation (heat input)	[W m^{-2}]	Measured meteorological data – Hintermartell station (Province of Bolzano/Bozen)
L_0	Total heat loss	[W m^{-2}]	250
k_{wa}	Heat transfer coefficient between water and air	[W m^2 K^{-1}]	80
$\alpha = (\rho\, c_p\, H)^{-1}$	Lumped coefficient	[W^{-1} s^{-1} m^2 K]	
ρ	Water density	[kg m^{-3}]	1000
c_p	Specific heat capacity	[J kg^{-1} K^{-1}]	4180 (for water)
H	Thickness of the thermally reactive layer	[m]	$H = H_0 + \Delta H \cdot Q/\max(Q)$ with H_0 = 0.2 m and ΔH = 0.4 m

Water density (ρ) was calculated based on the state equation for freshwater proposed by Chen & Millero (1986). For the assessment of the theoretical depth of intrusion of the inflow, water density was computed as a function of the estimated water temperature only.

Inflow suspended solids concentration

The concentration of inorganic suspended solids in the lake (hereafter, ISS) was modelled, providing the inflow ISS concentration and the settling velocity of particles. The concentration and composition of suspended solids in the lake shallow layers was available from the analysis described in Chapter 2. The measured concentrations of suspended solids were compared with the model output. Simulations were then iterated varying inflow ISS concentrations until the simulated ISS concentrations in the water column (averaged across the first two shallow layers) aligned with the measured values of total dry mass, at least in the order of magnitude. The optimal inflow concentration obtained was 200 mg/L.

ISS settling velocity

The settling velocity of the solids in the water column was assigned based on the available data obtained from the sediment characterisation (Chapter 2). To assign the settling velocity of the solids in the water column, an average particle diameter of 0.006 mm (i.e., fine silt) was assigned to the suspended solids. Settling velocity of particles in a water column is a function of the grain size, as described by the Stoke's law:

$$W_s = \frac{1}{18} \frac{g\,\Delta}{\nu} d^2, \tag{3. 8}$$

where g is the gravitational acceleration (9.8 m/s^2), Δ is the submerged specific gravity of sediments (here considered equal to 1.65 as an average value for inorganic sediments), ν is the kinematic viscosity of water (10^{-6} m^2/s at 20 °C) and d is the particle diameter (m). From the Stoke's law, the assigned settling velocity was 3.2 m/day.

Data analysis and model calibration

Model parameters were calibrated in order to minimise the error between modelled temperature data and field temperature data as measured by the thermistors chains positioned in L2 during summer 2023 (see methods section in this chapter). Temperature sensors were intercalibrated and mean errors for each sensor were applied to the dataset. For the calibration, hourly averaged temperature data were considered. The upstream temperature data were compared with the model output at segment 18, while the downstream temperature data were compared with the model output at segment 40 (Figure 3. 3). Root mean square error (RMSE) was computed separately for the upstream and the downstream segments, for each layer corresponding to the location of the thermistors, i.e., 0, 0.2, 0.4, 0.8, 1.6 m. RMSE was also calculated on longitudinal thermal differences, expressed as the difference between the downstream and upstream segments for each of the five layers, and the vertical differences, expressed as the differences between water temperature in the surficial layer and the temperature in the other layers.

Results

Field data

Water temperature

The temperature data measured in the littoral areas of the four Cevedale proglacial lakes during the monitoring seasons 2022 and 2023 are shown in Figure 3. 7 and Table 3. 3. Overall, the ice-contact lake, L1, was the coldest lake, with a mean temperature of 3.16 °C (min = 0.23, max = 8.38 °C). This condition potentially leads to continuous mixing due to the formation of thermal convection processes (Otto, 2019). The process can theoretically be described as follows: glacier runoff enters the lake at temperature below the temperature of maximum density of 3.98 °C (e.g, for L1, between 0.2 and 3.5 °C, as measured on 2 August 2022), the surface layers are heated by solar radiation, increasing their density and sinking in the water column until water reaches its maximum density and can drop to deeper layers. This process is likely not occurring in the other three lakes, L2, LC and L3, which showed an increasing trend in littoral water temperature going from L2 to L3.
Notably, L2 showed longitudinal thermaldifferences, with the downstream portion of the lake 0.8 °C warmer, on average, than the upstream portion (Table 3. 3). In 2022, the littoral water temperature measured in the upstream portion of the lake was on average 1.6 °C warmer than in the downstream portion, while, in 2023, littoral water temperatures in L2 were more uniform.

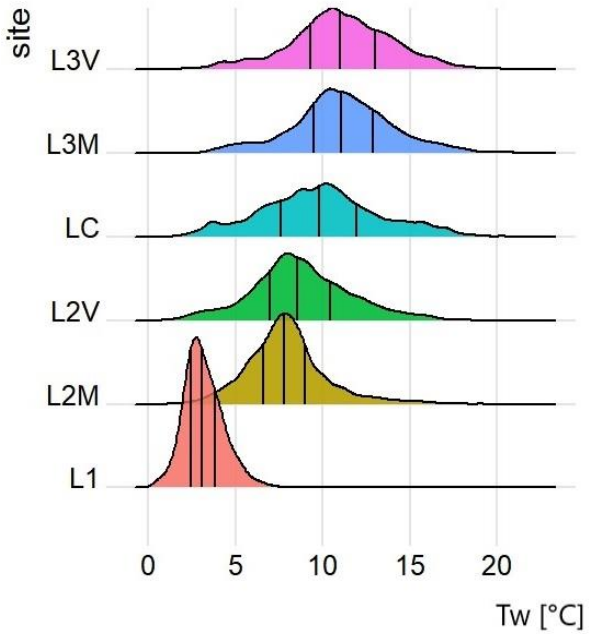

Figure 3. 7. Distribution of littoral water temperatures measured in the four Cevedale proglacial lakes (2022 and 2023). Vertical lines represent the median value of the distribution (central line) and 25th and 75th percentiles.

Table 3. 3. Littoral water temperature (minimum, maximum and average values, expressed in °C) measured in the Cevedale proglacial lakes over the two ice-free seasons 2022 and 2023. M = upstream; V = downstream.

Lake	2022			2023			2022 + 2023
	Min	Max	Average	Min	Max	Average	Average
L1	0.23	8.38	3.16	-	-	-	3.16
L2M	3.26	15.76	7.58	0.12	20.71	8.29	7.94
L2V	0.82	21.86	9.19	0.78	18.04	8.31	8.75
LC	-	-	-	1.44	22.14	9.86	9.86
L3M	2.94	17.95	10.79	2.94	22.43	11.49	11.14
L3V	2.02	19.03	10.83	1.55	21.38	11.28	11.06

Vertical temperature profiles in L2 and L3 (Figure 3. 8) showed that, overall, the water column in L3 was warmer than L2, with an average water temperature of, respectively, 10.3 °C and 7.5°C (7.3 °C upstream and 7.6 °C downstream). Also, temperature maxima were more pronounced in L3 than in L2, reaching 20.6 °C in L3 and 18.2 °C in L2. During warm and dry periods (e.g., during the period from 11 August to 25 August), when air temperatures were warm and precipitation events reduced, the lakes responded with a daily thermal stratification, with shallow layers becoming warmer than deeper layers. The temperature difference between the surface layer, 0 m, and the deepest layer, 1.6 m, increased from L2M to L3, and was on average 1.09 °C in L2M, 1.53 °C in L2V, and 1.9 °C in L3. Surface layers in L3 were warmer than in L2, with an average surface temperature of respectively 10.9 °C and 8.1 °C (7.9 °C upstream and 8.3 °C downstream). Layers at 1.6 m showed a similar pattern, increasing from 6.8 °C in L2M, to 6.7 °C in L2V, and 9.0 °C in L3.

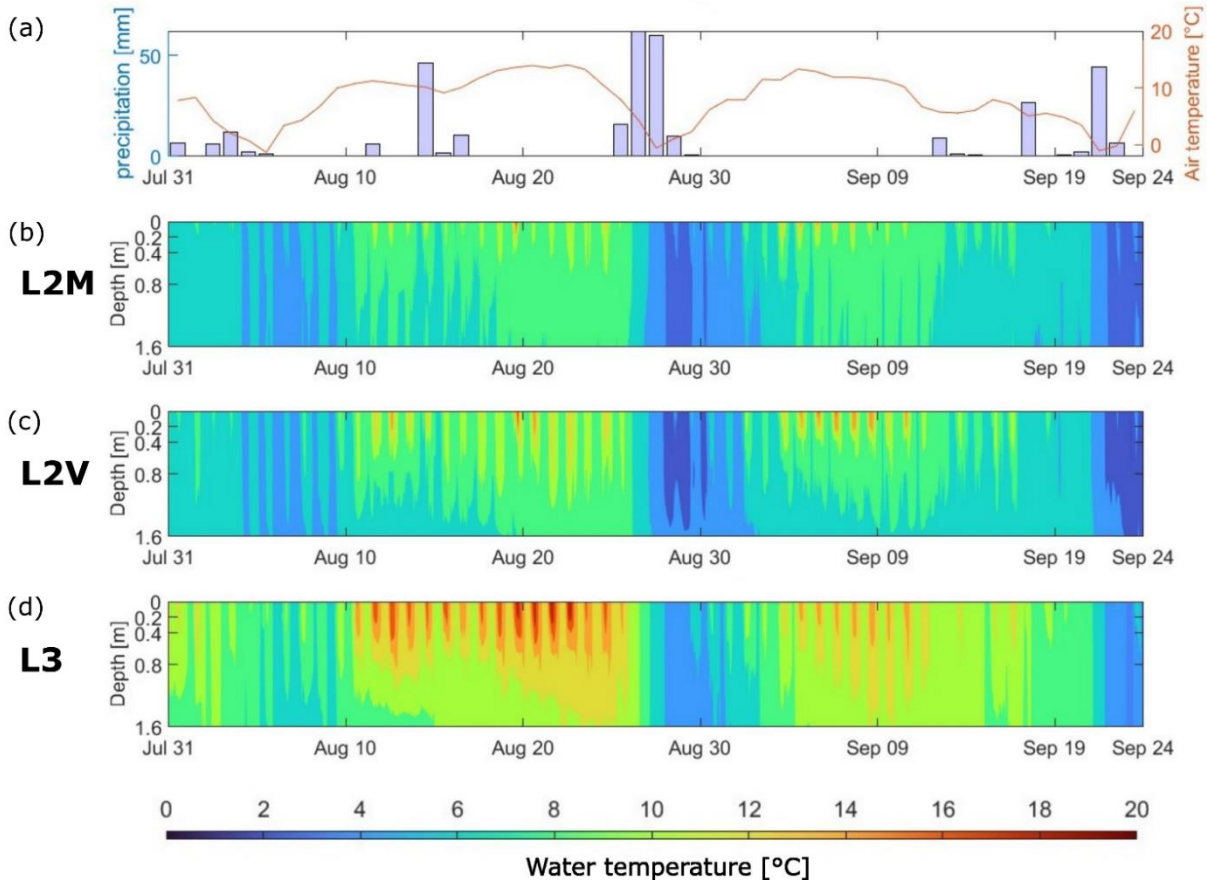

Figure 3. 8. (a) Meteorological conditions (daily cumulate precipitation registered in the Sulden meteorological station and mean air temperature at the Madritsch meteorological station); (b), (c), (d) water temperature profiles in L2 (upstream, L2M and downstream, L2V) and in L3.

The Schmidt stability (Figure 3. 9) was significantly higher in L3 (mean 2.57 J m^{-2}, max 9.4 J m^{-2}) than in L2 (upstream: mean 0.53 J m^{-2}, max 1.33 J m^{-2}; downstream: mean = 1.22 J m^{-2}, max = 3.18 J m^{-2}), thus indicating that the stratification was more stable in L3 than in L2. Both locations in L2, i.e., upstream and downstream, showed significant differences (Mann-Whitney test, $p < 0.05$) between each other and with L3. More pronounced differences in Schmidt stability between the three locations formed during the summer period (August), while in September the lakes were uniformly unstable.

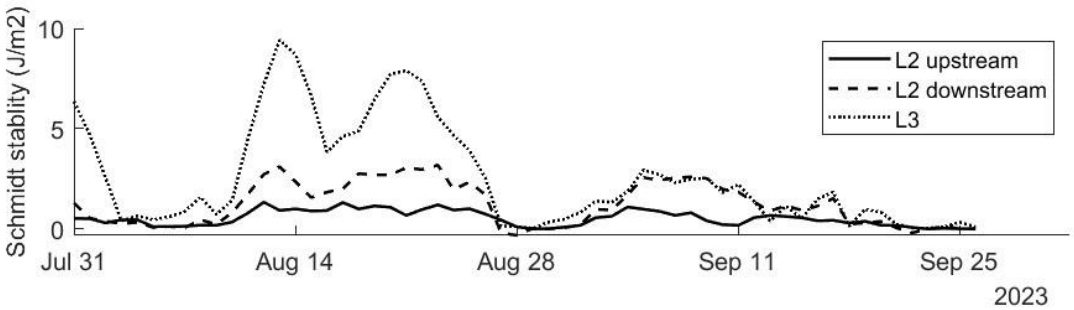

Figure 3. 9. Schmidt stability estimated from measured temperature data, during the ice-free season 2023.

In lake L2, similarly to what observed from measurements in the littoral area (Figure 3. 7), a longitudinal thermal difference formed along the lake (Figure 3. 10), especially in the surface layers (0, 0.2 and 0.4 m). Longitudinal thermal differences were more pronounced during warm and dry periods. The strongest difference, reaching, in the layer at 0 m, 2.1 °C on a daily average (i.e., downstream part 2.1 °C warmer than the upstream part), was observed on 21 August 2023. On the other hand, during periods with lower air temperature or precipitation events (e.g. during the period 26-30 August, Figure 3. 10) the cooling of surface water column produced-well mixed conditions, with uniform surface temperature along the lake.

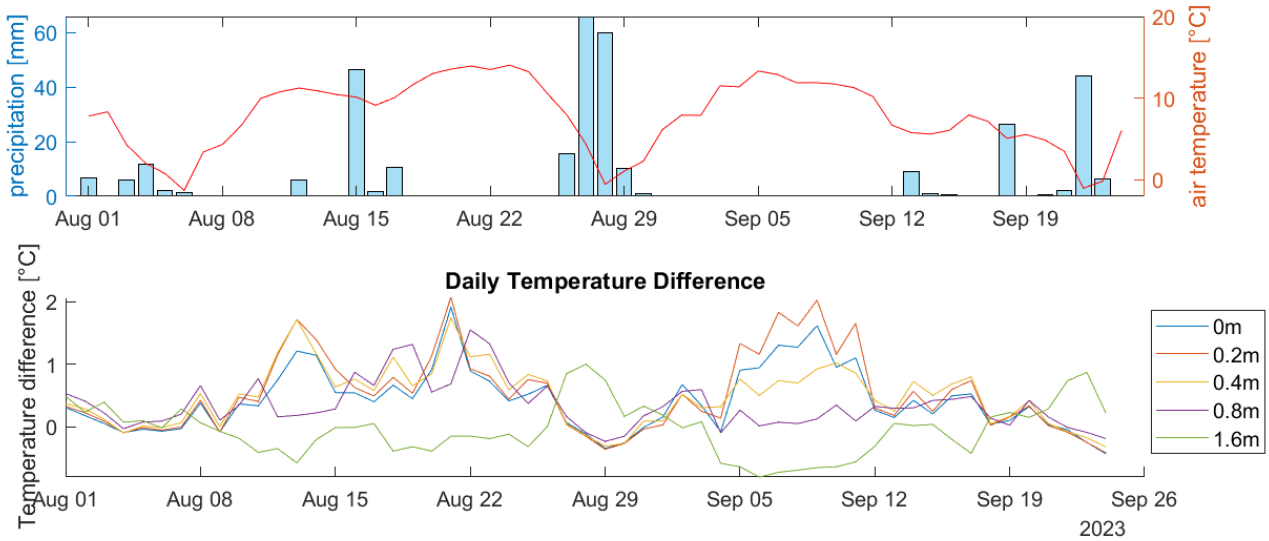

Figure 3. 10. Daily averaged air temperature and cumulative precipitation in Summer 2023 (upper plot) and the thermal longitudinal differences observed in L2 in the same period, in the five layers of the water column where thermistors were installed.

Water temperature measured in the first layer of the buoy chains (0m) showed good agreement with the temperature data measured in the littoral area (Figure 3. 11). In the upstream part of the lake, thermal variations of the littoral sensor were stronger than those registered by the buoy sensor, while water temperature in the downstream part was more laterally uniform.

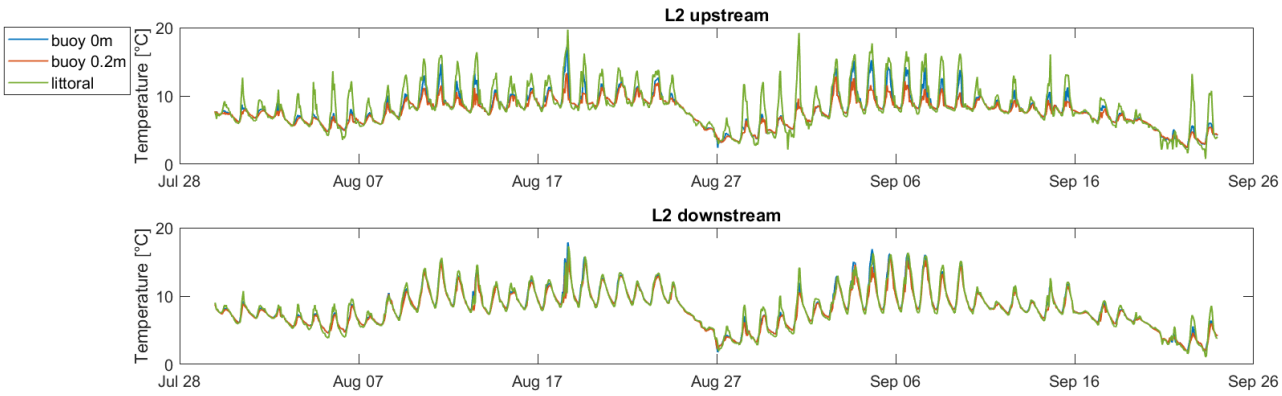

Figure 3. 11. Water temperature measured in 2023 in the shallow layers of the buoys and in the littoral area, in the upstream and downstream parts of L2.

Electrical conductivity

The lowest electrical conductivity was measured in lake L1 (average18 µS/cm, see Chapter 1). During the first month of the ice-free season of 2022 (25 June – 1 August), electrical conductivity was higher in L2 compared to L3 (Figure 3. 12). However, in the early days of August 2022, this trend reversed, with L3 showing higher electrical conductivity than L2. This condition persisted for the remaining part of 2022 and the whole season 2023. This shift is likely the result of the progressively reduced connection between L1 and L3. Initially, L3 received water from both L1 and L2, with L1 delivering water with low electrical conductivity (11-27 µS/cm). After the discharge of the channel connecting L1 and L3 decreased significantly, L3 primarily received water from L2. L2 outflow is progressively enriched in solutes along the chain of streams and lakes, resulting in a higher electrical conductivity in L3.

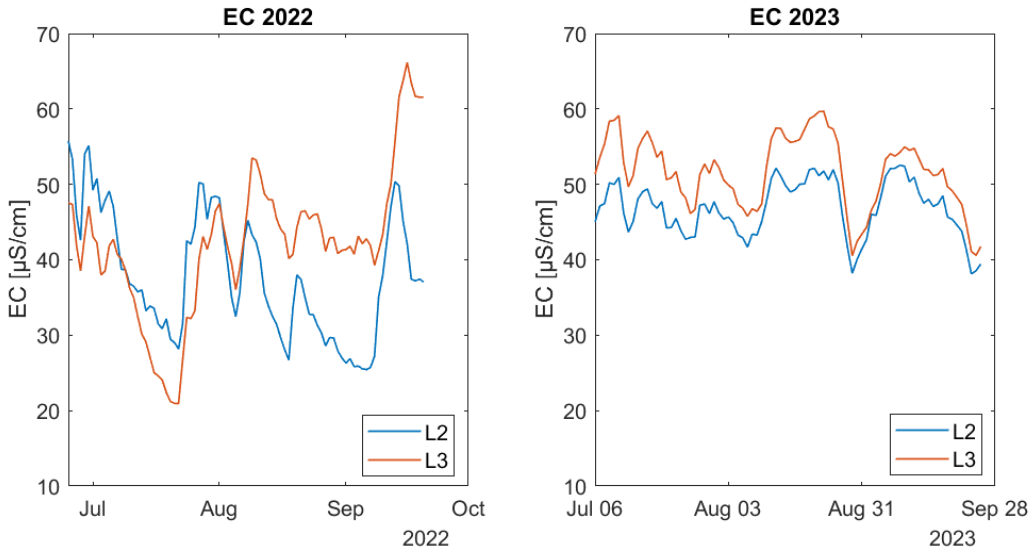

Figure 3. 12. Electrical Conductivity (EC, µS/cm) measured in L2 and L3, in the ice-free seasons 2022 and 2023.

Turbidity and light availability

The turbidity (*N*) and concentration of total suspended solids (*TSS*) measured in water samples showed a linear relationship (Figure 3. 13),

$$N = a_0 + a_1\, TSS, \tag{3. 9}$$

where a_0 = 3.88 NTU and a_1 = 0.68 NTU mg^{-1} L, with significant positive correlation (Spearman rho = 0.82, $p < 0.01$).

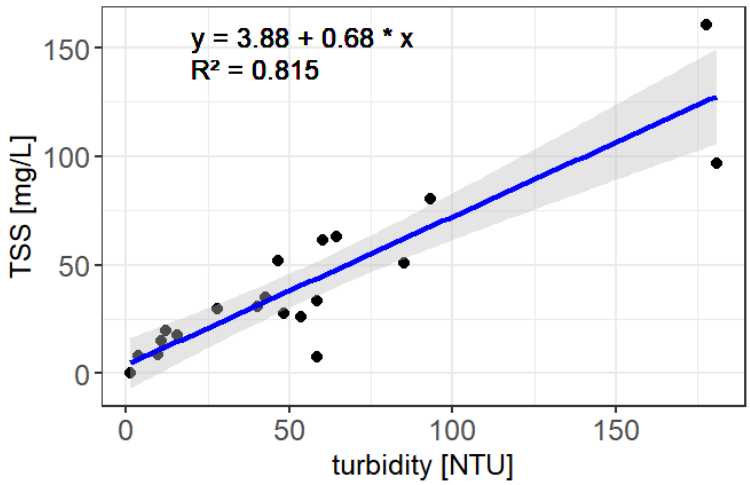

Figure 3. 13. Linear fit with 95% confidence interval between turbidity (NTU) and total suspended solids (TSS) measured in laboratory analyses on independent samples collected from the study area.

Considering the composition of the suspended solids, the predominant fraction was the inorganic, (ashes in Figure 3. 14), which represented from 94.5 to 96% of the dry mass in L1, from 90.2 to 96% in L2, from 87.9 to 84.2% in LC, from 76.5 to 94.4% in L3.

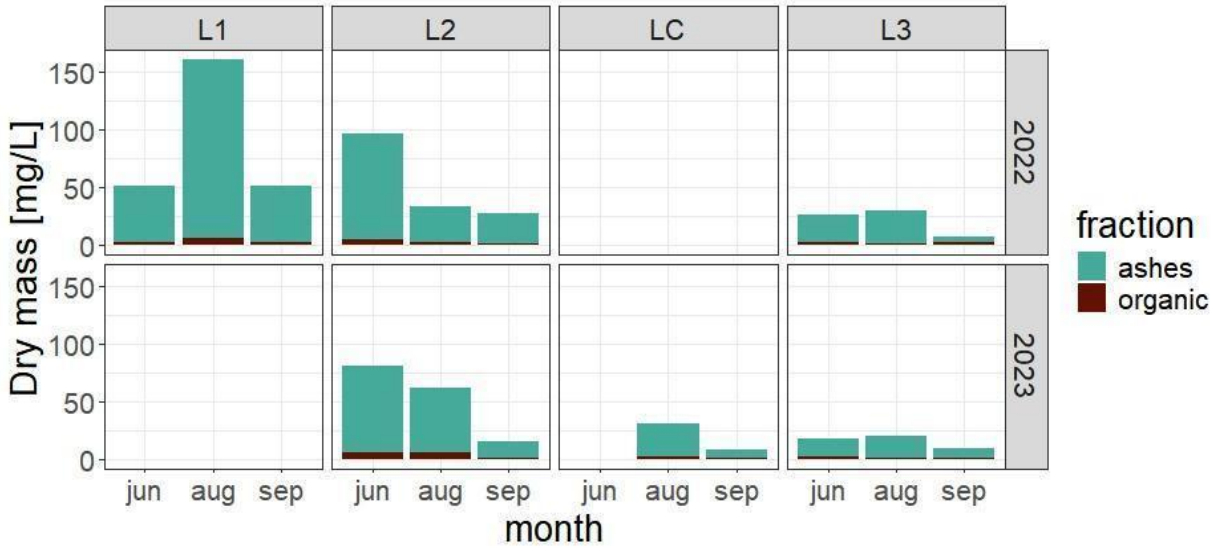

Figure 3. 14. Concentration of suspended solids measured in the four Cevedale proglacial lakes in 2022 and 2023 with laboratory analyses. Colours represent the dry mass of the two components of the suspended dry mass, obtained after ignition at 550 °C.

Therefore, the concentration of suspended solids, which was composed mainly by the inorganic mineral fraction, was adopted as a proxy for turbidity.

The most turbid lakes were L1 (mean = 103.1 NTU) and L2 (mean = 95.8 NTU in 2022, 54.7 NTU in 2023); due to the increasing distance from the glacier, LC and L3 had lower turbidity (mean = 33.8 and 29.5 NTU, respectively).

Turbidity gradually decreased with decreasing glacial influence, both considering NTU and the total amount of suspended solids in the water column. The glacier ablation period in summer, and the

consequent increase in glacial turbid runoff, induced a significant peak in the suspended solids only in the L1 lake, in 2022. In L2 and LC, turbidity gradually decreased during the season, while the concentration in L3 is lower than 50 mg/L throughout the entire season, and concentrations diminished mainly in September (i.e., early autumn). The presence of a summer turbidity peak in L1 suggests that the water temperatures around 4 °C induce a continuous mixing of the water column, and a continuous redistribution of suspended solids.

The high concentration of solids suspended in the water column impacts water transparency to light. In lake L2, the average light extinction coefficient was 5.87 m^{-1}, corresponding to a mean Secchi disk depth of 0.3 m. However, the estimated light extinction coefficient showed significant seasonal variation (Figure 3. 15). During sunny summer days, such as 20 August 2023, when glacier melting is sustained, light penetration is strongly reduced. At 14:00 on this day, the light extinction coefficient was 6.8 m^{-1}, corresponding to a Secchi disk depth of 0.25 m. Following the snowing event at the end of August 2023, light penetration in the deeper layers increased, and measured light was > 0 lux also at 1.6 m. On 1 September at 14:00, the light extinction coefficient decreased to 1.32 m^{-1}, corresponding to a Secchi disk depth of approximately 1.28 m. In contrast, Lake L3 exhibited overall lower light attenuation. For instance, on 20 August 2023, the light extinction coefficient at 14:00 in L3 was 2.38 m^{-1}, corresponding to a Secchi disk depth of 0.7 m.

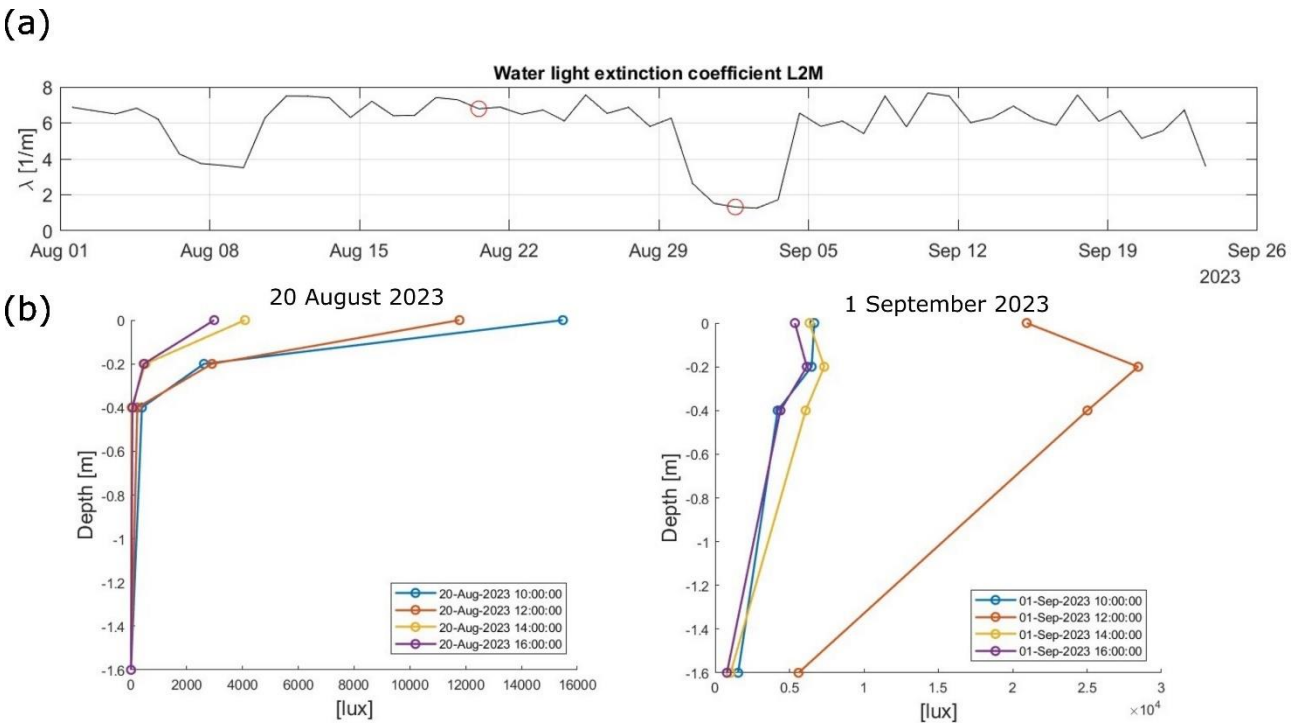

Figure 3. 15. (a) Water light extinction coefficient time series in L2, computed at 14:00 of each day. (b) Vertical profiles of light recorded in the water column, in two selected days (red circles in the upper panel).

The turbidity of the proglacial lakes, as previously pointed out, is determined by the presence of suspended fine glacial sediments. Within a lentic water body, relatively slow current velocities can allow suspended sediments to deposit (Otto, 2019). Sedimentation of suspended solids is a crucial process that can strongly influence the environmental characteristics of the downstream water bodies (Figure 3. 16).

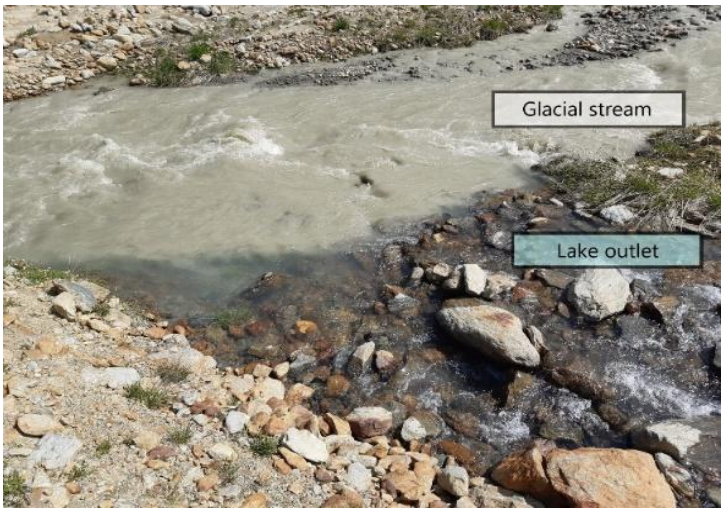

Figure 3. 16. Effect of sedimentation on stream turbidity: confluence between a stream directly fed from a glacier tongue (Fürkeleferner) and the outlet of the Cevedale lakes system (14 July 2023).

To estimate the order of magnitude of the sediment layer that deposits on the lake bottom of L2, we adopted the approach proposed by Steffen et al., 2022 and Hardmeier et al., 2024. According to this approach, the volume of sediment deposited in a glacial lake can be estimated based on the difference in suspended sediment concentration between the inlet and outlet streams, as described by the equation:

$$V_s = \frac{C_{in} - C_{out}}{\rho_s} V_w, \tag{3. 10}$$

where V_s is the volume of accumulated sediment during a time interval [m^3], C_{in} and C_{out} are the concentrations of suspended solids in the inlet and outlet streams [kg/m^3], ρ_s is the density of the deposited sediment [kg/m^3] and V_w is the cumulative glacial runoff during the time interval [m^3/s]. As an example, it is possible to estimate the order of magnitude of sedimentation during a day of glacier ablation (31 July 2023). The inlet and outlet concentrations of suspended solids were estimated from direct turbidity measured in the streams using equation Figure 3. 8), and amounted to 1.37 and 0.05 kg/m^3, respectively. ρs is assumed equal to 2200 kg/m^3 (Steffen et al., 2022; Hardmeier et al., 2024). The glacial runoff (V_w) for this day was calculated based on the inflow timeseries and amounted to approximately 1888.4 m^3. From equation (3. 10), the total amount of fine sediment deposited in lake L2 on 31 July 2023 was about 1.13 m^3.

Given the lake area of 4996.3 m^2 (here including the sediment delta estimated from orthophoto, see Chapter 2), the average thickness of the sediment layer deposited on the lake bottom was 0.2 mm per day. Over a month of glacier ablation, assuming all days are equal to 31 July, this corresponds to a total deposition of 6 mm.

The same procedure was applied to other days for which stream turbidity measurements and lake level data were available (Table 3. 4). The average daily deposition, based on these data, was 0.1 mm. Assuming uniform deposition over a three-month season (90 days), the average thickness of

the sediment layer deposited in L2 would be approximately 0.9 mm. However, these observations highlight the seasonal variability in the sedimentation processes. Sediment deposition during periods of sustained glacier ablation in 2022 and 31 July 2023 was higher than during autumn, as exemplified by the lowest value recorded on 26 September 2023. This reflects the reduced glacier runoff observed at the end of September, driven by lower air temperatures. In this period, inflow discharge was primarily sustained by snowmelt following a snowfall between 22 and 24 September (snow height at the Madritsch meteorological station, 6 cm on 23 September, http://meteobrowser.eurac.edu/). As a result of the limited ice melt contribution, the concentration of suspended solids in the water column was lower.

Table 3. 4. Parameters used to estimate the sediment deposition in lake L2. Q_{in} = daily average inflow discharge; C_{in}, C_{out} = concentrations of suspended solids estimated from turbidity measurements in inflow and outflow streams, respectively. H = average thickness of the sediment layer deposited on the day.

Date	Q_{in} [m^3/s]	C_{in} [kg/m^3]	C_{out} [kg/m^3]	H [mm/day]
1 August 2022	0.02	0.52	0.06	0.07
13 September 2022	0.01	0.84	0.02	0.08
31 July 2023	0.02	1.37	0.05	0.23
26 September 2023	0.002	0.22	0.001	0.003

Modelling

The model CE-QUAL-W2 was used to simulate the temperature and turbidity dynamics of lake L2 in the two ice-free seasons of 2022 and 2023. Details on the periods considered in the simulations and the respective meteorological forcings used in the model are reported in Table 3. 5.

Table 3. 5. Periods of CE-QUAL-W2 simulation in 2022 and 2023 and the main meteorological conditions.

	2022	**2023**
Simulation period	12 July – 21 September	12 July – 26 September
Air temperature (°C)	avg 7.29, min 6.8, max 16.9	avg 7.89, min, 5.3, max 17.2
Wind velocity (m/s)	avg 1.75, max 9.3	avg 2.06, max 8.6
Solar radiation (W/m^2)	avg 199.39, max 1095.6	avg 177.09, max 1140.5
Cumulate precipitation (mm)	159.9 mm	521.1 mm

Model calibration

The meteorological parameter with the largest degree of uncertainty was wind direction, due to the different location of the study site and the meteorological station adopted as reference (Madritsch). Indeed, the Madritsch meteorological station is located in an adjacent valley, Solda Valley, at a location where the presence and influence of glaciers is significantly reduced with respect to the widely glacierised Upper Martell Valley (Figure 3. 17c). Furthermore, the main orientations of Solda and Martell Valleys differ, with the Solda Valley S-N oriented and Martell Valley SW-NE oriented (Figure 3. 17c). Finally, microclimate conditions over glaciers are predominantly influenced by

downslope katabatic winds, often referred to as glacier winds (Smith, 1978; Obleitner, 1994; Van Den Broeke, 1997; Strasser et al., 2004; Oerlemans & Grisogono, 2002).

Therefore, in absence of in situ measurements at the Cevedale proglacial lakes of this parameter, different configurations of wind direction were explored, maintaining the measured wind speeds measured at the Madritsch station. In Figure 3. 17a, two wind scenarios are shown, the first (W1) with wind directions measured at the Madritsch station, the second (W2), with modified wind directions in the configuration that minimised the root mean square error. This configuration was obtained by adding 150 °C to the directions recorded at the Madritsch station. For wind directions corresponding to up-valley flows, a 180° adjustment was applied to convert them into katabatic wind directions. In the W2 scenario, the most frequent winds are oriented as Martell Valley, i.e., SW-NE, and originate from the area covered by the Zufallferner (Figure 3. 17c). This wind configuration resulted in a more accurate representation of the observed longitudinal thermal differences, with the downstream section of the lake being warmer than the upstream section (Figure 3. 17b). Anabatic winds reversed this difference. Indeed, the RMSE referred to the thermal difference was 1.22 °C in W2, compared to 1.87 °C in the W1 scenario.

While the precise wind direction remains a source of uncertainty in this model application, the W2 scenario is considered the most realistic based on both literature and the comparison of model outputs with field data. Consequently, the results shown in the next sections refer to this configuration.

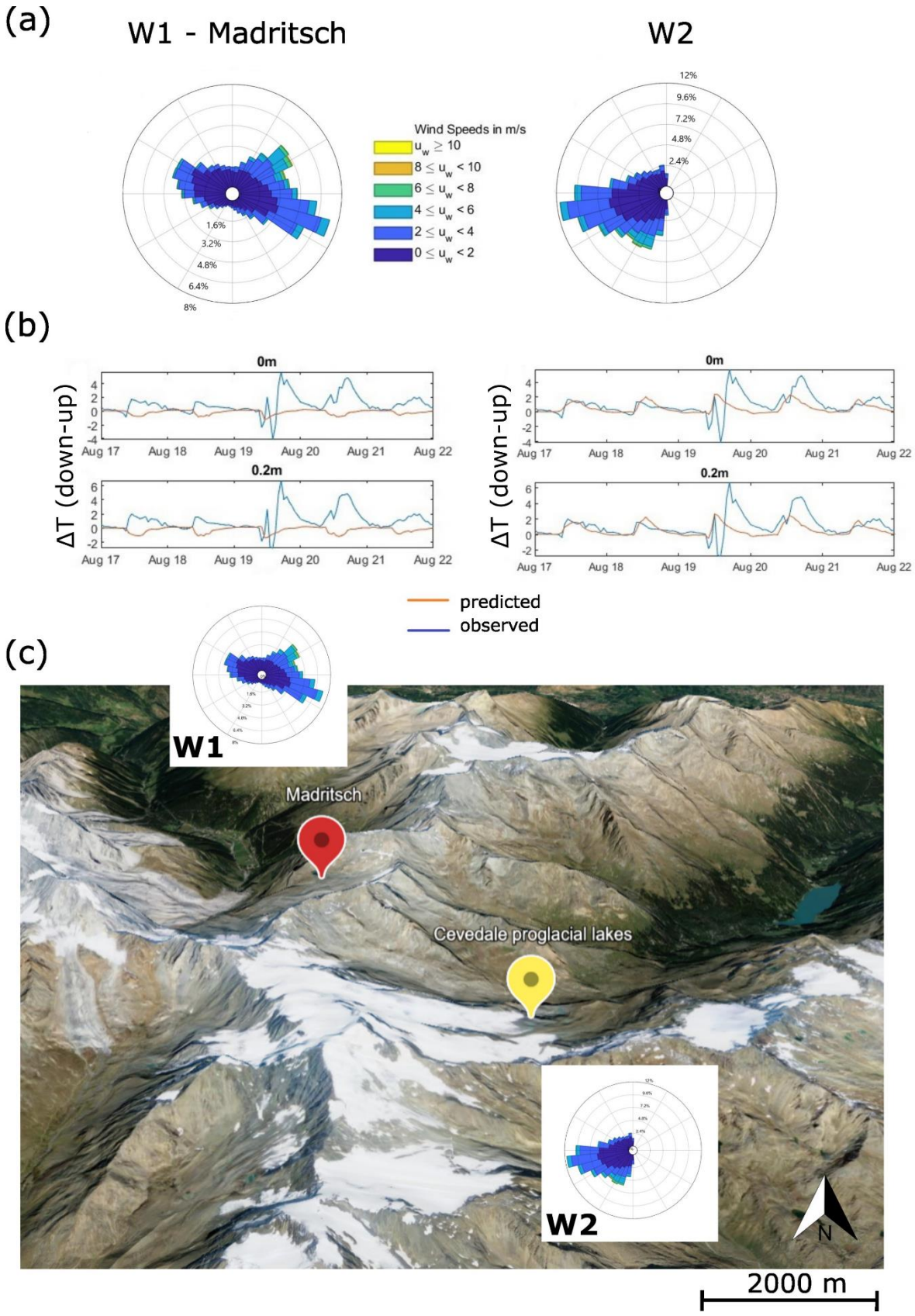

Figure 3. 17. (a) Windrose of two wind scenarios, W1 and W2 (described in the text); (b) longitudinal thermal differences obtained in the simulations adopting W1 and W2 scenarios, expressed as the difference in water temperature between the downstream and the upstream segments, predicted (orange) and observed (blue) in a warm and dry period. (c) Map of the study area showing the position of the Cevedale proglacial lakes and of the Madritsch meteorological station, with the respective windrose (Orthophoto: Autonomous Province of Bolzano/Bozen, 2023).

The inflow water temperatures were estimated with the simplified model in equation (3. 7). The results are presented in Figure 3. 18: temperatures range from 0 to 13.8 °C in 2022 and from 0 to 12.8 °C in 2023, with mean values of 5.82 °C in 2022 and 5.84 °C in 2023. The estimated values showed a good agreement with the available inflow water temperature measured during 2022.
During the 2022 season, the decrease in inflow water temperature was gradual. In contrast, the 2023 season was characterised by sharper temperature fluctuations, driven by variable meteorological conditions.

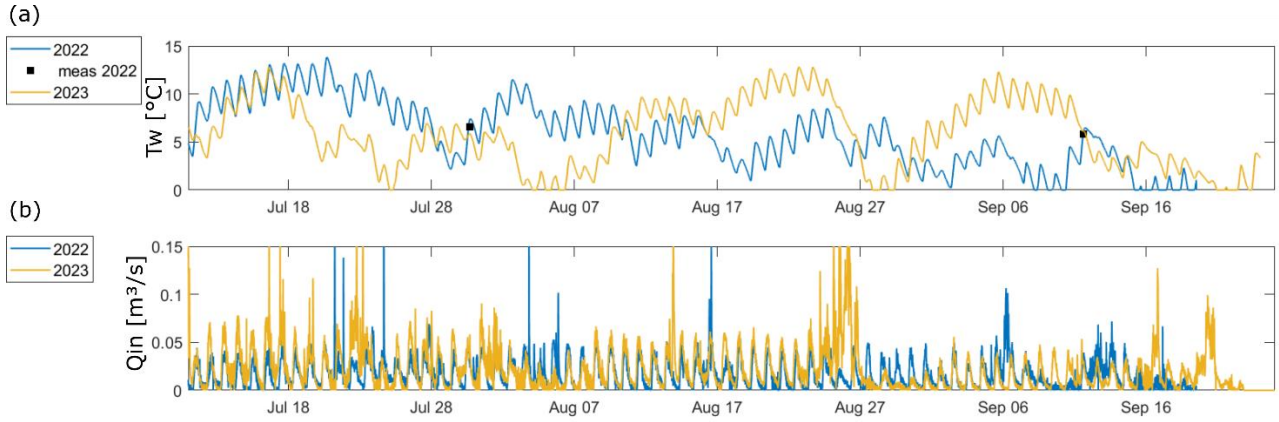

Figure 3. 18. (a) Estimated inflow water temperature and (b) inflow discharge of L2 in 2022 and 2023.

The model was calibrated manually, by adopting an expert-based trial and error procedure. Simulations were iterated (about two hundred times) changing the values of key parameters, observing the effects of the modifications on lake thermal dynamics and annotating RMSE, aiming to minimise errors. The final configuration of the model with the calibrated parameters is shown in Table 3. 6.
One of the most relevant factors in shaping the lake thermal dynamics, and influencing RMSE, was the inflow water temperature. The adoption of the modelling approach for this parameter significantly reduced the RMSE with respect to the adoption of a constant temperature value.
The assigned light extinction coefficient for water (EXH2O) was set at 1.3 m^{-1}, which is higher than the value of pure water (Cole & Wells, 2023) and corresponds to the lowest value of light extinction estimated from the field measurements of light intensity (for a description of this data, see the section “Turbidity and light availability” in the Results of this chapter). This adjustment was made to account for the presence of non-flocculated clays in the water column, that induce the background turbidity observed in the L2 lake, often characterised by the typical “milky” look of proglacial lakes (e.g. Sommaruga, 2015). Assuming the relationship (3. 2), a light extinction coefficient of 1.3 m^{-1} corresponds to a Secchi disk depth of 1.3 m. On top of this background light extinction, the extinction due to inorganic suspended solids (EXSS) was calibrated based on field observations. In August 2022, the measured concentration was 33 mg/L, and we observed that, in the same day, the Secchi disk depth was < 30 cm. It was possible to obtain this light extinction value at 33mg/L by attributing EXSS = 0.2 $m^{-1}/(g/m^3)$, corresponding to a total light extinction of 7.9 m^{-1} and a Secchi depth of 0.2 m. The default value, multiplied 33 mg/L, produced the unrealistic Secchi disk depth of 0.6 m.

Wind speed was reduced by scaling the measured wind speeds (at Madritsch meteorological station) by a factor of 0.5, which allowed a better replication of the mixing dynamics observed in the vertical profiles. This condition reflects the fact that the ground depression where L2 is impounded is surrounded by moraines, that partially shelter the surface of the lake from wind stress.
The critical shear stress for sediment resuspension was assigned from literature data referred to lakes in the adjacent Province of Trento (Righetti et al., 2010).

Table 3. 6. Calibrated parameters of the CE-QUAL-W2 model, applied to lake L2.

Description	Short name	Default	Calibrated	Unit
Water light extinction	EXH2O	0.25	2	1/m
Fraction of incident solar radiation absorbed at the water surface	BETA	0.45	0.3	-
Light extinction due to inorganic suspended solids	EXSS	0.1	0.2	$m^{-1}/(g/m^3)$
Wind sheltering		-	0.5	-
ISS concentration		-	200	mg/L
ISS settling velocity		-	3.2	m/day
Critical shear stress for sediment resuspension	TAUCR	-	0.5	$dynes/cm^2$

The calibrated numerical model simulated the thermal dynamics measured at the two buoys with an average RMSE of 1.54 °C. Errors were slightly higher in the upstream segment (1.57 °C) compared to the downstream segment (1.52 °C). The model allowed a good reproduction of the observed daily and seasonal thermal fluctuations of water temperature (Figure 3. 19) and of the temperature differences between the layers (Figure 3. 20, RMSE = 1.19 °C). In particular, the model coherently reproduced the changes of temperature that were observed between warm and dry periods (second half of August and first half of September), and the colder/stormy days (end of August). The period with the highest error was the end of September, when the model generally underestimated water temperatures in all layers. This uncertainty was reflected also in the vertical differences (Figure 3. 20), that were overestimated by the model simulations, while measured data suggested isothermal conditions. Finally, longitudinal thermal differences (Figure 3. 21, RMSE = 1.23 °C) were well reproduced in their general daily trends but were generally underestimated in the model outputs in all the lake layers.

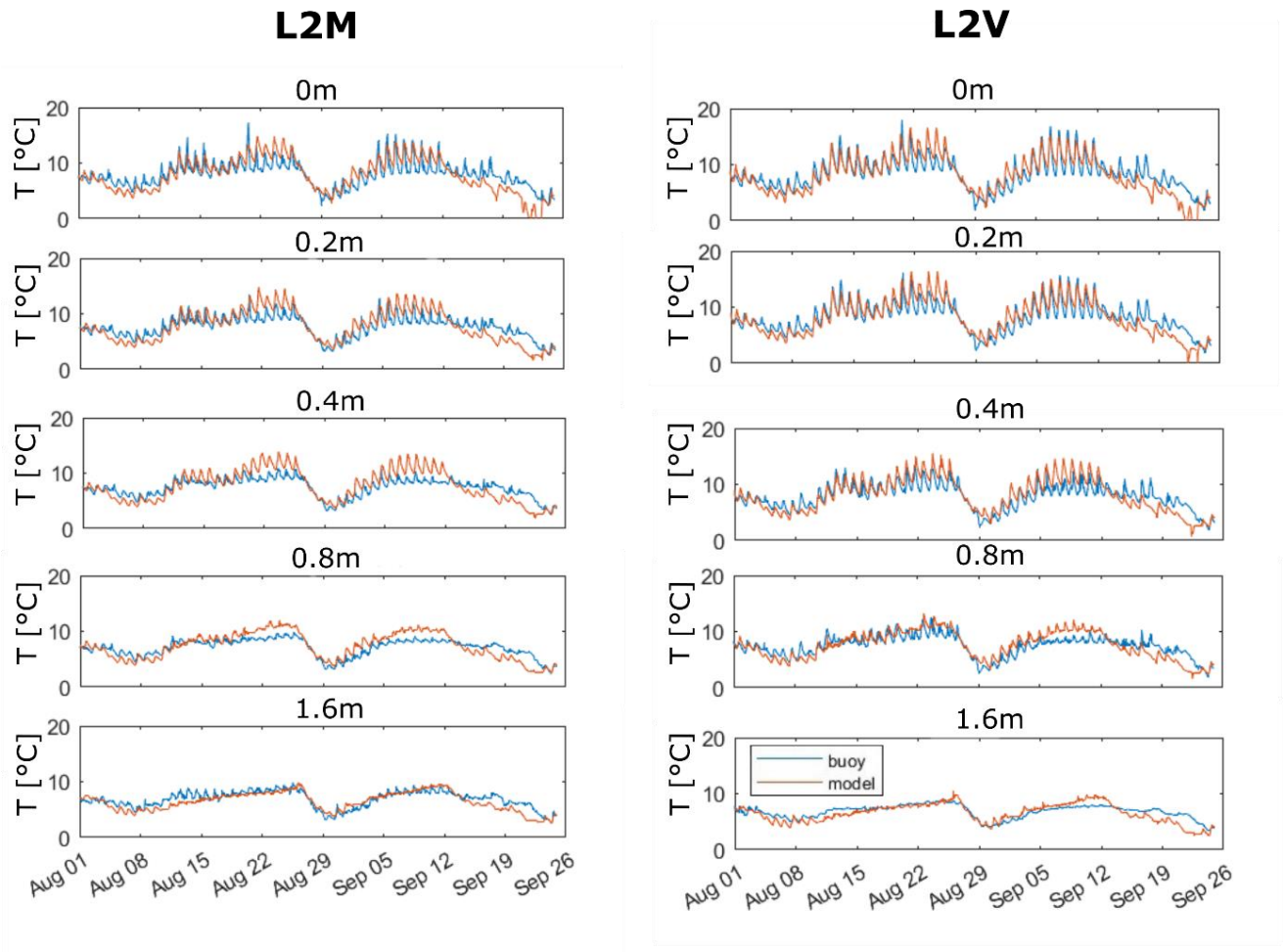

Figure 3. 19. Observed (buoy, blue) and modelled (model, orange) temperature data in the calibration period (1 August-26 September 2023), in the 5 layers of the upstream (L2M) and downstream (L2V) segments of L2.

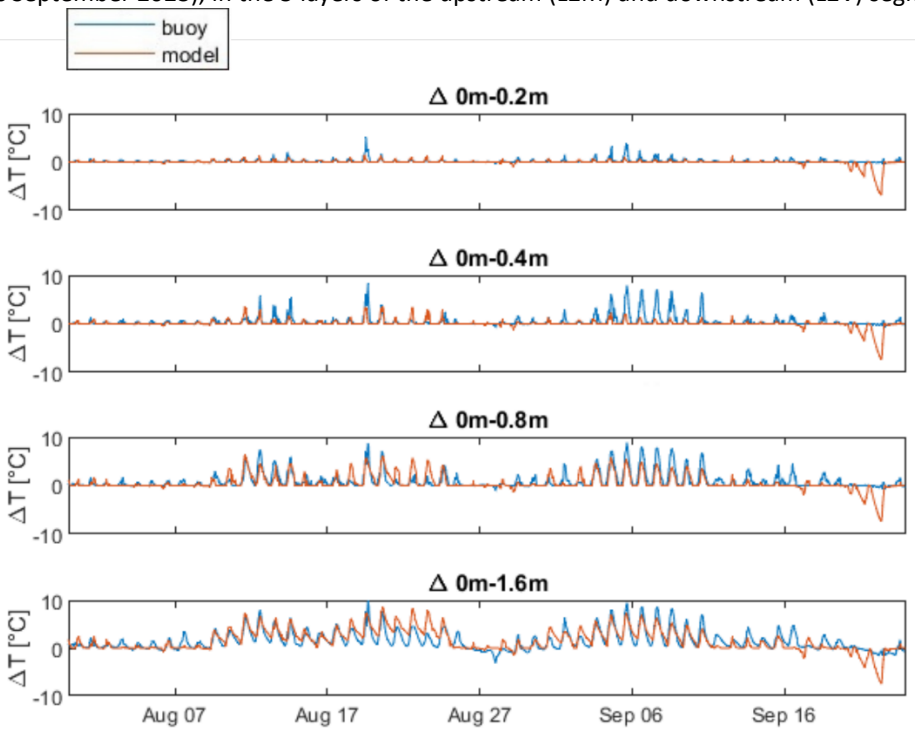

Figure 3. 20. Observed (buoy, blue) and modelled (model, orange) temperature differences between the surface layer and deeper layers.

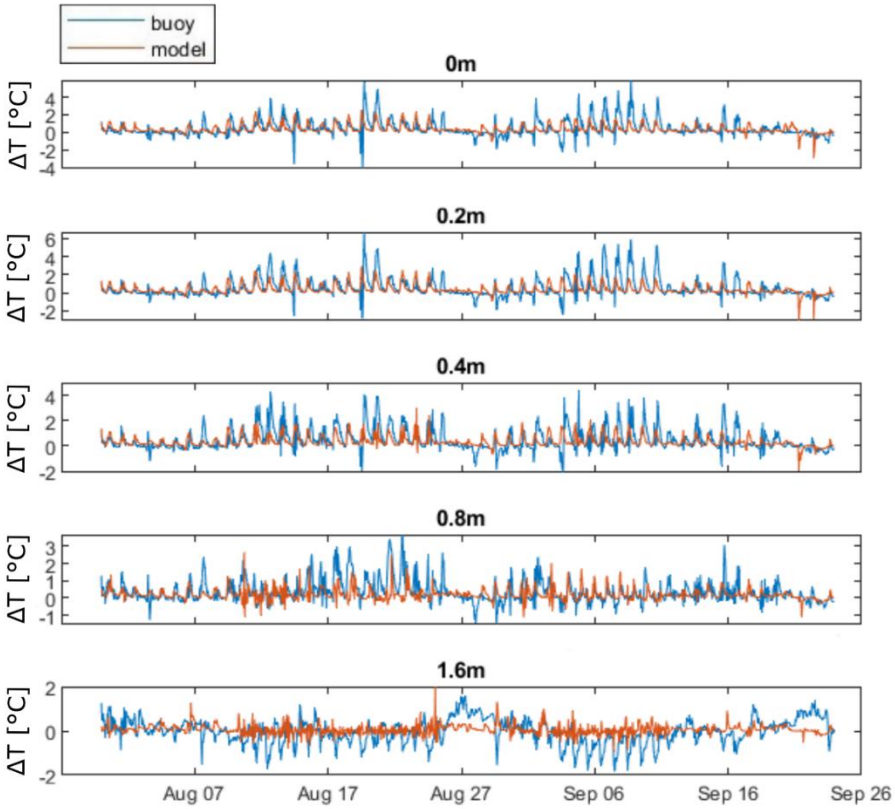

Figure 3. 21. Observed (buoy, blue) and modelled (model, orange) temperature differences between the upstream and downstream segments of the lake, at different depths.

Modelled concentrations of suspended solids were coherent with measurements of light intensity in the water column (Figure 3. 22). This means that higher modelled concentrations of ISS correspond to periods of decreased light intensity reaching the water column and vice versa.

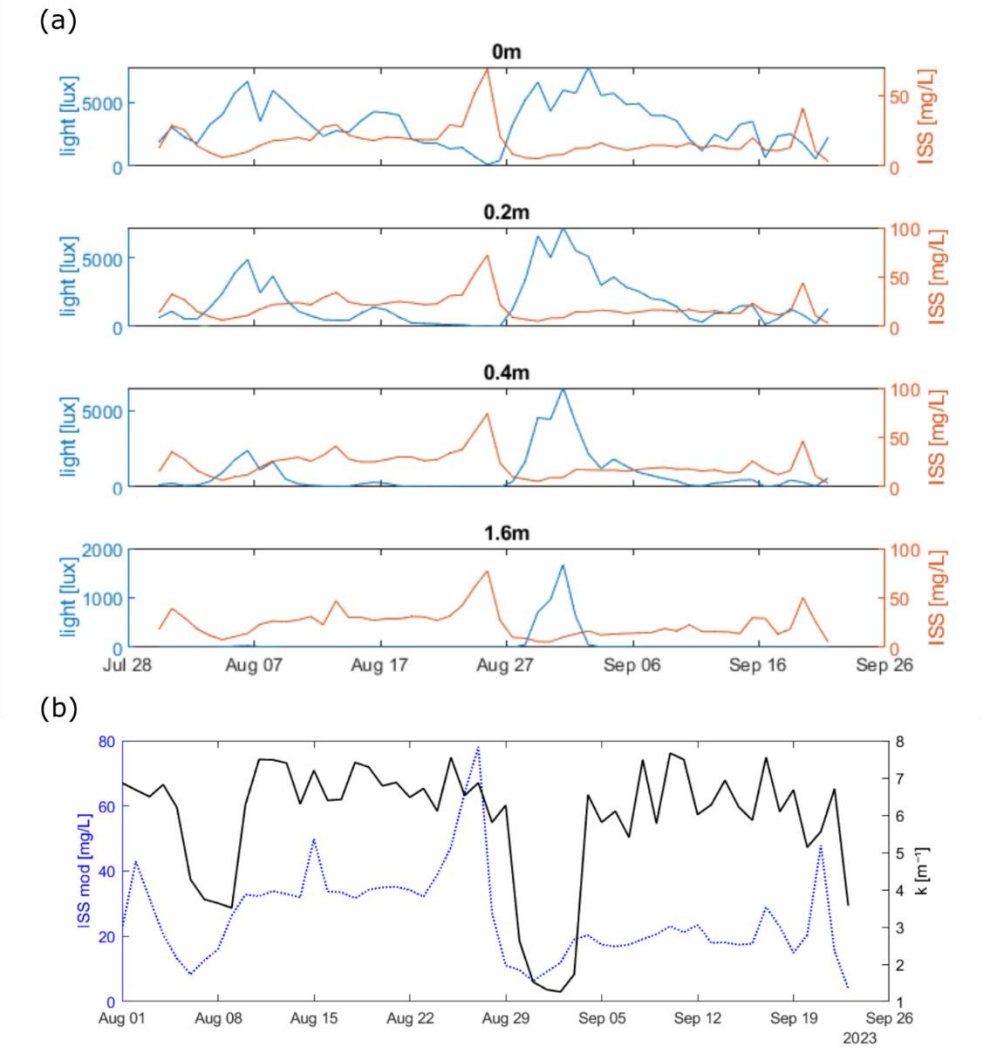

Figure 3. 22. (a) Light intensity measured by HOBO sensors (blue line) and the concentration of inorganic suspended solids predicted by model simulations (orange line), in four layers of the water column of the upstream part of L2. (b) Modelled concentration of ISS in the water column (mean of the five layers) at segment 18 (blue dotted line) and the light extinction coefficient computed from light measurements at the same location (black continuous line).

Stratification related dynamics

Lake surface is exposed to wind stress, which is crucial in determining the direction of the horizontal superficial current.

In a warm and dry day (Figure 3. 23), thermal stratification is typically observed in the lake, with shallow layers warmer than deeper layers. This stratification forms because water temperatures in these phases are constantly above 3.98 °C, i.e., the temperature of maximum density. Therefore, colder water is denser than warmer water, and the layers warmed by the solar radiation float on colder layers. Furthermore, as observed in the measured data, the shallow layers in the downstream part of the lake are warmer than those in the upstream part, thus determining a longitudinal thermal difference.

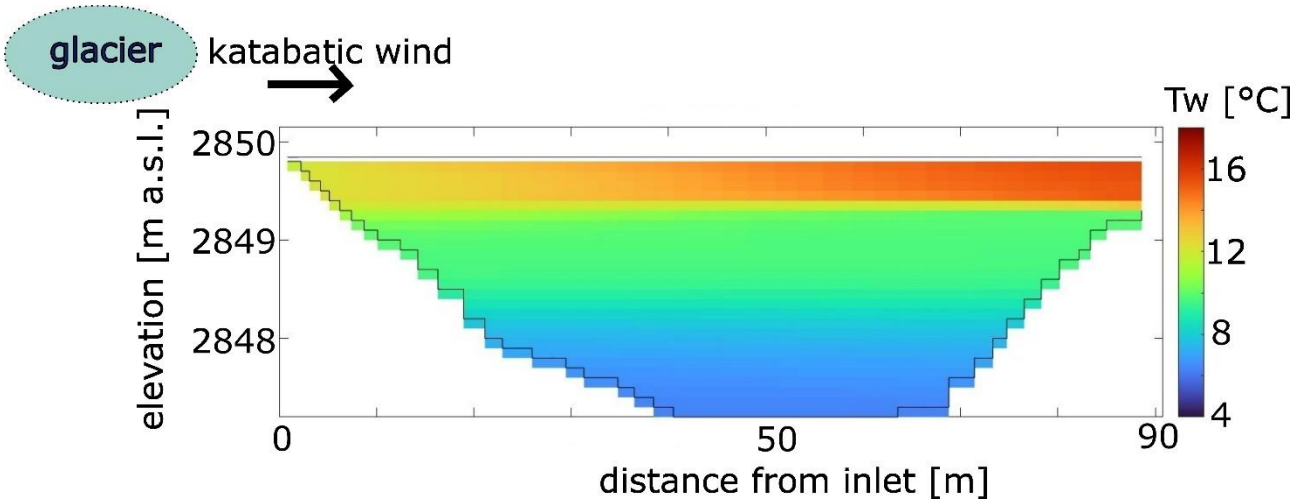

Figure 3. 23. Longitudinal section of L2 showing (colours) the modelled water temperature in L2 on a warm and dry day (20 August 2023, at 14:00).

In this stratified context, currents develop in different layers of the lake (Figure 3. 24). The strongest currents are observed in the horizontal direction and involve mainly the first meter of the water column, while in the deeper layers the horizontal velocities were weaker. As expected in shallow water systems, vertical velocities are always significantly weaker than horizontal ones.

With the katabatic glacier wind applied to the system, two circulations are observed, both counterclockwise in Figure 3. 24. The circulation in the shallow layers is more intense (higher horizontal velocities), whereas the one in deeper layers is weaker.

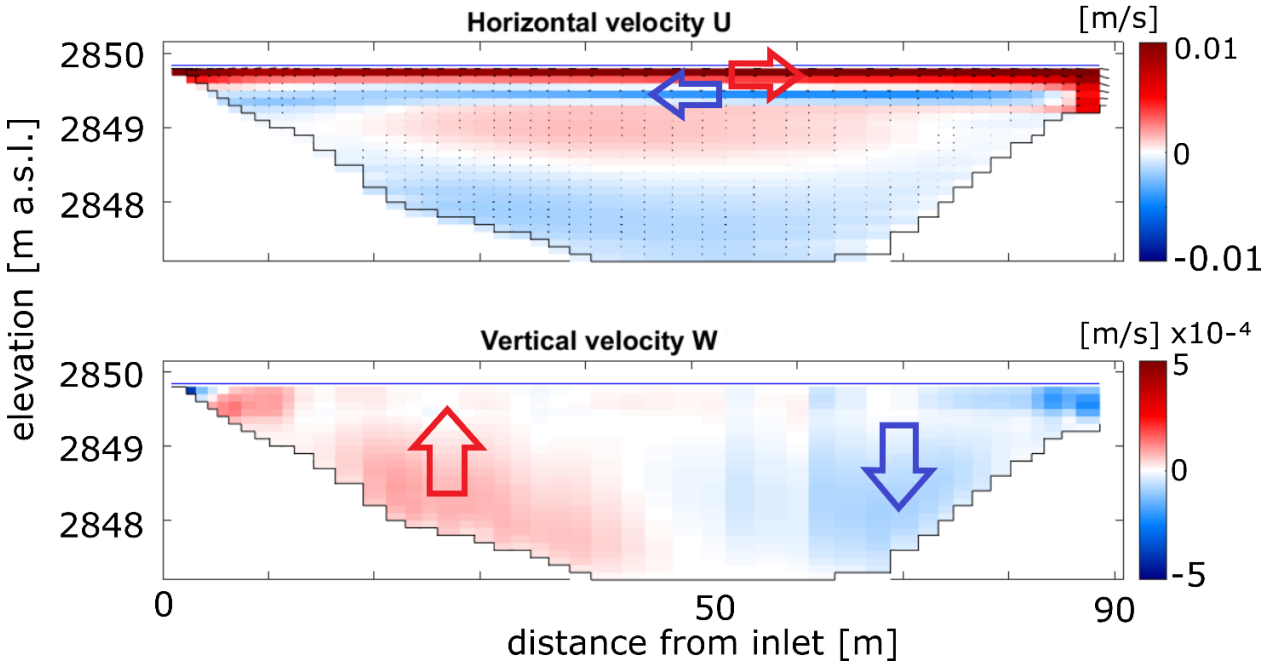

Figure 3. 24. Flow field modelled in the L2 lake on a warm and dry day in summer (20 August 2023 at 14:00). Note the different colour scales.

Periods of daily thermal stratification induced a stable density stratification in the lake and mixing processes involved only the upper layers, which responded directly to heat input from solar

radiation. On the other hand, deeper layers of L2 constitute a cold hypolimnion during warming periods, which is not involved in diurnal processes. This pattern can be clearly observed when considering water age, i.e., the time water has remained in the lake (Wells, 2023b), that increased in deeper layers after a period of stable thermal stratification (Figure 3. 25).

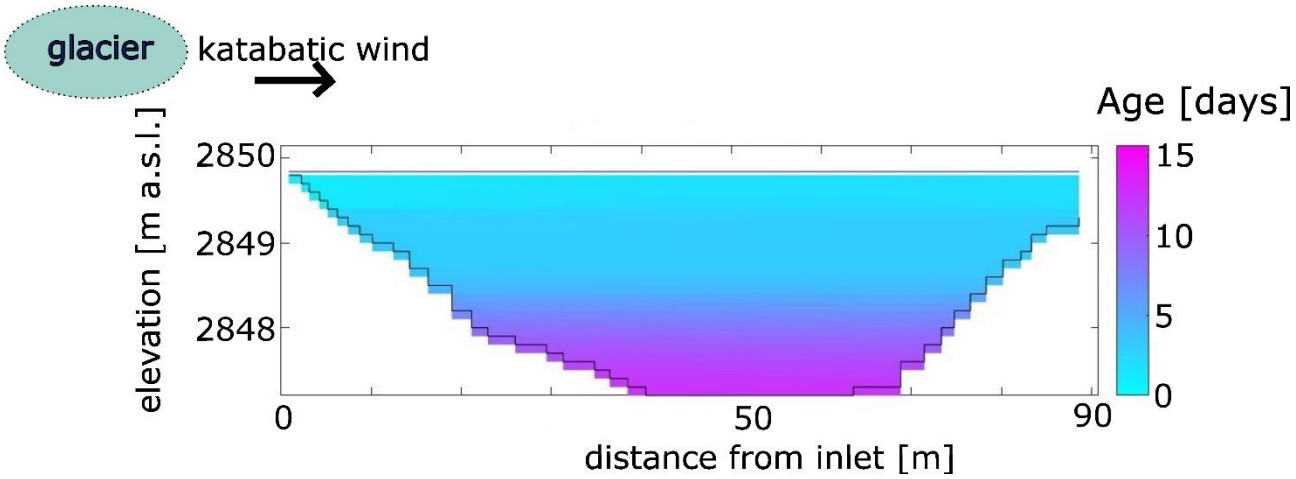

Figure 3. 25. Modelled water age in L2 on 20 August 2023 at 14:00.

The next element addressed in the modelling analysis was the concentration of suspended solids (glacial flour) in the water column. The turbid glacial inflow starts to enter the lake in the late morning, and the concentration of suspended solids simulated by the model in the surface layers (0, 0.2, 0.4 m, see Figure 3. 26) reaches its maximum at around midday in the upstream part. The maximum concentration of ISS reached in the shallow layers of the downstream part is lower than upstream. Therefore, in the first hours of the day, turbidity is limited, especially in the downstream segments (Figure 3. 27) and light can be available in the littoral area for photosynthetic organisms. In the late afternoon, the maximum ISS concentration is observed below the water surface. Consequently, in the afternoon of a warm and dry day, light limitation induced by glacial flour can be mitigated by sedimentation.

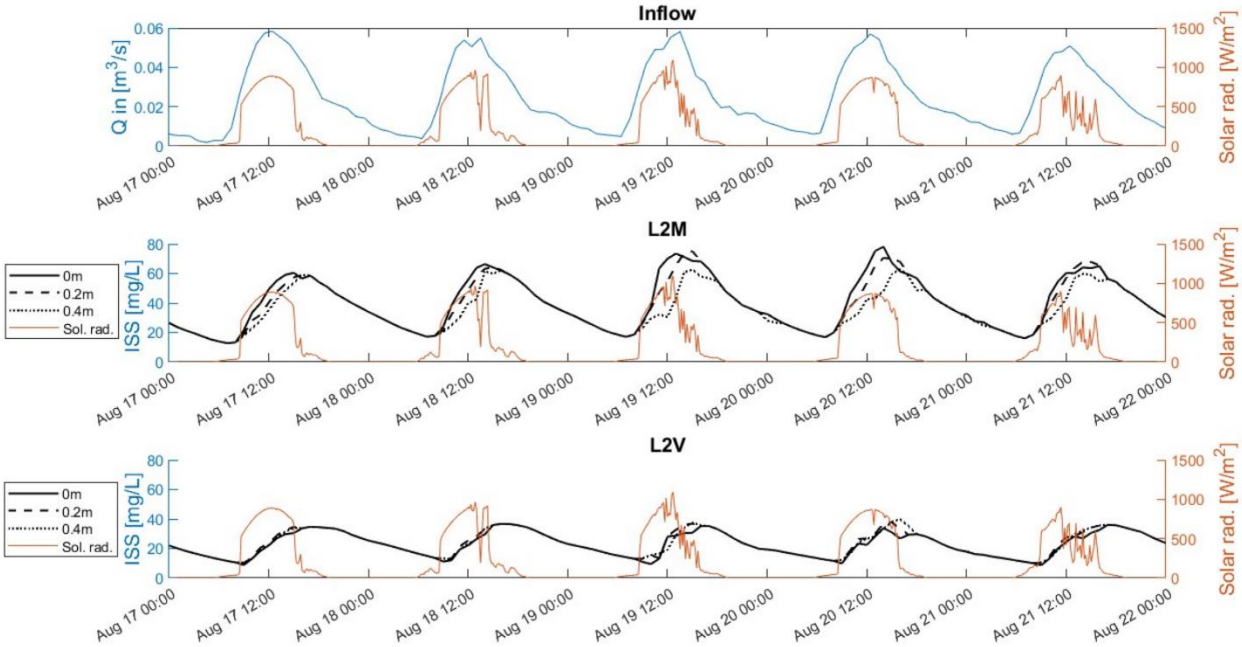

Figure 3. 26. Modelled concentration of suspended solids at 0, 0.2 and 0.4 m (black lines) and incident solar radiation (orange) during a warm and dry period.

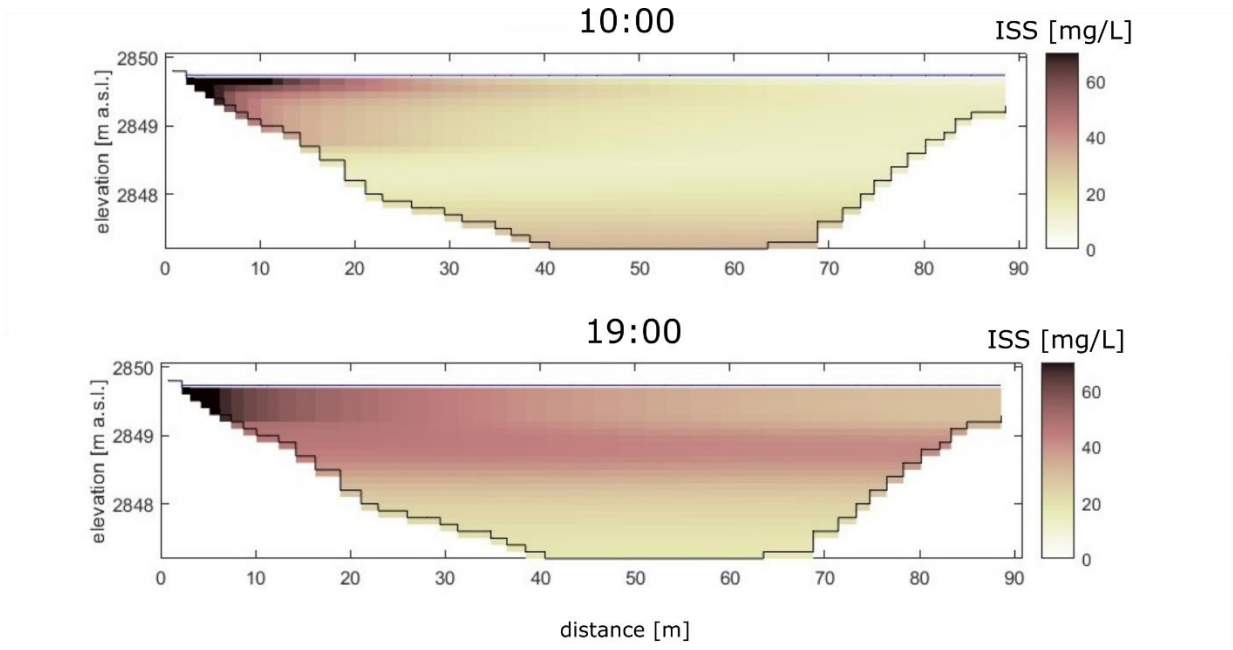

Figure 3. 27. Modelled concentration of suspended solids in the L2 lake on 20 August 2023, in the morning and in the afternoon.

The glacial inflow is heated to a lesser extent than the lake surface layer during warm and dry periods, thus determining a temperature difference between inlet and lake water. This difference in turn determines a difference in water density, which induces the inflow to often enter the lake as an interflow (Figure 3. 28). The cooling of the upper layer is the result of the upwelling current developing in the lake (see the upward arrow in Figure 3. 24), which shifts the colder glacial water from the layer of intrusion towards the surface layers. This movement also involves the suspended

solids, which are, therefore, transported toward the surface in the upstream part. On the other side, the downstream part of the lake is affected by downwelling currents (downward arrow in Figure 3. 24), which allow the sedimentation of suspended particles. This pattern can explain the reduction of turbidity peaks during summer, i.e., August sampling, both in 2022 and 2023 (shown in Figure 3. 14). Indeed, water samples were collected during warm and dry days in the central part of the lake, where suspended solids were already sinking towards the lake bottom.

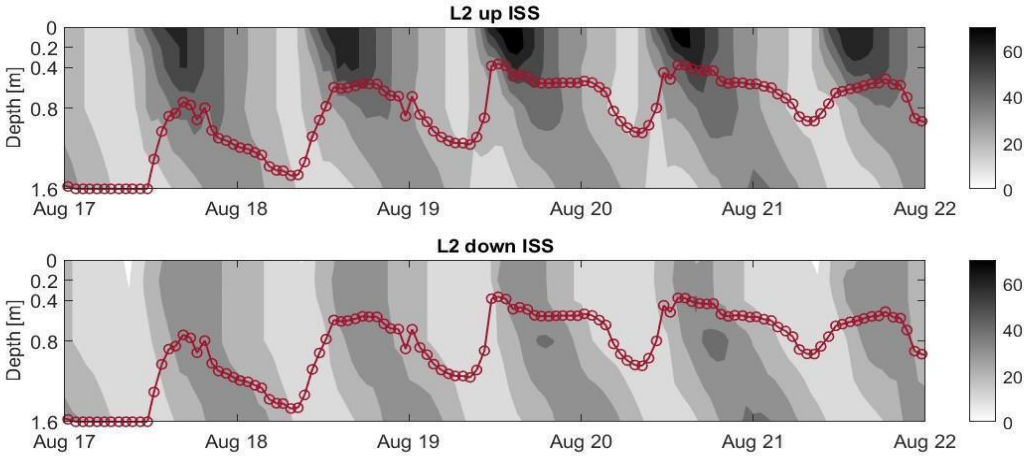

Figure 28. Concentration of inorganic suspended solids (ISS): temporal evolution of the profiles in the upstream and downstream part of the lake, in a warm and dry period. Red dots represent the theoretical depth of intrusion of the inflow, based on water density.

On a seasonal scale, the intensity of the vertical currents (Figure 3. 28 and Figure 3. 29) is reduced during warm and dry periods, whereas precipitation events or air temperature drops induce increased vertical velocity, both in the upstream and downstream parts of the lake.

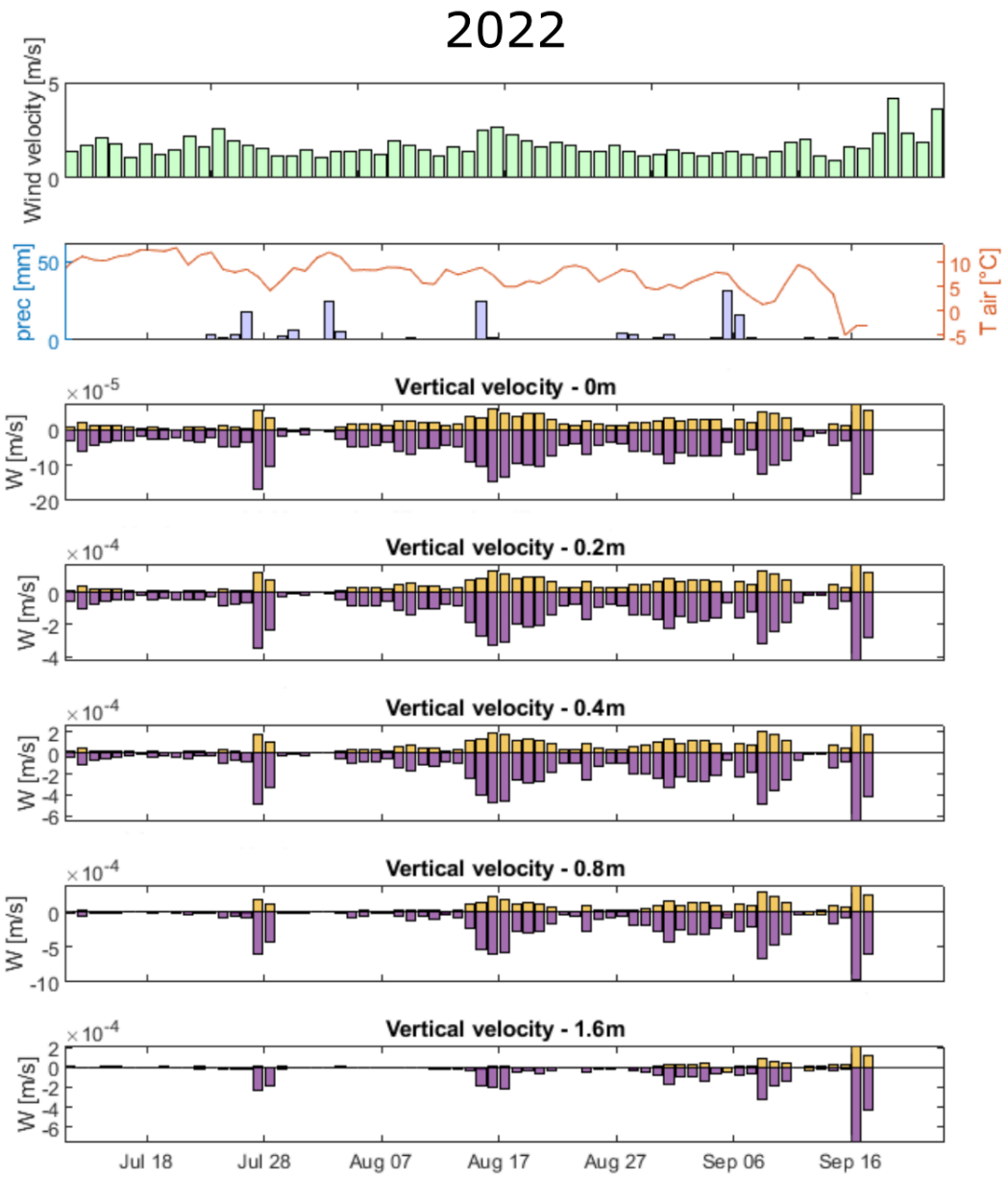

Figure 3. 28. Meteorological conditions (upper panels) and modelled vertical velocity at different depths, in the upstream (yellow bars) and downstream (purple bars) parts of L2, in 2022. Daily values.

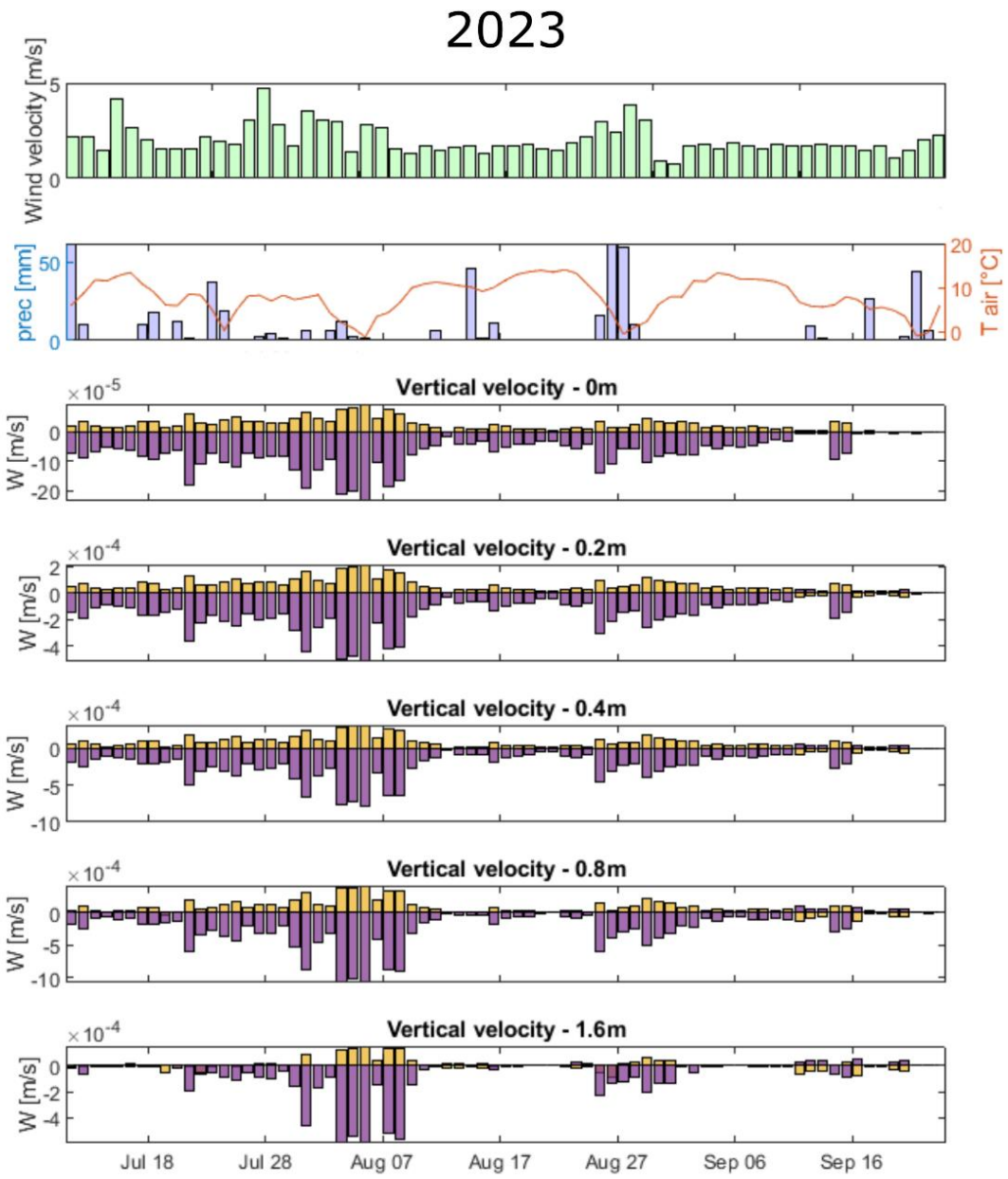

Figure 3. 29. Meteorological conditions (upper panels) and modelled vertical velocity at different depths, in the upstream (yellow bars) and downstream (purple bars) segments of L2, in 2023. Daily values.

Discussion

The loss of contact between proglacial lakes and the glacier is a critical phase for the thermal structure of proglacial lakes. Ice-contact lakes typically maintain uniformly cold thermal conditions, with water temperatures lower than 3.98 °C (e.g., Bird et al., 2022), and the water column is continuously mixed (Otto, 2019), as likely happened in lake L1. This thermal pattern was maintained by both the cold glacier runoff entering the lake and the direct contact of lake water with glacier ice, which in L1 involved at least half of the perimeter and the lake bottom. In contrast, ice-distal

lakes are no longer in contact with the glacier ice and receive warmer water. In L2, the contact with ice involved only one shore of the lake (upstream). Ice-distal proglacial lakes can experience considerable diurnal warming and the development of thermal stratification (Irwin & Pickrill, 1982; Peter & Sommaruga, 2017; Bird et al., 2022). Also, ice distal lakes can often develop longitudinal thermal differences, as observed in L2. For example, in Place Lake (Coast Mountains), a temperature increase of 1.8°C was observed from the inlet to the outlet (Richards et al., 2011); Roseg Lake in the European Alps exhibited a temperature rise of 3.3 °C in the summer period (Uehlinger et al., 2003); in the distal portion of the Bridge Lake in the Coast Mountains, water temperatures increased by 1.9 °C (Bird et al., 2022). In this study, lake L2, despite being in close proximity (about 270 m in 2023) to the glacier, exhibited significant longitudinal thermal differences, likely driven also by the contact with debris-covered ice in its upstream part. Specifically, the average longitudinal difference reached 2.1 °C in the surface layer in the central part of the lake, and 1.6 °C in the littoral area. According to these thermal differences and to the stratification patterns observed, L2 can be considered an ice-distal lake, even if it is very close to the glacier and in contact with debris-covered ice. In L3, longitudinal thermal differences were close to 0 or slightly negative (-0.1 °C in the two seasons), indicating a more homogeneous environment. Horizontal gradients in proglacial lakes can have deep influences on lake habitat characteristics. For instance, Hylander et al. (2011) observed that longitudinal differences in the water light extinction coefficient in a glacier-fed lake in the Andes, Lake Mascardi, influenced the depth distribution of phytoplankton and the relative abundances of zooplankton, within the same lake. Our results confirm that even small water bodies, such as L2, can exhibit significant longitudinal thermal differences with potential ecological consequences. These differences are particularly relevant when considering habitat heterogeneity and the potential for differential responses of aquatic organisms to temperature and light conditions within the same lake. In ice-distal lakes, where thermal stratification occurs, the thermocline separates lake layers (Ashley, 2002), and thermal stratification affects the distribution of suspended solids. The suspended glacial flour tends to sink to the deeper layers, at a depth of intrusion depending on temperature and turbidity differences, i.e., density, between the glacial inflow and lake water (Otto 2019). In the occurrence of underflows and interflows, cold meltwater moves along the lake bottom, as has been previously documented in other proglacial lakes (e.g., Robb et al., 2021, Hardmeier et al., 2024). The estimated depth of intrusion of the inflow in L2 is likely an underestimate, given that the presence of suspended particles can increase water density (Sugiyama et al., 2016; Hardmeier et al., 2024).

Sedimentation patterns in proglacial lakes are also strongly influenced by meteorological conditions (Chikita, 1999; Peter & Sommaruga, 2017). The local variability in mountain weather conditions can contribute to discrepancies in model predictions for L2, particularly evident in late September 2023. However, despite the weather data from the Madritsch meteorological station may not fully capture the specific conditions in the Cevedale proglacial area, the general seasonal trends were well reproduced, and the model provided valuable insights into the general response of the lake to meteorological forcing. In L2, events of meteorological instability were associated with total mixing and cooling of the water column, and increased vertical velocity compared to warm and dry periods. This corresponds to strong increases in turbulence and, in turn, possible resuspension of the glacial flour that results in an increase of turbidity. Conversely, under stable meteorological conditions,

with warm and dry weather, vertical velocity was reduced. When the turbid inflow enters the lake as an interflow, the patterns of circulation induced by katabatic glacier winds allow the sedimentation of solids in the downstream part of the lake. Therefore, sedimentation processes can mitigate the light limiting effect of glacier-derived turbidity in the shallow layers of L2, in the downstream part of the lake, creating more suitable conditions for primary production in the littoral area. This setting could open the possibility of additional Windows of Opportunity for periphyton growth in summer.

Windows of opportunity and periphyton growth

Benthic primary production in glacier-fed Alpine water bodies such as streams is typically inhibited during the summer period of glacier ablation (Uehlinger et al., 2010). We measured benthic growth in L2 during summer of 2022 and 2023 every month, as described in Chapter 2, both in terms of chlorophyll *a* and organic content in quantitative biofilm samples. Surprisingly, an enhanced benthic growth was observed in August 2022, both in terms of primary productivity (measured as chlorophyll *a*) and of the biofilm organic content (Figure 3. 30), while in August 2023 benthic communities showed a suppression of their growth.

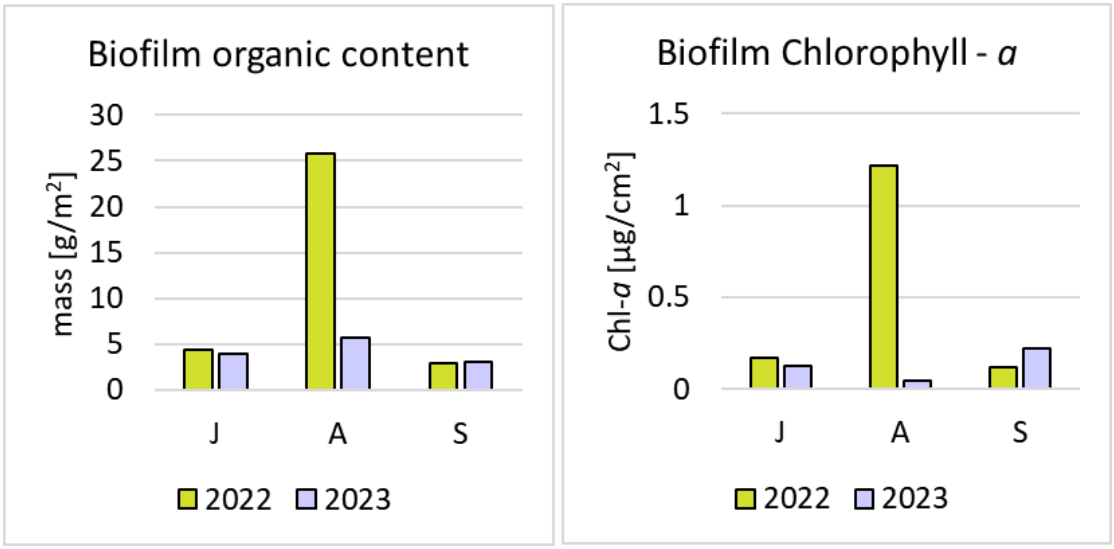

Figure 3. 30. Biofilm organic content and chlorophyll *a* in the littoral area of L2 lake. J = June, A = August, S = September.

The meteorological conditions and modelled habitat characteristics in the lake (water temperature and concentration of inorganic suspended solids) in the 10 days before the field campaigns in August are shown in Figure 3. 31 (2022) and Figure 3. 32 (2023). Meteorological conditions were characterised by higher mean air temperatures in 2022 than in 2023 (8.4 °C and 6.5 °C, respectively), with colder minima in 2023 and warmer maxima in 2022 (min = 2.2 °C in 2022, -1.8 °C in 2023; max = 16.7 °C in 2022, 11.8 °C in 2023). Furthermore, precipitations were more intense in 2023 (77.5 mm cumulated over the period, with a maximum of 37.1 mm in one day) than in 2022 (28.7 mm cumulated over the period, with a maximum of 18.3 mm in one day). Raining events can disrupt the thermal stratification of proglacial lakes, as precipitation flowing on glacier ice is cooled and enters the lake at low temperatures (Peter & Sommaruga, 2017), weakening the thermocline.

Furthermore, the limited heat input due to cloud cover does not induce the warming of surface layers, as observed in warm and dry days. The modelled response of the lake water column to this condition shows stronger surface heating in 2022 than in 2023: average surface (0 m) water temperature is 11.4 °C in 2022 and 7.2 °C in 2023, with a maximum of 18.9 °C in 2022, and of 10.9 °C in 2023. In 2023, less stable meteorological conditions induced more frequent mixing events, associated with higher vertical velocities in the period (Figure 3. 29). Therefore, littoral communities may have responded both to warmer water temperature with enhanced metabolic and replication rates (Teoh et al., 2010), and to light availability with enhanced photosynthetic rates, resulting in accelerated biofilm formation (Villanueva et al., 2011). No other significant patterns were recognised in other environmental factors (e.g., nutrient concentration), suggesting that temperature and light may be the dominant factors influencing benthic growth in L2. These windows of milder habitat conditions in summer may be further exploitable by photosynthetic organisms as they can occur in correspondence to longer photoperiod compared to autumn.

The littoral area of L2 was also characterised by the continuous deposition of fine sediment on the lake shores, which shapes the habitat characteristics where benthic littoral communities grow, potentially creating selective pressures that foster the establishment of specialised communities (e.g., epipelic). Furthermore, due to water level fluctuations induced by meltwater flow pulses, littoral communities are likely subject to daily periods of emersion, another potential selective environmental factor for algal communities.

The predicted alterations in air temperatures and in the distribution of rain events induced by climatic changes (Kotlarski et al., 2022) will likely alter the physical dynamics of proglacial lakes. A trend toward warmer and drier conditions during Alpine summers could accelerate colonisation processes in the littoral areas of proglacial lakes by inducing longer and more stable thermal stratification and increased algal growth. Furthermore, the shrinking and fragmentation of the glacier may cause a decay of katabatic wind currents and a progressive incursion of up-valley winds over the glacier area (Shaw et al., 2023), a condition that would alter the flow currents in the lake, and consequently sedimentation patterns.

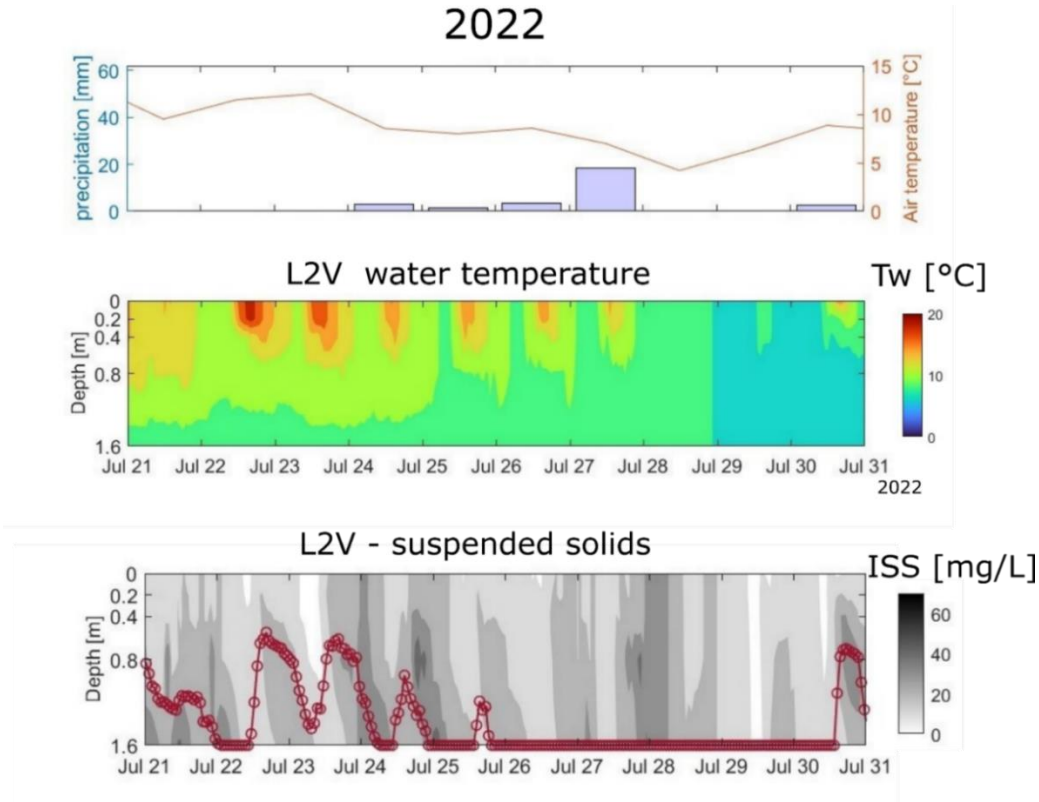

Figure 3. 31. Meteorological conditions and modelled lake water temperature and suspended solids concentration in the 10 days before the sampling in summer 2023 (1 August 2022). Red dots represent the theoretical depth of intrusion of the inflow, based on water density.

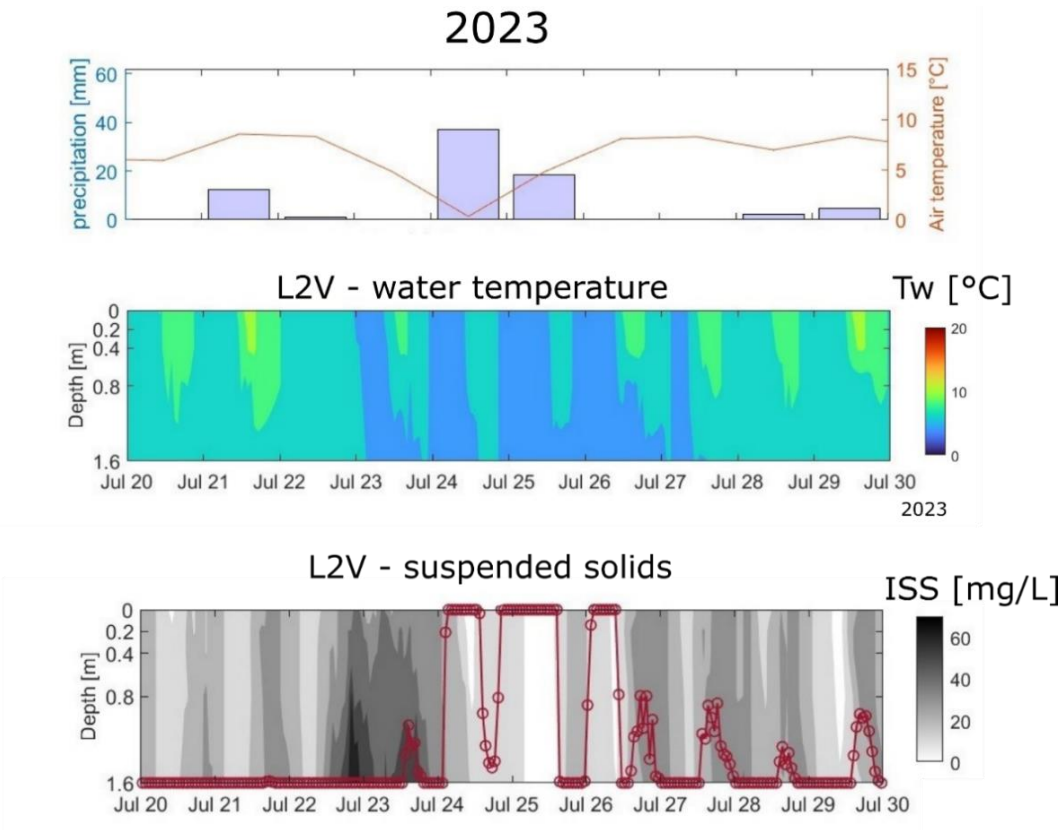

Figure 3. 32. Meteorological conditions and modelled lake water temperature and suspended solids concentration in the 10 days before the sampling in summer 2023 (31 July 2023). Red dots represent the theoretical depth of intrusion of the inflow, based on water density.

Concluding remarks

Among the Cevedale proglacial lakes, L1 can be classified as an ice-contact lake, while L2, LC and L3 are distal lakes. L2 showed typical characteristics of an ice-distal lake, such as thermal stratification, despite its recent appearance (approx. 2018, see Chapter 2) and its proximity to the glacier (about 270 m in September 2022, 300 m in September 2023), suggesting a particularly fast evolution of the system. The littoral habitat of L2 was influenced by thermal patterns. Thermal stratification formed during warm and dry periods and induced warming of surface layers, allowing the sedimentation of glacial flour, and mitigating the light limiting effect of fine suspended solids. Warm temperatures and light availability can affect the timing of windows of opportunity for littoral algal growth, inducing additional windows in summer (with respect to the typical ones occurring in autumn) and accelerating algal colonisation processes.

Chapter 4

Benthic diatom communities of the Cevedale proglacial lakes

Introduction

Diatoms (class *Bacillariophyceae*) are unicellular, eukaryotic algae that produce a siliceous cell-wall made by opaline silica (SiO_2, Round et al., 1990). Diatoms include mainly photosynthetic pigmented organisms that colonise all the aquatic ecosystems in the world, with a multitude of adaptations to different ecosystems and their environmental conditions (Stevenson et al., 2010). Diatom taxonomy is very developed, and more than 24000 species were already described (Julius & Theriot, 2010). Furthermore, their ecological preferences are largely investigated by the scientific community (e.g. Van Dam et al., 1994; Smol & Stoermer, 2010). Diatoms are used as bioindicators (e.g., U.S. Clean Water Act of 1972 and European Water Framework Directive 2000/60/EC), as they are widespread and highly sensitive to environmental conditions. Therefore, the analysis of diatom communities, while providing valuable biodiversity and conservation insights, allows to gather important information about the conditions of the habitats that host the community.

Diatoms are also among the main algal groups composing phytobenthic communities in high-altitude water bodies, together with cyanobacteria, chrysophytes, and chlorophytes (Rott et al., 2006; Fell et al., 2017; Busi et al., 2022; Sudlow et al., 2023). Benthic diatoms form distinct communities in turbid mountain lakes compared to clear mountain lakes (Feret et al., 2018).

The Alpine glacial summer is characterised by three main hydrological phases, i.e., snow melt, glacier ablation (ice melt) and glacial recession (base flow), that determine a seasonal succession of habitat conditions which are particularly evident in glacier-fed water bodies. Previous studies on benthic diatoms of Alpine proglacial lakes mainly focused on regional patterns (e.g., Feret et al., 2018) while rarely addressing the seasonal evolution of communities.

This chapter presents and discusses the results obtained from the analysis of the benthic diatom communities of the Cevedale proglacial lakes, based on the samples collected during the ice-free season of 2022 and 2023. No previous studies on the biological communities of the Cevedale proglacial lakes have been published to date. Diatom samples were analysed addressing diatom density, taxonomic composition and ecological strategies. This study aims at: (i) provide the first characterisation of the diatom flora of the Cevedale proglacial lakes; (ii) exploring role of varying glacial influence in shaping the density and taxonomical composition of diatom communities.

Material and methods

Benthic diatom communities of the Cevedale proglacial lakes were analysed by adopting a quantitative morphological approach. Samples were collected at each sampling occasion during the ice-free seasons in 2022 and 2023, i.e., in June/July (as soon as snowpack and ice conditions allowed

to reach the study site), early August, and middle/late September. In 2022, communities of lakes L1, L2 and L3 were investigated, while in 2023, after the flood and disappearance of L1, LC was added to the analysis. In 2022, one integrated sample was assembled for each lake at each sampling session, while in 2023 samples from L2 and L3 were collected separately in the upstream (M) and downstream (V) portions of these lakes. Periphyton samples were assembled by collecting the biofilm from the substrata that characterised the littoral area of the lakes, i.e., pebbles (epilithic samples) and cohesive sediment (epipelic samples). A known area of biofilm was collected by brushing the substratum with a clean toothbrush, to obtain quantitative samples. The reference area was delimited with a 3 x 3 cm nitrile frame, shown in Figure 4. 1a.

The collected material was preserved in polyethylene bottles in ethanol at a final concentration of 50%. Samples were treated according to the Italian and European guidelines for the analysis of benthic diatom communities (APAT 2007; CEN 2014). Diatom samples were transferred into 100 mL Pyrex flasks and organic matter, which hinders the observation of diatom frustules, was removed by oxidation, by adding 30% hydrogen peroxide (H_2O_2) and heating the mixture at 90 °C on a heating plate (Figure 4. 1b). Samples containing particularly resistant organic matter were finally treated with a small quantity of the strong oxidant potassium bichromate ($K_2Cr_2O_7$), until the colour of the solution turned from opaque green/yellow to limpid blue/purple. At the end of the oxidation, samples were added with a small volume of 37% HCl, to dissolve carbonates. Samples were then decanted overnight. The diatom suspension was transferred to a 50mL Falcon tube by using a Pasteur pipette. The solid phase, containing coarse mineral material, was removed after careful rinsing with distilled water. Samples were centrifuged at 1700 rpm for 15 minutes at 20 °C and the liquid phase was removed. The pellet was then resuspended in distilled water and centrifugation was repeated. This rinsing procedure was repeated 3 times, to completely remove the reagents. Finally, the pellet was resuspended with a small volume of distilled water to be transferred into glass vials. The clean diatom suspension was finally preserved in ethanol 90%.

To allow quantitative diatom analyses, all sample volumes were equalised at 6 ml. In the case of samples with a total volume > 6 ml, a subsample was extracted after homogenisation. Then, a known quantity of microscopic marker was added in each sample. Sample volumes of 6 ml were added with 1 ml of a standard solution of divinylbenzene microspheres (diameter 8-10 µm, concentration 8.02 10^6 ml^{-1}). The suspensions of diatoms added with the microspheres were used to prepare permanent slides. Few drops of each sample were collected with a clean Pasteur pipette and diluted in distilled water into a separate clean glass vial. After homogenisation, a small aliquot of the diluted suspension was withdrawn with a clean Pasteur pipette and distributed on three round cover glasses (13 mm diameter) placed on a clean slide (Figure 4. 1c). Drops were left to dry on cover glasses at room temperature. Permanent slides were mounted in Naphrax®, with 1.7 refraction index.

Dilutions were variable and were iterated until obtaining a suitable concentration of diatoms, microspheres and inorganic grains for the microscopical observation. Diatom identification and counting were performed using a Leica DM2500 optical microscope (LM) equipped with differential interference contrast optics at 1000x magnification (Figure 4. 1d). Micrographs and measurements of the specimens were taken at the LM using the Leica LASX Software (version 3.7.6.25977) for digital image acquisition and processing. Taxonomic identification of diatom valvae followed current

reference literature (Lange-Bertalot et al., 2017; Lange-Bertalot & Gankal, 1999; Krammer, 2000; Levkov et al., 2016; Krammer & Lange-Bertalot, 1986-2000), completed by recent papers for taxonomical updates at species level (e.g., Hlúbiková et al., 2009; Kulikovskiy et al., 2023). Diatom valvae were identified at the lowest taxonomic level (i.e., species or variety) whenever possible. The taxonomic identification of some critical species was validated by analysing samples with a scanning electron microscope (SEM, Jeol JSM-IT300LV), at the Micro-structural Analysis Laboratory of the Department of Industrial Engineering of the University of Trento.

Figure 4. 1. Main steps of the treatment of diatom samples, see text for details. a) Collection of samples by brushing a known area of substratum with a 9 cm^2 template; b) oxidation of organic matter and dissolution of carbonates in the samples, on the heating plate; c) drops of diluted samples drying on the cover glasses during permanent slide preparation; d) digital microphotography at the light microscope (magnification 100x), showing three microspheres and a diatom frustule (*Odonthidium mesodon* (Ehrenberg) Kützing, 1844), in girdle view.

The determination of diatom density per unit area was performed by counting at least 400 valvae per mount (CEN 2004) and simultaneously enumerating the microspheres present in each field. For very diluted permanent slides (<400 valvae in a slide), at least 1000 microspheres were counted. Diatom density per unit area was then estimated according to Battarbee et al. 2001. The total number of diatom valvae in one sample (N_s) was calculated as:

$$N_s = \frac{n_{m0}\, n_v}{n_m}, \tag{4. 1}$$

where $n_{m0} = (c_m\, V_m)$ is the number of microspheres introduced in the sample obtained as the concentration of divinylbenzene microspheres (c_m) multiplied the volume of solution added to the sample, n_v is the number of valvae counted in the sample, and $n_m$is the number of microspheres counted in the sample. Diatom density (D), expressed as the total number of valvae per cm^2, was then obtained as:

$$D = \frac{N_s}{A_s}, \tag{4. 2}$$

where N_s is the total number of valvae in the sample and A_s is the brushed area on the substratum (cm^2). All counts were performed in 3 replicates to calculate the standard error of the density estimates.

Diatom biodiversity was analysed based on the final community compositions. Species represented by less than 2 valvae (i.e., one cell frustule) in each sample were not considered in the computation. Similarly, specimens identified only at higher taxonomic level than genus were not considered in the biodiversity analyses. All analyses were performed in R version 4.3.2 (R Core Team 2023). Alpha-diversity was analysed using the *vegan* package (Oksanen et al., 2022), computing species richness (number of observed species in the sample) and the Shannon Index (Shannon & Weaver, 1949). The Pielou's Evenness (Pielou, 1975) was used to evaluate the heterogeneity of the diatom assemblages. Beta-diversity was analysed by computing a Bray-Curtis distance matrix of samples based on taxa relative abundances. The Bray-Curtis distance was also used to perform a Non-metric Multidimensional Scaling (NMDS, Kruskal & Wish, 1978). Statistical differences between diatom assemblage composition in the studied lakes were tested by computing the analysis of similarity (ANOSIM, Clarke, 1993). The relationship between environmental variables (log+1 transformed) and diatom community structure was examined by applying the *envfit* function of the *vegan* package, that fits environmental vectors into the NMDS ordination. Spearman rank order correlation coefficients between environmental variables and the NMDS ordination were computed to assess the significance of each relationship.

The presence of rare species within the diatom communities of the proglacial lakes was tested based on the German Red List of diatoms (Hofmann et al. 2018). To investigate the ecological traits of diatom communities, diatom taxa were grouped into functional groups according to data aggregated in the Diat.barcode database (Rimet et al., 2018; Rimet et al., 2019a). Ecological preferences toward presence of water and nutrients in the habitat (aerophily and trophic status, respectively) and pH were derived from van Dam et al., 1994 and Rimet et al., 2019a. Habitus and ecological guilds of the identified diatom species were classified based on Passy et al. (2007), which grouped diatom taxa into three ecological guilds—high-profile, low-profile, and motile—based on their competitiveness in utilizing resources (nutrients and light) and their ability to cope with disturbance. The low-profile guild comprises species that grow very near the substrate and firmly attached to it, including adnate, prostrate, and short-stalked forms. These species typically remain within the biofilm boundary layer, which confers increased resistance to physical disturbances. However, their position also limits access to light and nutrients. In contrast, the high-profile morphological guild includes taller forms, capable of extending beyond the biofilm boundary layer through the development of elongated structures such as stalks, tubes, or chains. This elevated position facilitates access to light and nutrients but increases exposure to physical disturbances, such as current scouring and grazing. Lastly, the motile guild consists of species that actively move across the substrate by gliding along their raphe, allowing them to selectively occupy microhabitats.

Results

Diatom density

Periphytic diatom density as determined under the light microscope showed an increasing spatial trend according to the decrease of glacial influences from L1 to L3 (Figure 4. 2).

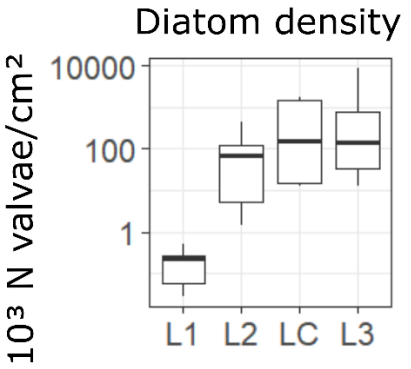

Figure 4. 2. Median, 25th percentile and 75th percentile of estimated diatom densities in the analysed samples, grouped by lake.

Benthic diatom assemblages were extremely diluted in the ice-contact lake L1, where the lowest density of the whole lake system was observed (0 – 0.2 10^3 valvae/cm^2). Density increased in L2, ranging from 2.87 10^3 to 405.76 10^3 valvae/cm^2, while the two samples analysed in LC in 2023 showed a significant benthic growth in September 2023 (1524.84 10^3 valvae/cm^2) compared with August 2023 (15.17 10^3 valvae/cm^2). Finally, density in L3 reached the highest values in the system, ranging from 19.00 10^3 to 4589.63 10^3 valvae/cm^2. L1 and L2 showed comparable seasonal changes, with density increase from June to the August maximum, followed by a pronounced drop from August to September (Figure 4. 3). Conversely, L3 showed increased and particularly intense diatom growth in August 2023, in the upstream portion of the lake.

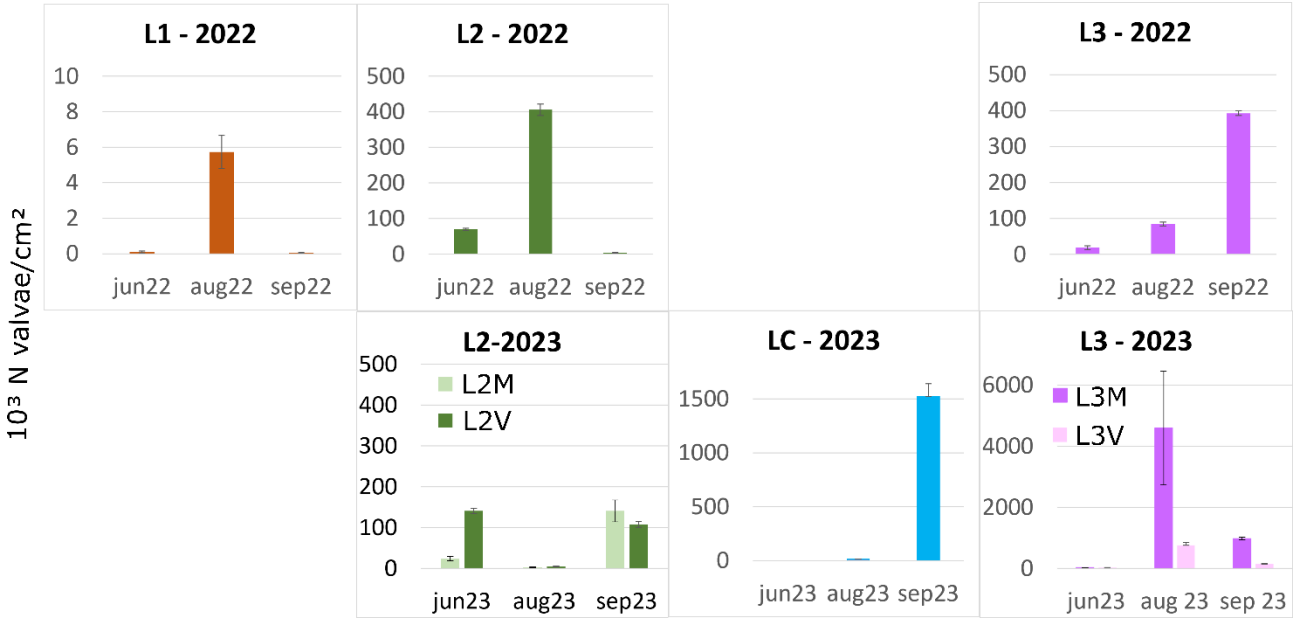

Figure 4. 3. Diatom density in the counted samples, grouped by lake and season, with error bars (standard error). In 2022 and 2023, both upstream (L2M and L3M) and downstream (L2V and L3V) samples, where available, are shown for each month.

Diatom taxonomic composition and diversity

In the 21 diatom samples collected from the Cevedale proglacial lakes, 36 diatom taxa were identified, belonging to 17 genera (Table 4. 1). The taxonomic composition of the analysed samples is show in Figure 4. 5. Micrographs of the main species identified in the samples are presented in supplementary material S4.1.

The most abundant genus across all analysed samples was *Achnanthidium* (38.6% average relative abundance), followed by *Encyonopsis* (14.7%), *Encyonema* (9.9%), *Pinnularia* (9.3%), *Caloneis* (7.3%), *Gomphonema* (5.8%), *Nitzschia* (5.8%) and *Surirella* (3.0%). Other genera showed relative abundances lower than 1%. Some of the most abundant genera showed remarkable spatial trends (Figure 4. 4). The genus *Achnanthidium* was predominantly represented by the species *Achnanthidium minutissimum* (mean relative abundance across all samples 38.5%), which was the most abundant species in all L2 samples, and the only species found in L1 in August 2022, albeit with a low number of valvae. In LC, the relative abundance of *A. minutissimum* ranged from 7.9% to 61.4%, while in L3 it was still present, but with lower relative abundance (0.5-14.2%). *Encyonopsis* exhibited variable abundance across the lake system and was represented by two species. In L2 and L3, *Encyonopsis falaisensis* was the most frequent species of the genus (mean relative abundance across all samples 10.2%), in LC *Encyonopsis microcephala* var. *robusta* was observed, reaching the remarkable relative abundance of 51.9% in September 2023. In this lake, *E. falaisensis* accounted for 24.2% to 27.1% of the community. *Encyonema* was almost exclusively found in L3, especially in the upstream part, where it made up to 64.6% of the community (September 2023). The genus *Pinnularia* was frequently observed in L3, especially in the downstream part, where it made up to 54.6% of the community (July 2023). Notably, the relative abundance of *Pinnularia* in L3 was higher in the epipelic (indicated with * in Figure 4. 5) than in the epilithic samples, ranging, respectively, from 20% to 54% and from 0.25% to 7.1% (Wilcoxon-Mann-Whitney test, $p < 0.05$). In only one sample from L1, *Pinnularia* accounted for 30.8% of the counted valvae. However, it is important to remark that only 26 valvae were counted in this whole slide, with *Pinnularia* sp. being represented by just 8 valvae. Similarly, the high relative abundances of *Caloneis* in L1 corresponded to few valvae counted (7 in June and 26 in August), attributed to *Caloneis aerophila* (mean relative abundance across all samples 6.1%). The genus *Gomphonema* was found exclusively in L3, where it appeared in all the samples and accounted for 3.9% to 38.9% of the diatom communities. The most abundant species of the genus in the dataset was *Gomphonema varioreduncum* (mean relative abundance 5.5%). *Nitzschia* was observed mainly in L2 and L3. *Surirella* showed a low but even distribution among the distal lakes and was absent only in L1.

Table 4. 1. List of diatom taxa identified in the samples collected in the Cevedale proglacial lakes in 2022 and 2023. N samples = number of samples where the species was observed; max% = maximum relative abundance of the species in the dataset; max n valvae = maximum number of valvae attributed to the species in one sample; + and – symbols indicate respectively presence (at least one observation in one sample) or absence of the species in each lake (no observations across all samples).

Taxon	n samples	max%	max n valvae	L1	L2	LC	L3
Achnanthidium minutissimum (Kützing) Czarnecki, 1994	22	100.0	431	+	+	+	+
Achnanthidium pyrenaicum (Hustedt) H.Kobayasi, 1997	2	2.2	4	-	-	+	+
Adlafia minuscula (Grunow) Lange-Bertalot, 1999	5	1.9	8	-	+	-	+
Amphora C.G. Ehrenberg ex F.T. Kützing, 1844	1	0.9	4	-	-	-	+
Caloneis P.T. Cleve, 1894	4	4.5	19	-	+	-	+
Caloneis aerophila W.Bock, 1963	7	100.0	28	+	-	-	+
Caloneis vasileyevae Lange-Bertalot, Genkal & Vekhov 2004	5	10.4	19	-	-	-	+
Denticula tenuis Kützing, 1844	1	1.6	8	-	-	+	-
Encyonema Kütz., 1833	6	14.2	57	-	+	-	+
Encyonema minutum (Hilse) D.G.Mann, 1990	5	3.7	15	-	-	-	+
Encyonema silesiacum (Bleisch) D.G.Mann, 1990	7	46.6	210	-	-	-	+
Encyonopsis falaisensis (Grunow) Krammer, 1997	20	31.5	143	-	+	+	+
Encyonopsis microcephala var. *robusta* (Hustedt) Krammer, 1997	9	51.9	255	-	+	+	+
Encyonopsis sp. (aff. *microcephala* var. *robusta* (Hustedt) Krammer, 1997)	2	8.6	42	-	-	+	-
Eucocconeis laevis (Østrup) Lange-Bertalot, 1999	2	0.5	2	-	+	-	-
Gomphonema C.G. Ehrenberg, 1832	7	1.2	5	-	-	+	+
Gomphonema varioreduncum Jüttner, Ector, E. Reichardt, Van de Vijver & E.J.Cox, 2013	9	37.7	160	-	-	-	+
Hantzschia amphioxys (Ehrenberg) Grunow, 1880	2	0.5	2	-	-	-	+
Mayamaea permitis (Hustedt) K.Bruder & L.K.Medlin, 2008	1	1.1	2	-	-	-	+
Navicula cryptocephala Kützing, 1844	8	7.3	31	+	+	-	+
Nitzschia A.H. Hassall, 1845	2	1.4	6	-	-	-	+
Nitzschia acidoclinata Lange-Bertalot, 1976	2	1.4	6	-	-	-	+
Nitzschia palea var. *debilis* (Kützing) Grunow, 1880	9	4.2	15	-	+	+	+
Nitzschia perminuta (Grunow) M.Peragallo, 1903	10	2.4	11	-	+	-	+
Nitzschia sp. (aff. *pura* Hustedt 1954)	18	38.6	129	-	+	+	+
Odontidium mesodon (Ehrenberg) Kützing, 1844	3	11.5	10	+	+	-	+
Pinnularia C.G. Ehrenberg, 1843	3	30.8	8	+	-	-	+
Pinnularia borealis Ehrenberg, 1843	2	0.5	2	-	+	-	+
Pinnularia brebissonii (Kützing) Rabenhorst 1864	1	1.0	2	-	-	+	-
Pinnularia bullacostae Krammer & Lange-Bertalot, 1999	10	30.1	127	-	+	-	+
Pinnularia microstauron var. *nonfasciata* Krammer, 2000	1	2.7	5	-	-	-	+
Pinnularia obscura Krasske, 1932	7	28.4	52	-	+	-	+
Pinnularia obscuriformis Krammer 2000	6	6.3	4	-	+	-	-
Psammothidium helveticum (Hustedt) Bukhtiyarova & Round, 1996	11	4.3	9	-	+	+	+
Surirella P.J.F. Turpin, 1828	11	4.8	13	-	+	+	+
Surirella terricola Lange-Bertalot & E.Alles, 1996	19	9.5	29	-	+	+	+

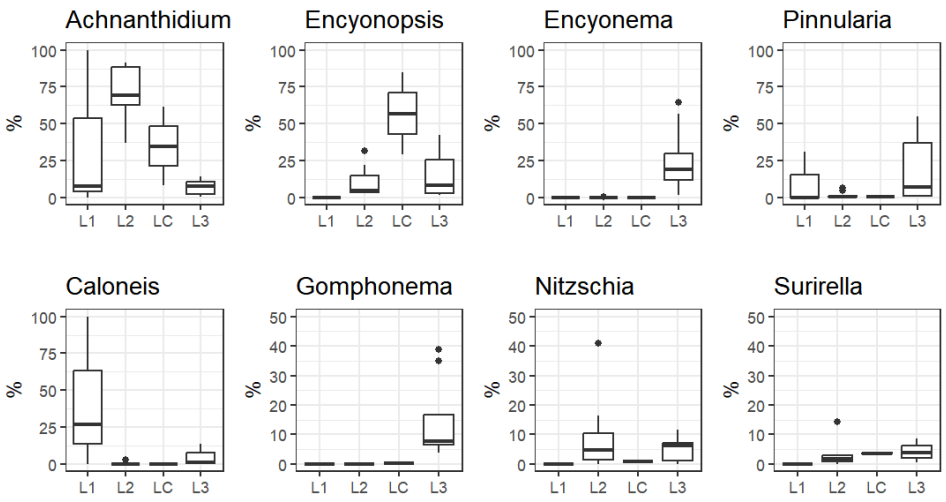

Figure 4. 4. Relative abundance of the four most represented genera found in the samples from the Cevedale lakes. Samples are ordered from left to right representing a gradient of glacial influence.

According to the German Red List of freshwater diatoms (Hofmann et al. 2018), two of the species identified in the studied lakes are considered as extremely rare: *Caloneis vasileyevae* and *Caloneis aerophila. Caloneis vasileyevae* was previously observed in alpine lakes and ponds of Turkey, including glacier-fed ones (Solak et al. 2023). *Pinnularia obscuriformis* and *Pinnularia microstauron* var. *nonfasciata*, are classified as very rare, and two, *Encyonopsis falaisensis* and *Eucocconeis laevis*, as rare. Several of the most common species in the lakes are classified as common (*Odontidium mesodon, Achnanthidium minutissimum, Adlafia minuscula, Achnanthidium pyrenaicum, Hantzschia amphyoxis, Navicula cryptocephala*) or very common (*Encyonema silesiacum, Encyonosis microcephala* var. *robusta, Pinnularia obscura, Psammothidium helveticum, Nitzschia perminuta, Encyonema minutum, Nitzschia acidoclinata, Denticula tenuis, Pinnularia brebissonii* and *Pinnularia borealis*). *Surirella terricola* and *Gomphonema varioreduncum* are widespread species in Europe (Guiry, 2016; Karlson et al., 2018). *Pinnularia bullacostae* (not included in the red list as typical for polar and subpolar ecosystems) has never been previously detected in the European Alps. Nonetheless, it formed a stable population on one shore in the downstream part of L3 covered with fine sediment (epipelic substratum), where it accounted for 16.6 to 30.1% of the total number of counted valvae in the samples. The species, whose identification could be validated at the SEM, was observed also in two samples of L2 in August 2022 and August 2023, with relative abundance 0.2 and 4.8%, respectively. In L1 and LC, the species has never been detected during the study period. More insights about this species and its distribution are described in supplementary material S4.2 (Tenci et al., 2025).

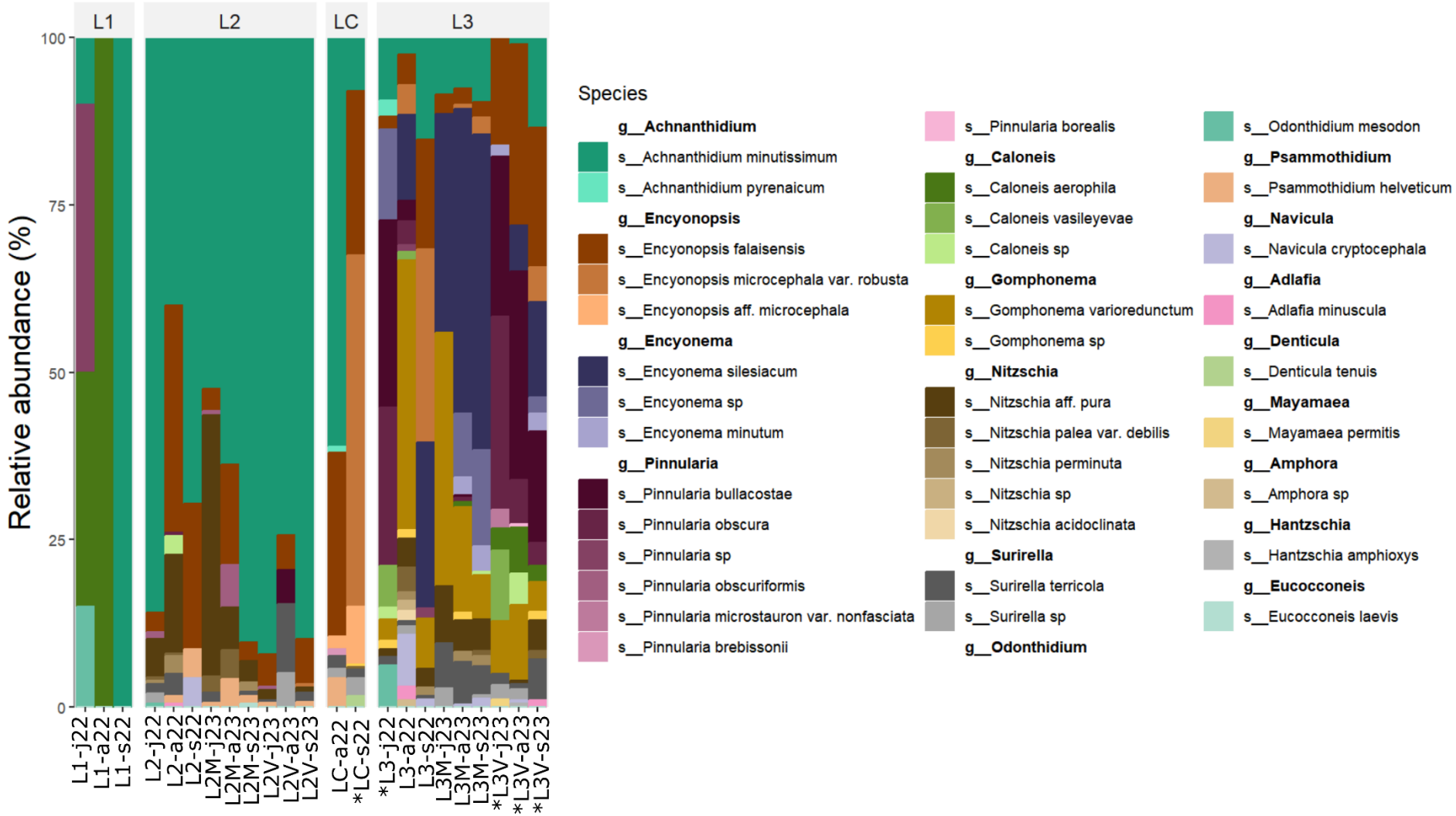

Figure 4. 5. Diatom taxonomical composition of all the analysed samples (relative abundance). Stars indicate epipelic samples.

The number of species (richness) observed in the samples varied from 1 to 20 (Table 4. 2) and showed a spatial gradient (Figure 4. 6a), gradually increasing from ice-contact conditions towards ice-distal conditions. In L1 very scarce and monospecific communities were observed in 2 out of 3 samples. Here, only up to 26 valvae were observed in a whole slide, and 5 species in total were identified in these samples, resulting in the lowest alpha diversity of the system (Figure 4. 6a). Conversely, the highest species richness was observed in L3, where well developed communities with rather high species richness (up to 20 species) were identified. Intermediate richness was observed in samples from L2, ranging from 5 to 10, and LC, ranging from 8 to 9. Similarly, the Shannon index showed a spatially increasing trend, ranging from 0 to 1.2 in L1, from 0.4 to 1.4 in L2, from 1.1 to 1.4 in LC and from 1.5 to 2.2 in L3 (Figure 4. 6b). The highest species evenness (0.9) was observed in L1, where the only non-monospecific sample was composed by 26 valvae belonging to only 4 taxa. Species evenness of the other three studied lakes gradually increased accordingly to ice-distal conditions.

In L2, the highest value of Shannon Index was recorded in August in both 2022 and 2023, i.e., during the glacier ablation period. In L3, alpha diversity (Shannon Index in Figure 4. 6) was more stable across the two seasons, with a slight increase in August in 2022 and in September in 2023. The samples collected in L2 and L3 during 2023 also reveal community patterns within lakes. In L2, the samples collected in the upstream portion (L2M in Figure 4. 5, Table 4. 2 and Figure 4. 6) had a slightly higher diversity than those collected in the downstream portion (L2V), while seasonal patterns were similar. The community compositions of L2M and L2V samples (Figure 4. 5) were similar as well, and characterised by the dominance of *A. minutissimum* in both groups of samples, followed by *Encyonopsis falaisensis* and *Nitzschia* sp. In L3, alpha diversity was slightly higher in the samples from the downstream portion (L3V) than the upstream portion (L3M), with a similar stable seasonal pattern and a slight increase in September 2023. The taxonomic composition of communities in L3 were more diversified than in L2. In L3M samples, the most abundant genera were *Encyonema* and *Gomphonema*, while in L3V samples *Pinnularia* was more abundant, as well as in the epipelic sample collected in June 2022. This pattern reflects the heterogeneity of littoral habitats in L3, where epilithic substrata prevailed upstream, while epipelic substrata prevailed downstream.

Table 4. 2. Diatom counts grouped by lake and values of diversity indexes in each sample.

lake	Sample id	N valvae	Richness	Shannon	Evenness
L1	ZL1-j22	26	4	1.25	0.90
	ZL1-a22	26	1	0.00	NA
	ZL1-s22	4	1	0.00	NA
L2	ZL2-j22	408	9	0.65	0.30
	ZL2-a22	454	10	1.45	0.63
	ZL2-s22	35	4	0.86	0.62
	ZL2M-j23	334	7	1.03	0.53
	ZL2V-j23	470	6	0.37	0.20
	ZL2M-a23	48	6	1.19	0.66
	ZL2V-a23	42	5	0.91	0.57
	ZL2M-s23	438	7	0.47	0.24
	ZL2V-s23	418	6	0.44	0.24
LC	ZLC-a23	210	8	1.09	0.53
	ZLC-s23	491	9	1.36	0.62
L3	ZL3-j22	178	13	2.05	0.80
	ZL3-a22	424	20	2.24	0.75
	ZL3-s22	443	10	1.78	0.77
	ZL3M-j23	231	7	1.54	0.79
	ZL3V-j23	183	11	1.91	0.80
	ZL3M-a23	471	15	1.83	0.68
	ZL3V-a23	422	15	1.92	0.71
	ZL3M-s23	401	14	1.83	0.69
	ZL3V-s23	410	15	2.33	0.86

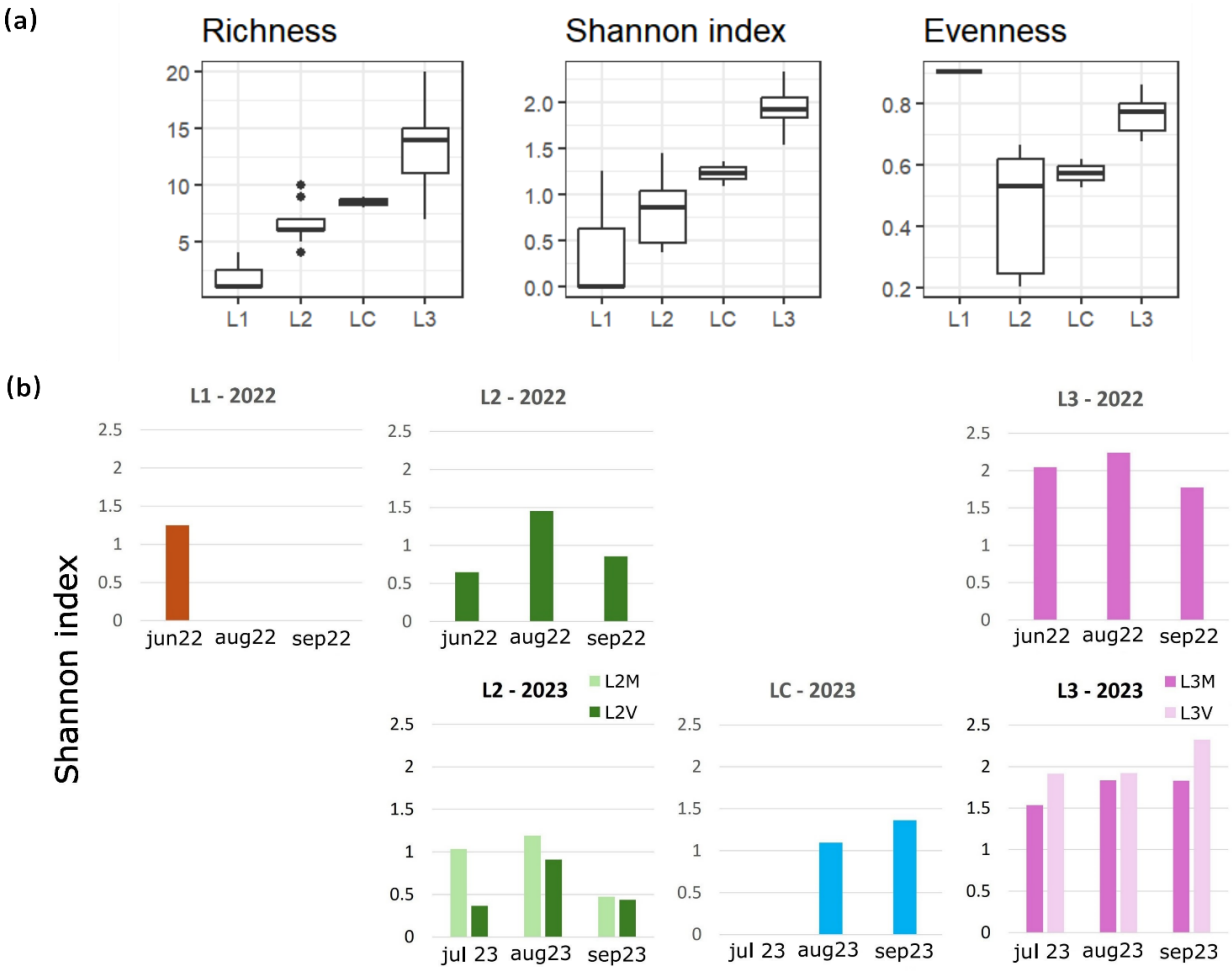

Figure 4. 6. (a) Alpha-diversity measures of the diatom samples, grouped by lake (median values, 25th and 75th percentiles); (b) seasonal evolution of the Shannon index in the samples collected in the four lakes, during the seasons 2022 and 2023.

The NMDS ordination (Figure 4. 7) showed a neat clustering of diatom samples collected from the different studied lakes (stress value = 0.12, R^2 = 0.99 in the Shepard plot). The diatom community composition was significantly different among the four lakes (ANOSIM R = 0.72, p = 0.001), suggesting that within-lake seasonal differences in community composition are less important than variations between lakes. The samples from L1 are clearly separated from the samples from the distal lakes L2, LC and L3, mainly along the first NMDS axis. Compared to the communities observed in the distal lakes, communities in L1 were extremely scarce and showed very low diversity. Among the distal lakes, samples collected in L2 and L3 formed two distinct clusters, separated from each other mainly along the vertical axis direction (NMDS2). The two samples available from LC are only partially separated from L2 and L3 and did not form a distinct cluster. Those taxa that significantly contributed to the grouping of samples along the first two NMDS axes are shown in Table 4. 3. The L2 cluster was characterised by the dominance of *Achnanthidium minutissimum* and the presence of *Psammothidium helveticum* in all the samples collected from this lake (relative abundance of *P. helveticum* ranging from 0.6 to 4.3%). In contrast, only one valva of this species was found in only one sample from L3, i.e., in June 2022. In the L3 cluster, other taxa that were not observed in L2 outnumbered *A. minutissimum*, such as *Gomphonema* spp., *Encyonema silesiacum* and *Pinnularia* spp. The two communities detected in LC did not form a distinct cluster. In August 2023, the

community was comparable to those observed in L2, and it was dominated by *A. minutissimum* (60.5%) and *Encyonopsis falaisensis* (27.1%), while in September 2023 the community was closer to those observed in L3 and dominated by *Encyonopsis microcephala* var. *robusta* (51.9%) and *E. falaisensis* (24.2%). *Denticula tenuis* was uniquely observed in LC in September 2023 (1.6%).

The environmental variables that were significantly correlated with the NMDS ordination axes ($p < 0.05$ in Table 4. 4) were suspended solids in the water column (TSS), electrical conductivity (EC), concentration of total nitrogen (TN), total phosphorus (TP) and silica (SiO2), as well as water temperature (Tw). Tw, SiO2, EC and P-PO4 all point toward the L3 cluster in the ordination plot, and L3 is indeed characterised by higher values of these environmental variables (see also Chapter 2 and 3), thus confirming that Tw, SiO2, EC and P-PO4 can be key drivers for diatom community compositions observed in samples from L3. On the other hand, NTU and TP arrows point toward the L1 cluster, where the highest water turbidity and total P concentrations were measured. Finally, the L2 cluster, which was characterised by intermediate conditions in water temperature and electrical conductivity, and was enriched in total nitrogen, occupies a rather central position in the NMDS ordination, close to the dimension origin.

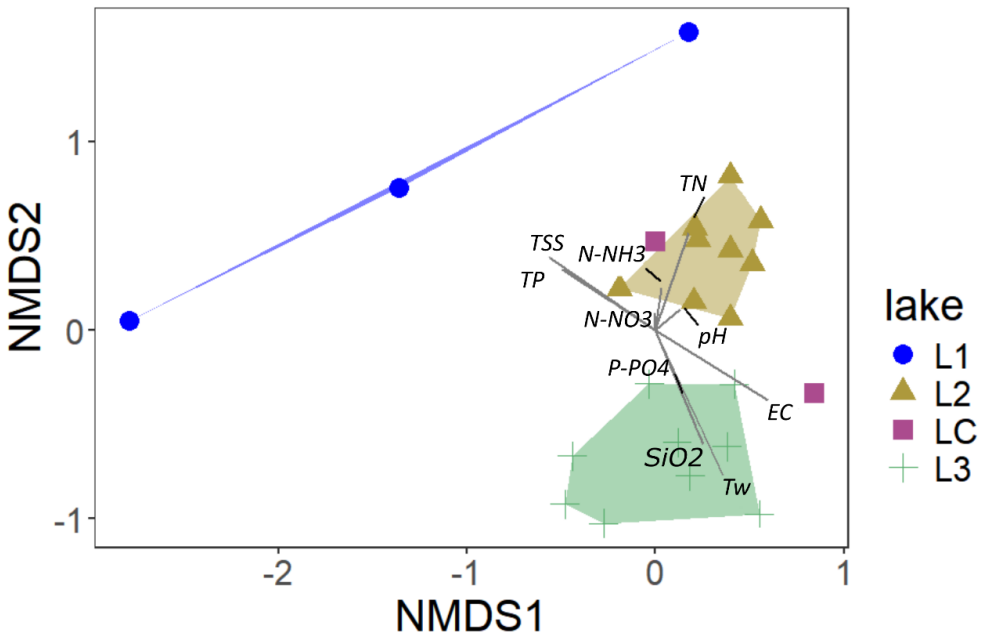

Figure 4. 7. Non-metric multidimensional scaling ordination plot of diatom samples, grouped according to lake of origin (point shapes).

Table 4. 3. Correlation between NMDS axes scores and taxa abundances. p-value refers to the significance of the correlations with |R|>0.5 (Spearman). Stars: * p ≤ 0.05, ** p ≤ 0.01, *** p ≤ 0.001.

Taxon	NMDS1	NMDS2
Achnanthidium minutissimum	0.23	0.78 ***
Caloneis aerophila	-0.62**	-0.26
Caloneis vasileyevae	-0.15	-0.58**
Encyonema silesiacum	0.18	-0.56**
Encyonema sp	-0.01	-0.52*
Encyonopsis microcephala var. *robusta*	0.53**	-0.43
Gomphonema sp	0.21	-0.62**
Gomphonema varioreduncum	-0.02	-0.79***
Nitzschia palea var. *debilis*	0.55**	-0.15
Nitzschia perminuta	0.53**	-0.31
Pinnularia bullacostae	-0.36	-0.68***
Pinnularia obscura	-0.21	-0.74***
Psammothidium helveticum	0.33	0.60**

Table 4. 4. Environmental variables fitted to the NMDS ordination, the loadings on axes NMDS1 and NMDS2, correlation coefficient (r^2, Spearman correlation), and associated p-values for each variable. Significant correlations are indicated by stars: * p ≤ 0.05, * p ≤ 0.01, *** p ≤ 0.001.

Variable	NMDS1	NMDS2	r2
EC	0.87	-0.49	0.51 ***
$N\text{-}NH_3$	0.16	0.99	0.05
$N\text{-}NO_3$	0.08	1.00	0.01
TN	0.27	0.96	0.29 *
pH	0.75	0.66	0.03
$P\text{-}PO_4^{3-}$	0.42	-0.91	0.10
TP	-0.86	0.51	0.35 *
SiO_2	0.42	-0.91	0.43 **
TSS	-0.85	0.52	0.50 **
Tw	0.45	-0.89	0.72 ***

Ecological traits

The diatom species identified in the Cevedale proglacial lakes are exclusively pennate benthic forms typical of freshwater habitats. The most abundant species, *Achnanthidium minutissimum*, is a widely distributed, generalist (Potapova et al., 2009) and pioneer species (Rimet et al., 2017). Several species, such as *Odontidium mesodon* and *Encyonopsis falaisensis* (Potapova, 2009; Bahls et al., 2013) are known to prefer cold water temperatures, while others, like *Nitzschia acidoclinata* and *O. mesodon* thrive in low-conductivity habitats (Potapova, 2009; Bahls, 2016).

According to the classification proposed by Van Dam et al. (1994), many taxa in the Cevedale proglacial lakes are circumneutral, occurring at pH values around 7, or alkaliphilous. Taxa that can

tolerate temporary desiccation are common in all the lakes (Figure 4. 8a). In L2, more than 80% of the community is composed of species that regularly occur both in water bodies and wet or moist places. *Caloneis aerophila*, which is among the few species found in the upper ice-contact lake L1, although in low absolute abundance, is a pseudaerial species (Lange-Bertalot et al., 2017; Rimet et al., 2017), able to colonise wet soils (Van Kerckvoorde et al., 2000). *Surirella terricola,* another aerial species (Cantonati et al., 2020), can be found in soils (Lange-Bertalot et al., 2017), as well as *Pinnularia bullacostae* (Patova & Novakovskaya, 2018; Foets et al., 2020; Patova et al., 2023). In L3, diatom communities shift towards predominantly aquatic taxa.

Regarding trophic status, the community of L2 was dominated by tolerant taxa that are not selective with respect to the trophic status, and by few eutraphentic forms (Figure 4. 8b). In L3, where the communities are more structured and diverse, the proportion of oligotraphentic species increased. The low-profile ecological guild prevailed in Lake L2 (Figure 4. 8c), while the high-profile guild prevailed in L3. Fast-moving species, such as Nitzschia spp, were observed throughout all the Cevedale lakes. Notably, in samples collected from the downstream section of L3 (marked with stars in Figure 4. 8c: ZL3-jun22 and ZL3V in 2023), the relative abundance of motile forms was significantly higher in the epipelic samples than in the epilithic samples (Wilcoxon-Mann-Whitney test, $p < 0.05$).

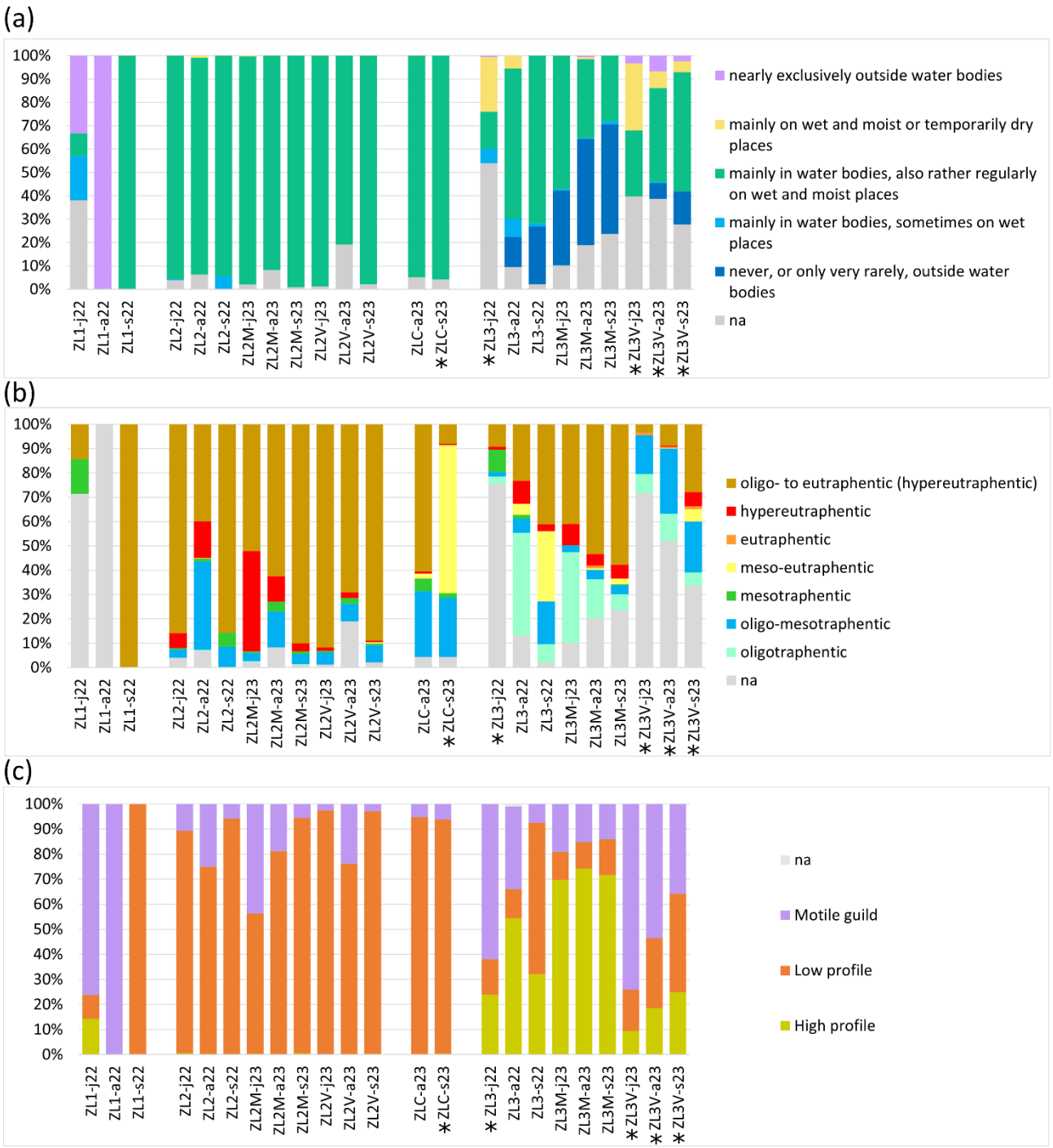

Figure 4. 8. Relative abundances of diatom groups with different preferences for moisture (a) and trophic status (b); (c) relative abundances of diatom ecological guilds observed in the Cevedale proglacial lakes. Stars highlight epipelic samples.

Discussion

The diatom flora of the four Cevedale proglacial lakes consists of distinct assemblages that reflect a gradient of decreasing glacial influence. These assemblages, characterised by different ecological strategies, provide insights into the dynamic interactions between benthic growth and environmental factors, such as glacial meltwater input and the connected physical disturbances in

glacier-fed lentic ecosystems. Diatom density also followed the gradient of glacial influence, with very low values in the ice-contact lake L1 and progressively increasing densities towards the ice-distal lakes, L2, LC and L3. The initial stages of colonization, specifically the communities in L1 and L2, were dominated by aerophilic and pioneer species. The presence of aerophilic and subaerial diatom species was already documented in glacier-fed lakes (Feret et al., 2017), where water level fluctuations can be an important selective pressure (Wantzen, 2008).

As expected according to the sparse previous investigation of biological communities in proglacial lakes (e.g., Sommaruga 2015), environmental factors showing significant correlations with the NMDS ordination axes included key indicators of glacial influence, i.e., mineral turbidity (determined by suspended glacial flour and higher near the glacier terminus), electrical conductivity and water temperature (both increasing towards distal conditions). Silica concentrations were lowest in water samples collected in L1, with slightly higher values in L2 and highest values in L3. In L2, LC and L3, SiO_2 showed similar seasonal trends, with minimum values in the August samples (Chapter 2), likely due to a dilution effect by increased inflow discharge of meltwater during the period of glacier ablation. These observations suggest that silica limitation may play a relevant role in constraining diatom growth in the upstream lakes. Regarding the other key algal nutrients, i.e., N and P, total phosphorus (TP) and nitrogen (TN) were significantly correlated with NMDS ordination axes. Indeed, total phosphorus exhibited a clear spatial trend, with higher concentrations in L1 and L2 with respect to LC and L3 (Chapter 2). On the other hand, concentrations of reactive phosphorus (PO_4) were extremely low, often below the detection limit of the analytical method (0.5 µg/L), across the entire system. Particulate phosphorus, primarily generated through the comminution of bedrock and sediment by glacier activity, is often rather abundant in glacial meltwater (Burpee et al., 2018; Ren et al. 2019), but it is not readily bioavailable to diatoms (Hodson et al., 2004). Therefore, due to the extremely low availability of bioavailable, soluble P, primary productivity in glacier-fed lakes is often clearly phosphorus-limited (Ren et al., 2019).

The very low diatom densities observed in the studied lakes, and especially in L1, align with findings from glacier-fed streams within high-altitude catchments of the same region (Rotta et al. 2018). Nonetheless, the increasing density toward distal lakes appears related to a combination of interconnected factors. First, L1 is a very young lake that started to form in proximity of the Cevedale glacier terminus in summer 2018 (Chapter 2), and little time was available for algal colonisation to occur. Second, L1 exhibits the highest turbidity and lowest water temperatures compared to other lakes in the system (Chapter 3), determining the harshest habitat conditions. Third, the water column in L1 is likely isothermal and subject to constant mixing, due to the thermal patterns induced by water temperatures around 4 °C (Chapter 3). This leads to the absence (or extremely reduced) mediation of thermal stratification on turbidity patterns. Consequently, constant light limitation and low water temperatures likely constrained diatom colonisation while cell growth is likely consistently slowed down by the low temperatures in lake L1. Although L2 shares a similarly recent origin, as it started to be visible in satellite images in summer 2017 (Chapter 2), diatom communities in L2 were denser and showed higher diversity than those in L1, thus suggesting a faster colonisation possibly due to more favourable conditions occurring in L2. Still, the diatom assemblage of L2 can be interpreted as the result of an early stage of colonisation, as suggested by the dominance of the pioneer species *Achnanthidium minutissimum*. As described in Chapter 3, a critical factor shaping

the habitat setting of proglacial lakes in their early stages of evolution is the loss of direct contact with the glacier ice. In summer 2017, L2 was still an ice-contact lake (Chapter 2), while in 2018 this connection was already lost. In 2022 and 2023, when we conducted the sampling campaigns, while L1 showed the typical characteristics of ice-contact lakes, L2 already showed the typical thermal patterns of distal lakes. In L2, surface water temperature was usually above 4 °C, especially during periods characterised by warm air temperatures and scarce (or absent) precipitation events. During these periods, identified in Chapter 3 as stratification-driven Windows of Opportunity for littoral periphyton growth, diatom communities could have experienced stable physical habitat conditions. Indeed, following a period of stable warm and dry weather conditions that induced thermal stratification in the lake water column (Chapter 3), diatom communities in L2 showed a density peak in August 2022. In contrast, in August 2023, after a period characterised by unstable weather conditions, diatom density did not increase. In addition, in the sample collected in L2 in August 2022, specimens of the two dominant species, i.e., *Achnanthidium minutissimum* (37.2 %) and *Encyonopsis falaisensis* (31.5 %), were characterised by small valvae size in August 2022 (Figure 4. 9). The presence of small-sized individuals is considered to reflect a period of fast asexual reproduction (Chepurnov et al., 2004). Indeed, after cytokinesis, each valva of the diatom frustule is inherited by one of the two daughter cells, that will complete the frustule by adding an hypovalva contained in the first valva (epivalva), thus decreasing progressively the size of the cells. With this mechanism, called MacDonald-Pfitzer rule (MacDonald, 1869; Pfitzer, 1871), asexual reproduction produces smaller generations of diatom cells, until sexual reproduction can re-establish the original cell size (Cherpurnov et al., 2004). This event has been observed to typically occur once a year for *Achnanthidium minutissimum* (Cyr, 2016). *A. minutissimum* frequently dominates benthic algal communities in the first stages of colonisation (e.g., Stockner & Armstrong, 1971; Cyr, 2016). However, during fast asexual reproduction phases, cells are particularly vulnerable to dislodgement, as the sibling cells after asexual replication are not attached and it takes time to the cells to securely attach to substrata through the production of short stalks (Peterson, 1996; Cyr, 2016). Similarly, *Encyonopsis falaisensis* is a not-attached species (Bahls, 2013; Rimet et al., 2017), suggesting early vulnerability to physical disturbance such as turbulence. Therefore, the accumulation of cell frustules on the shores of lake L2 Lake may be linked to different interplaying factors: absolute higher values of water temperature and light availability induced accelerated growth rates of pioneer R-strategist algae (Biggs et al., 1998), while environmental stability and reduced physical disturbance allowed communities to attach to substrata and establish. Considering ecological guilds, the communities observed in L2 are dominated by low-profile diatoms, which are in general more resistant to physical disturbances (Passy et al., 2007; Fell et al., 2017). In contrast, in L3, the high-profile guild was more frequent, if not predominant. High-profile forms are able to better exploit resources such as light (Tuji, 2000) and nutrients (McCormick, 1996), when habitat conditions become more stable. As observed in Chapter 3, the more stable thermal stratification (Schmidt stability) that characterises the water column in L3 makes this lake more resistant to holomixis than L2. Mixing events are associated with increased vertical motion and resuspension of sediments (Evans, 1994), a phenomenon that decreases the light availability for diatom growth even along the lake shores. Furthermore, although lake-specific wind measurements are not available, L3 may experience less wind stress on its surface, as the glacier deposited, in the area right upstream the

lake, a moraine with a considerable elevation that partially shelters the lake from katabatic glacier winds. L2 is directly exposed to glacier winds that produce a constant physical disturbance on biofilms in shallow layers (Rimet et al., 2019b). Therefore, species that are vulnerable to physical disturbance, such as high-profile species, are selectively removed from the biofilm, where only species adapted to suboptimal conditions are likely to survive (McCormick, 1996; Fell et al., 2017; Rimet et al., 2019b).

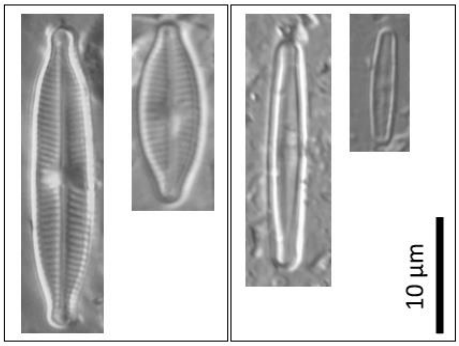

Figure 4. 9. Large and small specimens of *Encyonopsis falaisensis* (left) and *Achnanthidium minutissimum* (right) in the Cevedale proglacial lakes. Small specimens were photographed in the sample collected in August 2022 from L2.

A more stable environment ensures less physical disturbance on diatom communities, which in turn makes high-profile, larger forms more competitive and successful. According to the Intermediate Disturbance Hypothesis (IDH, Connell, 1978), intermediate and constant levels of disturbance can promote an increase in local biodiversity. In biofilms, dominant, high-profile species are periodically displaced by physical disturbance (Peterson, 1996), thus mitigating the effect of competitive interactions in structuring the communities (McCormick, 1996). This theory can be applied also to the studied Cevedale proglacial lake system to explain the higher diatom diversity observed with increasing distal conditions. The "intermediate disturbance" conditions can be identified as the daily increase in turbidity induced by meltwater pulses during the period of glacier ablation, observed both in L2 and L3. Higher levels of disturbance can be induced by factors that increase littoral turbidity, such as frequent mixing processes of the water column or wind stress on lake surface (Rimet et al., 2019b). These effects are amplified in concomitance with storms, that induce the total mixing and cooling of the water column (Chapter 3). A conceptual model of this ecological regulation is depicted in Figure 4. 10. High disturbance intensity and frequency in L2 selected diatom communities with high levels of adaptation to physical disturbance (low-profile and R-strategists), relatively low biodiversity, and reduced competition between species. During the warm and dry period in summer 2022, stable habitat conditions induced an increase in both diatom density and biodiversity, suggesting that warm and dry periods represent stages of reduced disturbance. On the other hand, diversity was higher in L3, where less resistant but more competitive high-profile diatom species established. At the same time, high-profile diatoms are periodically displaced, e.g., during storms, thus mitigating the effects of competitive exclusion and allowing the coexistence of resistant and competitive species, which in turn determines the highest diatom diversity in the system.

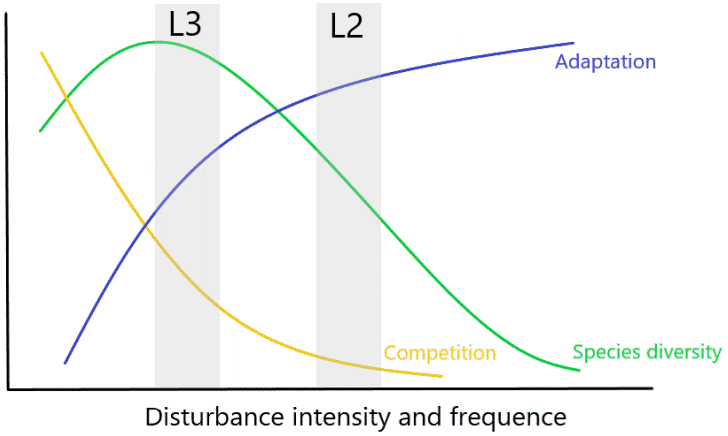

Figure 4. 10. Schematic representation of the relationship between the degree of intensity of disturbance and species diversity, competitive interactions in community structuring and adaptations to physical disturbance. The conditions hypothetically observed in L2 and L3 are highlighted. Adapted from McCormick 1996.

Finally, diatom species belonging to the motile guild were present in all the lakes. Motility has been demonstrated to be an advantageous trait in developing biofilms (Hill, 1996) and, especially, epipelic algal assemblages (Linares Cuesta et al., 2007). The capacity to glide over the raphe allows diatom species to migrate toward more suitable environmental conditions, thus compensating, for instance, the light attenuation related to sediment deposition over the substratum (Wetzel, 2001). In glacier-fed lakes, where fine sediment is continuously deposited on the lake bottom, motility may also give advantage to reach the surface after deposition of fine sediment on the biofilm (Round & Eaton, 1966; Passy et al., 2007), that increases during periods of glacier ablation.

Concluding remarks

The results of this study provide important insights on the diversity and ecology of benthic diatoms in proglacial lakes. The stability of the physical environment and the availability of light are crucial factors in determining the structure and dynamics of diatom communities in these unique ecosystems.

Glacial influence plays a significant role in shaping diatom community composition and distribution of recently formed proglacial lakes. As known for planktonic communities (Sommaruga, 2015), harsh environmental conditions in proglacial lakes pose important selective forces to lake communities, shaping unique algal assemblages with a rapid evolution. The variation in diatom density and diversity across the Cevedale proglacial lakes reflects differences in turbidity, water temperature, electrical conductivity, and, secondarily, nutrient availability. Physical conditions play a dominant role in constraining diatom growth and shaping community composition, surpassing the influence of chemical factors.

First stages of colonisation, i.e., communities in L1 and L2, were characterized by aerophilic and pioneer species. These early-stage colonisers reflect the exposition to continuous and intense physical disturbance induced by daily pulses of glacial meltwater, wind stress, and instability of the water column. With decreasing glacial influence, α-diversity increased. The distal lake L3 supported denser, stable, and more diversified diatom communities. The more stable environment allowed also the establishment of competitively dominant, high-profile diatom taxa.

These results underscore how the loss of contact of proglacial lakes with glacier ice represent a critical stage in the environmental and ecological evolution of these ecosystems, accelerating colonisation processes with longer windows of opportunity for periphyton growth (see also Chapter 3) and triggering the establishment of more stable and lake-typical communities.

Chapter 5
Prokaryotic and eukaryotic diversity of the Cevedale proglacial lakes

Introduction

Biological communities in glacier-fed lakes are often dominated by microorganisms (Sommaruga, 2015), which play a key role in the ecosystem functioning by connecting the biotic and abiotic compartments through their metabolism (Bartons et al., 2012), and represent key elements of food webs (Sommaruga, 2015; Tiberti et al., 2020). Previous studies of microbial communities in Alpine proglacial lakes have primarily focused on planktonic populations (e.g., Peter & Sommaruga, 2017), revealing that glacial meltwater can influence lake biodiversity. This influence decreases as the glacial meltwater contribution wanes, thus highlighting the dynamic relationship between glaciers and lake ecosystems. On the other hand, studies specifically focusing on benthic prokaryotic communities in proglacial lakes remain scarce, particularly in the European Alps (e.g., Kleinteich et al., 2022). Nonetheless, during early stages of lake formation, benthic biofilms may serve as a crucial source of biomass (Mez et al., 1998) and biodiversity (Liu et al., 2024), thus playing a vital role in ecosystem development. In addition, recent findings suggest that prokaryotic benthic communities may respond differently to deglaciation compared to planktonic communities (Liu et al., 2024). Knowledge on eukaryotic microbial communities of proglacial lakes is even scarcer. While planktonic eukaryotes have been more widely studied (e.g., Koenings et al., 1990; Sommaruga & Kandolf, 2014), benthic eukaryotes have predominantly been studied in relation to benthic macroinvertebrates (e.g., Khamis et al., 2014; Jennings, 2021; DeBiasi et al., 2022). Studies on benthic macroinvertebrates revealed the presence of indicator species of glacial influence (Khamis et al., 2014), and the occurrence of highly specialised communities that differentiate proglacial lakes from other high-altitude lakes (Miserendino et al., 2023). However, proglacial lakes are primarily microbially dominated ecosystems (Sommaruga, 2015), and while mountain lakes have been identified as biodiversity hotspots for planktonic eukaryotic microbes (Triadó-Margarit & Casamayor, 2012; Kammerlander et al., 2015), the benthic microbial component has largely been overlooked.

In this study, we investigated planktonic and benthic communities in the Cevedale proglacial lakes, focusing on both prokaryotic and eukaryotic components, using HTS (High Throughput Sequencing) metabarcoding of eDNA samples. This is the first exploration of the biodiversity inhabiting the Cevedale proglacial lakes. The metabarcoding approach was chosen to provide a preliminary overview of microbial and metazoan biodiversity, and to individuate key groups in the community composition of the proglacial lakes and their response to deglaciation. In addition, this approach has been adopted to overcome the technical challenges posed by the pronounced water turbidity in the studied lakes, which hinders the microscopic observation due to the abundance of mineral

particles (glacial flour) similar in size to cells (i.e., silts and clays, as described in Chapter 2). The investigation aimed at (i) characterising the microbial and animal diversity and community composition of the Cevedale proglacial lakes, providing baseline data for future monitoring, and (ii) identifying key groups driving the community composition of the proglacial lakes and the response of biodiversity to deglaciation processes. In addition, the study aimed at testing the hypotheses that benthic communities in proglacial lakes are more relevant than planktonic ones in terms of diversity, and that communities are composed of organisms adapted to cope with harsh physical constraints and scarce resources.

Methods

Samples for prokaryotic and eukaryotic metabarcoding were collected from the Cevedale proglacial lakes L1, L2, LC, L3, and from the clear (i.e., non-glacier-fed) mountain lake Marmotte Lake (MA). The location and main morphological and environmental characteristics of these lakes are described in Chapter 2. Sample collection occurred during the ice-free seasons 2022 and 2023, in June/July, August and September, which represent the main stages of the Alpine glacial summer. Samples of benthic epilithic biofilms were collected by brushing, with a sterile toothbrush, the surface of up to 10 pebbles (epilithon) and cohesive sediment (epipelon) in the littoral area of each lake. Sediment samples were collected by withdrawing small quantities of material from the surface (0-1 cm depth) sediment of the littoral area using a sterile plastic pipette. In 2022, 22 samples were collected: 9 epilithic, 9 sediment, and 5 plankton samples from L1, L2, and L3. In 2023, only epilithic (17) and plankton (9) samples were collected from L2, LC, L3 and MA, the latter sampled once in September 2023. Epilithic samples from L2 and L3 in 2023 were collected both in the upstream and downstream parts of the lakes, to account for habitat heterogeneity. L1 was not considered in 2023 as it totally drained in June (see Chapter 2). For a detailed list of samples collected, see supplementary material S5.2.

Epilithic and sediment samples were stored into sterile Falcon tubes and preserved at temperature < 20°C until laboratory processing and were treated in laboratory in the same way: water was removed from the samples by freeze-drying at -65 °C and aliquots of 150-250 mg of the dried material were sub-sampled to perform DNA extraction. DNA was extracted with the DNeasy Power Soil Kit (QIAGEN, USA), following the manufacturer's instructions. Planktonic samples consisted of 1 L lake water samples collected from the littoral zone using sterile PE bottles. Water samples were stored at 4 °C and filtered as soon as possible (within 24 h from the sampling) in the laboratory. Water samples passed through previously sterilised polycarbonate filters (0.45 µm-pore-size, Whatman). The filtered volume of water ranged from 250 to 1000 mL, depending on the water mineral turbidity. Each filter containing planktonic eDNA was preserved at -80 °C. DNA extraction was performed with the DNeasy PowerWater Kit (QIAGEN, USA) following the manufacturer's instructions. The final concentration of nucleic acids in the extracts was checked with a NanoDrop spectrophotometer ND-8000 (Thermo-Fischer Scientific Inc. Ma., USA).

PCA amplification, library preparation and DNA Illumina sequencing were performed by the FEM laboratory of Computational Biology. PCR amplification of the variable region V4 of the 16S rRNA

genes was performed by using the specific primer set (5' GTGYCAGCMGCCGCGGTAA 3') and (5' GGACTACNVGGGTWTCTAAT 3'). PCR amplification of the variable region V4 of the 18S rRNA genes was performed by using the specific primer set (5' CCAGCASCYGCGGTAATTCC 3') and (3' ACTTTCGTTCTTGATYRATGA 5'). For further details about amplification, library preparation, and DNA Illumina sequencing refer to Tolotti et al., 2020 (16S) and to Obertegger et al., 2019 (18S).

Raw 16S and 18S rRNA gene sequences were pre-processed with the open-source MICCA (version 1.7.2) software (Albanese et al., 2015). Paired-end reads were merged keeping only merged reads with minimum overlap length > 150 bp and with number of mismatches < 50 bp for 16S, and minimum overlap length > 120 bp and with number of mismatches < 30 bp for 18S. Forward and reverse primers were trimmed and reads shorter than 270 bp and expected error rate higher than 0.5% were removed (for both 16S and 18S datasets). Sequences were then clustered into Amplicon Sequence Variants (ASVs) with the UNOISE3 algorithm implemented in MICCA (Albanese et al., 2015). Prokaryotic ASVs were assigned to taxonomic groups using the RDP classifier dataset version 2.14 (Wang et al., 2007). Eukaryotic ASVs were assigned to taxonomic groups using the PR2 database version 5.0.1 (Guillou et al., 2013). ASVs assigned to chloroplasts and mitochondria, as well as those without assigned prokaryotic phylum or eukaryotic division, were removed from the rRNA amplicon datasets.

Community composition and diversity analyses were performed in R, version 4.3.2 (R Core Team 2023). The packages *phyloseq* v 1.46.0 (McMurdie & Holmes, 2013), *microeco* v 1.2.2 (Liu et al., 2021), and *vegan* (Oksanen et al., 2022). Plots were drawn with *ggplot2* package v 3.5.1 (Wickham, 2016).

16S dataset

To explore the taxonomic composition of the samples, the relative abundance of the taxa was considered, based on the total number of reads in each sample. For biodiversity analyses, a rarefaction without replacement was applied at 10000 reads per sample. Rarefaction curves are shown in the supplementary material S5.1. Eight samples (16%) had sequencing depth lower than 10000 reads and were removed from the dataset after rarefaction. The list of samples before and after rarefaction is shown in supplementary material S5.2.

Prokaryotic α-diversity was quantified based on the observed number of ASVs in each sample (ASV richness) and the Shannon Diversity Index. Significant differences in α-diversity among sample types were tested with the Kruskal-Wallis rank sum test and the pairwise Wilcoxon test. Beta-diversity was explored by building a Bray-Curtis dissimilarity matrix based on ASV relative abundance. The dissimilarity matrix was used to perform the NMDS analysis (non-metric multidimensional scaling) based on the ASV composition. Statistical significance of differences in community composition among types of samples was assessed with the non-parametric Analysis of Similarity (ANOSIM, Clarke & Green 1988). Plankton and epilithic samples were also analysed separately, but separate analysis was not performed on sediment samples because of the low number of samples. For each of the two datasets (plankton and epilithic), statistical differences in community composition between lakes were tested with ANOSIM and graphically represented in the NMDS with fitted environmental vectors. Environmental variables were those described in Chapter 2 and were log-transformed by log(x+1). Significant Spearman correlations between α-diversity metrics (ASV

richness, Shannon Index) and environmental variables were tested with the Benjamini-Hochberg correction.

18S dataset

The analysis of the 18S dataset focused on the identification of key groups, i.e., classes, characterising the epilithic and planktic communities in the different lakes, including both unicellular eukaryotes and pluricellular organisms (i.e., metazoans). Relative abundances across the whole community were not considered due bias originating from the high variability of the number of gene copies among unicellular eukaryotes (e.g., Gong et al., 2013), which can lead to misleading interpretations of abundances (Santi et al., 2021). New methodologies were recently proposed to gain a more accurate correspondence between number of sequences and biomass or number of individuals (Martin et al., 2022; Yabuki et al., 2024), however these studies are restricted to few taxonomic groups. For the aims of this study, i.e., to individuate key groups composing the up-to-date unknown community composition of eukaryotes the Cevedale proglacial lakes, and to inspect biodiversity patterns in response to glacial influence, community composition was explored in terms of presence/absence of genera and of ASV richness within key classes. Key classes were identified among the most diverse classes detected in the dataset, considering both the number of ASVs and the number of genera. These classes were then explored separately to assess biodiversity patterns in response to glacial influence in both benthic and plankton assemblages.

For biodiversity analyses, rarefaction without replacement was applied at 10000 reads per sample. Twelve samples (24%) had sequencing depth lower than 10000 reads and were removed from the dataset after rarefaction (supplementary material S5.1 and S5.2). Significant differences in ASV richness between sample types (epilithic, plankton, sediment) were tested with the Kruskal-Wallis test. The spatial variation of α-diversity was analysed by computing the number of ASVs in each sample on the rarefied dataset (ASV richness). Significant differences in planktonic and epilithic ASV richness in the lakes were tested with the Kruskal-Wallis test and the pairwise Wilcoxon test. Sediment samples were excluded due to the low number. Significant Spearman correlations between ASV richness and environmental variables were tested with the Benjamini-Hochberg correction, separately for plankton and epilithic samples. ASV richness was also computed separately on key groups, to observe group-specific biodiversity patterns.

The community composition of epilithic diatoms at the genus level obtained with the analysis of the 18S dataset was compared with the results obtained with the morphological analysis described in Chapter 4. Richness (number of diatom genera) was computed for each sample. Significant differences between richness obtained with the two methods were tested with the Wilcoxon signed-rank test. NMDS was built on the Bray-Curtis distance matrix and statistical differences in community composition among lakes were tested with ANOSIM.

Results and discussion

Prokaryotes

The metabarcoding of the V4 region of the prokaryotic 16S rRNA gene resulted in 13672 Amplicon Sequence Variants (ASVs), assigned to 33 phyla and 531 genera. The Cevedale proglacial lakes shared a core bacterial composition, at phylum level, with other cryosphere environments in the Alps (Kleinteich et al., 2022; Tolotti et al., 2024) and at the global level (Bourquin et al., 2022). In fact, the most abundant phylum across the analysed samples was *Pseudomonadota*, which contributed between 14.3 and 89.9 % to the total community composition (Figure 5. 1). Planktonic assemblages were predominantly composed of *Bacteroidota* (8.5 – 66.8%) and *Pseudomonadota* (31.4 – 89.8%). *Cyanobacteriota* were almost exclusively present in epilithic samples, where the phylum accounted for an average 23.6% of the whole community, while they contributed only 0 – 6.5% and 0 – 8.2% to the community composition in planktonic and sediment samples, respectively. *Deinococcota* exhibited the highest relative abundances in epilithic samples (up to 35.6%, in L1), while being scarcely represented in planktonic (0 – 0.1%) and sediment (0 – 0.7%) samples. *Bacillota* were mainly detected in sediment samples (0.7 – 63.8%).

Archaea were detected only in the plankton samples from L3 and MA (supplementary material S5.4). Abundances of archaea (number of reads) were overall very low, in accordance with other surveys of microbial communities of Alpine cryospheric freshwater habitats (Wilhelm et al., 2014; Tolotti et al., 2024). The presence of archaea in glacial streams has been interpreted as related to the transport of cells living in the glacier ice during intense glacier melting (Battin et al., 2001; Tolotti et al., 2024). However, in this study, archaea were exclusively found in the most distal lake and in the clear lake, suggesting that the glacier may not be the primary source of archaeal cells. All the archaeal reads were attributed to the genus *Nitrosarchaeum*, (phylum *Nitrososphaerota*), an aerobic autotrophic archaeon, able to fix carbon via ammonia oxidation to nitrite, found in soils and low salinity to freshwater habitats, including lakes (Tolar et al., 2019).

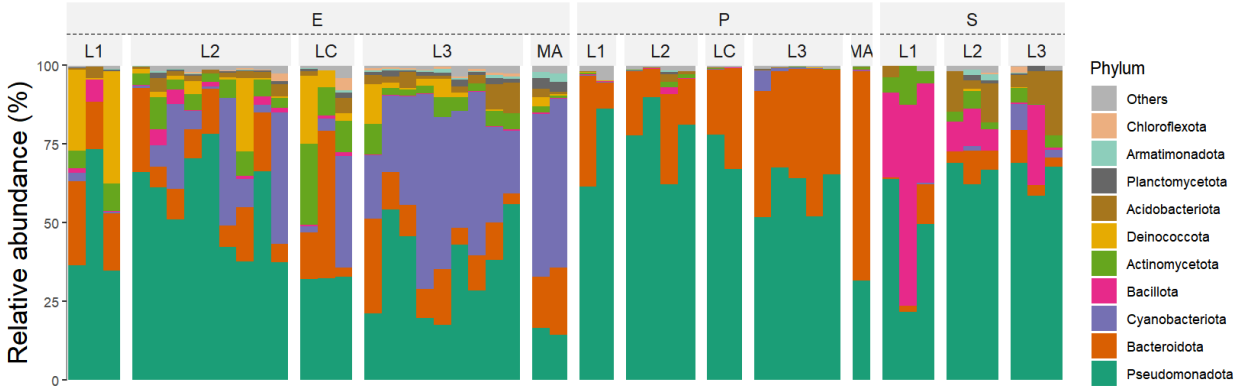

Figure 5. 1. Taxonomic composition at the phylum level of prokaryotic communities in all the examined samples, according to the analyses of the 16S rRNA gene. Samples are grouped by type (E = epilithic, P = plankton, S = sediment) and lake.

Several prokaryotic genera characteristic of specific community types were identified in the analysed samples (Figure 5. 2). *Polaromonas* (phylum *Pseudomonadota*) was the most abundant

genus across all samples, followed by *Rhodoferax* (*Pseudomonadota*) and *Aquirufa* (*Bacteroidota*). *Rhodoferax* and *Aquirufa* were predominant in planktonic samples, alongside *Methylophilus* and *Spingorhabdus* (*Pseudomonadota*), while were scarcely represented in both epilithic and sediment samples. Conversely, cyanobacterial genera such as *Anagnostidinema* and *Apatinema*, along with *Deinococcus* (*Deinococcota*) and *Ferruginibacter* (*Bacteroidota*), were more abundant in epilithic samples compared to planktonic and sediment samples. The abundance of these genera in the samples confirms the high specialisation of lake bacterial communities to cold conditions. Three genera, i.e., *Polaromonas*, *Rhodoferax*, and *Ferruginibacter* are important contributors of the world's cryospheric microbiome (Bourquin et al., 2022). *Polaromonas* is a widespread genus in cryospheric environments (Darcy et al., 2011; Margesin et al., 2012; Franzetti et al 2013; Franzetti et al., 2016; Varliero et al., 2024), including the glacier runoff entering proglacial lakes (Peter & Sommaruga, 2016). Strains of *Polaromonas* are psychrophilic, (Gosnik, 2015) or psychrotolerant (Ciok et al., 2018). *Rhodoferax* is a phototroph that has been previously observed in cold environments such as glaciers (Liu et al., 2015; Bourquin et al., 2022) and Antarctic lakes (Jung et al., 2004), and includes psychrophilic lineages (Jung et al., 2004; Baker et al., 2015).

Deinococcus is known for its exceptional resistance to extreme conditions and the related environmental stress (e.g., Slade & Radman, 2011) and was previously found in high-altitude Alpine catchments (Tolotti et al., 2024). *Anagnostidinema* (Strunecký et al., 2017, formerly members of the genus *Geitlerinema*) can colonise lake littoral areas, periphyton of stagnant waters and periodically wetted habitats such as soils (Strunecký et al., 2017). *Apatinema* is a soil cyanobacterium, first described by Davydov & Vilnet (2022) in podzol soil layers in the Apatity town, Murmansk Region of Russia.

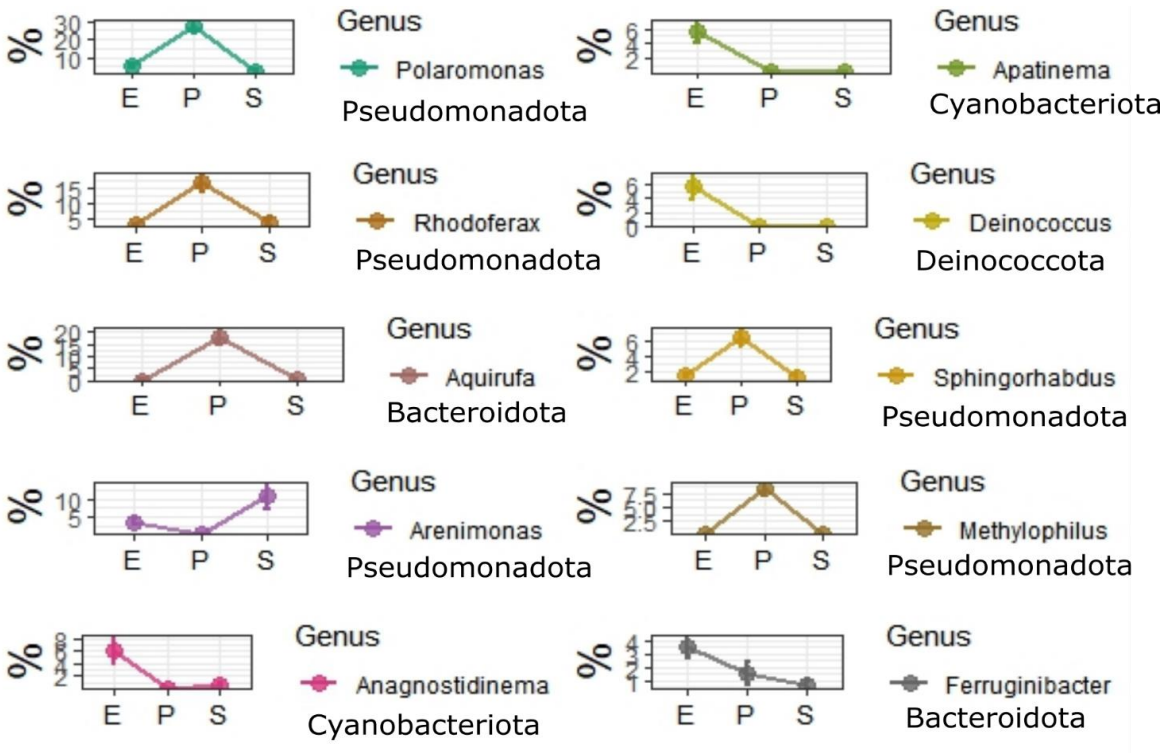

Figure 5. 2. Relative abundance of the 10 most abundant genera detected in the analysed samples, grouped by type: E = epilithic, P = plankton, S = sediment. Also the phylum is indicated.

Prokaryotic diversity in the Cevedale proglacial lakes (not considering the Marmotte Lake) was significantly different among the three different analysed types of samples, i.e., epilithic (E), plankton (P) and sediment (S) (Kruskal-Wallis test $p < 0.05$ for both ASV richness and Shannon Index). The pairwise Wilcoxon test highlighted that α-diversity values were significantly higher in the epilithic than in the planktonic and sediment samples (Figure 5. 3). The Shannon Index, which considers both the number of ASVs (higher in epilithic than in sediment) was significantly lower in the plankton than sediment and epilithon, which showed comparable values of the index (Figure 5. 3).

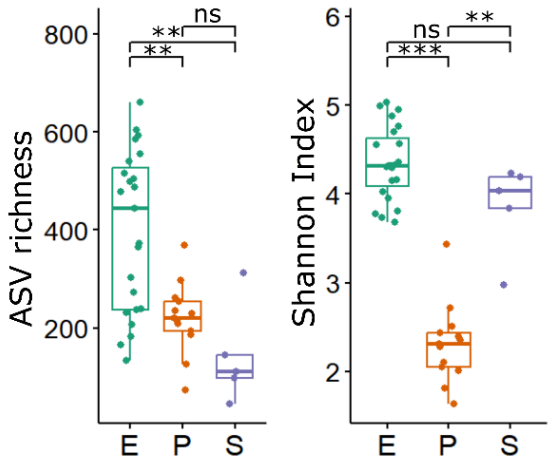

Figure 5. 3 . Prokaryotic α-diversity metrics in the samples collected from the Cevedale proglacial lakes, grouped by sample type: E = epilithic, P = plankton, S = sediment. Significance = Wilcoxon test, * $p < 0.05$, ** $p < 0.01$, *** $p < 0.001$.

The NMDS ordination (Figure 5. 4) showed a sample clustering according to the type of sample, i.e., epilithic, planktonic, sediment (stress = 0.14). The ANOSIM analysis confirmed that community composition of the three sample groups was significantly different ($R = 0.75$, $p = 0.001$). Specifically, while sediment and epilithic samples were partially overlapped, planktonic samples formed a distinct separated cluster with different taxonomic composition.

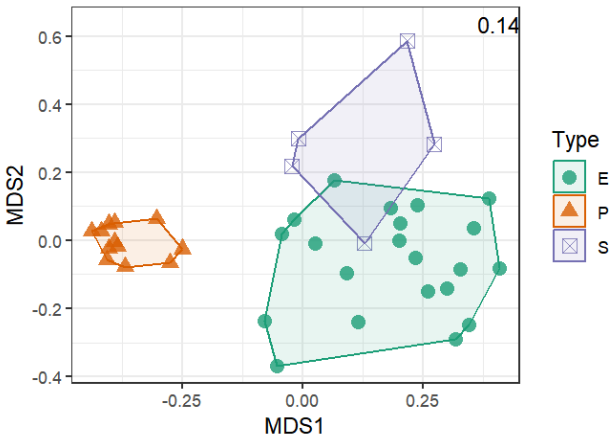

Figure 5. 4. NMDS ordination plot of the samples collected in the Cevedale lakes, grouped by sample type: E = epilithic, P = plankton, S = sediment. Stress value = 0.14.

Considering the lake spatial gradient, i.e., from ice-contact conditions (L1) toward distal (L2, LC, L3) and clear (MA) conditions, plankton samples did not show significant differences in α-diversity metrics between lakes (Kruskal-Wallis test, $p > 0.05$, see Figure 5. 5a). Conversely, α-diversity of bacterial epilithic samples showed a gradually increasing trend from L1 to L3 and MA (Figure 5. 5b). Alpha-diversity differences among lakes were significant only when considering ASV richness (Kruskal-Wallis test, $p < 0.05$), not the Shannon Index ($p > 0.05$).

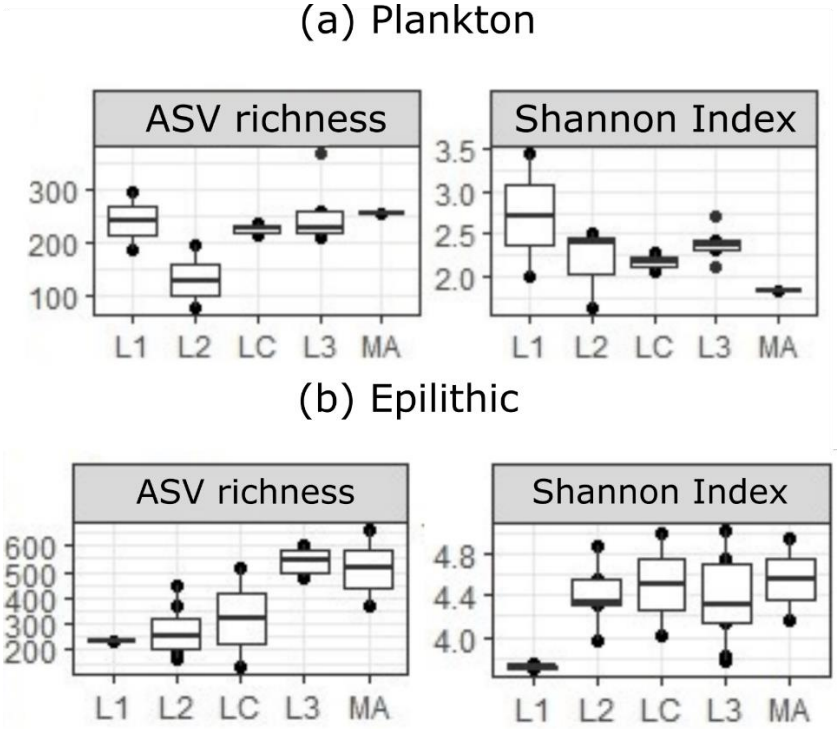

Figure 5. 5. Prokaryotic α -diversity metrics of the planktonic (a) and epilithic (b) samples analysed from the Cevedale proglacial lakes (L1, L2, LC, L3) and the Marmotte Lake (MA).

Planktonic α-diversity did not show significant correlations with key environmental variables (Spearman correlation, p adjusted > 0.05). In contrast, epilithic α-diversity metrics were significantly correlated with 6 environmental variables (Spearman correlation, adjusted $p < 0.05$, Figure 5. 6): concentration of suspended solids (total, TSS, inorganic, ISS, organic, OSS), water temperature (Tw), concentration of silica (SiO_2) and total nitrogen (TN). Specifically, both richness and the Shannon Index increased with warmer water temperatures and concentrations of silica. In contrast, both diversity metrics decreased with increasing concentrations of suspended solids. The Shannon Index also showed a negative correlation with total nitrogen.

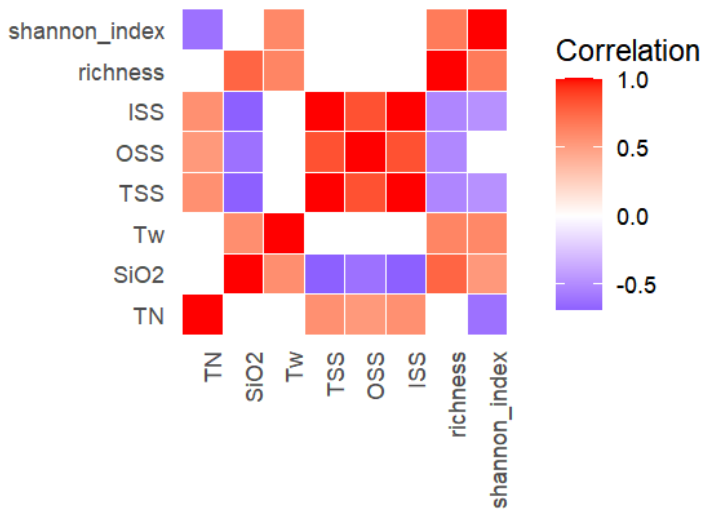

Figure 5. 6. Environmental variables with significant correlation (Spearman, p adjusted < 0.05) with ASV richness and the Shannon Index in the epilithic samples. Only significant correlations are shown.

The observed differences in community compositions among lakes were statistically significant for both plankton and epilithic samples (ANOSIM, $p < 0.05$, $R = 0.41$ and 0.86 respectively). The NMDS analysis (supplementary material S5.3) confirmed the importance of glacier-related factors in shaping lake prokaryotic communities. In both plankton and epilithic, samples from the distal lakes L2, LC and L3, and MA, were separated along axis 1, while samples from the ice-contact lake L1 were separated from the other groups mainly along axis 2. Environmental variables that showed a significant relationship with both ordination pattens (plankton and epilithic) were electrical conductivity (EC), concentration of silica (SiO2), and concentration of suspended solids in the water column (TSS). The ordination of epilithic samples showed also a significant relationship with water temperature (Tw) and total nitrogen (TN).

Planktonic communities

The comparable α-diversity observed in the proglacial lakes and the clear lake can be linked to different interacting factors. First, dispersal processes: planktonic communities of proglacial lakes receive the contribution of a metacommunity which is influenced by the glaciers included in the lake catchment area (Battin et al., 2007; Peter & Sommaruga, 2016; Liu et al., 2024), while the Marmotte catchment lacks the glacier source. Glacial microbial communities not only include several taxa which are adapted to the harsh glacial habitat (Anesio & Laybourn-Parry, 2012), but also can receive the input of allochthonous taxa through the atmospheric deposition, a vector of bacterial cells that are transported with aerosols and dust (Margesin & Miteva, 2011), deposited upon glacier surfaces with precipitation and released during the ice melting phases. Furthermore, proglacial lakes can receive contributions from other sources such as cryoconite holes (Cook et al., 2016), snow (Krug et al., 2020), and soils (Crump et al., 2012). Second, the reduced presence of key predators in the water column of turbid glacial lakes (Sommaruga, 2015; Peter & Sommaruga, 2016), such as heterotrophic nanoflagellates (Sommaruga & Kandolf, 2014) and Cladocera (Koenings et al., 1990), may reduce

the predatory pressure on bacterial communities, thus contributing to maintain relatively high abundance and biodiversity. Third, mineral turbidity, by attenuating UVR penetration in the water column (Rose et al., 2014), may provide protection to UV-sensitive bacteria (Sommaruga, 2001; Peter & Sommaruga, 2016), while plankton bacteria of the clear lake are highly exposed to UV stress (Sommaruga, 2001). Altogether, these factors may help mitigate the harsh environmental conditions in ice-contact lakes and contribute to maintaining bacterial diversity levels in both proglacial and clear lakes.

Bacterial planktonic communities of the analysed lakes were generally characterised by high relative abundance of the phyla *Pseudomonadota* and *Bacteroidota*, in agreement with previous studies about high-altitude Alpine headwaters (e.g., Tolotti et al., 2024) including glacier-fed lakes (Peter & Sommaruga, 2016). Some of the most represented planktonic genera identified in the studied lakes showed remarkable spatial gradients in their relative abundance, as shown in Figure 5. 7. *Polaromonas* (phylum *Pseudomonadota*) was the genus with the highest relative abundances in the plankton of proglacial lakes, where it accounted for 16.3% to 56.6% of the communities in L1, L2, LC and L3, while the relative abundance of the genus substantially dropped to 4.1% in the sample from the Marmotte Lake (MA). Another genus that was frequently observed in the plankton of the Cevedale proglacial lakes was *Aquirufa* (phylum *Bacteroidota*), which increased gradually in relative abundance, from L1 (0.33 – 0.35%) to L2 (8.04 – 19.19.28%), LC (20.16 – 32.19%), and L3 (29.96 – 34.01%), while it was not detected in MA (0 reads). Similarly, *Methylophilus* (phylum *Pseudomonadota*) accounted from 3.3 to 15.2 % of the proglacial planktonic communities, while was not detected in the MA (0 reads). *Sphingorhabdus* (phylum *Pseudomonadota*) exhibited low relative abundance in L1 (0 – 0.01%) and MA (0.03%), while in the proglacial distal lakes was more frequent (3.93 – 12.84% in L2, 8.28 – 10.52% in LC, 2.79 – 10.61% in L3). *Arcicella*, a bacterial genus that was previously found as characteristic glacier fed lakes (Peter & Sommaruga, 2016; Liu et al., 2024) (phylum *Bacteroidota*) showed a strong spatial gradient. The highest relative abundance was observed in L1 (3.9 - 18.3 % of the community) and gradually decreased in the other lakes. *Ferruginibacter* showed the highest relative abundance in L1 (1.44 – 12.67%) and MA (4.99%), while in L2, LC and L3 it had relative abundances lower than 1% in all samples. *Flavobacterium* had the highest relative abundance in L3. Similarly to *Polaromonas*, *Flavobacterium* constitutes the core microbiome of the cryosphere (Bourquin et al., 2022). In contrast, *Haliscomenobacter* (phylum *Bacteroidota*) was a characteristic genus of the Marmotte Lake. Here, the genus accounted for 59.16% of the planktonic community, while in the proglacial Cevedale lakes it was not detected (L1 and LC) or in extremely low relative abundances (0 – 0.1% in L2, 0 – 0.04% in L3). This bacterial genus was previously found as characteristic of clear lake conditions and absent in glacier-fed lakes (Peter & Sommaruga, 2016). Finally, the genus *Rhodoferax* (phylum *Pseudomonadota*), which was very common in all the analysed samples, did not show spatial gradients.

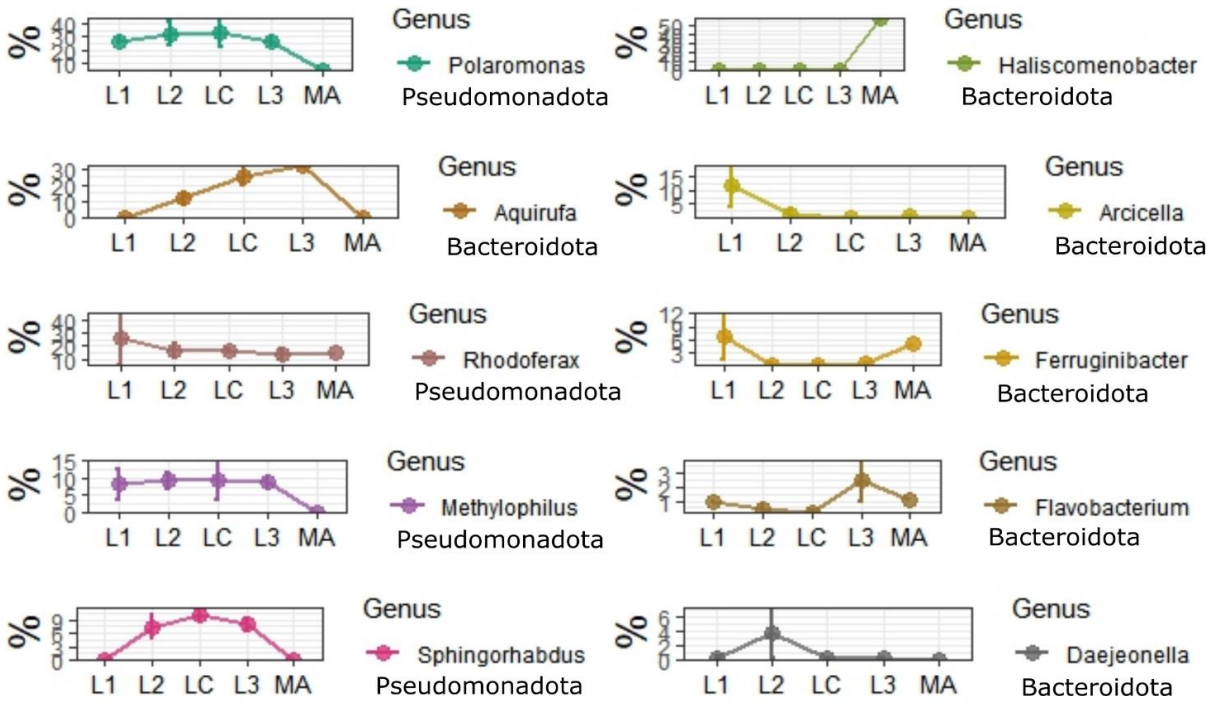

Figure 5. 7. Relative abundance of the 10 most abundant prokaryotic genera detected in the analysed planktonic samples, grouped by lake. The phylum is also indicated.

Epilithic communities

The most representative genera (in terms of highest relative abundance in reads) identified in littoral epilithic communities belonged to the phyla *Cyanobacteriota*, *Deinococcota*, *Pseudomonadota* and *Bacteroidota* (Figure 5. 8). The cryospheric genera that were common in the plankton samples, such as *Polaromonas, Rhodoferax* and *Ferruginibacter*, were common also in epilithic samples, as well as *Deinococcus*. All these genera exhibited a similar decreasing trend from L1 to MA. *Polaromonas* accounted for 14.1 - 19.26% of the community in L1, 2.29 - 9.82% in L2, 1.74 - 2.6% in LC, 1.42 - 4.75% in L3, and 1.85 - 2.13% in MA. A similar trend was observed for *Ferruginibacter* (phylum *Bacteroidota*), that gradually decreased from L1 (8.8 – 19.54%) toward distal lakes (0.9 – 5.99% in L2, 0 – 2.03% in LC, 0.26 – 1.66% in L3). In the clear lake, MA, the abundance of *Ferruginibacter* ranged from 2.9 to 5.83%. *Deinococcus* was highly represented in L1 (25–33.7%) but decreased in the samples from other lakes.

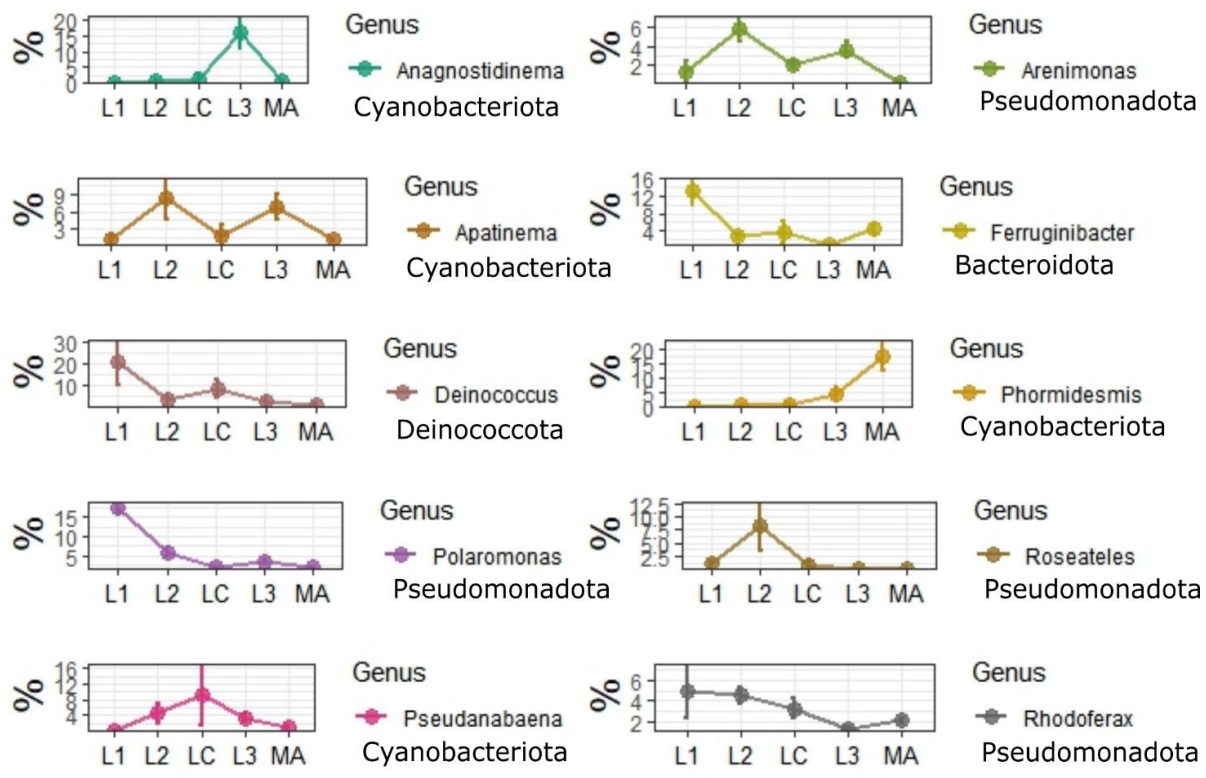

Figure 5. 8. Relative abundance of the 10 most abundant prokaryotic genera detected in the analysed epilithic samples, grouped by lake.

Being cyanobacteria one of the key components of the autotrophic benthos, were further explored. The ASVs attributed to cyanobacteria were 142, belonging to 28 coded genera. The diversity of epilithic cyanobacteria was generally higher in MA than in the Cevedale proglacial lakes (Figure 5. 9). The observed number of cyanobacterial genera identified from the analysis of the 16S rRNA gene increased going from 2 in L1, 2 – 11 in L2, 5 – 6 in LC and 9 – 15 in L3, to 17 – 19 genera in MA.

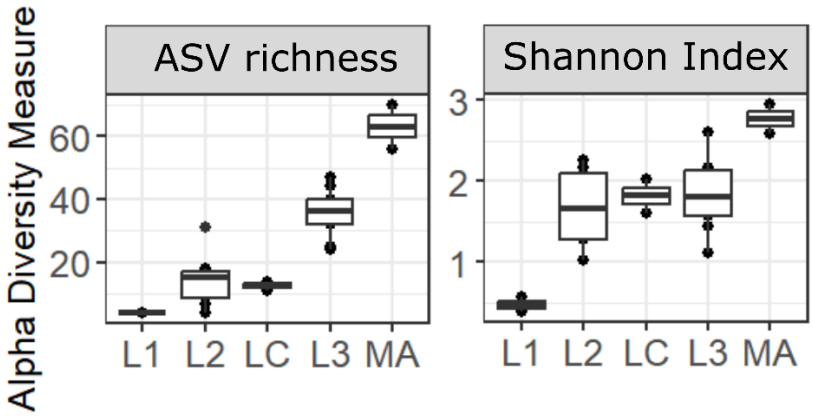

Figure 5. 9. α-diversity metrics of ASVs belonging to the phylum *Cyanobacteriota* in the epilithic samples.

Epilithic cyanobacteria formed distinct assemblages in the lakes (Figure 5. 10), as confirmed by the ANOSIM ($R = 0.52$, $p < 0.01$). In L1, the cyanobacteria community was composed solely of

Pseudanabaena and *Apatinema*. *Pseudanabaena*, which was also observed in living samples collected in the proglacial lakes (Figure 5. 11), is a cosmopolitan cyanobacterium (Komárek & Anagnostidis, 2005) characteristic of epipelic algal assemblages (Poulíčková et al., 2008), which has been previously found in cryospheric environments, including glacial soil (e.g., Yang et al., 2016). *Pseudanabaena* was detected in all the epilithic samples, with a median relative abundance 1.94%. The highest relative abundance was observed in LC in September 2023 (24%), while in L1 and MA the genus was less abundant. The soil cyanobacterium *Apatinema* was detected in all the epilithic samples. The genus showed highest relative abundances in L2 and L3, where it accounted for 0.14 – 28.71% and 0.56 – 17.56% of the communities, respectively. The high relative abundance of *Apatinema* and *Pseudanabaena* in the samples from the proglacial lakes suggests that proglacial soils represent a relevant source of microbial diversity for the Cevedale proglacial lakes.

In L2, while being still mainly composed of *Pseudanabaena* and *Apatinema,* the community was more diversified. *Anagnostidinema* and *Phormidesmis* appeared in L2 and became increasingly more represented in L3. The cyanobacterium *Anagnostidinema* was particularly abundant in the samples collected from L3, where it represented on average the 17.85% (0.63 – 38.28%) of the community and was not detected in only one sample, in June 2022. *Anagnostidinema* was detected with lower relative abundances also in L2 (0 – 3.61%), LC (0 – 4.04%) and MA (0.20 – 0.47%), while in samples from L1 it was never detected. *Phormidesmis* is a widespread genus of cyanobacteria that can colonise soils, rocks and lake littoral areas, although some species appear to be restricted to specific niches (Raabova et al., 2019). The genus *Crinalium*, which was detected uniquely in L2, is a cosmopolitan but rare member of the family *Gomontiellaceae* (Mikhailyuk et al., 2019), that includes also one cryosphere-related species, *Crinalium glaciale*, isolated from cryoconitic ponds of Antarctica (Broady & Kibblewhite, 1991). *Altericista*, a recently described genus (Averina et al., 2021) detected in L2, L3 and MA, is capable to synthesise accessory chlorophylls and to rearrange the phycobilisome apparatus, thus acquiring the ability to photo acclimate. This trait may explain its ability to colonise habitats with different light conditions such as proglacial and clear lakes. The epilithic samples from L3 were also characterised by the presence of *Wilmottia*, a cosmopolitan genus that is found in many environments, including Antarctica (Radzi et al., 2021). *Gloeobacter* was detected only in samples from L3 and MA.

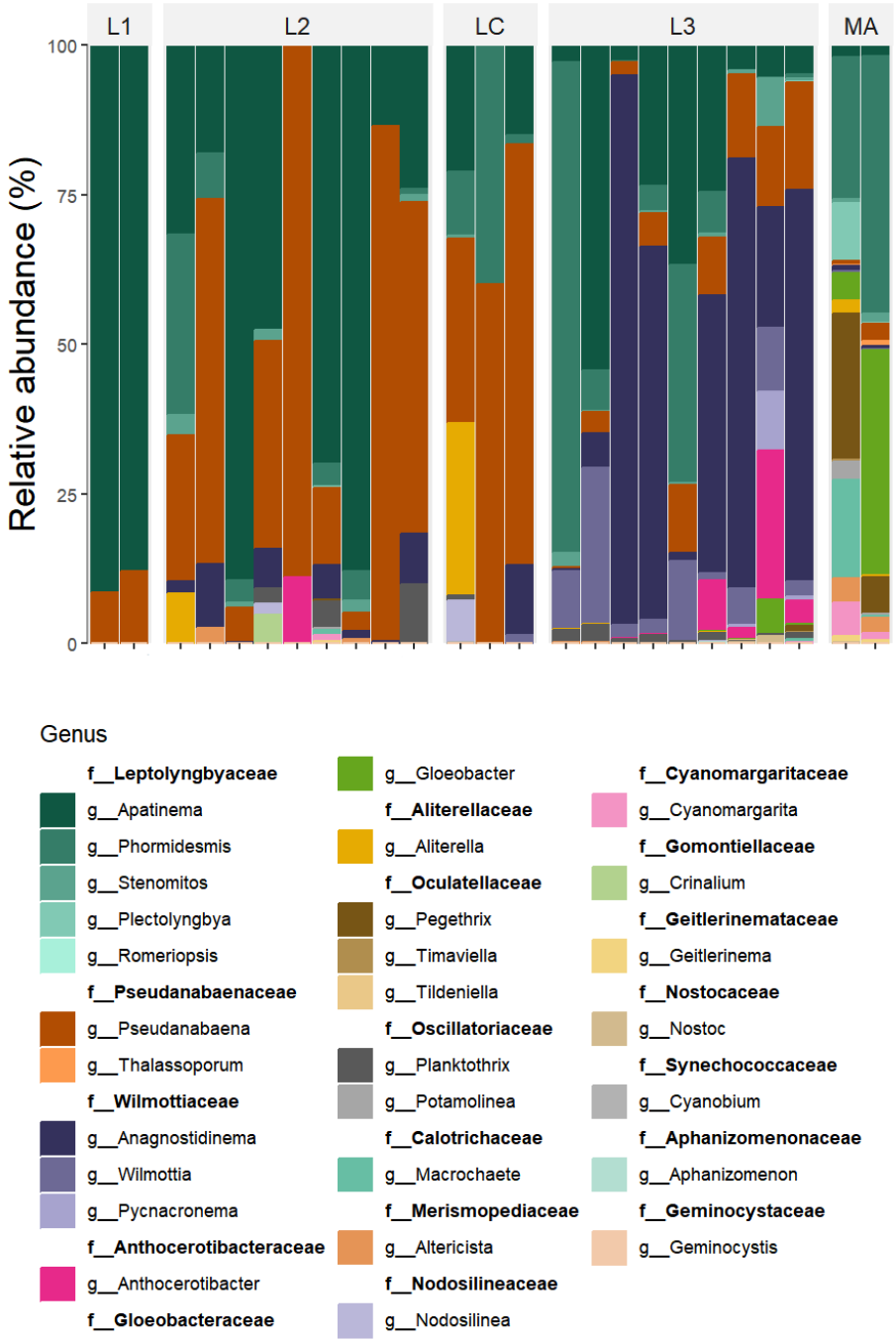

Figure 5. 10. Taxonomic composition at the family and genus level of the phylum *Cyanobacteriota* in the epilithic samples, grouped by lake.

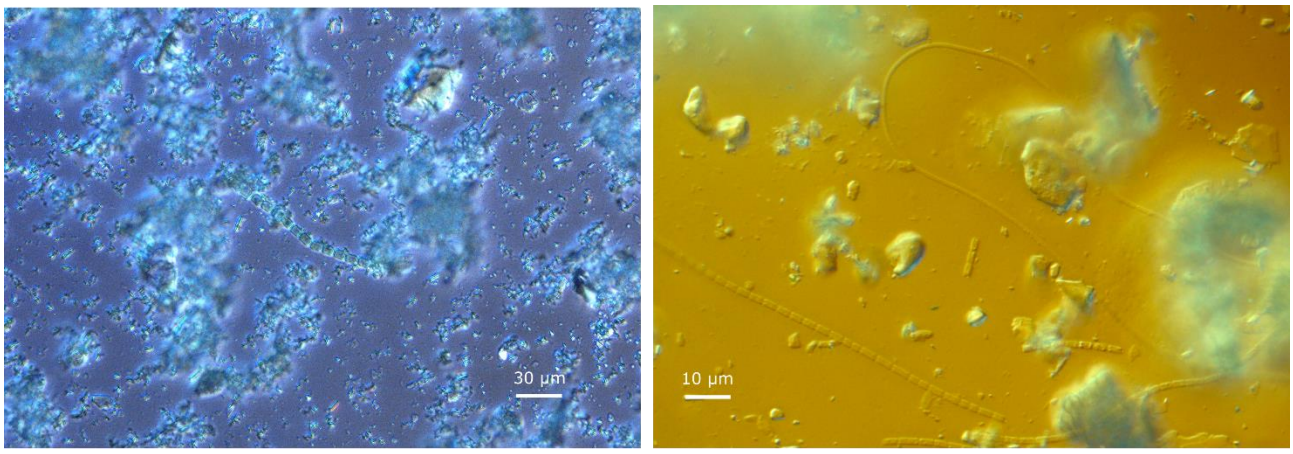

Figure 5. 11. Left: *Pseudanabaena* sp. in L1, 1 October 2021; Right: *Pseudanabaena* sp. and another filamentous cyanobacterium in L3, 12 July 2022.

Eukaryotes

The metabarcoding of the V4 region of the 18S ribosomal RNA gene resulted in the identification of 2387 ASVs, assigned to 473 genera belonging to 18 eukaryotic divisions. The ASV richness did not show significant differences among sample types (Kruskal-Wallis test, $p > 0.05$). The highest number of unique (i.e., not shared with other sample types) ASVs was detected in epilithic samples (690), followed by planktonic and sediment samples (supplementary material S5.5). A high fraction of ASVs (1250) was shared between plankton and epilithic sample types, and a core group of 120 ASVs was detected in all the lakes studies (Figure 5. 12). Lake Marmotte was the lake with the highest number of unique ASVs and the highest ASV richness (523-742 ASVs in epilithic samples). In the proglacial lakes, the highest number of unique ASVs was detected in L3 (362), followed by L1 (79), L2 (65), and LC (20). This taxa distribution confirms the homogeneity of the samples from the proglacial lakes in comparison with the only clear lake in the dataset.

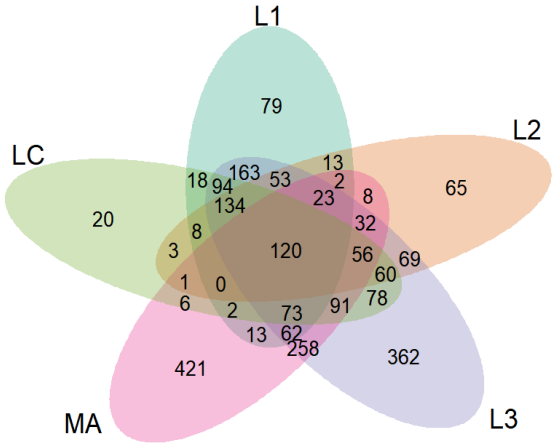

Figure 5. 12. Venn diagram showing the number of shared and unique ASVs detected in the analysed samples (18S dataset), grouped by lake.

The taxonomic composition at the division level (Figure 5. 13) displayed a relatively uniform distribution across the dataset. The most diverse division, in terms of ASV richness, was *Opisthokonta*, followed by *Stramenopiles*, *Chlorophyta*, *Rhizaria*, and *Alveolata* (supplementary material S5.7a). All other divisions included less than 50 ASVs. It is important to note that *Opisthokonta* includes multicellular organisms such as metazoans and fungi (supplementary material S5.6), for which the number of reads does not correspond to the number of individuals. At the class level (supplementary material, S5.7b), the highest proportion of ASVs was attributed to the *Filosa-Sarcomonadea* class (14%), followed by *Chytridiomycota* (11%), *Chrysophyceae* (7%), *Chlorophyceae* (6%), *Nematoda* (6%), *Bacillariophyceae* (4%), *Basidiomycota* (4%), *Trebouxiophyceae* (3%), *Oligohymenophorea* (3%), and *Litostomatea* (2%). The remaining 40% of ASVs were distributed among classes containing less than 2% of the total ASVs, indicating a highly diverse but uneven distribution of taxa within the sampled environments.

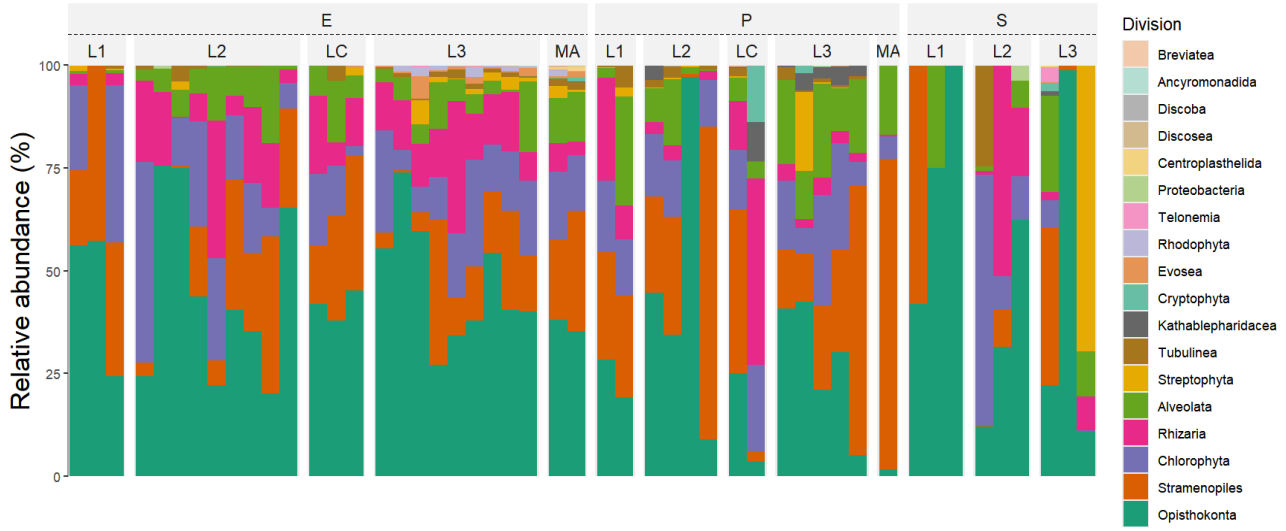

Figure 5. 13. Taxonomic composition (relative abundance of reads in the sample) at the division level of the analysed samples, grouped by type (E = epilithic, P = plankton, S = sediment) and lake.

Eukaryotic ASV richness of epilithic and planktonic samples from the proglacial lakes showed different spatial patterns (Figure 5. 14). Among planktonic samples, richness did not differ significantly between lakes (Kruskal-Wallis test, $p > 0.05$), while it significantly differed in the epilithic samples (Kruskal-Wallis test, $p < 0.05$). Particularly, the epilithic richness in L2 was significantly lower than in L3 (Wilcoxon test, $p < 0.05$). Planktonic ASV richness was not significantly correlated with any of the environmental variables, while epilithic richness showed a positive correlation with silica concentrations and water temperature, and a negative correlation with water turbidity (Spearman correlations, $p < 0.05$).

The highest epilithic richness was found in MA, followed by L3 and L1. L2 and LC had overall lower epilithic diversity than the other lakes. On the other hand, planktonic samples showed high diversity in L1, which dropped in L2 and increased again in LC and L3, where the numbers of detected ASVs were comparable to those found in L1. Finally, MA exhibited the lowest planktonic richness. The high diversity in the plankton samples from L1 resembles the pattern observed in the prokaryotic dataset, and can be explained by the contributions from glacier meltwater (Peter & Sommaruga,

2016), which can collect and transport organisms from the diverse microbial communities of cryoconite holes (Edwards et al., 2013b; Cook et al., 2016), snow (Hoham & Remias, 2020), and the glacier ice microbiome (Anesio et al., 2017). In contrast, the high diversity in LC and L3 may reflect a condition of "intermediate disturbance" (Fox & Connell, 1979), where the thermally more stable water column ensures mild conditions in shallow layers during warm and dry periods (Chapter 3). In contrast, in the ice-contact lakes the unstable physical environment exerts a constant selective pressure on the lake biota. Especially the communities of L2 may be related to a "high disturbance" condition, where only pioneer species are likely to survive (as seen in benthic diatoms in Chapter 4), and where the partial loss of connection with the glacier significantly reduces the contribution from the upstream metacommunity. In contrast, physical disturbance is reduced in MA, which is a mature lake, by the complete absence of glaciers in the catchment (Chapter 2), so that interactions among organisms, such as competitive exclusion, likely play a more important role in shaping communities (Reynolds, 2006). Furthermore, planktonic communities of clear mountain lakes are particularly subject to UVR stress, which may further reduce the biodiversity of plankton communities in the shallow layers of the water column (Sommaruga, 2001). In turbid lakes, the UVR stress is significantly reduced by the suspended glacial flour (Kammerlander et al., 2016). However, this effect is likely counterbalanced by the physical disturbance of glacial flour on cells (Sommaruga & Kandolf, 2014).

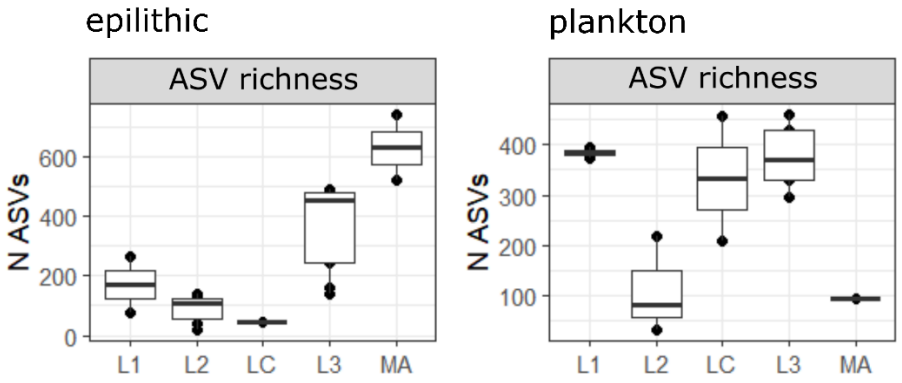

Figure 5. 14. Eukaryotic ASV richness in the analysed epilithic and plankton samples, grouped by lake.

The ASV richness (number of ASV) of the most diverse classes within the dataset is shown in Figure 5. 15. In the epilithic communities, both *Nematoda* and *Bacillariophyceae* displayed an increasing trend in ASV richness from the ice-contact lake toward the ice-distal lakes. Nematodes were not detected in the epilithic samples from L1 but were present in all epilithic samples from L2, LC, and L3, reflecting an increase in taxonomic diversity with decreasing glacial influence. In L1, epilithic communities were dominated by rotifers, with a significant increase in diversity in L2 and LC, where nematodes, *Platyhelminthes*, *Nemertea*, *Rotifera*, and even insects (*Baetis* sp.) were also detected. L3 exhibited the highest diversity of metazoans, including *Nematoda*, *Rotifera*, and *Tardigrada* (data not shown). Two epilithic samples from L3 contained the arachnid genus *Tectocepheus*, a pioneer and parthenogenetic oribatid mite that is one of the first colonisers of young soils after glacier retreat (Hågvar et al., 2009) and can be found in lichen tundra habitats (Leonov, 2020). Fungal ASV richness, especially of the two most diverse classes, Chytridiomycota and Basidiomycota, showed a

similar pattern to metazoans. The highest fungal diversity was observed in planktonic samples from L1. An exceptionally high number of basidiomycetes ASVs was detected in L1, largely attributed to the family *Microbotryomycetes*, which was extensively detected in both planktonic and epilithic samples from this lake. In contrast, *Microbotryomycetes* were only sparsely represented in the samples from the Marmotte. This family includes the genus *Leucosporidium*, a psychrophilic basidiomycete (de García et al., 2015), which was exclusively found in proglacial lake samples. These findings suggest that glaciers serve as reservoirs of cold-adapted fungal biodiversity, a source that becomes progressively less abundant in the absence of ice cover (Tsuji et al., 2022).

The taxonomic richness of protozoa and algae in planktonic samples also varied with glacial influence. Notably, amoebae of the class *Filosa-Sarcomonadea*, ciliates of the classes *Oligohymenophorea* and *Litostomatea*, as well as chlorophytes of the classes *Chlorophyceae* and *Trebouxiophyceae*, exhibited higher ASV richness in L1 than in L2 and, in some cases, with values comparable to those found in L3 (e.g., planktonic *Litostomatea*). Among *Sarcomonadea*, many ASVs were detected exclusively in the proglacial lakes, with 19 ASVs found only in L1 and 27 ASVs restricted to L3.

Chlorophyta, one of the most diverse algal groups in the samples analysed in this study, similarly showed a high richness in planktonic samples from L1, in both classes *Chlorophyceae* and *Trebouxiophyceae.* Epilithic *Chlorophyceae* exhibited the highest richness in the samples from MA. The species *Planophila bipyrenoidosa* was detected in all epilithic samples, with particularly high number of reads in the samples from L2, LC, and L3. This species may be a key player in the colonization processes of these young, glacier-fed environments by algal communities. Epilithic *Trebouxiophyceae* exhibited the highest richness in L3. Interestingly, *Koliella* sp. was found mainly in the proglacial lakes (max. 5 reads in MA), where it was among the most abundant chlorophytes in the plankton of L1. The presence of *Koliella* sp. was previously observed in the plankton of a highly turbid proglacial lake in Austria (Kammerlander et al., 2016). Algae of the genus *Koliella* (such as *K. antarctica*) are adapted to low temperature and light conditions and can promptly modulate the composition of their photosynthetic apparatus to acclimate to changing irradiance (La Rocca et al., 2015).

Another well represented algal group was the class *Chrysophyceae*. Epilithic samples from MA exhibited a higher richness of chrysophytes compared to the proglacial lakes. All planktonic samples from the proglacial lakes were characterised by the presence of *Hydrurus foetidus*, a cold stenotherm species (Klaveness, 2019). Since *H. foetidus* is typically a benthic rheophilic alga (Traaen & Lindstrøm, 1983; Rott et al., 2006), its presence in the plankton of proglacial lakes may be due to drift from inlet streams. Only a few reads of chrysophytes, including *H. foetidus*, were detected in the samples from MA, thus confirming field observations (Tolotti, pers. comm.) indicating an overall scarcity of chrysophytes.

Other algal groups detected in the analysed samples were Dinophyceae, found mainly in MA, while sparsely detected in the proglacial lakes, *Bangiophyceae*, almost exclusively detected in L3, *Zygnemophyceae*, mainly found in L3 with *Cosmarium* sp. and in MA with *Mougeotia* sp., and *Xanthophyceae*, detected mainly in the proglacial lakes. The relevance of dinoflagellates in MA agrees with their important role in the phytoplankton of this lake, as observed in previous morphological surveys in 2017 and 2021 (Tolotti, unpublished data).

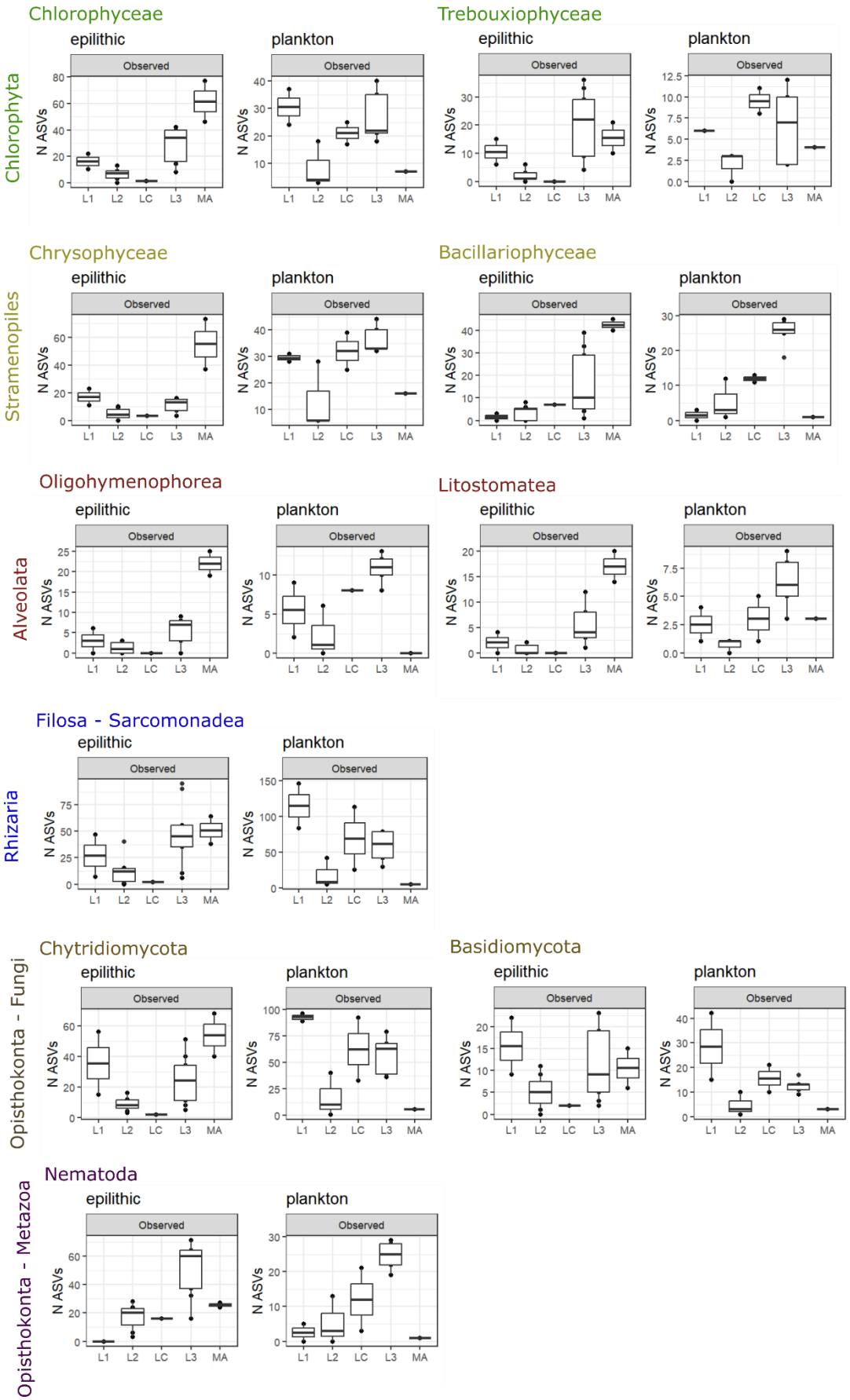

Figure 5. 15. ASV richness of the most diversified (n ASV > 50) classes detected in the analysed samples, divided into epilithic and plankton samples.

Diatoms – comparison of two methods for assessing diversity

Diatoms (division *Stramenopiles*, subdivision *Gyrista*, class *Bacillariophyceae*) were detected mainly in epilithic samples of L2, LC, L3 and MA, with number of ASVs gradually increasing from contact to distal proglacial lakes (Figure 5. 15). Planktonic ASV richness increased in the distal proglacial lakes. The samples from the clear lake, MA, displayed the highest diatom richness among epilithic samples. In contrast, planktonic diatom richness was extremely low in MA, where only the genera *Fragilaria* and *Gomphonema* were identified, and comparable with L1.

Diatom ASVs were attributed to a total of 19 diatom genera, 14 of which were detected in the proglacial lakes. This result was compared with the taxonomic composition at the genus level obtained from the morphological analysis (Chapter 4), which identified an analogous (17) number of diatom genera. However, the richness estimates (number of genera) differed significantly when measured using the two approaches (Wilcoxon signed-rank test, $p < 0.05$), as richness estimated with the morphological method was higher than that estimated from 18S analysis (mean number of genera equal to 6 and 4.2, respectively). The community composition of benthic diatoms obtained with the 18S analysis was significantly different among lakes (ANOSIM, $R = 0.42$, $p = 0.001$), thus confirming that the four proglacial lakes are characterised by distinct diatom assemblages (Figure 5. 16), as found with the morphological analysis in Chapter 4. However, some differences in taxonomic composition obtained with the two methods were observed. Three genera that were not detected by the microscopy observation, i.e., *Craticula*, *Cymbopleura*, and *Reimeria,* were instead detected with the 18S analysis. On the other hand, the morphological observations identified 7 genera that were not detected with the 18S method: *Caloneis, Psammothidium,* and 5 quite rare genera, i.e., *Adlafia*, *Amphora*, *Denticula*, *Eucocconeis*, *Hantzschia*, that were observed in < 2 samples, and with few valvae. In LC, the taxonomic compositions obtained with the two methods differed consistently. In the NMDS ordination plot, samples from LC analysed with the morphologic approach were close to samples from L2 and L1, while the community compositions obtained with the 18S analysis were closer to the L3 cluster (Figure 5. 16).

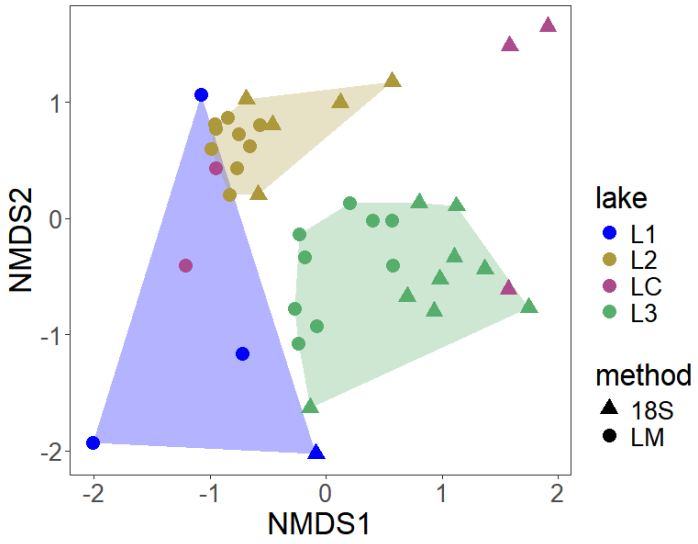

Figure 5. 16. Ordination plot of epilithic diatom samples grouped by lake, based on the method used for the determination of the taxonomic composition at the genus level: 18S = metabarcoding of the 18S rRNA gene; LM = light microscopy. NMDS stress = 0.13.

Concluding remarks

This study provides a preliminary analysis of the taxonomic composition and distribution of prokaryotes and eukaryotes in the Cevedale proglacial lakes. The metabarcoding approach provided insight into biodiversity patterns and allowed to identify the most diverse and common taxonomic groups which compose the biological communities of the studied lakes. However, the methodology presents an important limitation. The analysis of DNA sequences instead of individual cells or organisms does not allow the direct quantification of the abundance of individuals, thus hindering the evaluation of ecological weight of each group within the whole community.

Higher diversity was observed in the epilithic than in the planktonic prokaryotic communities, thus confirming the relevant role played by epilithic biofilms in shaping proglacial lake ecosystems.

The microbial communities of the studied proglacial lakes exhibited pronounced individuality in their taxonomic profiles, both in comparison to each other and to the clear Marmotte Lake. This suggests the presence of a specialised biodiversity in the proglacial lakes, such as cold-adapted bacteria.

The microbial response of diversity to decreasing glacial influence appeared more pronounced in benthic communities, that showed significant correlations with glacier-related environmental factors, than in planktonic ones. Planktonic communities in L1 were notably enriched with cryosphere-related taxa, such as the bacterium *Polaromonas* and the basidiomycetes *Leucosporidium*, which are characteristic of glacial environments. However, although glacial runoff is an important contributor to planktonic biodiversity (Peter & Sommaruga, 2016), it remains unclear whether these organisms are integrated into resident communities within the water column or if they simply drift through the system. Furthermore, the role of ecological interactions, such as the scarcity of bacterial predators, in shaping bacterial diversity requires further investigation.

These findings support the hypothesis that stochastic processes, such as dispersion, are the primary drivers of the planktonic assemblages of the studied lakes (Peter & Sommaruga, 2016; Liu et al., 2021; Liu et al., 2024). On the other hand, key groups of the photosynthetic littoral benthos, such as diatoms and cyanobacteria, appeared more strictly constrained by the harsh physical conditions, and the diversity of these groups progressively increased with decreasing glacial influence.

Chapter 6

Conclusions

This thesis provides new insights into the ecological features and evolution of Alpine proglacial lakes, focusing on the Cevedale proglacial lake system in the Ortles-Cevedale Massif. This system, formed due to the progressive retreat of the Zufallferner/Vedretta del Cevedale glacier, serves as a natural laboratory to study how deglaciation influences lake ecosystems. By analysing a cluster of four lakes, which include both ice-contact (L1) and distal lakes (L2, LC, and L3), this study enhances our understanding of the physical, chemical, and biological factors that shape these dynamic environments over time. The adoption of the integrated approach combining field data (physical, chemical, biological) and hydrodynamic modelling was particularly useful in a context where data collection is logistically challenging. The integration of different disciplines was of utmost importance to disentangle the environmental controls on biological communities, especially in these ecosystems, where physical factors play a dominant role over chemical characteristics.

Hydrochemistry was relatively uniform across the proglacial lakes, also due to the hydrological connection between the lakes. Concentrations of bioavailable nutrients phosphorus and nitrogen were consistently low throughout the system. In contrast, notable gradients were observed in key physical factors such as turbidity and water temperature.

The investigation of physical dynamics revealed that, among the Cevedale proglacial lakes, L1 is a typical ice-contact lake, characterised by cold water temperatures (around 4°C) and high turbidity. The other lakes, L2, LC, and L3, are distal lakes, where temperatures above 4°C allow thermal stratification to form during warm and dry summer periods, as observed in the field data from L2 and L3. Notably, L2 exhibits characteristics typical of an ice-distal lake, such as thermal stratification, despite its relatively recent formation and its proximity to the glacier terminus. The detailed analysis of stratification dynamics in L2, conducted by integrating field data and hydrodynamic modelling, revealed that thermal stratification is triggered during warm and dry periods, and results in a more stable water column. This condition promotes the warming of the surface water layer and the sedimentation of glacial flour, which mitigates the light-limiting effect of fine suspended solids. Therefore, light limitation decreases in the surface layers of the lake, including the littoral area, even when glacier ablation is sustained. These physical changes appear to control the seasonal development of the littoral periphyton by influencing the timing of windows of opportunity (WOs) for periphyton growth, and allowing additional WOs during summer months besides the typical autumn WO observed in glacier-fed streams. The key role of physical conditions in influencing littoral periphyton was confirmed by the results of analyses conducted on biofilm samples, which addressed different communities with different methodologies (diatoms with the morphological approach, prokaryotes and eukaryotes with HTS). Quantitative data about biofilm development in L2 (organic content, chlorophyll *a*, and diatom density) supported this thesis, as littoral periphyton growth peaked in August 2022, after a period of warm and dry meteorological conditions, while, in August 2023, the unstable lake environment resulted in reduced periphyton biomass.

As warm and dry periods are predicted to increase with the progressing climate change, longer periods of stratification and the establishment of longer WOs are expected in distal lakes, thus resulting in the acceleration of colonisation processes. However, seasonal measurements of littoral biofilm biomass at more frequent intervals are necessary to validate this thesis.

The study also highlights that stochastic processes, such as dispersion, likely play an important role in shaping the planktonic assemblages of proglacial lakes, which are enriched with microorganisms sourcing from ice and snow. On the other hand, benthic assemblages, and in particular diatoms and cyanobacteria, are more constrained by the habitat conditions found in proglacial lakes, and are likely more influenced by deterministic ecological processes, such as resource availability and environmental stability.

Benthic communities, and especially primary producers, such as diatoms and cyanobacteria, responded to glacial influence in terms of taxonomic composition, diversity and biomass. Early stages of colonisation, represented by L1 and L2, were characterised by soil cyanobacteria, amoebae, fungi, chlorophytes and chrysophytes. Diatom communities were dominated by aerophilic, pioneer and low-profile species that can cope with the exposure to intense physical disturbances induced by daily pulses of glacial meltwater, water level fluctuations, wind stress on lake surface, and water column instability. The strong physical constraints explain the extremely low biomass and diversity observed in L1. In contrast, despite the very recent formation of L2, benthic diatom communities in this lake were more diverse and abundant than those in L1, especially during periods of more favourable environmental conditions. These periods were characterised by reduced (intermediate) physical disturbance, depending on the stability of the thermal stratification established in the lake. In the distal lake L3, both benthic α-diversity and biomass increased, and diatom community composition shifted toward more lake-typical and high-profile species.

Finally, benthic communities found in the proglacial lakes varied along the deglaciation chronosequence and were clearly distinct from those observed in the studied clear lake. In agreement with recent findings from glacial and non-glacial Alpine streams, this study confirmed that the decrease of glacial influence induces an increase in lake α-diversity, paralleled by a net β-diversity loss at the landscape level. Further research is required to investigate γ-diversity of benthic communities of proglacial lakes at the regional scale.

These findings underscore the pronounced vulnerability of proglacial lake habitats in the present context of global warming and deglaciation. The vulnerability of these habitats and of their unique biological assemblages opens a conservation issue. Glacial ecosystems are protected by the EU legislation as the Habitat 8340 in the Habitat Directive, even if none of the species inhabiting this habitat type are included in the Natura 2000 Annexes, due to scarce knowledge (Gobbi et al., 2021). However, specific protection measures for glacial aquatic ecosystems are extremely rare even in natural parks and other protected areas of the Alps. Including proglacial habitats into conservation strategies would represent a far-sighted action to protect them at least from local anthropogenic pressures, and to contribute to the preservation of Alpine biodiversity at a broader scale.

References

Albanese, D., Fontana, P., De Filippo, C., Cavalieri, D., & Donati, C. (2015). MICCA: A complete and accurate software for taxonomic profiling of metagenomic data. *Scientific Reports*, *5*(1), 9743. https://doi.org/10.1038/srep09743

Al-Yaari, A., Condom, T., Junquas, C., Rabatel, A., Ramseyer, V., Sicart, J., Masiokas, M., Cauvy-Fraunié, S., & Dangles, O. (2023). Climate Variability and Glacier Evolution at Selected Sites Across the World: Past Trends and Future Projections. *Earth's Future*, *11*(10), e2023EF003618. https://doi.org/10.1029/2023EF003618

Andersen, T., Hessen, D.O. (1991) Carbon, nitrogen, and phosphorus content of freshwater zooplankton*. Limnology and Oceanography, 36*, 807–814.

Anesio, A. M., Hodson, A. J., Fritz, A., Psenner, R., & Sattler, B. (2009). High microbial activity on glaciers: Importance to the global carbon cycle. *Global Change Biology*, *15*(4), 955–960. https://doi.org/10.1111/j.1365-2486.2008.01758.x

Anesio, A. M., & Laybourn-Parry, J. (2012). Glaciers and ice sheets as a biome. *Trends in Ecology & Evolution*, *27*(4), 219–225. https://doi.org/10.1016/j.tree.2011.09.012

Anesio, A. M., Lutz, S., Chrismas, N. A. M., & Benning, L. G. (2017). The microbiome of glaciers and ice sheets. *Npj Biofilms and Microbiomes*, *3*(1), 10. https://doi.org/10.1038/s41522-017-0019-0

APAT (2008). Metodi biologici per le acque. Parte I. Roma: APAT. Available from: https://www.isprambiente.gov.it/it/pubblicazioni/manuali-e-linee-guida/metodi-biologici-per-le-acque-parte-i

Ashley, G. M. (2002). Glaciolacustrine environments. In: *Modern and Past Glacial Environments* (pp. 335–359). Elsevier. https://doi.org/10.1016/B978-075064226-2/50014-3

Autonomous Province of Bolzano/Bozen - APB (2005). Carta dell'uso del suolo 1:10.000. Online Geobrowser v.3. Available from http://geokatalog.buergernetz.bz.it/geokatalog

Averina, S., Polyakova, E., Senatskaya, E., & Pinevich, A. (2021). A new cyanobacterial genus *Altericista* and three species, *A. lacusladogae* sp. Nov., *A. violacea* sp. Nov., and *A. variichlora* sp. Nov., described using a polyphasic approach. *Journal of Phycology*, *57*(5), 1517–1529. https://doi.org/10.1111/jpy.13188

Bahls, L. (2013). *Encyonopsis falaisensis*. In Diatoms of North America. Retrieved December 06, 2024, from https://diatoms.org/species/encyonopsis_falaisensis

Baker, J., Riester, C., Skinner, B., Newell, A., Swingley, W., Madigan, M., Jung, D., Asao, M., Chen, M., Loughlin, P., Pan, H., Lin, Y., Li, Y., Shaw, J., Prado, M., Sherman, C., Tang, J., Blankenship, R., Zhao, T., … Sattley, W. (2017). Genome Sequence of *Rhodoferax antarcticus* ANT.BRT; A Psychrophilic Purple Nonsulfur Bacterium from an Antarctic Microbial Mat. *Microorganisms*, *5*(1), 8. https://doi.org/10.3390/microorganisms5010008

Baroni, C., Bondesan, A., Carturan, L., Chiarle, M., & Scotti, R. (2022). Annual glaciological survey of Italian glaciers (2021). *Geografia Fisica e Dinamica Quaternaria*, *45*(1), 69-167. DOI 10.4461/ GFDQ.2022.45.5

Baroni, C., Bondesan, A., Carturan, L., Chiarle, M., & Scotti, R. (2023). Annual glaciological survey of Italian glaciers (2022). *Geografia Fisica e Dinamica Quaternaria*, *46*(1), 3–123. https://doi.org/10.4454/gfdq.v46.883

Barta, B., Mouillet, C., Espinosa, R., Andino, P., Jacobsen, D., & Christoffersen, K. S. (2018). Glacial-fed and páramo lake ecosystems in the tropical high Andes. *Hydrobiologia*, *813*(1), 19–32. https://doi.org/10.1007/s10750-017-3428-4

Bartrons, M., Catalan, J., & Casamayor, E. O. (2012). High Bacterial Diversity in Epilithic Biofilms of Oligotrophic Mountain Lakes. *Microbial Ecology*, *64*(4), 860–869. https://doi.org/10.1007/s00248-012-0072-4

Battarbee, R. W., Jones, V. J., Flower, R. J., Cameron, N. G., Bennion, H., Carvalho, L., & Juggins, S. (2001). Diatoms, p. 155–202. *In* Tracking Environmental Change Using Lake Sediments. Kluwer Academic Publishers.

Battin, T. J., Sloan, W. T., Kjelleberg, S., Daims, H., Head, I. M., Curtis, T. P., & Eberl, L. (2007). Microbial landscapes: New paths to biofilm research. *Nature Reviews Microbiology*, *5*(1), 76–81. https://doi.org/10.1038/nrmicro1556

Beniston, M., Farinotti, D., Stoffel, M., Andreassen, L. M., Coppola, E., Eckert, N., Fantini, A., Giacona, F., Hauck, C., Huss, M., Huwald, H., Lehning, M., López-Moreno, J.-I., Magnusson, J., Marty, C., Morán-Tejéda, E., Morin, S., Naaim, M., Provenzale, A., … Vincent, C. (2018). The European Mountain cryosphere: A review of its current state, trends, and future challenges. *The Cryosphere*, *12*(2), 759–794. https://doi.org/10.5194/tc-12-759-2018

Bird, L. A., Moyer, A. N., Moore, R. D. & Koppes, M. N. (2022). Hydrology and thermal regime of an ice-contact proglacial lake: implications for stream temperature and lake evaporation. *Hydrological Processes, 36*(4), e14566. https://doi.org/10.1002/HYP.14566.

Birkmann, J., E. Liwenga, R. Pandey, E. Boyd, R. Djalante, F. Gemenne, W. Leal Filho, P.F. Pinho, L. Stringer, and D. Wrathall, 2022: Poverty, Livelihoods and Sustainable Development. In: Climate Change 2022: Impacts, Adaptation and Vulnerability. Contribution of Working Group II to the Sixth Assessment Report of the Intergovernmental Panel on Climate Change [H.-O. Portner, D.C. Roberts, M. Tignor, E.S. Poloczanska, K. Mintenbeck, A. Alegria, M. Craig, S. Langsdorf, S. Loschke, V. Moller, A. Okem, B. Rama (eds.)]. Cambridge University Press, Cambridge, UK and New York, NY, USA, pp. 1171–1274, doi:10.1017/9781009325844.010.

Boenigk, J., & Novarino, G. (2004). Effect of suspended clay on the feeding and growth of bacterivorous flagellates and ciliates. *Aquatic Microbial Ecology*, *34*, 181–192. https://doi.org/10.3354/ame034181

Bogen, J., Xu, M., & Kennie, P. (2015). The impact of pro-glacial lakes on downstream sediment delivery in Norway. *Earth Surface Processes and Landforms*, *40*(7), 942–952. https://doi.org/10.1002/esp.3669

Bollati, I. M., Viani, C., Masseroli, A., Mortara, G., Testa, B., Tronti, G., Pelfini, M., & Reynard, E. (2023). Geodiversity of proglacial areas and implications for geosystem services: A review. *Geomorphology*, *421*, 108517. https://doi.org/10.1016/j.geomorph.2022.108517

Bosson, J. B., Huss, M., Cauvy-Fraunié, S., Clément, J. C., Costes, G., Fischer, M., Poulenard, J., & Arthaud, F. (2023). Future emergence of new ecosystems caused by glacial retreat. *Nature*, *620*(7974), 562–569. https://doi.org/10.1038/s41586-023-06302-2

Bourquin, M., Busi, S. B., Fodelianakis, S., Peter, H., Washburne, A., Kohler, T. J., Ezzat, L., Michoud, G., Wilmes, P., & Battin, T. J. (2022). The microbiome of cryospheric ecosystems. *Nature Communications*, *13*(1), 3087. https://doi.org/10.1038/s41467-022-30816-4

Brahney, J., Ballantyne, A. P., Kociolek, P., Spaulding, S., Otu, M., Porwoll, T., & Neff, J. C. (2014). Dust mediated transfer of phosphorus to alpine lake ecosystems of the Wind River Range, Wyoming, USA. *Biogeochemistry*, *120*(1–3), 259–278. https://doi.org/10.1007/s10533-014-9994-x

Broady, P. A., & Kibblewhite, A. L. (1991). Morphological characterization of Oscillatoriales (Cyanobacteria) from Ross Island and southern Victoria Land, Antarctica. *Antarctic Science*, *3*(1), 35–45. https://doi.org/10.1017/S095410209100007X

Brown, L. E., Hannah, D. M., & Milner, A. M. (2007). Vulnerability of alpine stream biodiversity to shrinking glaciers and snowpacks. *Global Change Biology*, *13*(5), 958–966. https://doi.org/10.1111/j.1365-2486.2007.01341.x

Burpee, B. T., Anderson, D., & Saros, J. E. (2018). Assessing ecological effects of glacial meltwater on lakes fed by the Greenland Ice Sheet: The role of nutrient subsidies and turbidity. *Arctic, Antarctic, and Alpine Research*, *50*(1), S100019. https://doi.org/10.1080/15230430.2017.1420953

Busi, S. B., Bourquin, M., Fodelianakis, S., Michoud, G., Kohler, T. J., Peter, H., Pramateftaki, P., Styllas, M., Tolosano, M., De Staercke, V., Schön, M., De Nies, L., Marasco, R., Daffonchio, D., Ezzat, L., Wilmes, P., & Battin, T. J. (2022). Genomic and metabolic adaptations of biofilms to ecological windows of opportunity in glacier-fed streams. *Nature Communications*, *13*(1), 2168. https://doi.org/10.1038/s41467-022-29914-0

Callieri, C. (2017). Synechococcus plasticity under environmental changes. *FEMS Microbiology Letters*, *364*(23). https://doi.org/10.1093/femsle/fnx229

Cantonati, M., Kelly, M. G., Demartini, D., Angeli, N., Dörflinger, G., Papatheodoulou, A., & Armanini, D. G. (2020). Overwhelming role of hydrology-related variables and river types in driving diatom species distribution and community assemblage in streams in Cyprus. Ecological Indicators, 117, 106690. https://doi.org/10.1016/j.ecolind.2020.106690

Carrivick, J. L., & Tweed, F. S. (2013). Proglacial lakes: Character, behaviour and geological importance. *Quaternary Science Reviews*, *78*, 34–52. https://doi.org/10.1016/j.quascirev.2013.07.028

Carrivick, J. L., & Tweed, F. S. (2016). A global assessment of the societal impacts of glacier outburst floods. *Global and Planetary Change*, *144*, 1–16. https://doi.org/10.1016/j.gloplacha.2016.07.001

Carturan, L., & Gasperini, N. (2021). Geomorphic imprint of a small glacier and its rapid vanishing during 20th century: The Marmotte Glacier (Ortles-Cevedale, Italy). *Geografia Fisica e Dinamica Quaternaria, 44*(2), 139–157. https://doi.org/10.4461/GFDQ.2021.44.11

Carturan, L., Zuecco, G., Seppi, R., Zanoner, T., Borga, M., Carton, A., & Dalla Fontana, G. (2016). Catchment-scale permafrost mapping using spring water characteristics. *Permafrost and Periglacial Processes, 27*(3), 253–270. https://doi.org/10.1002/ppp.1875

Cauvy-Fraunié, S., & Dangles, O. (2019). A global synthesis of biodiversity responses to glacier retreat. *Nature Ecology & Evolution*, *3*(12), 1675–1685. https://doi.org/10.1038/s41559-019-1042-8

CEN. 2004. Water quality - Guidance standard for the identification, enumeration and interpretation of benthic diatom samples from running waters. EN 14407:2004.

CEN. 2014. Water quality - Guidance for the routine sampling and preparation of benthic diatoms from rivers and lakes. EN 13946:2003.

Chanudet, V., & Filella, M. (2008). Size and composition of inorganic colloids in a peri-alpine, glacial flour-rich lake. *Geochimica et Cosmochimica Acta*, *72*(5), 1466–1479. https://doi.org/10.1016/j.gca.2008.01.002

Chen, C. A., & Millero, F. J. (1986). Thermodynamic properties for natural waters covering only the limnological range. *Limnology and Oceanography, 31*(3), 657–662. https://doi.org/10.4319/lo.1986.31.3.0657

Chepurnov, V. A., Mann, D. G., Sabbe, K., & Vyverman, W. (2004). Experimental Studies on Sexual Reproduction in Diatoms. In International Review of Cytology (Vol. 237, pp. 91–154). Elsevier. https://doi.org/10.1016/S0074-7696(04)37003-8

Chiarle, M., Bondesan, A., Carturan, L., & Scotti, R. (2024). Annual glaciological survey of Italian glaciers (2023). Campagna glaciologica annuale dei ghiacciai italiani (2023). *Geografia Fisica e Dinamica Quaternaria, 47*(1), 3–127. https://doi.org/10.4454/g5672anf

Chikita, K., Jha, J., & Yamada, T. (1999). Hydrodynamics of a supraglacial lake and its effect on the basin expansion: Tsho Rolpa, Rolwaling Valley, Nepal Himalaya. *Arctic, Antarctic, and Alpine Research, 31*(1), 58-70.

Ciok, A., Budzik, K., Zdanowski, M. K., Gawor, J., Grzesiak, J., Decewicz, P., Gromadka, R., Bartosik, D., & Dziewit, L. (2018). Plasmids of psychrotolerant Polaromonas spp. isolated from Arctic and Antarctic Glaciers – Diversity and role in adaptation to polar environments. *Frontiers in Microbiology*, *9*, 1285. https://doi.org/10.3389/fmicb.2018.01285

Clarke, K. R. (1993). Non-parametric multivariate analyses of changes in community structure. *Austral Ecology*, *18(1)*, 117-143. DOI: 10.1111/j.1442-9993.1993.tb00438.x

Cole, T. & Wells, S. (2023). Input and Output Files Data Description in CE-QUAL-W2: A two-dimensional, laterally averaged, hydrodynamic and water quality model, version 4.5, user manual part 3, model input and output files, ed. by S. Wells, Department of Civil and Environmental Engineering, Portland State University, Portland, OR.

Collins, T., Gerday, C. (2017). Enzyme catalysis in psychrophiles. In: Margesin, R. (eds) Psychrophiles: From Biodiversity to Biotechnology. Springer, Cham. https://doi.org/10.1007/978-3-319-57057-0_10

Colombo, N., Bocchiola, D., Martin, M., Confortola, G., Salerno, F., Godone, D., D'Amico, M. E., & Freppaz, M. (2019). High export of nitrogen and dissolved organic carbon from an Alpine glacier

(Indren Glacier, NW Italian Alps). *Aquatic Sciences*, *81*(4), 74. https://doi.org/10.1007/s00027-019-0670-z

Cook, J., Edwards, A., Takeuchi, N., & Irvine-Fynn, T. (2016). Cryoconite: The dark biological secret of the cryosphere. *Progress in Physical Geography: Earth and Environment*, *40*(1), 66–111. https://doi.org/10.1177/0309133315616574

Crump, B. C., Amaral-Zettler, L. A., & Kling, G. W. (2012). Microbial diversity in arctic freshwaters is structured by inoculation of microbes from soils. *The ISME Journal*, *6*(9), 1629–1639. https://doi.org/10.1038/ismej.2012.9

Cyr, H. (2016). Wind-driven thermocline movements affect the colonisation and growth of *Achnanthidium minutissimum*, a ubiquitous benthic diatom in lakes. Freshwater Biology. 61. 10.1111/fwb.12806.

D'Amico, S., Collins, T., Marx, J., Feller, G., Gerday, C., & Gerday, C. (2006). Psychrophilic microorganisms: Challenges for life. *EMBO Reports*, *7*(4), 385–389. https://doi.org/10.1038/sj.embor.7400662

Darcy, J. L., Lynch, R. C., King, A. J., Robeson, M. S., & Schmidt, S. K. (2011). Global Distribution of Polaromonas Phylotypes—Evidence for a Highly Successful Dispersal Capacity. *PLoS ONE*, *6*(8), e23742. https://doi.org/10.1371/journal.pone.0023742

Davydov, D., & Vilnet, A. (2022). Review of the Cyanobacterial Genus Phormidesmis (Leptolyngbyaceae) with the Description of Apatinema gen. Nov. *Diversity*, *14*(9), 731. https://doi.org/10.3390/d14090731

de García, V., Coelho, M. A., Maia, T. M., Rosa, L. H., Vaz, A. M., Rosa, C. A., Sampaio, J. P., Gonçalves, P., van Broock, M., & Libkind, D. (2015). Sex in the cold: taxonomic reorganization of psychrotolerant yeasts in the order Leucosporidiales. *FEMS yeast research*, *15*(4), fov019. https://doi.org/10.1093/femsyr/fov019

Debiasi, D., Franceschini, A., Paoli, F., & Lencioni, V. (2022). How do macroinvertebrate communities respond to declining glacial influence in the Southern Alps? *Limnetica*, *41*(1), 121–137. https://doi.org/10.23818/limn.41.10

DeMott, W. R. (1986). The role of taste in food selection by freshwater zooplankton. *Oecologia*, *69*(3), 334–340. https://doi.org/10.1007/BF00377053

Drenkhan, F., Guardamino, L., Huggel, C., & Frey, H. (2018). Current and future glacier and lake assessment in the deglaciating Vilcanota-Urubamba basin, Peruvian Andes. *Global and Planetary Change*, *169*, 105–118. https://doi.org/10.1016/j.gloplacha.2018.07.005

Echeverría-Vega, A., Chong, G., Serrano, A. E., Guajardo, M., Encalada, O., Parro, V., Blanco, Y., Rivas, L., Rose, K. C., Moreno-Paz, M., Luque, J. A., Cabrol, N. A., & Demergasso, C. S. (2018). Watershed-Induced Limnological and Microbial Status in Two Oligotrophic Andean Lakes Exposed to the Same Climatic Scenario. *Frontiers in Microbiology*, *9*, 357. https://doi.org/10.3389/fmicb.2018.00357

Edwards, A., Douglas, B., Anesio, A. M., Rassner, S. M., Irvine-Fynn, T. D. L., Sattler, B., & Griffith, G. W. (2013a). A distinctive fungal community inhabiting cryoconite holes on glaciers in Svalbard. *Fungal Ecology*, *6*(2), 168–176. https://doi.org/10.1016/j.funeco.2012.11.001

Edwards, A., Pachebat, J. A., Swain, M., Hegarty, M., Hodson, A. J., Irvine-Fynn, T. D. L., Rassner, S. M. E., & Sattler, B. (2013b). A metagenomic snapshot of taxonomic and functional diversity in an alpine glacier cryoconite ecosystem. *Environmental Research Letters*, *8*(3), 035003. https://doi.org/10.1088/1748-9326/8/3/035003

Elser, J. J., Wu, C., González, A. L., Shain, D. H., Smith, H. J., Sommaruga, R., Williamson, C. E., Brahney, J., Hotaling, S., Vanderwall, J., Yu, J., Aizen, V., Aizen, E., Battin, T. J., Camassa, R., Feng, X., Jiang, H., Lu, L., Qu, J. J., … Saros, J. E. (2020). Key rules of life and the fading cryosphere: Impacts in alpine lakes and streams. *Global Change Biology*, *26*(12), 6644–6656. https://doi.org/10.1111/gcb.15362

Evans, R. D. (1994). Empirical evidence of the importance of sediment resuspension in lakes. Hydrobiologia, 284(1), 5–12. https://doi.org/10.1007/BF00005727

Ezzat, L., Fodelianakis, S., Kohler, T. J., Bourquin, M., Brandani, J., Busi, S. B., Daffonchio, D., De Staercke, V., Marasco, R., Michoud, G., Oppliger, E., Peter, H., Pramateftaki, P., Schön, M., Styllas, M., Tadei, V., Tolosano, M., & Battin, T. J. (2022). Benthic Biofilms in Glacier-Fed Streams from Scandinavia to the Himalayas Host Distinct Bacterial Communities Compared with the Streamwater. *Applied and Environmental Microbiology*, *88*(12), e00421-22. https://doi.org/10.1128/aem.00421-22

Fell, S. C., Carrivick, J. L., & Brown, L. E. (2017). The multitrophic effects of climate change and glacier retreat in mountain rivers. *BioScience*, *67*(10), 897–911. https://doi.org/10.1093/biosci/bix107

Feret, L., Bouchez, A., & Rimet, F. (2017). Benthic diatom communities in high altitude lakes: A large scale study in the French Alps. *Annales de Limnologie - International Journal of Limnology*, *53*, 411–423. https://doi.org/10.1051/limn/2017025

Foets, J., Wetzel, C. E., Teuling, A. J., & Pfister, L. (2020). Temporal and spatial variability of terrestrial diatoms at the catchment scale: Controls on communities. PeerJ, 8, e8296. https://doi.org/10.7717/peerj.8296.Pfx, J. F., & Connell, J. H. (1979). Intermediate disturbance hypothesis. *Science*, *204*, 1344–5.

Föllmi, K. B., Hosein, R., Arn, K., & Steinmann, P. (2009). Weathering and the mobility of phosphorus in the catchments and forefields of the Rhône and Oberaar glaciers, central Switzerland: Implications for the global phosphorus cycle on glacial–interglacial timescales. *Geochimica et Cosmochimica Acta*, *73*(8), 2252–2282. https://doi.org/10.1016/j.gca.2009.01.017

Franzetti, A., Tatangelo, V., Gandolfi, I., Bertolini, V., Bestetti, G., Diolaiuti, G., D'Agata, C., Mihalcea, C., Smiraglia, C., & Ambrosini, R. (2013). Bacterial community structure on two alpine debris-covered glaciers and biogeography of *Polaromonas* phylotypes. *The ISME Journal*, *7*(8), 1483–1492. https://doi.org/10.1038/ismej.2013.48

Gallegos, C. L., Davies-Colley, R. J., & Gall, M. (2008). Optical closure in lakes with contrasting extremes of reflectance. *Limnology and Oceanography*, *53*(5), 2021–2034. https://doi.org/10.4319/lo.2008.53.5.2021

Gantt, E., Edwards, M. R., & Provasoli, L. (1971). Chloroplast structure of the Chryptophyceae. *The Journal of Cell Biology*, *48*(2), 280–290. https://doi.org/10.1083/jcb.48.2.280

Gaskill, J. A., Harris, T. D., & North, R. L. (2020). Phytoplankton Community Response to Changes in Light: Can Glacial Rock Flour Be Used to Control Cyanobacterial Blooms? *Frontiers in Environmental Science*, *8*, 540607. https://doi.org/10.3389/fenvs.2020.540607

Gervais, F. (1997). Light-dependent growth, dark survival, and glucose uptake by chrysophytes isolated from a freshwater chemocline. *Journal of Phycology*, *33*(1), 18–25. https://doi.org/10.1111/j.0022-3646.1997.00018.x

Gobbi, M., & Lencioni, V. (2021). Glacial biodiversity: lessons from ground-dwelling and aquatic Insects. IntechOpen. doi: 10.5772/intechopen.92826

Gobbi, M., Ambrosini, R., Casarotto, C., Diolaiuti, G., Ficetola, G. F., Lencioni, V., Seppi, R., Smiraglia, C., Tampucci, D., Valle, B., & Caccianiga, M. (2021). Vanishing permanent glaciers: Climate change is threatening a European Union habitat (Code 8340) and its poorly known biodiversity. *Biodiversity and Conservation*, *30*(7), 2267–2276. https://doi.org/10.1007/s10531-021-02185-9

Gong, J., Dong, J., Liu, X., & Massana, R. (2013). Extremely High Copy Numbers and Polymorphisms of the rDNA Operon Estimated from Single Cell Analysis of Oligotrich and Peritrich Ciliates. *Protist*, *164*(3), 369–379. https://doi.org/10.1016/j.protis.2012.11.006

Gordon, N. D., MacMahon, T. A., & Finlayson, B. L. (1992). Stream hydrology: an introduction for ecologists. John Wiley & Sons: New York. ISBN: 978-0-470-84358-1

Gosink, J.J. (2015) *Polaromonas*. Bergey's Manual of Systematics of Archaea and Bacteria. John Wiley & Sons, Ltd; 2015. p. 1–6. Available from: https://doi.org/10.1002/9781118960608.gbm00950

Guiry, M.D. in Guiry, M.D. & Guiry, G.M. 13 June 2016. AlgaeBase. World-wide electronic publication, National University of Ireland, Galway. https://www.algaebase.org; searched on 02 December 2024

Haeberli, W., Buetler, M., Huggel, C., Friedli, T. L., Schaub, Y., & Schleiss, A. J. (2016). New lakes in deglaciating high-mountain regions – opportunities and risks. *Climatic Change*, *139*(2), 201–214. https://doi.org/10.1007/s10584-016-1771-5

Hågvar, S., Solhøy, T., & Mong, C. E. (2009). Primary Succession of Soil Mites (Acari) in a Norwegian Glacier Foreland, with Emphasis on Oribatid Species. *Arctic, Antarctic, and Alpine Research*, *41*(2), 219–227. https://doi.org/10.1657/1938-4246-41.2.219

Hall, S. R., Leibold, M. A., Lytle, D. A., & Smith, V. H. (2004). Stoichiometry and planktonic grazer composition over gradients of light, nutrients, and predation risk. *Ecology*, *85*(8), 2291–2301. https://doi.org/10.1890/03-0471

Hardmeier, F., Schmidheiny, N., Suremann, J., Lüthi, M., & Vieli, A. (2024). Evolution, sedimentation and thermal state of the emerging pro-glacial lakes at Witenwasserengletscher, Switzerland. *Earth Surface Processes and Landforms, 49*, 4055–4073.

Hauer, F. R., & Lamberti, G. A. (1996). *Methods in stream ecology*. Academic Press Ed., San Diego, CA. 877 pp.

Herman, F., Beyssac, O., Brughelli, M., Lane, S. N., Leprince, S., Adatte, T., Lin, J. Y. Y., Avouac, J.-P., & Cox, S. C. (2015). Erosion by an Alpine glacier. *Science*, *350*(6257), 193–195. https://doi.org/10.1126/science.aab2386

Hill, W. (1996). Effects of light. In: Stevenson, R.J., Bothwell, M.L., Lowe, R.L. (Eds.), Algal Ecology: Freshwater Benthic Ecosystems. Academic Press, San Diego, CA, pp. 229–252.

Hinder, B., Baur, I., Hanselmann, K., & Schanz, F. (1999). Microbial food web in an oligotrophic high mountain lake (Jöri Lake III, Switzerland). *Journal of Limnology*, *58*(2), 162. https://doi.org/10.4081/jlimnol.1999.162

Hlúbiková, D., Blanco, S., Falasco, E., Gomà, J., Hoffmann, L., & Ector, L. (2009). NITZSCHIA ALICAE SP. NOV. AND N. PURIFORMIS SP. NOV., NEW DIATOMS FROM EUROPEAN RIVERS AND COMPARISON WITH THE TYPE MATERIAL OF N. SUBLINEARIS AND N. PURA. Journal of Phycology, 45(3), 742–760. https://doi.org/10.1111/j.1529-8817.2009.00692.x

Hock, R., G. Rasul, C. Adler, B. Cáceres, S. Gruber, Y. Hirabayashi, M. Jackson, A. Kääb, S. Kang, S. Kutuzov, Al. Milner, U. Molau, S. Morin, B. Orlove, and H. Steltzer, 2019: High Mountain Areas. In: IPCC Special Report on the Ocean and Cryosphere in a Changing Climate [H.-O. Pörtner, D.C. Roberts, V. Masson-Delmotte, P. Zhai, M. Tignor, E. Poloczanska, K. Mintenbeck, A. Alegría, M. Nicolai, A. Okem, J. Petzold, B. Rama, N.M. Weyer (eds.)]. Cambridge University Press, Cambridge, UK and New York, NY, USA, pp. 131-202. https://doi.org/10.1017/9781009157964.004.Hu, Y., Yao, X., Wu, Y., Han, W., Zhou, Y., Tang, X., Shao, K., & Gao, G. (2020). Contrasting Patterns of the Bacterial Communities in Melting Ponds and Periglacial Rivers of the Zhuxi glacier in the Tibet Plateau. *Microorganisms*, *8*(4), 509. https://doi.org/10.3390/microorganisms8040509

Hodder, K.R. (2009). Flocculation: a key process in the sediment flux of a large, glacier-fed lake. *Earth Surface Processes and Landforms 34*, 1151–1163. https://doi.org/10.1002/esp.1807

Hodson, A., Mumford, P., & Lister, D. (2004). Suspended sediment and phosphorus in proglacial rivers: Bioavailability and potential impacts upon the P status of ice-marginal receiving waters. *Hydrological Processes*, *18*(13), 2409–2422. https://doi.org/10.1002/hyp.1471

Hofmann G, Lange-Bertalot H, Werum M, Klee R (2018) Rote Liste der limnischen Kieselalgen. Naturschutz und Biologische Vielfalt 70(7):601–708. Available from: https://www.rote-liste-zentrum.de/de/Limnische-Kieselalgen-Bacillariophyta-1772.html

Hofmeister, F., Arias-Rodriguez, L. F., Premier, V., Marin, C., Notarnicola, C., Disse, M., & Chiogna, G. (2022). Intercomparison of Sentinel-2 and modelled snow cover maps in a high-elevation Alpine catchment. *Journal of Hydrology X, 15*, 100123. https://doi.org/10.1016/j.hydroa.2022.100123

Hoham, R. W., & Remias, D. (2020). Snow and Glacial Algae: A Review. *Journal of Phycology*, *56*(2), 264–282. https://doi.org/10.1111/jpy.12952

Hood, E., Battin, T. J., Fellman, J., O'Neel, S., & Spencer, R. G. M. (2015). Storage and release of organic carbon from glaciers and ice sheets. *Nature Geoscience*, *8*(2), 91–96. https://doi.org/10.1038/ngeo2331

Huss, M., Bookhagen, B., Huggel, C., Jacobsen, D., Bradley, R. S., Clague, J. J., Vuille, M., Buytaert, W., Cayan, D. R., Greenwood, G., Mark, B. G., Milner, A. M., Weingartner, R., & Winder, M. (2017). Toward mountains without permanent snow and ice. *Earth's Future*, *5*(5), 418–435. https://doi.org/10.1002/2016EF000514

Hylander, S., Jephson, T., Lebret, K., Von Einem, J., Fagerberg, T., Balseiro, E., Modenutti, B., Souza, M. S., Laspoumaderes, C., Jonsson, M., Ljungberg, P., Nicolle, A., Nilsson, P. A., Ranaker, L., & Hansson, L.-A. (2011). Climate-induced input of turbid glacial meltwater affects vertical

distribution and community composition of phyto- and zooplankton. *Journal of Plankton Research, 33*(8), 1239–1248. https://doi.org/10.1093/plankt/fbr025

IPBES (2019): Global assessment report on biodiversity and ecosystem services of the Intergovernmental Science-Policy Platform on Biodiversity and Ecosystem Services. E. S. Brondizio, J. Settele, S. Díaz, and H. T. Ngo (eds.). IPBES secretariat, Bonn, Germany. 1148 pages. https://doi.org/10.5281/zenodo.3831673

IPCC (2022). Climate Change 2022: Impacts, Adaptation, and Vulnerability. Contribution of Working Group II to the Sixth Assessment Report of the Intergovernmental Panel on Climate Change [H.-O. Pörtner, D.C. Roberts, M. Tignor, E.S. Poloczanska, K. Mintenbeck, A. Alegría, M. Craig, S. Langsdorf, S. Löschke, V. Möller, A. Okem, B. Rama (eds.)]. Cambridge University Press. Cambridge University Press, Cambridge, UK and New York, NY, USA, 3056 pp., doi:10.1017/9781009325844.

Irwin, J., & Pickrill, R. A. (1982). Water temperature and turbidity in glacially fed Lake Tekapo. *New Zealand Journal of Marine and Freshwater Research, 16*(2), 189–200. https://doi.org/10.1080/00288330.1982.9515962

ISPRA – Servizio Geologico d'Italia (2012). Carta Geologica d'Italia. Foglio 024 Bormio. Available from https://www.isprambiente.gov.it/Media/carg/note_illustrative/24_Bormio.pdf, last access on 02 January 2025.

Jennings, D. R. H. (2021). Does glacial retreat impact benthic chironomid communities? A case study from Rocky Mountain National Park, Colorado. *SN Applied Sciences*, *3*(12), 855. https://doi.org/10.1007/s42452-021-04835-7

Julius, M. L., & Theriot, E. C. (2010). The diatoms: A primer. In J. P. Smol & E. F. Stoermer (Eds.), The Diatoms: Applications for the Environmental and Earth sciences 2nd Edition. Cambridge University Press. https://doi.org/10.1017/CBO9780511763175.003

Jung,D.O., Achenbach, L. A., Karr, E. A., Takaichi, S., & Madigan, M. T. (2004). A gas vesiculate planktonic strain of the purple non-sulfur bacterium *Rhodoferax antarcticus* isolated from Lake Fryxell, Dry Valleys, Antarctica. *Archives of Microbiology*, *182*(2–3). https://doi.org/10.1007/s00203-004-0719-8

Kammerlander, B., Breiner, H.-W., Filker, S., Sommaruga, R., Sonntag, B., & Stoeck, T. (2015). High diversity of protistan plankton communities in remote high mountain lakes in the European Alps and the Himalayan mountains. *FEMS Microbiology Ecology*, *91*(4). https://doi.org/10.1093/femsec/fiv010

Kammerlander, B., Koinig, K. A., Rott, E., Sommaruga, R., Tartarotti, B., Trattner, F., & Sonntag, B. (2016). Ciliate community structure and interactions within the planktonic food web in two alpine lakes of contrasting transparency. *Freshwater Biology*, *61*(11), 1950–1965. https://doi.org/10.1111/fwb.12828

Karlson, B., Andreasson, A., Johansen, M., Karlberg, M., Loo, A. & Skjevik, A.-T. (2018). Nordic Microalgae. World-wide electronic publication http://nordicmicroalgae.org. Norrköping: Swedish Meteorological and Hydrological Institute.

Kawahara, H. (2017). Cryoprotectants and Ice-Binding Proteins. In: Margesin, R. (eds) Psychrophiles: From Biodiversity to Biotechnology. Springer, Cham. https://doi.org/10.1007/978-3-319-57057-0_11

Khamis, K., Hannah, D. M., Brown, L. E., Tiberti, R., & Milner, A. M. (2014). The use of invertebrates as indicators of environmental change in alpine rivers and lakes. *Science of The Total Environment*, *493*, 1242–1254. https://doi.org/10.1016/j.scitotenv.2014.02.126

Kirk, K. L. (1991). Inorganic particles alter competition in grazing plankton: the role of selective feeding. *Ecology*, *72*(3), 915–923. https://doi.org/10.2307/1940593

Klaveness, D. (2019). Hydrurus foetidus (Chrysophyceae): An update and request for observations. *ALGAE*, *34*(1), 1–5. https://doi.org/10.4490/algae.2019.34.1.15

Kleinteich, J., Hanselmann, K., Hildebrand, F., Kappler, A., & Zarfl, C. (2022). Glacier melt-down changes habitat characteristics and unique microbial community composition and physiology in alpine lake sediments. *FEMS Microbiology Ecology*, *98*(7), fiac075. https://doi.org/10.1093/femsec/fiac075

Koenings, J. P., Burkett, R. D., & Edmundson, J. M. (1990). The Exclusion of Limnetic Cladocera from Turbid Glacier-Meltwater Lakes. *Ecology*, *71*(1), 57–67. https://doi.org/10.2307/1940247

Komárek, J., & Anagnostidis, K. (2005). Cyanoprokaryota 2. Teil/2nd Part: Oscillatoriales. In Süsswasserflora von Mitteleuropa 19/2; Büdel,B., Krienitz, L., Gärtner, G., Schagerl, M., Eds.; Elsevier/Spektrum: Heidelberg, Germany, 2005; p. 759.

Kotlarski, S., Gobiet, A., Morin, S., Olefs, M., Rajczak, J., & Samacoïts, R. (2023). 21st Century alpine climate change. Climate Dynamics, 60(1–2), 65–86. https://doi.org/10.1007/s00382-022-06303-3

Kottek, M., Grieser, J., Beck, C., Rudolf, B., & Rubel, F. (2006). World Map of the Köppen-Geiger climate classification updated. *Meteorologische Zeitschrift, 15*(3), 259–263. https://doi.org/10.1127/0941-2948/2006/0130.

Krammer K., Lange-Bertalot H., 1986, 1988, 1991a, 1991b, 2000. - Bacillariophyceae. Teil: Naviculaceae; Bacillariaceae, Epithemiaceae, Surirellaceae; Centrales, Fragilariaceae, Eunotiaceae; Achnathaceae. Kritische Erganzungen zu Navicula und Gomphonema; and french translation of the keys. Süβwasserflora von Mitteleuropa, 2/1-5, Fischer, Stuttgart.

Krammer, K. (2000). The genus Pinnularia. In: H. Lange-Bertalot (ed.). Diatoms of Europe, vol. 1 (pp. 1–703). Ruggell: A. R. G. Gantner Verlag K.G.

Krug, L., Erlacher, A., Markut, K., Berg, G., & Cernava, T. (2020). The microbiome of alpine snow algae shows a specific inter-kingdom connectivity and algae-bacteria interactions with supportive capacities. *The ISME Journal*, *14*(9), 2197–2210. https://doi.org/10.1038/s41396-020-0677-4

Kruskal, J.B., Wish, M. (1978). Multidimensional scaling. Sage Publications, Beverly Hills: 93 pp.

Kulikovskiy, M., Glushchenko, A., Kezlya, E., Kuznetsova, I., Kociolek, J. P., & Maltsev, Y. (2023). The Genus Pinnularia Ehrenberg (Bacillariophyta) from the Transbaikal Area (Russia, Siberia): Description of Seven New Species on the Basis of Morphology and Molecular Data with

Discussion of the Phylogenetic Position of Caloneis. Plants, 12(20), 3552. https://doi.org/10.3390/plants12203552

La Rocca, N., Sciuto, K., Meneghesso, A., Moro, I., Rascio, N., & Morosinotto, T. (2015). Photosynthesis in extreme environments: Responses to different light regimes in the Antarctic alga *Koliella antarctica*. *Physiologia Plantarum*, *153*(4), 654–667. https://doi.org/10.1111/ppl.12273

Lange-Bertalot, H., & Genkal, S.I. (1999). Diatoms from Siberia I. Islands in the Arctic Ocean (Yugorsky-Shar Strait). In: H. Lange-Bertalot (ed.). Iconographia Diatomologica, vol. 6 (pp.1–292). Vaduz: A. R. G. Gantner Verlag K.G.

Lange-Bertalot, H., Hofmann, G., Werum, M., Cantonati, M. (2017). Freshwater benthic diatoms of Central Europe: over 800 common species used in ecological assessment. English edition with updated taxonomy and added species. Koeltz Botanical Books, Schmitten-Oberreifenberg

Laspoumaderes, C., Modenutti, B., Souza, M. S., Bastidas Navarro, M., Cuassolo, F., & Balseiro, E. (2013). Glacier melting and stoichiometric implications for lake community structure: Zooplankton species distributions across a natural light gradient. *Global Change Biology*, *19*(1), 316–326. https://doi.org/10.1111/gcb.12040

Leonov, V. D. (2020). The first report on the oribatid mites (Acari: Oribatida) in tundra of the Chunatundra Mountains on the Kola Peninsula, Russia. *Acarologia*, *60*(4), 722–734. https://doi.org/10.24349/acarologia/20204398

Levkov, Z., Mitic-Kopanja, D. & Reichardt, E. (2016). The diatom genus *Gomphonema* in the Republic of Macedonia. In: *Diatoms of Europe. Diatoms of the European inland waters and comparable habitats. Volume 8*. (Lange-Bertalot, H. Eds), pp. 1-552. Oberreifenberg: Koeltz Botanical Books.

Linares Cuesta, J. E., Olofsson, L., & Sánchez-Castillo, P. (2007). Comunidades de diatomeas epipélicas en las lagunas de alta montaña de Sierra Nevada (Granada, España). *Limnetica, 26*(1), 89–97. https://doi.org/10.23818/limn.26.09

Liu, Q., Zhou, Y.-G., & Xin, Y.-H. (2015). High diversity and distinctive community structure of bacteria on glaciers in China revealed by 454 pyrosequencing. *Systematic and Applied Microbiology*, *38*(8), 578–585. https://doi.org/10.1016/j.syapm.2015.09.005

Liu, Y., Xie, J., & Wang, X. (2020). microeco: An R package for microbiome analysis with environmental metadata. *Journal of Open Source Software*, *5*(52), 2126. https://doi.org/10.21105/joss.02126

Liu, K., Yan, Q., Guo, X., Wang, W., Zhang, Z., Ji, M., Wang, F., & Liu, Y. (2024). Glacier retreat induces contrasting shifts in bacterial biodiversity patterns in glacial lake water and sediment: bacterial communities in glacial lakes. *Microbial Ecology*, *87*(1), 128. https://doi.org/10.1007/s00248-024-02447-3

Lorenzen, C. J. (1967). Determination of Chlorophyll and Pheopigments: Spectrophotometric Equations. *Limnology and Oceanography, 12*, 343-346. http://dx.doi.org/10.4319/lo.1967.12.2.0343

Ma, J., Song, C., & Wang, Y. (2021). Spatially and temporally resolved monitoring of glacial lake changes in Alps during the recent two decades. *Frontiers in Earth Science*, *9*, 723386. https://doi.org/10.3389/feart.2021.723386

MacDonald, J. D. (1869). On the structure of the diatomaceous frustule and its genetic cycle. Ann. Mag. Nat. Hist. ser. 4, 3, 1–8.

Mareš, J., Hrouzek, P., Kaňa, R., Ventura, S., Strunecký, O., & Komárek, J. (2013). The Primitive Thylakoid-Less Cyanobacterium Gloeobacter Is a Common Rock-Dwelling Organism. *PLoS ONE*, *8*(6), e66323. https://doi.org/10.1371/journal.pone.0066323

Margesin, R., & Miteva, V. (2011). Diversity and ecology of psychrophilic microorganisms. *Research in Microbiology*, *162*(3), 346–361. https://doi.org/10.1016/j.resmic.2010.12.004

Margesin, R., Spröer, C., Zhang, D.-C., & Busse, H.-J. (2012). *Polaromonas glacialis* sp. Nov. And *Polaromonas cryoconiti* sp. Nov., isolated from alpine glacier cryoconite. *International Journal of Systematic and Evolutionary Microbiology*, *62*(Pt_11), 2662–2668. https://doi.org/10.1099/ijs.0.037556-0

Martin, J. L., Santi, I., Pitta, P., John, U., & Gypens, N. (2022). Towards quantitative metabarcoding of eukaryotic plankton: An approach to improve 18S rRNA gene copy number bias. *Metabarcoding and Metagenomics*, *6*, e85794. https://doi.org/10.3897/mbmg.6.85794

Masetti, M., Diolaiuti, G., D'Agata, C., & Smiraglia, C. (2010). Hydrological Characterization of an Ice-Contact Lake: Miage Lake (Monte Bianco, Italy). *Water Resources Management, 24*(8), 1677–1696. https://doi.org/10.1007/s11269-009-9519-x

McCormick, P.V. (1996). Resource competition and species coexistence in freshwater algal assemblages. In: Stevenson, R.J., Bothwell, M.L., Lowe, R.L. (Eds.), Algal Ecology: Freshwater Benthic Ecosystems. Academic Press, San Diego, CA, pp. 229–252.

McMurdie, P. J., & Holmes, S. (2013). phyloseq: An R package for reproducible interactive analysis and graphics of microbiome census data. *PLOS ONE*, *8*(4), e61217. https://doi.org/10.1371/journal.pone.0061217

Mez, K., Hanselmann, K., & Preisig, H. R. (1998). Environmental conditions in high mountain lakes containing toxic benthic cyanobacteria*. Hydrobiologia 368*, 1–15.

Mikhailyuk, T., Vinogradova, O., Holzinger, A., Glaser, K., Samolov, E., & Karsten, U. (2019). New record of the rare genus Crinalium Crow (Oscillatoriales, Cyanobacteria) from sand dunes of the Baltic Sea, Germany: Epitypification and emendation of Crinalium magnum Fritsch et John based on an integrative approach. *Phytotaxa*, *400*(3), 165. https://doi.org/10.11646/phytotaxa.400.3.4

Milner, A. M., Khamis, K., Battin, T. J., Brittain, J. E., Barrand, N. E., Füreder, L., Cauvy-Fraunié, S., Gíslason, G. M., Jacobsen, D., Hannah, D. M., Hodson, A. J., Hood, E., Lencioni, V., Ólafsson, J. S., Robinson, C. T., Tranter, M., & Brown, L. E. (2017). Glacier shrinkage driving global changes in downstream systems. *Proceedings of the National Academy of Sciences*, *114*(37), 9770–9778. https://doi.org/10.1073/pnas.1619807114

Miserendino, M. L., Epele, L. B., Brand, C., Uyua, N., Santinelli, N., & Sastre, V. (2023). Uncovering aquatic diversity patterns in two Patagonian glacial lakes: Does habitat heterogeneity matter? *Aquatic Sciences*, *85*(2), 52. https://doi.org/10.1007/s00027-023-00949-9

Modenutti, B., Pérez, G., Balseiro, E., & Queimaliños, C. (2000). The relationship between light attenuation, chlorophyll *a* and total suspended solids in a Southern Andes glacial lake. *SIL Proceedings, 1922-2010*, *27*(5), 2648–2651. https://doi.org/10.1080/03680770.1998.11898147

Montrasio, A., Berra, F., Cariboni, M., Ceriani, M., Deichmann, N., Ferliga, C., Gregnanin, A., Guerra, S., Guglielimin, M., Jadoul, F., Longhin, M., Mair, V., Mazzoccola, D., Sciesa, E., & Zappone, A. (2012). Note illustrative sulla Carta Geologica d'Italia 1:50.000, foglio 024, Bormio. LTS Land Technology & Services – Padova e Treviso.

Muhlfeld, C. C., Giersch, J. J., Hauer, F. R., Pederson, G. T., Luikart, G., Peterson, D. P., Downs, C. C., & Fagre, D. B. (2011). Climate change links fate of glaciers and an endemic alpine invertebrate: A letter. *Climatic Change*, *106*(2), 337–345. https://doi.org/10.1007/s10584-011-0057-1

Napolitano, M. J., & Shain, D. H. (2004). Four kingdoms on glacier ice: Convergent energetic processes boost energy levels as temperatures fall. *Proceedings of the Royal Society of London. Series B: Biological Sciences*, *271*(suppl_5). https://doi.org/10.1098/rsbl.2004.0180

Nie, Y., Sheng, Y., Liu, Q., Liu, L., Liu, S., Zhang, Y., & Song, C. (2017). A regional-scale assessment of Himalayan glacial lake changes using satellite observations from 1990 to 2015. *Remote Sensing of Environment*, *189*, 1–13. https://doi.org/10.1016/j.rse.2016.11.008

Nimma, D., Devi, O. R., Laishram, B., Ramesh, J. V. N., Boddupalli, S., Ayyasamy, R., Tirth, V., & Arabil, A. (2025). Implications of climate change on freshwater ecosystems and their biodiversity. *Desalination and Water Treatment*, *321*, 100889. https://doi.org/10.1016/j.dwt.2024.100889

Obertegger, U., Pindo, M., & Flaim, G. (2019). Multifaceted aspects of synchrony between freshwater prokaryotes and protists. *Molecular Ecology*, *28*(19), 4500–4512. https://doi.org/10.1111/mec.15228

Obleitner, F. (1994). Climatological features of glacier and valley winds at the Hintereisferner (Ötztal Alps, Austria). *Theoretical and Applied Climatology, 49*(4), 225–239. https://doi.org/10.1007/BF00867462

Oerlemans, J., & Grisogono, B. (2002). Glacier winds and parameterisation of the related surface heat fluxes. *Tellus A: Dynamic Meteorology and Oceanography, 54*(5), 440. https://doi.org/10.3402/tellusa.v54i5.12164

Oksanen, J., Guillaume, B., Friendly, M., Kindt, R., Legendre, P., McGlinn, D., Minchin, P. R., O'Hara, R. B., Simpson, G. L., Solymos, P., Stevens, M. H. H., Szoecs, E., & Wagner, H. (2023). vegan: Community ecology package (Version 2.6-4) [R package]. https://cran.r-project.org/package=vegan

Otto, J.-C. (2019). Proglacial Lakes in High Mountain Environments. In T. Heckmann & D. Morche (Eds.), *Geomorphology of Proglacial Systems* (pp. 231–247). Springer International Publishing. https://doi.org/10.1007/978-3-319-94184-4_14

Passy, S. I. (2007). Diatom ecological guilds display distinct and predictable behavior along nutrient and disturbance gradients in running waters. Aquatic Botany, 86(2), 171–178. https://doi.org/10.1016/j.aquabot.2006.09.018.

Patova, E. N., & Novakovskaya, I. V. (2018). Soil algae of the Northeastern European Russia. Novosti sistematiki nizshikh rastenii, 52(2), 311–353. (In Russ.). https://doi.org/10.31111/nsnr/2018.52.2.311.

Patova, E., Novakovskaya, I., Gusev, E., & Martynenko, N. (2023). Diversity of Cyanobacteria and Algae in Biological Soil Crusts of the Northern Ural Mountain Region Assessed through Morphological and Metabarcoding Approaches. Diversity, 15(10), 1080. https://doi.org/10.3390/d15101080.

Pepin, N. C., Arnone, E., Gobiet, A., Haslinger, K., Kotlarski, S., Notarnicola, C., Palazzi, E., Seibert, P., Serafin, S., Schöner, W., Terzago, S., Thornton, J. M., Vuille, M., & Adler, C. (2022). Climate Changes and Their Elevational Patterns in the Mountains of the World. *Reviews of Geophysics*, *60*(1), e2020RG000730. https://doi.org/10.1029/2020RG000730

Pernthaler, J. (2005). Predation on prokaryotes in the water column and its ecological implications. *Nature Reviews Microbiology*, *3*(7), 537–546. https://doi.org/10.1038/nrmicro1180

Peter, H., & Sommaruga, R. (2016). Shifts in diversity and function of lake bacterial communities upon glacier retreat. *The ISME Journal*, *10*(7), 1545–1554. https://doi.org/10.1038/ismej.2015.245

Peter, H., & Sommaruga, R. (2017). Alpine glacier-fed turbid lakes are discontinuous cold polymictic rather than dimictic. *Inland Waters, 7*(1), 45–54. https://doi.org/10.1080/20442041.2017.1294346

Peterson, C.G. (1996). Response of Benthic Algal Communities to Natural Physical Disturbance In: Stevenson, R.J., Bothwell, M.L., Lowe, R.L. (Eds.), Algal Ecology: Freshwater Benthic Ecosystems. Academic Press, San Diego, CA, pp. 375-403.

Pfitzer, E. (1871). Untersuchungen u¨ber Bau und Entwickelung der Bacillariaceen (Diatomaceen). Bot. Abhandl. (ed. Hanstein) 1(2), 1–189.

Pielou, E.C. (1975). Ecological diversity. J. Eiley & Sons, New York: 165 pp.

Poole, H. H., & Atkins, W. R. G. (1929). Photo-electric Measurements of Submarine Illumination throughout the Year. *Journal of the Marine Biological Association of the United Kingdom, 16*(1), 297–324. https://doi.org/10.1017/S0025315400029829

Potapova, M. (2009). *Odontidium mesodon*. In Diatoms of North America. Retrieved December 06, 2024, from https://diatoms.org/species/odontidium_mesodon

Potapova, M., Allen, L., Edlund, M. (2009). *Achnanthidium minutissimum*. In Diatoms of North America. Retrieved December 06, 2024, from https://diatoms.org/species/achnanthidium_minutissimum

Poulíčková, A., Hašler, P., Lysáková, M., & Spears, B. (2008). The ecology of freshwater epipelic algae: An update. *Phycologia*, *47*(5), 437–450. https://doi.org/10.2216/07-59.1

Puspitarini, H. D., François, B., Zaramella, M., Brown, C., & Borga, M. (2020). The impact of glacier shrinkage on energy production from hydropower-solar complementarity in alpine river basins. *Science of the Total Environment 719*, 137488 https://doi.org/10.1016/j. scitotenv.2020.137488.

R Core Team (2023). R: A Language and Environment for Statistical Computing. R Foundation for Statistical Computing, Vienna, Austria. https://www.R-project.org/.

Raabová, L., Kovacik, L., Elster, J., & Strunecký, O. (2019). Review of the genus Phormidesmis (Cyanobacteria) based on environmental, morphological, and molecular data with description

of a new genus Leptodesmis. *Phytotaxa*, *395*(1), 1–16. https://doi.org/10.11646/phytotaxa.395.1.1

Rabot, C. (1905). Glacial Reservoirs and Their Outbursts. *The Geographical Journal, 25*(5), 534. https://doi.org/10.2307/1776694

Radzi, R., Merican, F., Broady, P., Convey, P., Muangmai, N., Omar, W. M. W., & Lavoué, S. (2021). First record of the cyanobacterial genus Wilmottia (Coleofasciculaceae, Oscillatoriales) from the South Orkney Islands (Antarctica). *ALGAE*, *36*(2), 111–121. https://doi.org/10.4490/algae.2021.36.5.6

Rae, R., Howard-Williams, C., Hawes, I., Schwarz, A.-M., & Vincent, W. F. (2001). Penetration of solar ultraviolet radiation into New Zealand lakes: Influence of dissolved organic carbon and catchment vegetation. *Limnology*, *2*(2), 79–89. https://doi.org/10.1007/s102010170003

Ramel, C., Rey, P.-L., Fernandes, R., Vincent, C., Cardoso, A. R., Broennimann, O., Pellissier, L., Pradervand, J.-N., Ursenbacher, S., Schmidt, B. R., & Guisan, A. (2020). Integrating ecosystem services within spatial biodiversity conservation prioritization in the Alps. *Ecosystem Services*, *45*, 101186. https://doi.org/10.1016/j.ecoser.2020.101186

Ramskogler, K., Knoflach, B., Elsner, B., Erschbamer, B., Haas, F., Heckmann, T., … Tasser, E. (2023). Primary succession and its driving variables – a sphere-spanning approach applied in proglacial areas in the upper Martell Valley (Eastern Italian Alps). *Biogeosciences, 20*(14), 2919–2939. https://doi.org/10.5194/bg-20-2919-2023.

Ren, Z., Martyniuk, N., Oleksy, I. A., Swain, A., & Hotaling, S. (2019). Ecological Stoichiometry of the Mountain Cryosphere. *Frontiers in Ecology and Evolution*, *7*, 360. https://doi.org/10.3389/fevo.2019.00360

Reynolds, C. S. (2006). The Ecology of Phytoplankton. Cambridge University Press.

Richards, J., Moore, R.D., & Forrest, A.L. (2011). Late-summer thermal regime of a small proglacial lake. *Hydrological processes, 26*, 2687–2695.

Righetti, M., & Lucarelli, C. (2010). Resuspension phenomena of benthic sediments: The role of cohesion and biological adhesion. *River Research and Applications, 26*(4), 404–413. https://doi.org/10.1002/rra.1296

Rimet F., Gusev E., Kahlert M., Kelly M., Kulikovskiy M., Maltsev Y., Mann D., Pfannkuchen M., Trobajo R., Vasselon V., Zimmermann J., Bouchez A., 2019. Diat.barcode, an open-access curated barcode library for diatoms. Scientific Reports. https://www.nature.com/articles/s41598-019-51500-6

Rimet, F., & Bouchez, A. (2012). Life-forms, cell-sizes and ecological guilds of diatoms in European rivers. Knowledge and Management of Aquatic Ecosystems, 406, 01. https://doi.org/10.1051/kmae/2012018.

Rimet, Frederic; Chonova, Teofana; Gassiole, Gilles; Gusev, Evgenuy; Kahlert, Maria; Keck, François; Kelly, Martyn; Kochoska, Hristina; Kulikovskiy, Maxim; Levkov, Zlatko; Maltsev, Yevhen; Mann, David; Pfannkuchen, Martin; Trobajo, Rosa; Vasselon, Valentin; Vidakovic, Danijela; Wetzel, Carlos; Zimmermann, Jonas; Bouchez, 2018, "Diat.barcode, an open-access barcode library for diatoms", https://doi.org/10.15454/TOMBYZ, Portail Data INRAE

Rinke, K., Robinson, C. T., & Uehlinger, U. (2001). A Note on Abiotic Factors that Constrain Periphyton Growth in Alpine Glacier Streams. *International Review of Hydrobiology, 86*(3), 361–366. https://doi.org/10.1002/1522-2632(200106)86:3<361::AID-IROH361>3.0.CO;2-Z

Robb, D. M., Pieters, R., & Lawrence, G. A. (2021). Fate of turbid glacial inflows in a hydroelectric reservoir. *Environmental Fluid Mechanics, 21*(6), 1201–1225. https://doi.org/10.1007/s10652-021-09815-4

Robinson, C. T., Tonolla, D., Imhof, B., Vukelic, R., & Uehlinger, U. (2016). Flow intermittency, physico-chemistry and function of headwater streams in an Alpine glacial catchment. Aquatic Sciences, 78(2), 327–341. https://doi.org/10.1007/s00027-015-0434-3

Rogora, M., Massaferro, J., Marchetto, A., Tartari, G., & Mosello, R. (2008). The water chemistry of some shallow lakes in Northern Patagonia and their nitrogen status in comparison with remote lakes in different regions of the globe. *Journal of Limnology*, *67*(2), 75. https://doi.org/10.4081/jlimnol.2008.75

Rose, K. C., Hamilton, D. P., Williamson, C. E., McBride, C. G., Fischer, J. M., Olson, M. H., Saros, J. E., Allan, M. G., & Cabrol, N. (2014). Light attenuation characteristics of glacially-fed lakes. *Journal of Geophysical Research: Biogeosciences*, *119*(7), 1446–1457. https://doi.org/10.1002/2014JG002674

Rott, E., Cantonati, M., Füreder, L., & Pfister, P. (2006). Benthic algae in high altitude streams of the Alps – a neglected component of the aquatic biota. *Hydrobiologia*, *562*(1), 195–216. https://doi.org/10.1007/s10750-005-1811-z

Rotta, F., Cerasino, L., Occhipinti-Ambrogi, A., Rogora, M., Seppi, R., & Tolotti, M. (2018). Diatom diversity in headwaters influenced by permafrost thawing: First evidence from the Central Italian Alps. *Advances in Oceanography and Limnology, 9*(2). https://doi.org/10.4081/aiol.2018.7929

Round, F. E., & Happey, C. M. (1965). Persistent, vertical-migration rhythms in benthic microflora: Part IV a diurnal rhythm of the epipelic diatom association in non-tidal flowing water. *British Phycological Bulletin*, *2*(6), 463–471. https://doi.org/10.1080/00071616500650081

Russell, N. J. (1997). Psychrophilic bacteria—Molecular adaptations of membrane lipids. *Comparative Biochemistry and Physiology Part A: Physiology*, *118*(3), 489–493. https://doi.org/10.1016/S0300-9629(97)87354-9

Salerno, F., Thakuri, S., Guyennon, N., Viviano, G., & Tartari, G. (2016). Glacier melting and precipitation trends detected by surface area changes in Himalayan ponds. *The Cryosphere*, *10*(4), 1433–1448. https://doi.org/10.5194/tc-10-1433-2016

Santi, I., Kasapidis, P., Karakassis, I., & Pitta, P. (2021). A Comparison of DNA Metabarcoding and Microscopy Methodologies for the Study of Aquatic Microbial Eukaryotes. *Diversity*, *13*(5), 180. https://doi.org/10.3390/d13050180

Saros, J. E., Rose, K. C., Clow, D. W., Stephens, V. C., Nurse, A. B., Arnett, H. A., Stone, J. R., Williamson, C. E., & Wolfe, A. P. (2010). Melting Alpine Glaciers Enrich High-Elevation Lakes with Reactive Nitrogen. *Environmental Science & Technology*, *44*(13), 4891–4896. https://doi.org/10.1021/es100147j

Schenone, L., Balseiro, E. G., Bastidas Navarro, M., & Modenutti, B. E. (2020). Modelling the consequence of glacier retreat on mixotrophic nanoflagellate bacterivory: A Bayesian approach. *Oikos*, *129*(8), 1216–1228. https://doi.org/10.1111/oik.07170

Servizio Glaciologico Alto Adige (2023). Ghiacciaio del Cevedale. Available from http://www.servizioglaciologico.com/ortler%20cevedale.htm

Shannon, C.E., & Weaver, W. (1949). The mathematical theory of comunication. University of Illinois Press, Urbana: 132 pp.guity Buri, P., McCarthy, M., Miles, E. S., Ayala, Á., & Pellicciotti, F. (2023). The decaying near-surface boundary layer of a retreating Alpine glacier. *Geophysical Research Letters, 50*, e2023GL103043. https://doi.org/10.1029/2023GL103043

Shaw, T. E., Buri, P., McCarthy, M., Miles, E. S., Ayala, Á., & Pellicciotti, F. (2023). The decaying near-surface boundary layer of a retreating Alpine glacier. *Geophysical Research Letters*, 50, e2023GL103043. https://doi.org/10.1029/2023GL103043

Shugar, D. H., Burr, A., Haritashya, U. K., Kargel, J. S., Watson, C. S., Kennedy, M. C., Bevington, A. R., Betts, R. A., Harrison, S., & Strattman, K. (2020). Rapid worldwide growth of glacial lakes since 1990. *Nature Climate Change*, *10*(10), 939–945. https://doi.org/10.1038/s41558-020-0855-4

Singer, G. A., Fasching, C., Wilhelm, L., Niggemann, J., Steier, P., Dittmar, T., & Battin, T. J. (2012). Biogeochemically diverse organic matter in Alpine glaciers and its downstream fate. *Nature Geoscience*, *5*(10), 710–714. https://doi.org/10.1038/ngeo1581

Slade, D., & Radman, M. (2011). Oxidative Stress Resistance in *Deinococcus radiodurans*. *Microbiology and Molecular Biology Reviews*, *75*(1), 133–191. https://doi.org/10.1128/MMBR.00015-10

Slemmons, K. E. H., & Saros, J. E. (2012). Implications of nitrogen-rich glacial meltwater for phytoplankton diversity and productivity in alpine lakes. *Limnology and Oceanography*, *57*(6), 1651–1663. https://doi.org/10.4319/lo.2012.57.6.1651

Slemmons, K. E. H., Rodgers, M. L., Stone, J. R., & Saros, J. E. (2017). Nitrogen subsidies in glacial meltwaters have altered planktonic diatom communities in lakes of the US Rocky Mountains for at least a century. *Hydrobiologia*, *800*(1), 129–144. https://doi.org/10.1007/s10750-017-3187-2

Slemmons, K. E. H., Saros, J. E., & Simon, K. (2013). The influence of glacial meltwater on alpine aquatic ecosystems: A review. *Environmental Science: Processes & Impacts*, *15*(10), 1794. https://doi.org/10.1039/c3em00243h

Smiraglia, C. & Diolaiuti, G. (2015) - *Il Nuovo Catasto dei Ghiacciai Italiani*. Ev-K2-CNR Ed., Bergamo, 400 pp.

Smith, N. D. (1978) Sedimentation processes and patterns in a glacier fed lake with low sediment input. *Canadian Journal of Earth Sciences, 15*, 741–756.

Smol, J. P., & Stoermer, E. F. (2010). Applications and uses of diatoms: prologue. In J. P. Smol & E. F. Stoermer (Eds.), The Diatoms: Applications for the Environmental and Earth sciences 2nd Edition. Cambridge University Press. https://doi.org/10.1017/CBO9780511763175.003

Solak, C.N., Hamilton, P., Peszek, L., Bąk, M., Yilmaz, E., Özkan, K., & Ertorun, N. (2023). Alpine Lake Environments and Psychrophile Diatoms Around the World with a Particular Emphasis on Turkish Glacial Lakes. In: Srivastava, P., Khan, A.S., Verma, J., Dhyani, S. (eds) Insights into the

World of Diatoms: From Essentials to Applications. Plant Life and Environment Dynamics. Springer, Singapore. https://doi.org/10.1007/978-981-19-5920-2_4

Sommaruga, R. (2001). The role of solar UV radiation in the ecology of alpine lakes. *Journal of Photochemistry and Photobiology B: Biology*, *62*(1–2), 35–42. https://doi.org/10.1016/S1011-1344(01)00154-3

Sommaruga, R. (2015). When glaciers and ice sheets melt: Consequences for planktonic organisms. *Journal of Plankton Research*, *37*(3), 509–518. https://doi.org/10.1093/plankt/fbv027

Sommaruga, R., & Kandolf, G. (2014). Negative consequences of glacial turbidity for the survival of freshwater planktonic heterotrophic flagellates. *Scientific Reports*, *4*(1), 4113. https://doi.org/10.1038/srep04113

Song, C., Sheng, Y., Wang, J., Ke, L., Madson, A., & Nie, Y. (2017). Heterogeneous glacial lake changes and links of lake expansions to the rapid thinning of adjacent glacier termini in the Himalayas. *Geomorphology*, *280*, 30–38. https://doi.org/10.1016/j.geomorph.2016.12.002

Steffen, T., Huss, M., Estermann, R., Hodel, E., & Farinotti, D. (2022). Volume, evolution, and sedimentation of future glacier lakes in Switzerland over the 21st century. *Earth Surface Dynamics*, *10*(4), 723–741. https://doi.org/10.5194/esurf-10-723-2022

Steinmann, A. D., Lamberti, G. A., & Leavitt, P. L. (1996). Biomass and pigments of benthic algae. In Hauer, F. R., & Lamberti, G. A. (Eds.). *Methods in stream ecology*. Academic Press, San Diego, CA

Sterner, R. W., Elser, J. J., Fee, E. J., Guildford, S. J., & Chrzanowski, T. H. (1997). The Light: Nutrient Ratio in Lakes: The Balance of Energy and Materials Affects Ecosystem Structure and Process. *The American Naturalist*, *150*(6), 663–684. https://doi.org/10.1086/286088

Stevenson, R. J., Bothwell, M. L., & Lowe, R. L. (1996). *Algal ecology: Freshwater benthic ecosystems*. Academic Press.

Stockner, J. G., & Armstrong, F. A. J. (1971). Periphyton of the Experimental Lakes Area, Northwestern Ontario. Journal of the Fisheries Research Board of Canada, 28, 215–229.

Stokes, C. R., Popovnin, V., Aleynikov, A., Gurney, S. D., & Shahgedanova, M. (2007). Recent glacier retreat in the Caucasus Mountains, Russia, and associated increase in supraglacial debris cover and supra-/proglacial lake development. *Annals of Glaciology*, *46*, 195–203. https://doi.org/10.3189/172756407782871468

Strasser, U., Corripio, J., Pellicciotti, F., Burlando, P., Brock, B., & Funk, M. (2004). Spatial and temporal variability of meteorological variables at Haut Glacier d'Arolla (Switzerland) during the ablation season 2001: Measurements and simulations. *Journal of Geophysical Research: Atmospheres, 109*(D3), 2003JD003973. https://doi.org/10.1029/2003JD003973

Strunecký, O., Bohunická, M., Johansen, J. R., Čapková, K., Raabová, L., Dvořák, P., & Komárek, J. (2017). A revision of the genus Geitlerinema and a description of the genus Anagnostidinema gen. Nov. (Oscillatoriophycidae, Cyanobacteria). *Fottea*, *17*(1), 114–126. https://doi.org/10.5507/fot.2016.025

Sudlow, K., Tremblay, S. S., & Vinebrooke, R. D. (2023). Glacial stream ecosystems and epilithic algal communities under a warming climate. *Environmental Reviews*, *31*(3), 471–483. https://doi.org/10.1139/er-2022-0114

Sugiyama, S., Minowa, M., Sakakibara, D., Skvarca, P., Sawagaki, T., Ohashi, Y., Naito, N., & Chikita, K. (2016). Thermal structure of proglacial lakes in Patagonia. *Journal of Geophysical Research: Earth Surface, 121*(12), 2270–2286. https://doi.org/10.1002/2016JF004084

Tartarotti, B., Saul, N., Chakrabarti, S., Trattner, F., Steinberg, C. E. W., & Sommaruga, R. (2014). UV-induced DNA damage in Cyclops abyssorum tatricus populations from clear and turbid alpine lakes. *Journal of Plankton Research*, *36*(2), 557–566. https://doi.org/10.1093/plankt/fbt109

Tartarotti, B., Trattner, F., Remias, D., Saul, N., Steinberg, C. E. W., & Sommaruga, R. (2017). Distribution and UV protection strategies of zooplankton in clear and glacier-fed alpine lakes. *Scientific Reports*, *7*(1), 4487. https://doi.org/10.1038/s41598-017-04836-w

Taylor, C., Robinson, T. R., Dunning, S., Rachel Carr, J., & Westoby, M. (2023). Glacial lake outburst floods threaten millions globally. *Nature Communications, 14*(1), 487. https://doi.org/10.1038/s41467-023-36033-x

Tenci, M. V., Bruno, M. C., & Tolotti, M. (2025). First record of *Pinnularia bullacostae* Krammer & Lange-Bertalot 1999 in proglacial lakes of the European Alps (Italy). *Nova Hedwigia*, 106514. https://doi.org/10.1127/nova_hedwigia/2025/1108

Teoh, M.L., Chu, W.L., Phang, S.M. (2010). Effect of temperature change on physiology and biochemistry of algae: A review. *Malaysian Journal of Science, 29*(2), 82–97

Tiberti, R., Buscaglia, F., Callieri, C., Rogora, M., Tartari, G., & Sommaruga, R. (2020). Food Web Complexity of High Mountain Lakes is Largely Affected by Glacial Retreat. *Ecosystems*, *23*(5), 1093–1106. https://doi.org/10.1007/s10021-019-00457-8

Toffolon, M., & Piccolroaz, S. (2015). A hybrid model for river water temperature as a function of air temperature and discharge. *Environmental Research Letters*, *10*(11), 114011. https://doi.org/10.1088/1748-9326/10/11/114011

Tolar, B.B., Mosier, A.C., Lund, M.B., Francis, C.A. (2019). *Nitrosarchaeum*. Bergey's Manual of Systematics of Archaea and Bacteria. John Wiley & Sons, Ltd; 2015. p. 1–6. Available from: https://doi.org/10.1002/9781118960608.gbm01289

Tolotti, M., Brighenti, S., Bruno, M. C., Cerasino, L., Pindo, M., Tirler, W., & Albanese, D. (2024). Ecological "Windows of opportunity" influence biofilm prokaryotic diversity differently in glacial and non-glacial Alpine streams. *Science of The Total Environment*, *944*, 173826. https://doi.org/10.1016/j.scitotenv.2024.173826

Tolotti, M., Cerasino, L., Donati, C., Pindo, M., Rogora, M., Seppi, R., & Albanese, D. (2020). Alpine headwaters emerging from glaciers and rock glaciers host different bacterial communities: Ecological implications for the future. *Science of The Total Environment*, *717*, 137101. https://doi.org/10.1016/j.scitotenv.2020.137101

Traaen, T. S., & Lindstrøm, E.-A. (1983). Influence of current velocity on periphyton distribution. In R. G. Wetzel (Ed.), *Periphyton of Freshwater Ecosystems* (pp. 97–99). Springer Netherlands. https://doi.org/10.1007/978-94-009-7293-3_15

Tsuji, M., Vincent, W. F., Tanabe, Y., & Uchida, M. (2022). Glacier Retreat Results in Loss of Fungal Diversity. *Sustainability*, *14*(3), 1617. https://doi.org/10.3390/su14031617

Tuji, A. (2000). The effect of irradiance on the growth of different diatom forms of freshwater diatoms: implications for succession in attached diatom communities. *Journal of Phycology*, *36*(4), 659–661. https://doi.org/10.1046/j.1529-8817.2000.99212.x

Tweed, F. S., & Carrivick, J. L. (2015). Deglaciation and proglacial lakes. *Geology Today*, *31*(3), 96–102. https://doi.org/10.1111/gto.12094

Uehlinger, U., Malard, F., & Ward, J. V. (2003). Thermal patterns in the surface waters of a glacial river corridor (Val Roseg, Switzerland). *Freshwater Biology, 48*(2), 284–300. https://doi.org/10.1046/j.1365-2427.2003.01000.x

Uehlinger, U., Robinson, C. T., Hieber, M., & Zah, R. (2010). The physico-chemical habitat template for periphyton in alpine glacial streams under a changing climate. *Hydrobiologia, 657*(1), 107–121. https://doi.org/10.1007/s10750-009-9963-x

Van Dam, H., Mertens, A., & Sinkeldam, J. (1994). A coded checklist and ecological indicator values of freshwater diatoms from The Netherlands. *Netherlands Journal of Aquatic Ecology*, *28*(1), 117–133. https://doi.org/10.1007/BF02334251.

Van Den Broeke, M. R. (1997). Structure and diurnal variation of the atmospheric boundary layer over a mid-latitude glacier in summer. *Boundary-Layer Meteorology, 83*(2), 183–205. https://doi.org/10.1023/A:1000268825998

Van Kerckvoorde, A., Trappeniers, K., Nijs, I., & Beyens, L. (2000). Terrestrial soil diatom assemblages from different vegetation types in Zackenberg (Northeast Greenland). *Polar Biology*, *23*(6), 392–400. https://doi.org/10.1007/s003000050460

Vanderwall, J. W., Muhlfeld, C. C., Tappenbeck, T. H., Giersch, J., Ren, Z., & Elser, J. J. (2024). Mountain glaciers influence biogeochemical and ecological characteristics of high-elevation lakes across the northern Rocky Mountains, USA. *Limnology and Oceanography*, *69*(1), 37–52. https://doi.org/10.1002/lno.12434

Varliero, G., Lebre, P. H., Adams, B., Chown, S. L., Convey, P., Dennis, P. G., Fan, D., Ferrari, B., Frey, B., Hogg, I. D., Hopkins, D. W., Kong, W., Makhalanyane, T., Matcher, G., Newsham, K. K., Stevens, M. I., Weigh, K. V., & Cowan, D. A. (2024). Biogeographic survey of soil bacterial communities across Antarctica. *Microbiome*, *12*(1), 9. https://doi.org/10.1186/s40168-023-01719-3

Viani, C., Colombo, N., Bollati, I. M., Mortara, G., Perotti, L., & Giardino, M. (2022). Socio-environmental value of glacier lakes: Assessment in the Aosta Valley (Western Italian Alps). *Regional Environmental Change*, *22*(1), 7. https://doi.org/10.1007/s10113-021-01860-5

Viani, C., Giardino, M., Huggel, C., Perotti, L., & Mortara, G. (2016). An overview of glacier lakes in the Western Italian Alps from1927 to 2014 based on multiple data sources (historical maps, orthophotos and reports of the glaciological surveys). *Geografia Fisica e Dinamica Quaternaria, 39*(2),203–214. https:// doi. org/ 10. 4461/ GFDQ. 2016. 39. 19

Villanueva, V. D., Font, J., Schwartz, T., & Romaní, A. M. (2011). Biofilm formation at warming temperature: Acceleration of microbial colonization and microbial interactive effects. *Biofouling, 27*(1), 59–71. https://doi.org/10.1080/08927014.2010.538841

Viviroli, D., Dürr, H. H., Messerli, B., Meybeck, M., & Weingartner, R. (2007). Mountains of the world, water towers for humanity: typology, mapping, and global significance. *Water Resources Research*, *43*(7), 2006WR005653. https://doi.org/10.1029/2006WR005653

Wang, W., Xiang, Y., Gao, Y., Lu, A., & Yao, T. (2015). Rapid expansion of glacial lakes caused by climate and glacier retreat in the Central Himalayas. *Hydrological Processes*, *29*(6), 859–874. https://doi.org/10.1002/hyp.10199

Wantzen, K. M., Rothhaupt, K.-O., Mörtl, M., Cantonati, M., -Tóth, L. G., & Fischer, P. (Eds.). (2008). *Ecological Effects of Water-Level Fluctuations in Lakes*. Springer Netherlands. https://doi.org/10.1007/978-1-4020-9192-6

Warner, K. A., Saros, J. E., & Simon, K. S. (2017). Nitrogen Subsidies in Glacial Meltwater: Implications for High Elevation Aquatic Chains. *Water Resources Research*, *53*(11), 9791–9806. https://doi.org/10.1002/2016WR020096

Wells, S. A., editor (2023a). CE-QUAL-W2: A two-dimensional, laterally averaged, hydrodynamic and water quality model, version 4.5, user manual part 1, introduction. Department of Civil and Environmental Engineering, Portland State University, Portland, OR.

Wells, S. A. editor (2023b). CE-QUAL-W2: A two-dimensional, laterally averaged, hydrodynamic and water quality model, version 4.5, user manual part 2, hydrodynamic and water quality model theory. Department of Civil and Environmental Engineering, Portland State University, Portland, OR.

Wetzel, R.G. (2001). Limnology: Lake and River Ecosystems. Third Edition, Academic Press, San Diego, 1006 p.

WGMS 2023. Global Glacier Change Bulletin No. 5 (2020–2021). Zemp, M., Gärtner-Roer, I., Nussbaumer, S.U., Welty, E.Z., Dussaillant, I., and Bannwart, J. (eds.), ISC(WDS)/IUGG(IACS)/UNEP/UNESCO/WMO, World Glacier Monitoring Service, Zurich, Switzerland, 134 pp., publication based on database version: doi:10.5904/wgms-fog-2023-09.

Wilhelm, L., Besemer, K., Fasching, C., Urich, T., Singer, G. A., Quince, C., & Battin, T. J. (2014). Rare but active taxa contribute to community dynamics of benthic biofilms in glacier-fed streams. *Environmental Microbiology*, *16*(8), 2514–2524. https://doi.org/10.1111/1462-2920.12392

Williams, J. J., Nurse, A., Saros, J. E., Riedel, J., & Beutel, M. (2016). Effects of glaciers on nutrient concentrations and phytoplankton in lakes within the Northern Cascades Mountains (USA). *Biogeochemistry*, *131*(3), 373–385. https://doi.org/10.1007/s10533-016-0264-y

Yabuki, A., Hoshino, T., Nakamura, T., & Mizuno, K. (2024). The copy number of the eukaryotic rRNA gene can be counted comprehensively. *MicrobiologyOpen*, *13*(2), e1399. https://doi.org/10.1002/mbo3.1399

Yang, G. L., Hou, S. G., Le Baoge, R., Li, Z. G., Xu, H., Liu, Y. P., Du, W. T., & Liu, Y. Q. (2016). Differences in Bacterial Diversity and Communities Between Glacial Snow and Glacial Soil on the Chongce Ice Cap, West Kunlun Mountains. *Scientific Reports*, *6*(1), 36548. https://doi.org/10.1038/srep36548

Supplementary material

S2.1. Sediment delta in L2

1 October 2021

4 July 2023

S4.1. Diatom micrographs

Diatoms species representative for the samples investigated Cevedale proglacial lakes summer 2022 and 2023. A = *Achnanthidium minutissimum*; B = *Encyonopsis falaisensis*; C = *Encyonopsis microcephala*; D = *Encyonopsis microcephala* var. *robusta*; E = *Encyonema silesiacum*; F = *Encyonema minutum*; G = *Caloneis aerophila;* H = *Caloneis vasileyevae*; I = *Gomphonema varioreduncum*; J = *Adlafia minuscula;* K = *Psammothidium helveticum;* L = *Denticula tenuis*; M = *Surirella terricola*; N = *Nitzschia* aff. *pura*; O = *Nitzschia perminuta*; P = *Nitzschia palea* var. *debilis*; Q = *Pinnularia bullacostae*; R = *Pinnularia obscuriformis*; S = *Pinnularia obscura*.

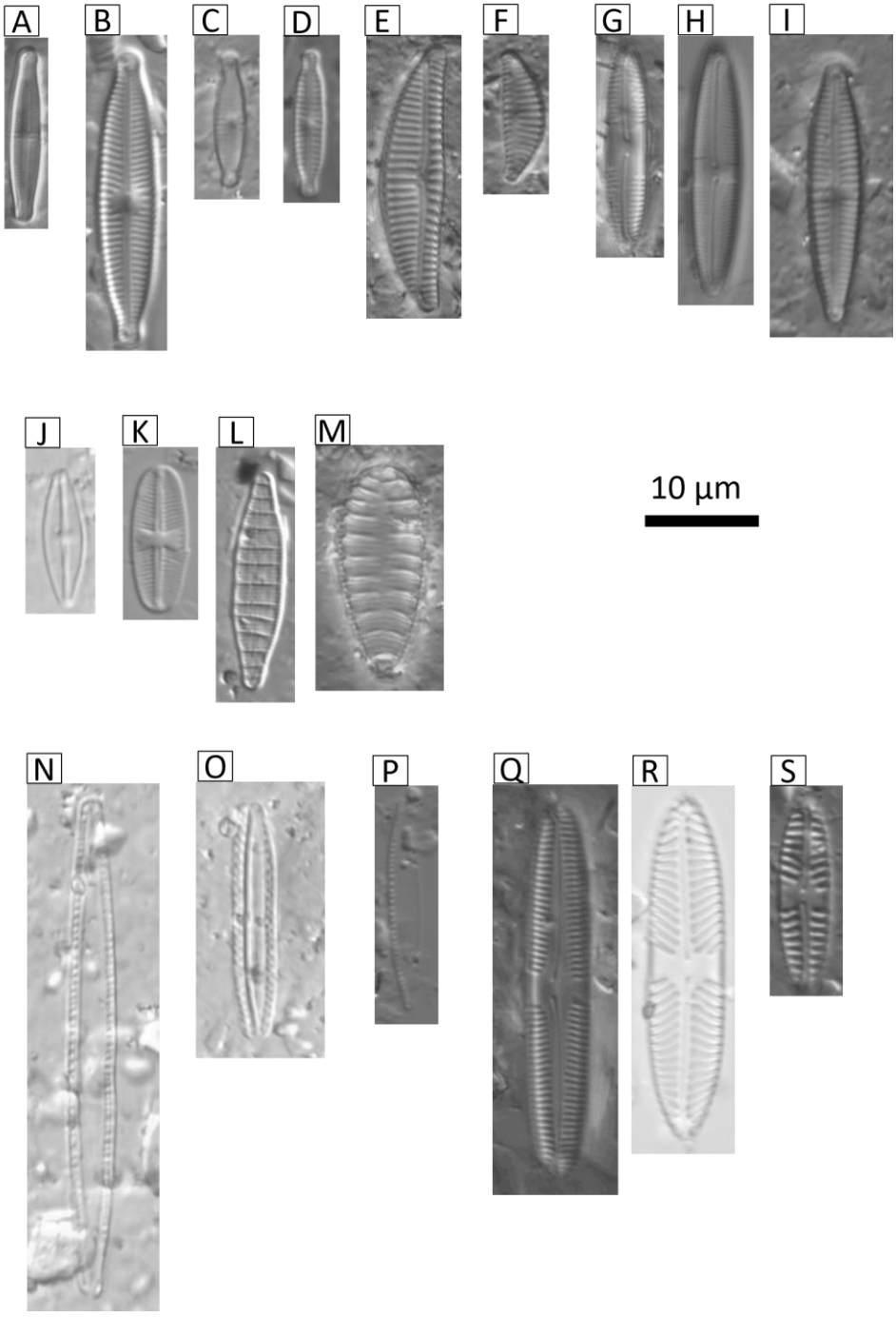

S4.2 *Pinnularia bullacostae*

Draft submitted to Nova Hedwigia in 2024, published in March 2025 (Tenci et al., 2025)

Title: First record of *Pinnularia bullacostae* Krammer & Lange-Bertalot 1999 in proglacial lakes of the European Alps (Italy)

Authors: Tenci Maria Vittoria (1,2), Bruno Maria Cristina (2, 3), Tolotti Monica (2, 3)

1. Department of Civil, Environmental and Mechanical Engineering, University of Trento, Italy
2. Research and Innovation Centre, Fondazione Edmund Mach, S. Michele all'Adige, Italy
3. National Biodiversity Future Center (NBFC), Università di Palermo, Palermo, Italy

Introduction

Pinnularia bullacostae Krammer & Lange-Bertalot 1999 was first described as living between river mosses of a small arctic island close to the Yugorsky peninsula, Siberia (Lange-Bertalot & Genkal 1999). At the best of our knowledge, the known distribution of this species (Guiry 2024: www.algaebase.org, last access on 16th October 2024) encompasses the Kotelny Island (Genkal & Gabyshev 2020), the Arctic and Subarctic tundra (Genkal & Yarushina 2016; Kopyrina et al. 2021; Barinova et al. 2023; Barinova & Gabyshev 2024), the Subpolar Urals (Patova & Novakovskaya 2018 and citations therein; Patova et al. 2023), the Bureya River catchment (Medvedeva & Nikulina 2019), and the Attert River catchment in Luxembourg (Barragán et al. 2018; Foets et al. 2020). One observation is also reported in a sediment core of the Nettilling Lake, a glacial lake in the Canadian Arctic Archipelago (Beaudoin 2014). The species is frequently associated with soil habitats (Patova & Novakovskaya 2018; Foets et al. 2020; Foets et al. 2021; Patova et al. 2023), lentic water bodies and pools (Beaudoin 2014; Genkal & Yarushina 2016; Genkal & Gabyshev 2020; Kopyrina et al. 2021; Barinova & Gabyshev 2024).

Here, we report the first record of *Pinnularia bullacostae* for the European Alps, in a cluster of proglacial lakes almost exclusively fed by glacial meltwater, aiming at updating and complementing the current distribution and ecological knowledge of the species.

Materials and methods

The study area (Figure 1) is located in the upper Martell Valley, in the Ortles-Cevedale Mountain group (Central Alps, South Tyrol, Italy). The proglacial lake cluster is located above the tree line, between 2700 and 2900 m a.s.l., and the surrounding landscape is composed of glaciers, permafrost, bedrock and moraines, where primary vegetational succession is occurring (Ramskogler et al. 2023). According to the Köppen-Geiger classification map (Kottek et al 2006), the climate in the area is classified as alpine tundra (ET). The lakes formed in the few past decades due to the retreat of the Cevedale Glacier and are mainly fed by turbid glacier runoff. The uppermost lake is located approximately 150 m downstream from the visible glacier ice and part of the lake bottom is in direct contact with debris-covered ice. The three lakes are connected to each other by small streams and represent different stages of evolution in the deglaciation process, i.e., ice contact (CL),

intermediate (IL) and ice distal (DL) conditions. No previous data on physical and chemical settings, as well as on biodiversity, are available for these lakes.

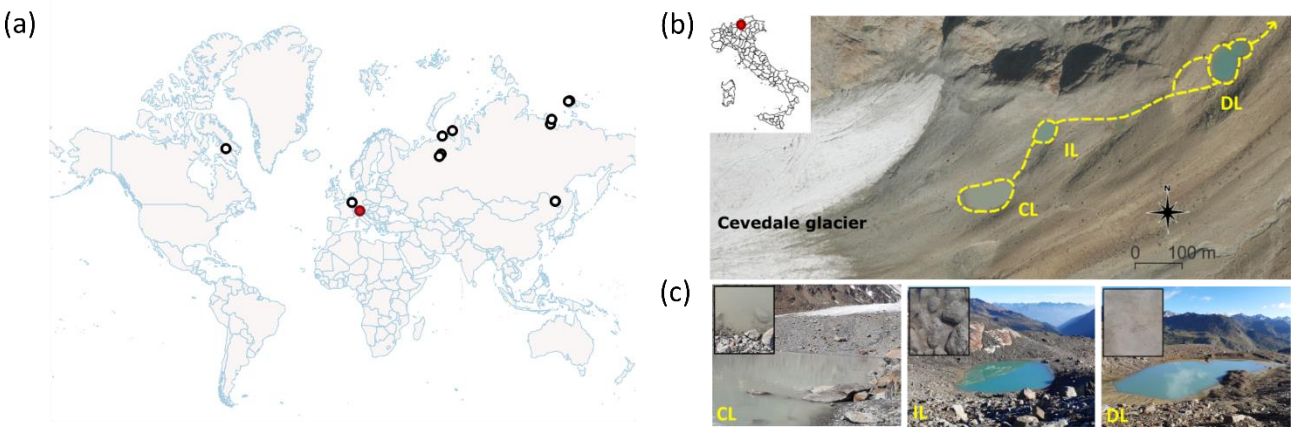

Figure 1. (a) Known distribution of *P. bullacostae* (white dots) and the study site in the European Alps (red dot); (b) The study site in Martell Valley (orthophoto: Province of Bolzano 2023, available at: http://geokatalog.buergernetz.bz.it); (c) the three studied proglacial lakes and the substrates where diatom samples were collected. CL = ice-contact lake with stones and pebbles along the shore (epilithon), IL = intermediate lake with pebbles covered by sediment (epipelon), DL = distal lake with a shore covered with fine sediment (epipelon).

Benthic diatom samples were collected in 2022 and 2023 during the ice-free seasons, in July, August and September, which represent the major hydrological stages of the Alpine glacial summer (characterised by prevalent snowmelt, ice melt, and baseflow, respectively). We collected pooled periphyton samples by brushing a known area of pebbles (epilithic samples) and cohesive sediment (epipelic samples) along the lake littoral area (Figure 1c). In 2022, one sample was assembled for each lake for each month, while in 2023 samples from the ice contact and the ice distal lakes were collected both in the upstream (U) and the downstream (D) part of the lakes. The collected material was preserved in ethanol at a final concentration of 50%. Samples were treated according to the European guidelines for the analysis of benthic diatom communities (European Committee for Standardisation 2014). Organic matter was removed by oxidation with 30% H_2O_2 at 90 °C. After dissolution of carbonates with HCl, the samples were centrifuged and rinsed with distilled water. Permanent slides were mounted in Naphrax®, with 1.7 refraction index. We counted at least 400 diatom valves and identified diatom valves at the species level whenever possible. We counted the whole slide in the case of samples with very low diatom density. Counts were made using a Leica DM2500 optical microscope (LM) equipped with differential interference contrast optics at 1000x magnification. We took micrographs of the specimens at LM using the Leica LAS X Software (version 3.7.6.25977) for image acquisition and processing, and with a Jeol JSM-IT300LV scanning electron microscope (SEM).

Results

Morphology of the observed *P. bullacostae* specimens

Valve. Length 34.3 – 39.2 µm. Width 5.8 – 7.0 µm. Linear outline, with central portion of the sides slightly concave, and flat surface in the SEM (Figure 2g). Ends rounded, not protracted.

Raphe. Narrow, linear, lateral in its central parts. Central pores drop-shaped and turned to one side. Terminal fissures ?-shaped.

Axial area. Narrow, broadening towards the central area.

Central area. An asymmetric fascia reaching the valve margins.

Striae. Weakly radiate at the centre of the valves, weakly convergent towards the ends, 15 – 16 / 10 µm, alveoli composed of 3 - 5 rows of offset areolae, sometimes with irregular arrangement (Figure 2i, visible only at SEM).

At SEM, the internal part of the valve is provided with characteristic siliceous papillae-like structures on the virgae (as described in Krammer 2000), also known in literature as “knopfartige Höcker” (Krammer & Lange-Bertalot 1999 in Lange-Bertalot & Genkal) or “elevated siliceous outgrowth” (Zidarova 2016). These structures are clearly visible only at SEM (Figure 2h) and can appear at the LM as a translucent line (Figure 2b, e, f) on the valve face.

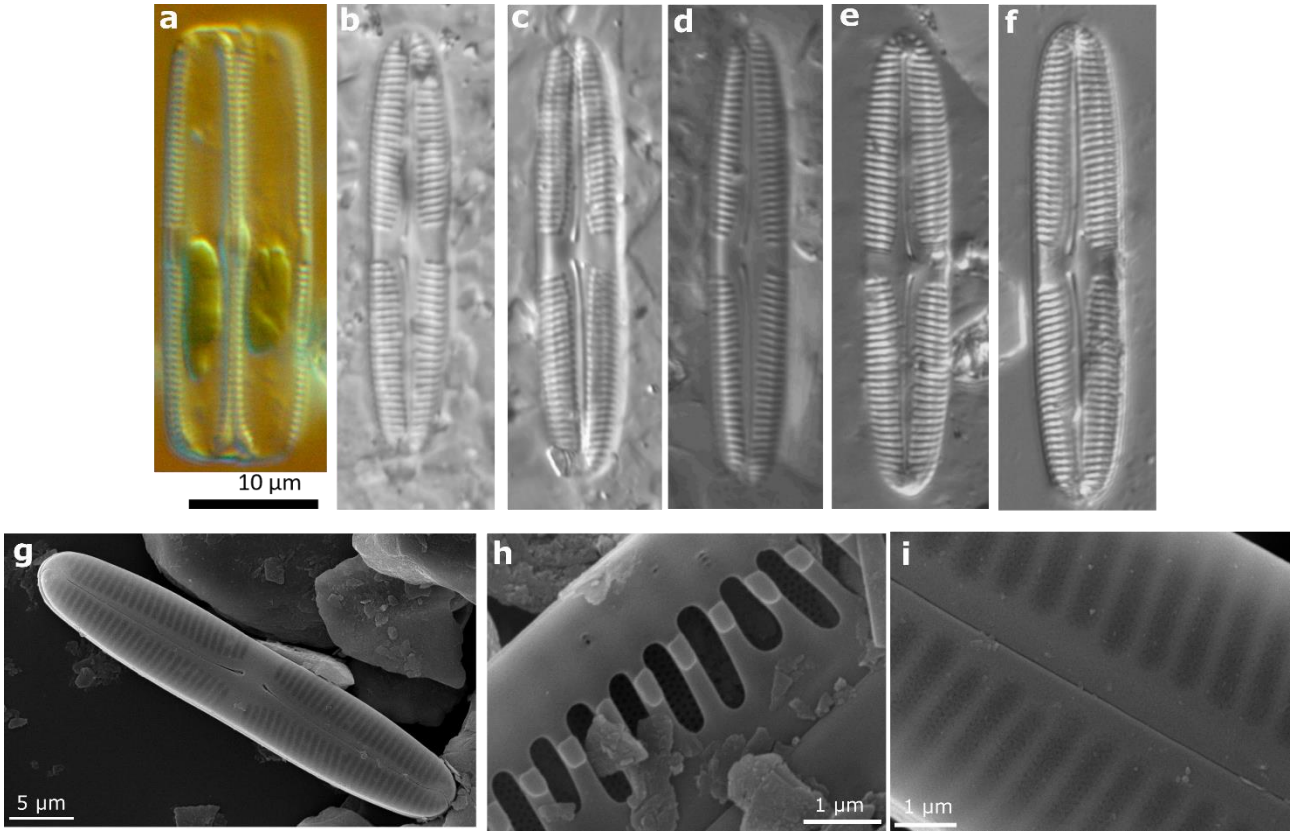

Figure 2. Micrographs of *Pinnularia bullacostae* in the specimens of the Cevedale proglacial lakes, at LM (a-f) and SEM (g-i). (a) living specimens connected to each other after the cell division, with condensed chloroplasts (interferential contrast); (b-f) oxidised specimens at LM; (g) entire valve view; (h) inner structure of the virgae with the typical papillae-like structures; (i) external view showing the alveoli as composed by 3 - 5 rows of offset areolae.

Distribution and ecology

Pinnularia bullacostae was found in the ice-contact (CL) and the ice-distal (DL) lakes (Figure 3a). In CL, the species was observed only in two samples, i.e., in August 2022 and August 2023, with relative abundance 0.2 and 4.8%, respectively. In DL, we found a stable population established on one shore covered with fine sediment (epipelic substrate) in the downstream part of the lake. Here, the species accounted for 16.6 to 30.1% of the total number of counted diatoms. In the upstream epilithic samples (U in Figure 3a), the species relative abundance was always lower than 3% (0.2 – 2.8%). In the intermediate lake, IL, the species has been never detected during the study period. In general, *P. bullacostae* was present (> 2 valves in the count) mainly in the epipelic samples (Figure 3b). The main habitat characteristics of the sites where *P. bullacostae* was observed are shown in Table 1.

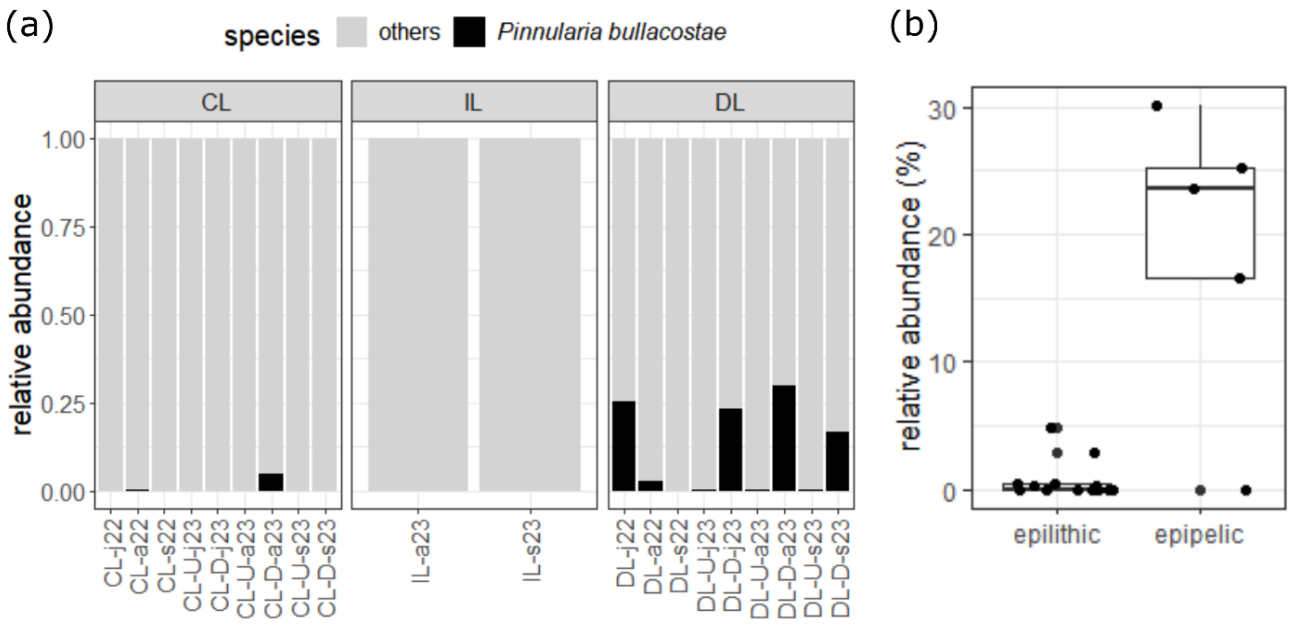

Figure 3. (a) Relative abundance of *Pinnularia bullacostae* in the analysed diatom samples. CL, IL, DL=ice-contact, intermediate, distal lake. U=upstream sample; D=downstream sample; j=July, a=August, s=September; (b) Relative abundance of *P. bullacostae* in all the analysed epilithic and epipelic samples.

Table 1. Habitat characteristics of the sites where *Pinnularia bullacostae* was observed. Subs. = substrate: E = epilithic, EP = epipelic; Tw = average littoral water temperature in the sampling day (°C); EC = Electrical Conductivity in the littoral area in the sampling day (µS/cm); TSS = Total Suspended Solids in the water column in the sampling day (mg/L). N *P.b.* = number of valves attributed to *Pinnularia bullacostae* in the sample. Name abbreviations: *A = Achnanthidium; C = Caloneis; E = Ec = Encyonema; Ep = Encyonopsis; G = Gomphonema; P = Pinnularia; S = Surirella.*

Lake	Sample	Subs.	pH	Tw	EC	TSS	N *P.b.*	Most abundant taxon	Other taxa
CL	CL- D-a22	E	7.2	11.0	71	33.6	1	*A. minutissimum* s.l. (37%)	*Ep. falaisensis* (31%)
	CL-D-a23	E	6.2	9.0	54	61.2	2	*A. minutissimum* s.l. (69%)	*S. terricola* (9%)
DL	DL-j22	E/EP	6.8	10.8	69	26.3	45	*P. bullacostae* (25%)	*P. obscura* (21%)
	DL-a22	E	7.1	12.1	59	29.8	12	*G. varioreduncum* (37%)	*Ec. silesiacum* (12%)
	DL-U-j23	E	6.6	11.2	83	17.4	1	*G. varioreduncum* (35%)	*Ec. silesiacum* (30%)
	DL-D-j23	EP	6.6	11.0	83	17.4	43	*P. obscura* (28%)	*P. bullacostae* (23%)
	DL-U-a23	E	6.3	12.7	83	30.8	2	*Ec. silesiacum* (41%)	*G. varioreduncum* (15%)
	DL-D-a23	EP	6.3	12.5	83	30.8	127	*P. bullacostae* (30%)	*Ep. falaisensis* (26%)
	DL-U-s23	E	6.6	5.9	100	8.8	1	*Ec. silesiacum* (39%)	*A. minutissimum* s.l. (9%)
	DL-D-s23	EP	6.6	6.5	100	8.8	68	*Ep. falaisensis* (21%)	*P. bullacostae* (17%)

Discussion

Morphology

Compared to values reported for the type material (Krammer & Lange-Bertalot 1999 in Lange-Bertalot & Genkal), the valves of the specimens of *P. bullacostae* identified in the Cevedale proglacial lakes are slightly longer (i.e., 34.3 – 39.2 µm versus 33 – 34 µm), and the largest specimens are slightly wider (5.8 – 7.0 µm versus 5.8 – 6.7 µm). The number of striae (15 – 16 in 10 µm) is perfectly coherent with the type material (around 15 in 10 µm).

Similar species

Pinnularia stricta Hustedt 1934 is considered to be possibly confused with *P. bullacostae* at the LM due to its size and general valve outline. However, *P. stricta* has a wider central area and is not provided with the siliceous papillae on the transapical virgae (Krammer 2000). Zidarova (2016) and Kulikovsky et al. (2023) described *Pinnularia pinseelliana* Zidarova, Kopalová & Van de Vijver 2016 and *Pinnularia microfrauenbergiana* Glushenko, Kezlya & Maltsev 2023, both similar to *P. bullacostae* due to the presence of the siliceous papillae in the inner side of the virgae. However,

both species can be easily distinguished from *P. bullacostae* by their general outline and central area (see Kulikovsky et al. 2023): an outline with slightly concave sides is present only in *P. bullacostae*, while *P. pinseelliana* and *P. microfrauenbergiana* have elliptical to lanceolate convex outlines. The central area of *P. microfrauenbergiana* is wider than in *P. bullacostae*, while in *P. pinseelliana* it is wedge-shaped as delimited by strongly radiate striae. Furthermore, *P. bullacostae* is longer (33 – 34 µm vs 20 – 25 µm and 24 – 30 µm, respectively) and wider (5.8 – 6.7 µm vs 4.5 – 5 µm and 4.5 – 5.5 µm) than these two species.

Distribution and ecology

The population of *Pinnularia bullacostae* identified in the distal proglacial lake (DL) shares the habitat with *Pinnularia obscura* Krasske 1932, which made up to the 28.4% of the samples where it is present. Diatom species of the genus *Pinnularia* are frequently found in epipelic algal assemblages (Round et al. 2007; Poulíčková et al. 2008) and can be common, if not abundant, in littoral communities of high mountain lakes (Buczkó 2016; Şahin et al. 2019; Muñoz-López & Rivera-Rondón 2021). However, previous investigations in high-altitude Alpine lakes, including proglacial turbid ones, did not report the presence of *Pinnularia bullacostae* (e.g., Tolotti 2001; Robinson & Kawecka 2005; Feret et al. 2017; Rimet et al. 2019a; Lepori & Tolotti 2023). *P. bullacostae* was previously observed in lentic habitats, such as a shallow lake of the Tit-Ary island with a sandy-silty bottom (Kopyrina et al. 2021), a lake in the Yamal Peninsula (Genkal & Yarushina 2016), a pool of the Kuchchugui-Sulbut River (Genkal & Gabyshev 2020), and the Arctic Lake Nettilling, fed by glacial meltwater from the Penny Ice Cap (Beaudoin 2014). In the Cevedale proglacial lakes, the habitat where *P. bullacostae* was more frequent or dominant (epipelic samples in the distal lake) is subject to intermittently semi-dry conditions, due to the daily fluctuations of the lake level during the diurnal cycle of summer glacier melting. In this context, the ability of *P. bullacostae* to colonise wet soils (Barragan et al. 2018; Patova & Novakovskaya 2018; Foets et al. 2020; Foets et al. 2021; Patova et al. 2023) represents an advantageous trait to survive in an environment subject to periodic desiccation.

Previous sites with records of *P. bullacostae* are included in the snow and tundra climates of the Köppen-Geiger climate classification (Kottek et al. 2006). The habitat characteristics of the Cevedale proglacial lakes are consistent with the known distribution of *P. bullacostae*, as the Ortles-Cevedale Massif is located in the alpine tundra (ET) cluster in the European Alps. Future climate projections (Rubel et al. 2017; Hock et al. 2019) predict a marked reduction in the extension of tundra and snow climate areas in the Alpine environment (Barredo et al. 2020). The related habitat alterations, e.g., shifts in hydrological regimes, higher water temperatures, increasing water transparency (Sommaruga 2015; Huss et al. 2017; Milner et al. 2017) are expected to strongly impact the biological communities in proglacial ecosystems (Tartarotti et al. 2014; Tiberti et al. 2020). The communities hosted by proglacial aquatic ecosystems, which are especially selected by the glacier derived turbidity (Sommaruga 2015; Sommaruga & Kandolf 2014), appear, therefore, as strongly threatened by the reduction of their habitat related to global warming and mountain deglaciation.

Our findings contribute to updating the known distribution of *Pinnularia bullacostae* by adding a first record in the European Alps, in the littoral area of turbid and shallow proglacial lakes in the Ortles-Cevedale Mountain group. These observations extend the area of distribution of the species to cold tundra habitats outside Arctic and Subarctic areas.

In the context of the present deglaciation, new proglacial lake ecosystems deserve special attention due to their potential in hosting specialised biodiversity and the related risk of climate-driven habitat loss. A wider geographical range of study sites is needed to assess whether *P. bullacostae* is present in other proglacial lakes in the Alps and other mountain districts at global scale. Furthermore, paleolimnological studies could assess the temporal extension of the presence of *P. bullacostae* in the European Alps in relation to suitable glacial, cold conditions.

Acknowledgements

This work is part of the EVERLAKE PhD project, co-funded by the Research and Innovation Centre of the Edmund Mach Foundation and the Department of Civil, Environmental and Mechanical Engineering of the University of Trento. We gratefully thank Walter Bertoldi and Marco Toffolon for their support and fruitful collaboration. The authors wish to express their gratitude to Alfredo Maule, Francesca Bearzot, Stefano Brighenti, Matteo De Vincenzi, Gaia Donini, Michele Combatti and Lukas Leonardi for their precious contribution to field activities and sample collection.

References

Barinova, S., Gabyshev, V., & Genkal, S. (2023). Diversity of Diatom Algae in the Lena Delta Nature Reserve and the Adjacent Territory in the Specific Ecological Factors of the Arctic. *Diversity*, *15*(7), 802. https://doi.org/10.3390/d15070802.

Barinova, S., & Gabyshev, V. (2024). The Influence of Arctic Conditions on the Formation of Algae and Cyanobacteria Diversity and on the Water Quality of Freshwater Habitats on Kotelny Island, Lena Delta Wildlife Reserve, Yakutia. *Water*, *16*(9), 1231. https://doi.org/10.3390/w16091231.

Beaudoin, A. (2014). Reconstitution paléoenvironnementale de la région du lac Nettilling, (Nunavut): Une analyse multi-proxy (mémoire). Retrieved from Library and Archives Canada (LAC) collection. (OCLC number: 1273289671).

Barragán, C., Wetzel, C. E., & Ector, L. (2018). A standard method for the routine sampling of terrestrial diatom communities for soil quality assessment. *Journal of Applied Phycology*, *30*(2), 1095–1113. https://doi.org/10.1007/s10811-017-1336-7.

Barredo, J. I., Mauri, A., & Caudullo, G. (2020). Alpine Tundra Contraction under Future Warming Scenarios in Europe. *Atmosphere*, *11*(7), 698. https://doi.org/10.3390/atmos11070698.

Buczkó, K. (2016). Guide to diatoms in mountain lakes in the Retezat Mountains, South Carpathians, Romania. *Studia Botanica Hungarica*, *47*(Suppl), 9–214. https://doi.org/10.17110/StudBot.2016.47.Suppl.9.

European Committee for Standardization (2014). European Standard 13946. Water quality - Guidance for the routine sampling and preparation of benthic diatoms from rivers and lakes. Brussels: CEN.

Feret, L., Bouchez, A., & Rimet, F. (2017). Benthic diatom communities in high altitude lakes: A large scale study in the French Alps. *Annales de Limnologie - International Journal of Limnology*, *53*, 411–423. https://doi.org/10.1051/limn/2017025.

Foets, J., Wetzel, C. E., Teuling, A. J., & Pfister, L. (2020). Temporal and spatial variability of terrestrial diatoms at the catchment scale: Controls on communities. *PeerJ*, *8*, e8296. https://doi.org/10.7717/peerj.8296.

Foets, J., Stanek-Tarkowska, J., Teuling, A. J., Van De Vijver, B., Wetzel, C. E., & Pfister, L. (2021). Autecology of terrestrial diatoms under anthropic disturbance and across climate zones. *Ecological Indicators*, *122*, 107248. https://doi.org/10.1016/j.ecolind.2020.107248.

Genkal, S.I., & Gabyshev, V. (2020). ДИАТОМОВЫЕ (BACILLARIOPHYTA) ВОДОЕМОВ И ВОДОТОКОВ ОСТРОВА КОТЕЛЬНЫЙ (НОВОСИБИРСКИЕ ОСТРОВА). *БОТАНИЧЕСКИЙ ЖУРНАЛ 105(8)*, 750-761. https://doi.org/10.31857/S0006813620080049 (In Russian).

Genkal, S. I., & Yarushina, M. I. (2016). A Study of Flora of Bacillariophyta in Water Bodies and Water Courses of the Naduiyakha River Basin (Yamal Peninsula, Russia). *International Journal on Algae*, *18*(1), 39–56. https://doi.org/10.1615/InterJAlgae.v18.i1.40.

Guiry, M.D., in Guiry, M.D. & Guiry, G.M. (2024). AlgaeBase. World-wide electronic publication, National University of Ireland, Galway. https://www.algaebase.org; searched on 16 October 2024.

Hock, R., Rasul, G. Adler, C., Cáceres, B., Gruber, S., Hirabayashi, Y., ... & Steltzer, H. (2019). High Mountain Areas. In: IPCC Special Report on the Ocean and Cryosphere in a Changing Climate [H.-O. Pörtner, D.C. Roberts, V. Masson-Delmotte, P. Zhai, M. Tignor, E. Poloczanska, K. Mintenbeck, A. Alegría, M. Nicolai, A. Okem, J. Petzold, B. Rama, N.M. Weyer (eds.)]. Cambridge University Press, Cambridge, UK and New York, NY, USA, pp. 131-202. https://doi.org/10.1017/9781009157964.004.

Huss, M., Bookhagen, B., Huggel, C., Jacobsen, D., Bradley, R.S., Clague, J.J., … Winder, M. (2017). Toward mountains without permanent snow and ice. *Earth's Future, 5,* 418-435. https://doi.org/10.1002/2016EF000514.

Kopyrina, L. I., Genkal, S. I., & Remigailo, P. A. (2021). Diatom Algae of Waterbodies in the Subarctic Tundra. *Inland Water Biology*, *14*(2), 125–132. https://doi.org/10.1134/S1995082921020085.

Kottek, M., Grieser, J., Beck, C., Rudolf, B., & Rubel, F. (2006). World Map of the Köppen-Geiger climate classification updated. *Meteorologische Zeitschrift*, *15*(3), 259–263. https://doi.org/10.1127/0941-2948/2006/0130.

Krammer, K. (2000). The genus Pinnularia. In: H. Lange-Bertalot (ed.). Diatoms of Europe, vol. 1 (pp. 1–703). Ruggell: A. R. G. Gantner Verlag K.G.

Kulikovskiy, M., Glushchenko, A., Kezlya, E., Kuznetsova, I., Kociolek, J. P., & Maltsev, Y. (2023). The Genus Pinnularia Ehrenberg (Bacillariophyta) from the Transbaikal Area (Russia, Siberia): Description of Seven New Species on the Basis of Morphology and Molecular Data with Discussion of the Phylogenetic Position of Caloneis. *Plants*, *12*(20), 3552. https://doi.org/10.3390/plants12203552.

Lange-Bertalot, H., & Genkal, S.I. (1999). Diatoms from Siberia I. Islands in the Arctic Ocean (Yugorsky-Shar Strait). In: H. Lange-Bertalot (ed.). Iconographia Diatomologica, vol. 6 (pp.1–292). Vaduz: A. R. G. Gantner Verlag K.G.

Lepori, F., & Tolotti, M. (2023). Effects of nitrogen on benthic diatom assemblages in high-elevation central and eastern alpine lakes. *Arctic, Antarctic, and Alpine Research*, *55*(1), 2270821. https://doi.org/10.1080/15230430.2023.2270821.

Medvedeva, L. A., Nikulina, T. (2019). Species diversity of Cyanobacteria and algae in the Bureya River basin (Khabarovsk territory). *Vladimir Ya. Levanidov's Biennial Memorial Meetings*, *8*, 91–113. (In Russian). https://doi.org/10.25221/levanidov.08.10.

Milner, A. M., Khamis, K., Battin, T. J., Brittain, J. E., Barrand, N. E., Füreder, L., … & Brown, L. E. (2017). Glacier shrinkage driving global changes in downstream systems. *Proceedings of the National Academy of Sciences*, *114*(37), 9770–9778. https://doi.org/10.1073/pnas.1619807114.

Muñoz-López, C. L., & Rivera-Rondón, C. A. (2022). Diatom response to environmental gradients in the high mountain lakes of the Colombia's Eastern Range. *Aquatic Sciences*, *84*(1), 15. https://doi.org/10.1007/s00027-021-00838-z.

Patova, E. N., & Novakovskaya, I. V. (2018). Soil algae of the Northeastern European Russia. *Novosti sistematiki nizshikh rastenii*, *52*(2), 311–353. (In Russ.). https://doi.org/10.31111/nsnr/2018.52.2.311.

Patova, E., Novakovskaya, I., Gusev, E., & Martynenko, N. (2023). Diversity of Cyanobacteria and Algae in Biological Soil Crusts of the Northern Ural Mountain Region Assessed through Morphological and Metabarcoding Approaches. *Diversity*, *15*(10), 1080. https://doi.org/10.3390/d15101080.

Poulíčková, A., Hašler, P., Lysáková, M., & Spears, B. (2008). The ecology of freshwater epipelic algae: An update. *Phycologia*, *47*(5), 437–450. https://doi.org/10.2216/07-59.1.

Province of Bolzano (2023). Available from: http://geokatalog.buergernetz.bz.it.

Ramskogler, K., Knoflach, B., Elsner, B., Erschbamer, B., Haas, F., Heckmann, T., … Tasser, E. (2023). Primary succession and its driving variables – a sphere-spanning approach applied in proglacial areas in the upper Martell Valley (Eastern Italian Alps). *Biogeosciences*, *20*(14), 2919–2939. https://doi.org/10.5194/bg-20-2919-2023.

Rimet, F., Feret, L., Bouchez, A., Dorioz, J.-M., & Dambrine, E. (2019). Factors influencing the heterogeneity of benthic diatom communities along the shoreline of natural alpine lakes. *Hydrobiologia*, *839*(1), 103–118. https://doi.org/10.1007/s10750-019-03999-z.

Robinson, C. T., & Kawecka, B. (2005). Benthic diatoms of an Alpine stream/lake network in Switzerland. *Aquatic Sciences*, *67*(4), 492–506. https://doi.org/10.1007/s00027-005-0783-4.

Rott, E., Cantonati, M., Füreder, L., & Pfister, P. (2006). Benthic algae in high altitude streams of the Alps – a neglected component of the aquatic biota. *Hydrobiologia, 562*(1), 195–216. https://doi.org/10.1007/s10750-005-1811-z

Round, F.E., Crawford, R.M., & Mann, D.G. (2006). Diatoms: Biology and Morphology of the Genera. Cambridge: Cambridge University Press.

Rubel, F., Brugger, K., Haslinger, K., & Auer, I. (2017). The climate of the European Alps: Shift of very high resolution Köppen-Geiger climate zones 1800–2100. *Meteorologische Zeitschrift*, *26*(2), 115–125. https://doi.org/10.1127/metz/2016/0816.

Şahin, B., Akar, B., Barinova, S. (2019). Algal Flora and Ecology of the High Mountain Lakes in the Artabel Lakes Nature Park (Gümüşhane, Turkey), I- Bacillariophyta. *International Journal of Advanced Research in Botany*, *5*(2). https://doi.org/10.20431/2455-4316.0502003.

Sommaruga, R. (2015). When glaciers and ice sheets melt: Consequences for planktonic organisms. *Journal of Plankton Research*, *37*(3), 509–518. https://doi.org/10.1093/plankt/fbv027.

Sommaruga, R., & Kandolf, G. (2014). Negative consequences of glacial turbidity for the survival of freshwater planktonic heterotrophic flagellates. *Scientific Reports*, *4*(1), 4113. https://doi.org/10.1038/srep04113.

Stevenson, R. J., Pan, Y., & Van Dam, H. (2010). Assessing environmental conditions in rivers and streams with diatoms. In J. P. Smol & E. F. Stoermer (Eds.), *The Diatoms* (2nd ed., pp. 57–85). Cambridge University Press. https://doi.org/10.1017/CBO9780511763175.005

Stockner, J. G., & Armstrong, F. A. J. (1971). Periphyton of the Experimental Lakes Area, Northwestern Ontario. *Fisheries Research Board of Canada 28*, 215-229.

Tartarotti, B., Saul, N., Chakrabarti, S., Trattner, F., Steinberg, C. E. W., & Sommaruga, R. (2014). UV-induced DNA damage in *Cyclops abyssorum tatricus* populations from clear and turbid alpine lakes. *Journal of Plankton Research*, *36*(2), 557–566. https://doi.org/10.1093/plankt/fbt109.

Tiberti, R., Buscaglia, F., Callieri, C., Rogora, M., Tartari, G., & Sommaruga, R. (2020). Food Web Complexity of High Mountain Lakes is Largely Affected by Glacial Retreat. *Ecosystems*, *23*(5), 1093–1106. https://doi.org/10.1007/s10021-019-00457-8.

Tolotti, M. (2001). Littoral diatom communities in high mountain lakes of the Adamello-Brenta Regional Park (Trentino, Italy) and their relation to acidification. In: R., Jahn, J.P. Kociolek, A., Witkowski & P., Compèere (eds), Lange-Bertalot Festschrift - Studies on Diatoms (pp. 327 – 352). Ruggell: A. R. G. Gantner Verlag K.G., ISBN 3-904144-26-X.

Guiry, G.M. in Guiry, M.D. & Guiry, G.M. 20 October 2023. AlgaeBase. World-wide electronic publication, National University of Ireland, Galway. Available from: https://www.algaebase.org.

Zidarova, R., Kopalová, K., & Van De Vijver, B. (2016). Ten new Bacillariophyta species from James Ross Island and the South Shetland Islands (Maritime Antarctic Region). *Phytotaxa*, *272*(1), 37. https://doi.org/10.11646/phytotaxa.272.1.2.

S5.1. Rarefaction curves

Rarefaction curves of 16S and 18S samples before and after rarefaction at 10000 reads.

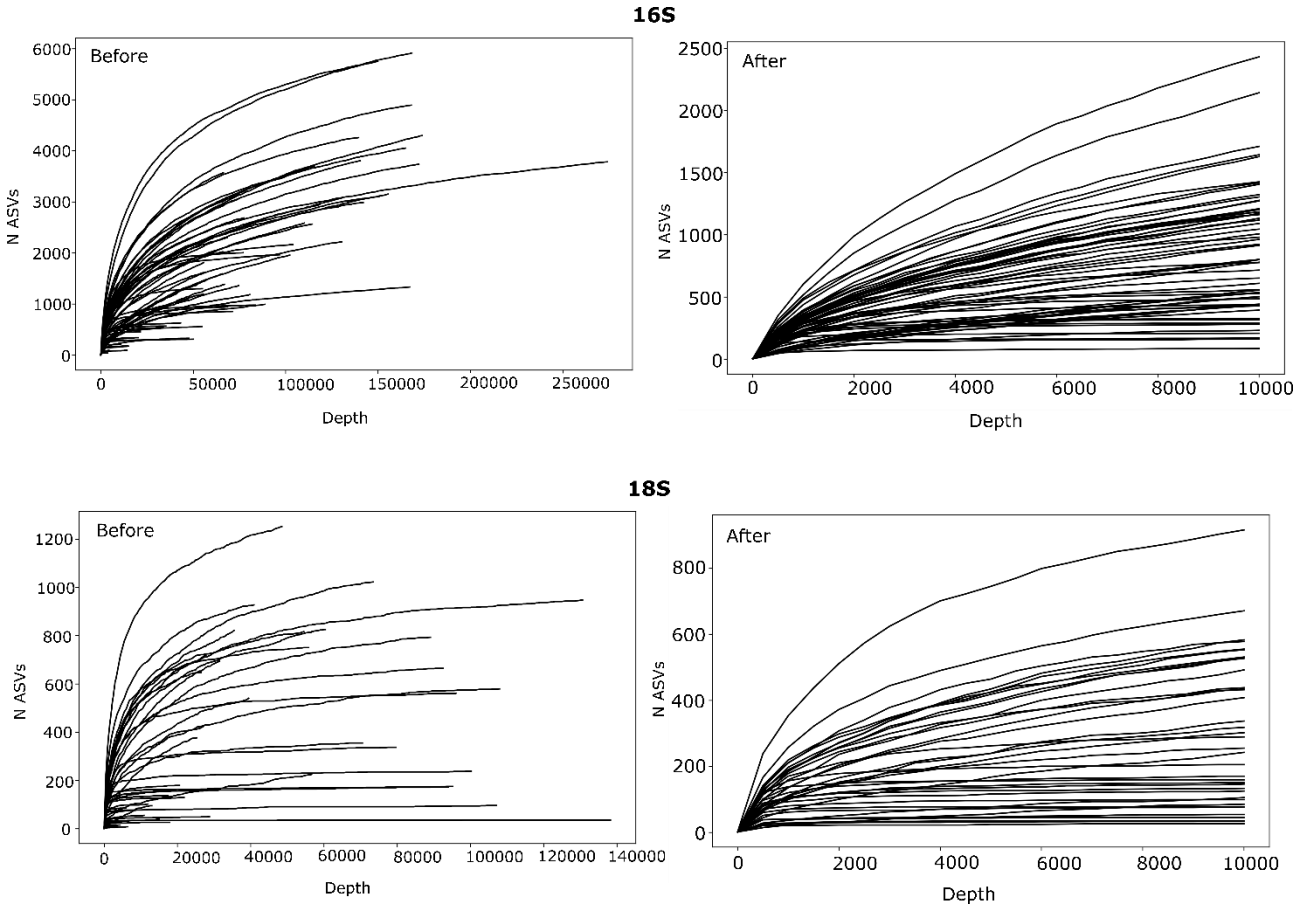

S5.2. List of eDNA samples

List of samples collected in 2022 and 2023 from the Cevedale proglacial lakes and the Marmotte Lake. Yellow shading = removed from the dataset after rarefaction (sequencing depth < 10000 reads).

Epilithic				
Sample	month	year	depth 16S	depth 18S
L1	J	2022	54745	107021
L1	A	2022	4406	3233
L1	S	2022	88828	107958
L2	J	2022	68641	95168
L2	A	2022	50091	17832
L2	S	2022	35169	28744
L3	J	2022	141982	130606
L3	A	2022	103950	79619
L3	S	2022	96655	100241
L2M	J	2023	1631	693
L2M	A	2023	33729	21823
L2M	S	2023	43182	31718
L2V	J	2023	17961	2118
L2V	A	2023	83578	17381
L2V	S	2023	21381	17858
LC	J	2023	747	6968
LC	A	2023	54974	5890
LC	S	2023	12842	10864
L3M	J	2023	65939	35533
L3M	A	2023	74858	54512
L3M	S	2023	74719	73398
L3V	J	2023	68358	27147
L3V	A	2023	77366	55828
L3V	S	2023	76947	20570
MARMM	S	2023	66330	48525
MARMV	S	2023	58659	40908

Plankton				
Sample	month	year	depth 16S	depth 18S
L1	J	2022	47202	92525
L1	S	2022	167101	96090
L2	S	2022	80564	70503
L3	J	2022	55635	60398
L3	S	2022	102224	89084
L2	J	2023	909	477
L2	A	2023	47609	11992
L2	S	2023	15041	15015
LC	A	2023	74573	26417
LC	S	2023	65707	25254
L3	J	2023	51886	27808
L3	A	2023	66855	31509
L3	S	2023	55669	39446
MARM	S	2023	56697	56629

Sediment				
Sample	month	year	depth 16S	depth 18S
L1	J	2022	3631	1336
L1	A	2022	529	4
L1	S	2022	1388	887
L2	J	2022	4432	671
L2	A	2022	10903	4351
L2	S	2022	14661	138239
L3	J	2022	71225	93925
L3	A	2022	14201	6426
L3	S	2022	20371	13007

S5.3. NMDS prokaryotes

Non-metric multidimensional scaling ordination plots of plankton (a) and epilithic (b) 16S samples, grouped according to lake of origin (point shapes). Tables show the loadings of environmental vectors on NMDS axes 1 and 2 and the correlation coefficient (r2, Spearman correlation). Significant correlations are indicated by stars (* $p \leq 0.05$, ** $p \leq 0.01$, *** $p \leq 0.001$).

(a) Plankton

stress value = 0.07, R^2 = 0.99 in the Shepard plot

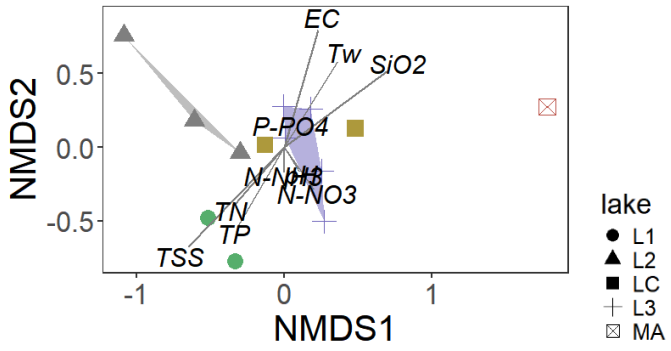

	NMDS1	NMDS2	r2
pH	0.53	-0.85	0.04
EC	0.28	0.96	0.68**
N-NO3	0.57	-0.82	0.12
N-NH3	-0.04	-1.00	0.03
TN	-0.65	-0.76	0.26
P-PO4	0.28	0.96	0.02
TP	-0.51	-0.86	0.38
SiO2	0.81	0.59	0.76**
Tw	0.53	0.85	0.47
TSS	-0.69	-0.72	0.87***

(b) Epilithic

stress value = 0.08, R^2 = 0.99 in the Shepard plot

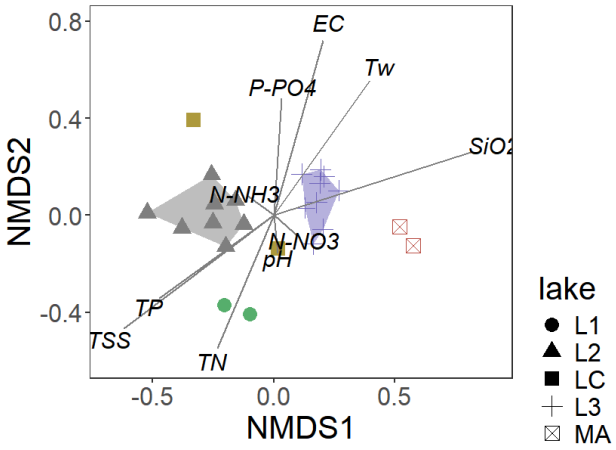

	NMDS1	NMDS2	r2
pH	0.10	-1.00	0.03
EC	0.27	0.96	0.56***
N-NO3	0.76	-0.65	0.02
N-NH3	-0.80	0.60	0.02
TN	-0.39	-0.92	0.35 *
P-PO4	0.07	1.00	0.23
TP	-0.81	-0.59	0.34
SiO2	0.95	0.30	0.75 ***
Tw	0.58	0.82	0.47 **
TSS	-0.80	-0.60	0.60 ***

S5.4. Archaea

Number of reads attributed to Archaea (genus *Nitrosarchaeum*) in plankton samples from the Cevedale proglacial lakes and the Marmotte Lake.

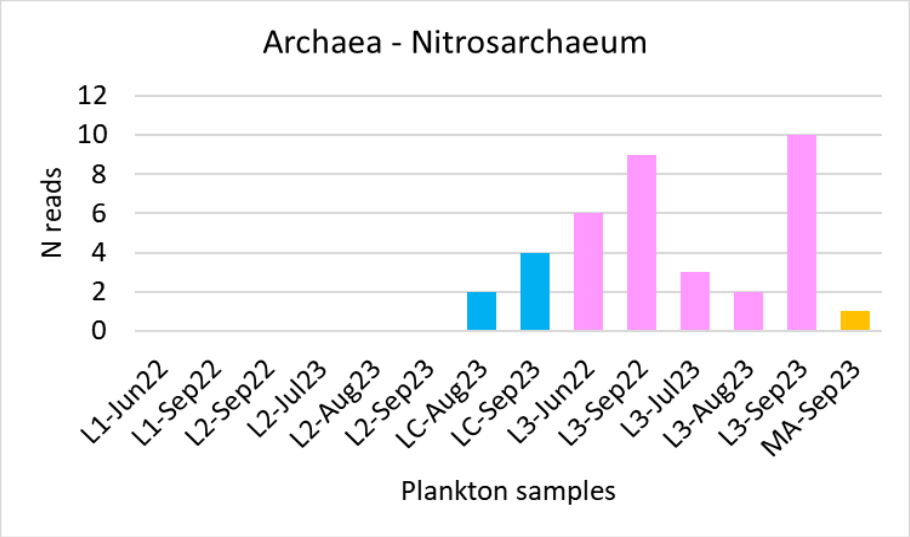

S5.5. Shared and unique eukaryotic ASVs in sample types

Venn diagram of shared and unique eukaryotic ASVs detected in the analysed samples (18S dataset), grouped by sample type (E = epilithic, P = plankton, S = sediment).

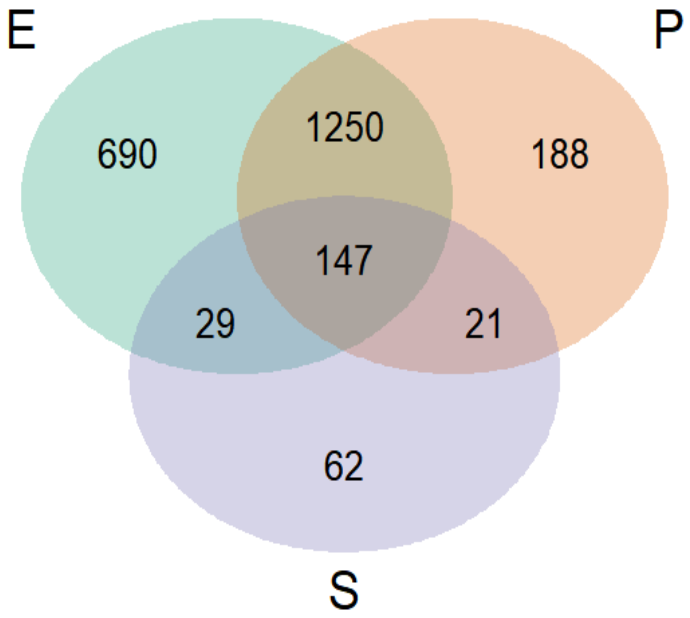

S5.6. Eukaryotic taxonomic composition

Taxonomic composition of eukaryotes at the division (d) and subdivision (s) level in the analysed samples, grouped by sample type (E = epilithic, P = plankton, S = sediment) and lake.

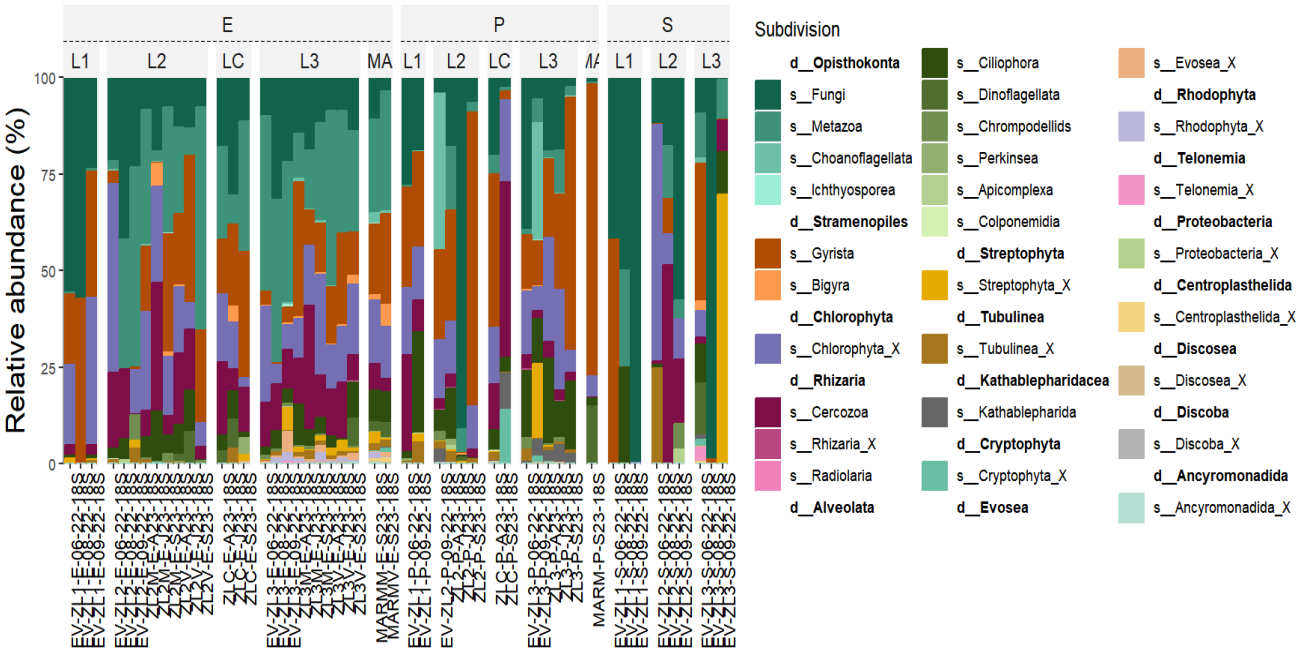

S5.7. ASV richness in divisions and classes

(a) Number of ASVs detected in each division, for the samples from the Cevedale proglacial lakes. **(b)** Number of ASV detected in each Class (only classes with >10 ASV). **(c)** Number of genera detected in each class (only classes with > 2 genera).

(a)

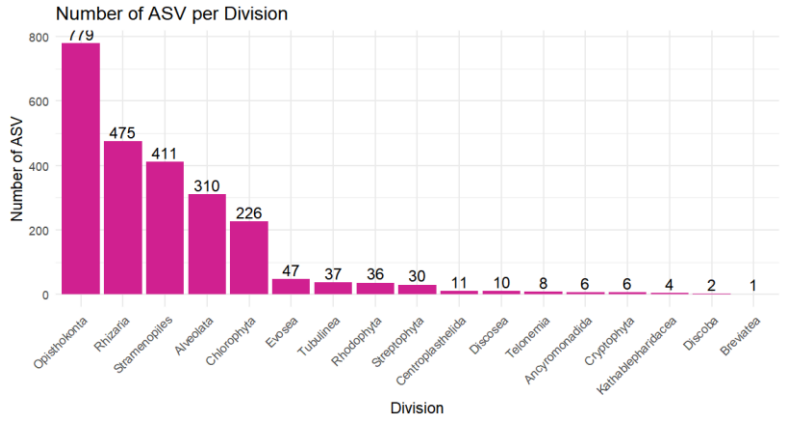

(b)

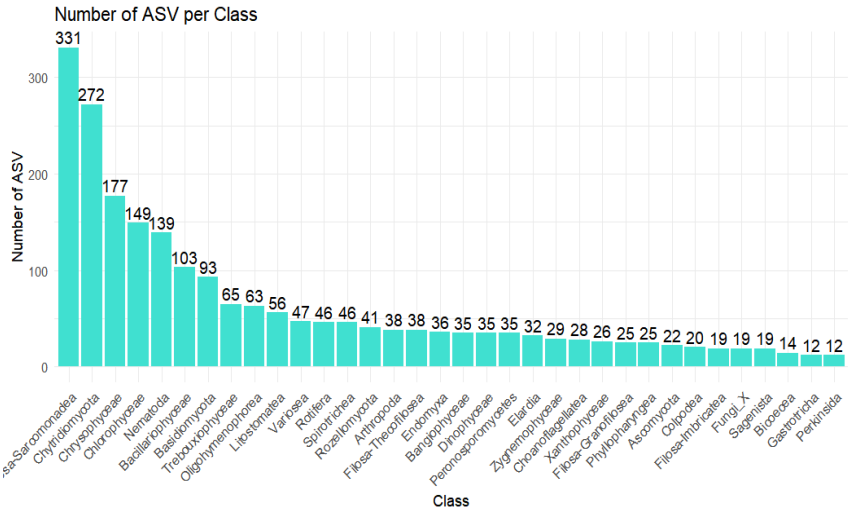

(c)

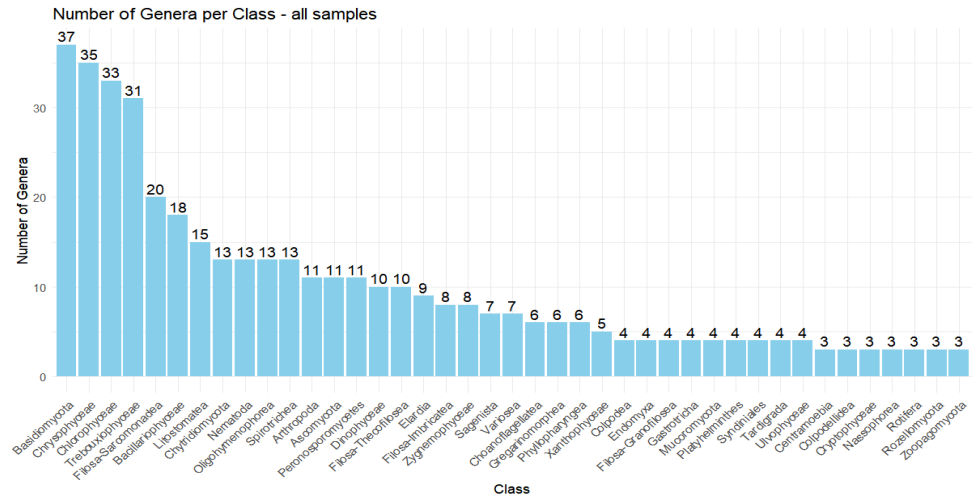

Acknowledgements

Words cannot express my gratitude to my supervisors, Monica, Cristina, Marco and Walter, for guiding and inspiring my PhD journey with competence, dedication and infinite patience. I am deeply grateful for the opportunity they gave me and for their support along the way, for believing in me, for encouraging me to go beyond my limits.

I wish to express my sincere appreciation to the reviewers, Diego Fontaneto and Tom Shatwell, and to the entire committee, for the time and energy they dedicated in reading this thesis, and for the valuable comments and feedback.

Fieldwork would not have been the same without the enthusiastic help of Nicola Accordini, Simone Speltoni, Sebastiano Piccolroaz, Gaia Donini, Matteo De Vincenzi, Michele Combatti, Enrico Pandrin, Alfredo Maule, Francesca Bearzot, Stefano Brighenti, and all my fantastic four supervisors. Thank you all for your invaluable support and good company in the field.

I would also like to warmly thank Bruno and Maria Luigia, and all the staff of Martellerhütte, for their fundamental logistical support and their warm hospitality.

Thanks to Francesco Comiti and Stefano Brighenti from the University of Bolzano, and to Luca Carturan from the University of Padova, for their collaboration in planning research and field activities, and for providing crucial insights into the study area.

I gratefully acknowledge the Geotechnical Laboratory of the University of Trento, for their technical expertise in the grain size analyses.

To all my colleagues in Mesiano and in San Michele: for their fundamental support and presence, for sharing their competence and knowledge with me. I am especially grateful to the Physical Limnology Laboratory of the University of Trento, and to the wonderful people in the GIAMT group, for their commitment in environmental studies and protection, and for creating a constructive and welcoming environment where I truly felt at home.

To all the friends and beautiful souls that populate my life, in Trento and around the world. For the moments of joy, the inspiration and the connection, and the silent, gentle closeness you gifted me, even in the darkest time.

To my parents, Antonella and Andrea, and grandparents, brothers, aunts and uncles and cousins. Thank you for being my roots.

And to Michele, thank you for sharing this PhD journey with me, and for walking shoulder to shoulder on many other paths.

Financing

This PhD project was co-financed by the Department of Civil, Environmental and Mechanical Engineering of the University of Trento and the Research and Innovation Centre of Fondazione Edmund Mach.